UNIVERSITÀ DEGLI STUDI DI MILANO
SCUOLA DI DOTTORATO
TERRA, AMBIENTE E BIODIVERSITÀ

Dottorato di Ricerca in Scienze della Terra
Ciclo XXIII

Facies distribution of a rimmed carbonate platform and overlying regressive carbonates: the Esino Limestone and Calcare Rosso facies in the Central Southern Alps (*Lombardy, Italy*)

Ph.D. Thesis

Marco Binda
Matricola R07617

Tutore
Prof.Fabrizio Berra

Co-Tutore
Prof. Flavio Jadoul

Coordinatore
Prof. Stefano Poli

Anno Accademico
2009-2010

TABLE OF CONTENENTS:

Chapter 1

DEPOSITIONAL ARCHITECTURE OF THE ESINO LIMESTONE

The evolution of a carbonate succession can be subdivided in different stages, as episodes of platform growth can be separated by intervals of reduced or absent carbonate production. The most important parameters which drive the evolution of a carbonate platform are the changes in base level (i.e. Kendall & Schlager, 1981; Handford & Loucks, 1993), in the environmental conditions (e.g. climate, nutrients; Mutti & Hallock, 2003) and in the type of the carbonate-producing organisms (as a response to biotic evolution; i.e. Pomar, 2001), whose interplay affects the efficiency of the carbonate factory as a whole and the final geometry of the carbonate platform. The changes in these parameters drive the evolution of carbonate factories, from inception to demise and, eventually, to the reprisal of a new carbonate factory.

Complete recordings of the evolution form the inception to the demise and renewed return of carbonate production are recorded in subsurface settings and can be reconstructed by the integration of seismic and core/well data. The geometric architecture of these settings is generally well constrained, nevertheless it is generally difficult to obtain detailed information on the characteristics and distribution of the different carbonate facies, so to create a large database of facies distribution and lithological-petrophysical characteristics. On the contrary well-preserved outcrop analogues which preserve the geometry of a complete evolution of carbonate systems (from inception, to demise, to renewed return to carbonate productions) are generally scarce and confined to a few numbers of well-known cases, randomly distributed in time and space. Therefore, the identification of new case histories is required to increase the understanding of the behaviour of carbonate systems different for age and depositional settings. Favourable cases should honour a number of requirements that can be summarized as follows:

- preservation of the original relationships among the different subenvironments (from platform top to the basin)
- well-exposed geometry
- preserved facies and microfacies
- preserved relationships between deposits related to different evolutionary stages.

A further major point is related to the reconstruction of the interplay between sea-level changes and subsidence (i.e. creation of accommodation space) and carbonate production. The detection of the effects of this interplay can especially be achieved only in well-preserved settings.

As all these requirements are extremely difficult to be honoured, it follows that only a small number of cases are really helpful in understanding a complete evolution of carbonate systems and of the environmental conditions and processes which control changes in the depositional regime and architecture.

A carbonate system which fully honours all these requirements is preserved in the Upper Anisian to Lower Carnian succession of the Southern Alps of Lombardy (Brembana platform, Northern Italy). It consists of a flat-topped, rimmed T-factory (*sensu* Schlager, 2003) platform with steep slopes, which enucleate after the drowning of a former Anisian platform. The evolution of this platform is characterized, after the nucleation stage, at first by aggradation and later by progradation and interfingering with basinal limestones. The top of this platform is marked by a regressive trend responsible for the repeated subaerial exposure of the flat-topped platform, followed by the reprise of inner platform facies on its top and by the onlap of shales on the slopes of the former system. The geometry and facies distribution of this well-preserved carbonate system allowed us 1) to describe and discuss the complete evolutionary history of a seismic-scale green-house carbonate platform; 2) to reconstruct the relationships of the different facies assemblages in space and time and 3) to reconstruct the response of the carbonate factory to the changes in accommodation space and carbonate production.

GEOLOGICAL SETTING

The Late Anisian to Early Carnian succession of the Southern Alps is characterised by the presence of thick carbonate platform successions separated by basinal troughs and seaways onto which they prograde (Fig. 1.1). The carbonate system evolves from prevailing attached platforms to the west-south-west (Esino Limestone) to isolated platforms toward the north-east (Dolomites; Latemar Limestone, Marmolada Limestone, Sciliar Dolomite). In the Lombardy Basin (Fig. 1.1, 1.2) the succession (Assereto & Casati, 1965; Forcella & Jadoul, 2000) consists of Late Anisian basinal to peritidal facies (peritidal Dolomite in Jadoul & Rossi, 1982; Camorelli Limestone in Berra et al., 2005) which, after drowning, are covered by a prograding carbonate platform (Esino Limestone) mainly represented by inner platform facies rimmed by narrow reefal and sandy margin facies. The reef facies laterally pass to thick bodies of slope breccias (Rossetti, 1967; Jadoul et al., 1992; Berra 2007) which interfinger with resedimented basinal limestones.

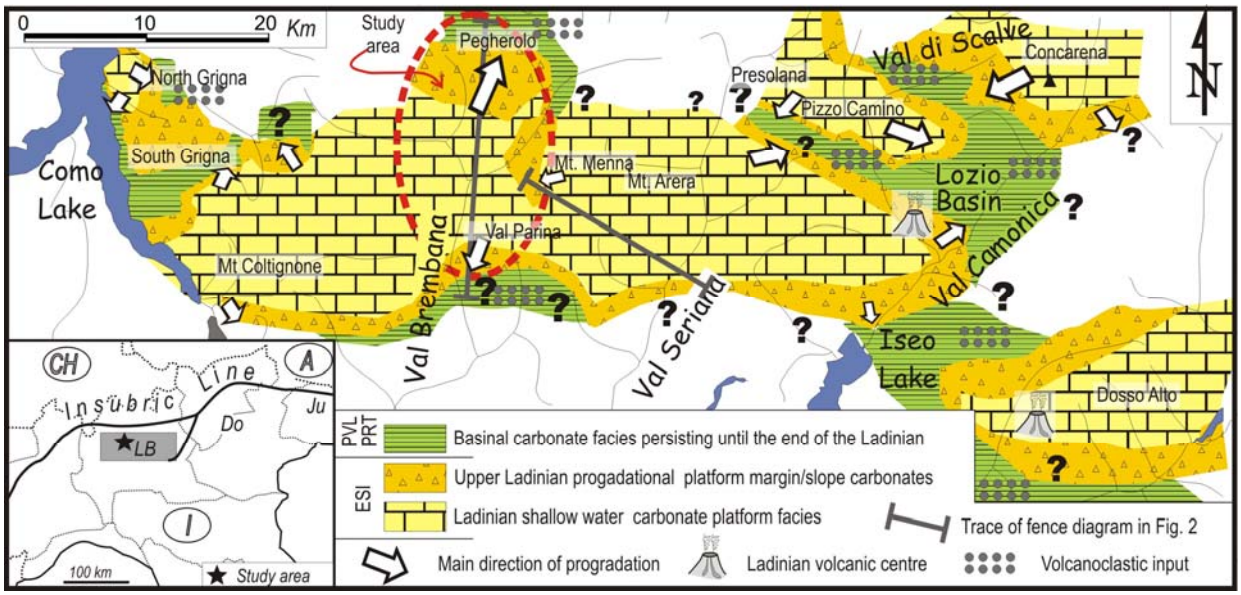

Fig. 1.1 *– Paleogeographic distribution of the carbonate highs and intraplatform basins in the Lombardy Basin at the end of the deposition of the Esino Limestone.*

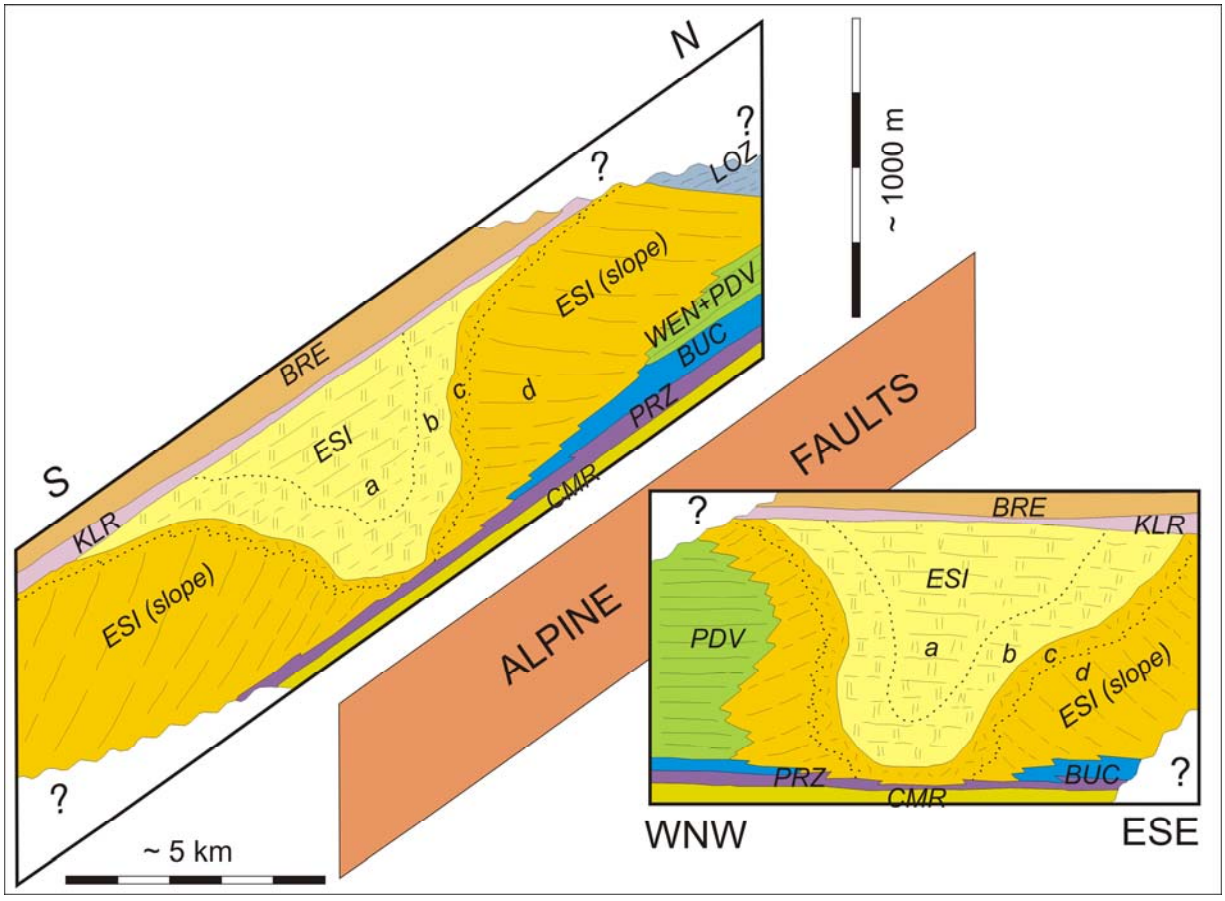

Fig. 1.2 *– Fence diagram of the facies distribution in the study area (Brembana platform). The trace of the stratigraphic sections in indicated in Fig. 1.1 CAM: Camorelli Limestone; PRZ: Prezzo Limestone; BUC: Buchenstein Fm.; PDV: Perledo-Varenna Limestone; WEN: Wengen Formation; ESI: Esino*

Limestone, consisting of: ***a-*** *bedded inner platform facies;* ***b-*** *massive bioclastic facies (open platform);* ***c-*** *reef belt;* ***d-*** *slope breccias; KLR: Calcare Rosso; LOZ: Lozio Shale; BRE: Breno Formation.*

In western Lombardy shallow-water facies prevail and basinal facies were deposited in narrow seaways and troughs. Before the end of the Ladinian, the basinal facies were generally overlain by shallow-water successions due to the progradation of the Esino Limestone carbonate platform. In the Lozio Basin, middle Val Camonica (Costa Volpino) and Brembana platform the basinal facies persisted throughout the Ladinian as platform progradation was not sufficient to close the intraplatform basins (Fig. 1.2). In these areas, the flat-topped Esino Limestone platform reaches a maximum thickness of about 700-800 m and rapidly pinches out basinward with steep slopes (about 35°) consisting of clinostratified deposits (Fig. 1.3).

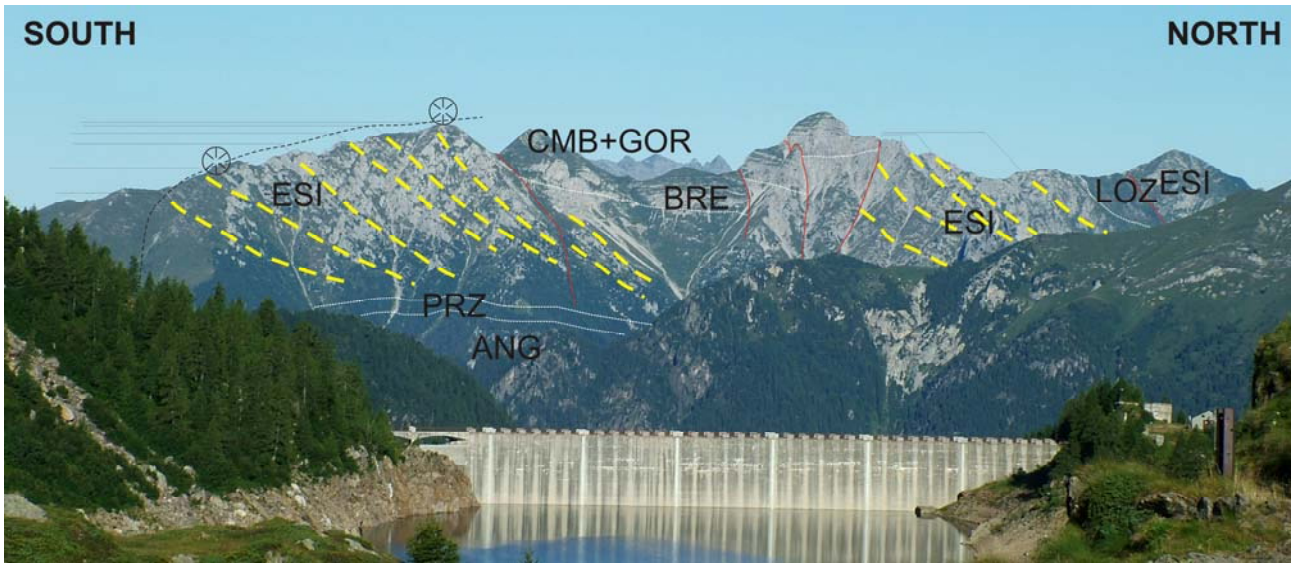

Fig- 1.3 *– Panoramic view or the prograding platform of the Brembana platform from East.*

The Ladinian basinal succession, coeval with different stages of evolution of the Esino Limestone, begins with the deposition of marly limestones (Prezzo Limestone) and nodular cherty limestones (Buchenstein Fm.), covered by dark, bedded limestones (referred to by various local stratigraphic names). The calcareous basinal facies are mainly developed in the Grigna Massif (western Lombardy; Perledo-Varenna Limestone), Val Seriana, in the Pegherolo-Menna Massif and in the Concarena-Pizzo Camino Massif (where the basinal limestone are known as Pratotondo Limestone). Volcanoclastic sandstones (Wengen Formation) interfinger, in the wider basins and close to the toe-of-the-slope, with the dark bedded limestone. Where the basinal limestone are not covered by the slope facies of the Esino Limestone (i.e. Pegherolo and Concarena Massifs), the sedimentation shifts to dark shales and siltstones (Carnian, Lozio Shale;

Rossetti, 1967; Balini et al., 2000; Berra, 2007). The volcanic input is generally scarce in the central-western Lombardy basin and documented by the Wengen Formation: therefore the distinction between the pre-volcanic and post-volcanic Ladinian platforms used in the Dolomites to the east is applicable only east of the Val Camonica.

The overall stratigraphic characteristics of the succession resemble those of many Ladinian inner platform successions studied throughout the Southern Alps (i.e. Latemar: Goldhammer et al., 1990; Esino Limestone: Jadoul et al., 1992b; Marmolada: Blendinger, 2001). Syndepositional tectonic activity was limited to the central-eastern part of the Southern Alps and is not recorded westward in the Lombardy Basin. Probably due to the different paleogeographic setting and volcano-tectonic activity in the Lombardy Basin (Central Southern Alps) and the Dolomites (Eastern Southern Alps), significant stratigraphic differences characterize the two sectors. The Ladinian platforms of the Dolomites (Marmolada Limestone, Latemar Limestone and Sciliar Dolomite; Bosellini, 1984; Bosellini & Stefani, 1991) are generally represented by partly isolated carbonate build-ups, whereas in the Lombardy basins the intraplatform seaways were narrower and most of the platform coalesced. Furthermore, sedimentary deposits in the seaways of the Dolomites include proximal volcanoclastics (including lava flows), which represent only a minor source of sediments in the Lombardy Basin.

Close to the Ladinian-Carnian boundary, a major sea-level fall is recorded in the Lombardy Basin by a lithostratigraphic unit ("Calcare Rosso", Italian for "Red Limestone", Assereto et al., 1977; Assereto & Kendall, 1977; Assereto & Folk, 1980; Mutti, 1994; Berra, 2007) characterised by karst structures, paleosols, collapse and sedimentary breccias which were developed at the top of the Ladinian carbonate platform (Esino Limestone). The Calcare Rosso is particularly well exposed in Val Brembana, where it consists of about 50 m of limestones with evidence for multiple episodes of carbonate deposition, that record karstification, abundant early carbonate-cement precipitation and development of paleosols. Eastward (Val Seriana), the Calcare Rosso is represented by a few meters of red to grey paleosols and erosional breccias documenting a longer subaerial exposure and/or reduced accommodation on the inner platform facies. The subaerial exposure of the Ladinian platforms can be traced throughout the Lombardy Basin and probably all over the Southern Alps (Jadoul et al., 2002), but the precise dating is prevented by the absence of index fossils. Mutti (1994) interprets the Calcare Rosso as a complete third order sequence, bounded at the base and at the top by two main erosional surfaces that represent the sequence boundaries.

The Ladinian-Carnian fall in sea level is well known in shallow-water carbonate platform settings of the western Southern Alps and can be related to a starvation episode in the basin (Berra, 2007).

STRATIGRAPHY

Geometry and facies distribution allow to define the entire history of the evolution of the Late Ladinian-Early Carnian carbonate factory in the area of the Brembana platform in the Lombardy Alps (Fig. 1.3). The architecture of this carbonate system is described in terms of evolutionary stages: inception, growth, demise and "rebirth" of the carbonate factory.

PLATFORM INCEPTION (LATE ANISIAN, EARLIEST LADINIAN; LOWER ESINO LIMESTONE)

The end of the Anisian carbonate platform (Angolo and Camorelli Limestone, Jadoul & Rossi, 1982; Berra et al., 2005) in the Lombardy Basin is marked by a rapid marine transgression which leads to the deposition of dark, bedded marly limestones yielding a rich ammonoid fauna (Prezzo Limestone; Balini, 1992). The deposition of the Prezzo Limestone marks a rapid drowning of the previous shallower successions (Gaetani et al., 1996). This transgression is rapidly followed by the nucleation of a new carbonate system which will last for all the Ladinian. Nucleation starts on relative highs where the Prezzo Limestone is thinner and rests on the peritidal carbonate facies of the Camorelli Limestone (Fig. 1.2). During the inception stage it is possible to identify bioclastic-rich margins ("Lumachella di Ghegna"; Tommasi, 1911; 1913; Patrini, 1927) which document the first reef associations of the Esino Limestone. From these small highs, scattered in the Lombardy Basin, the carbonate factory spreads basinward, gradually enlarging its surface and the sites of carbonate production (Fig. 1.4).

The precise identification of the nucleation areas is complex, as these zones have been later covered by the different facies of the prograding Esino Limestone. In the Brembana platform the nucleation zone was probably located in its southern part. The geometry of the first stages of the platform evolution can be described in detail more to the south, where it is possible to observe a rapid aggradation of the Ladinian Esino Limestone on the basinal facies of the Prezzo Limestone. Observations in this area (Fig. 1.4 b) can help the understanding of the evolution of the Esino Limestone in the initial stages, which can be exported to the Brembana platform. The observed presence of about 50 m of slope facies above the Prezzo Limestone suggest that this was the shelf to basin relief close to the nucleation highs (Fig. 1.4 b). The massive, clinostratified

slope facies are capped by bedded peritidal limestones which document the aggradation of the Ladinian platform postdating the progradation which follows the nucleation of the platform.

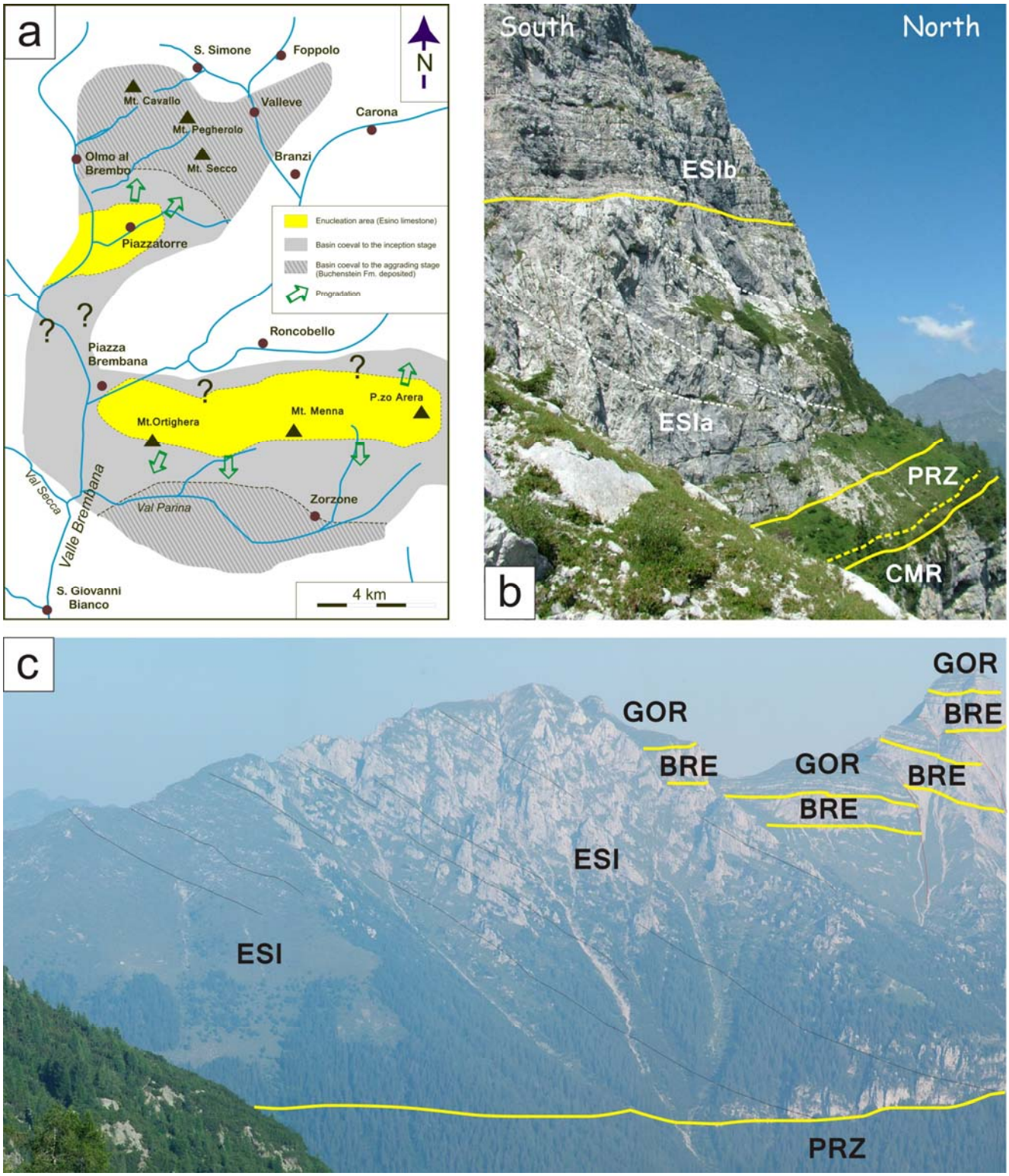

Fig. 1.4 *– Geometry and paleogeography of the Esino Limestone during the inception stage:* ***a****- paleogeographic reconstruction of the enucleation areas of the Esino Limestone, with the distribution of*

the surrounding basinal facies (the distribution of the Buchenstein Fm., corresponding to the aggradation stage is indicated); ***b****- geometry of the basal part of the Esino Limestone prograding from the inception area (northern Arera Mt.);* ***c****- view or the southernmost part of the Brembana platform, with the geometry of the aggrading stage, immediately predating the major progradation of the platform.*

This evolution reflect the transition from the keep-up to the catch-up stage. A regressive stage in the lower part of the Esino Limestone is locally observed (Assereto et al., 1977). This regressive lower lithozone of the Esino Limestone (lithozone 2 of Jadoul et al., 1992, 50-60 m thick) consists of well-bedded limestone and dolostones organized in peritidal cycles capped by stromatolitic beds, associated to dolomitized peritidali-supratidal horizons and tepees (Assereto & Kendall, 1977). This regression probably favoured the definitive onset of the carbonate platform of the Esino Limestone, which predates platform aggradation recorded at the beginning of the following stage (platform growth).

PLATFORM GROWTH (LADINIAN; MIDDLE AND UPPER ESINO LIMESTONE)

Most of the Ladinian is characterized by the progradation from the nucleation area of the Ladinian carbonate platform of the Esino Limestone, which interfingers with and covers coeval basinal limestones and mixed deposits (carbonate and volcanoclastic sediments, Wengen Formation).The carbonate platform succession can be subdivided in three main facies associations which characterize all the Esino Limestone from the inception to its demise: inner platform facies, reef facies and slope facies (Fig. 1.5). This stage records a general trend characterized by decreased accommodation and increased progradation.

a) bedded to massive inner platform facies

Calcareous, light-coloured, bedded, intra-bioclastic packstones, with dasycladaceans green algae, crinoids and molluscans, oncolitic rudstone horizons and stromatolitic bindstones characterize the inner platform facies. The vertical distribution of the inner platform facies (which reach a total thickness of up to 700-800 m) allows the definition, from base to top, of two lithozones (Jadoul et al., 1992) which cover the lower lithozone (lithozone 2 of Jadoul et al., 1992; that represents the basal part of the Esino Limestone corresponding to the platform inception stage):

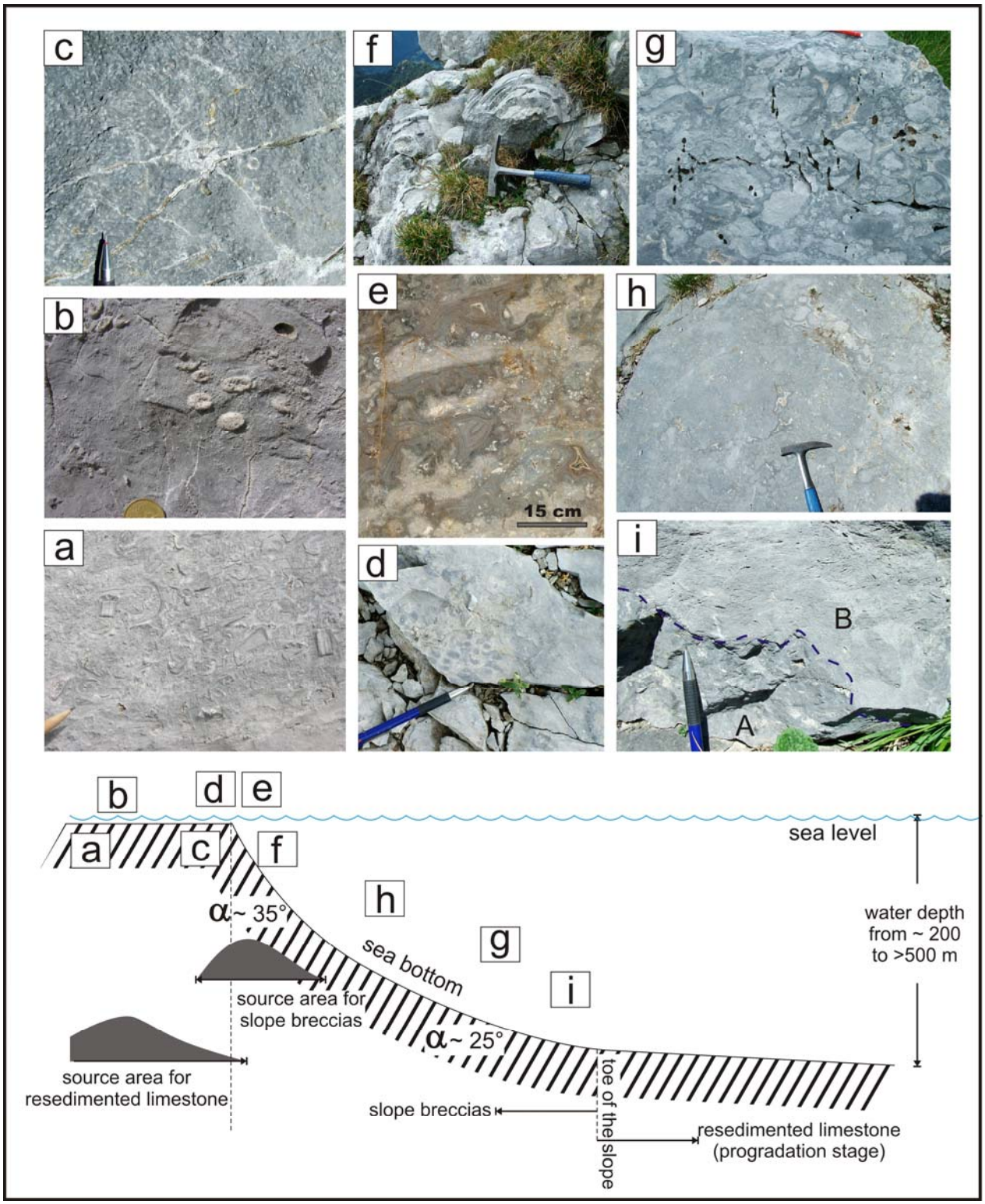

Fig. 1.5 *– Ideal profile and facies distribution along the depositional profile (from platform rim to the basin) during the growth stage (lower part of the figure).* ***a-*** *bioclastic rudstone yielding abundant crinoids and bivalves, open platfor/backreef facies;* ***b-*** *bioclastic sand with small coral colonies, backreef facies;* ***c-*** *Tubiphytes in the reef facies;* ***d-*** *coral framestone, reef facies;* ***e-*** *microbialitic mound with abundant cavities filled by early isopacous cements, upper slope facies;* ***f-*** *large cavity filled with early isopacous cement (evinospingia), upper slope;* ***g, h-*** *mud-free slope breccias, stabilized by early, marine*

isopacous cements, slope facies; ***i-*** *sharp contact between slope breccias (A) and a bivalve (daonellids) coquina (B) which marks the interval between two breccia flows. Letters in boxes in the slope model (base of the figure) indicate the approximate position of the pictures along the depositional profile.*

1) middle lithozone of the Esino Limestone (lithozone 4 of Jadoul et al., 1992; 300 to 450 m thick), consisting of thick bedded prevailing subtidal limestones (mainly packstone and wackestone) rich in large oncoids, gastropods, bivalves and green algae, as well as intraclasts and peloids. Stromatolitic limestones are generally thin and mark the top of shallowing upward cycles up to a few meters thick. Cycles generally show a shallowing-upward trend, consisting in the lower part of subtidal thick-bedded to massive packstone and wackestone, capped by fenestral packstone and/or stromatolites;

2) upper lithozone (lithozone 6 of Jadoul et al., 1992; 150 to 350 m thick), consisting of bedded limestones organized in subtidal and peritidal cycles (thickness ranging from a few decimetres to a few metres), which are often associated to intertidal-supratidal structures, such as pisoids. The stromatolitic beds are more common and generally thicker and bedding is thinner with respect to the underlying unit (middle lithozone). The top of this lithozone corresponds to the top of the Esino Limestone and is marked by a regressive unit with evidence of prolonged subaerial exposures (Calcare Rosso).

The transition between upper lithozone and the underlying middle lithozone and is gradual. In the area of nucleation of the Ladinian platform, the Esino Limestone is characterized by the presence of all the three lithozones (lower, platform inception stage, and middle and upper, platform growth stage), which laterally evolve to coeval basinal facies, where different types of basinal sediments (from the Calcare di Prezzo to the Buchenstein Formation, Wengen Formation and Pratotondo or Perledo Varenna Limestone) were deposited in different time intervals.

The inner platform facies become massive close to the reef area (Fig. 1.5), where deposition of a large belt (several tens of meters in lateral width) of thick-bedded, bioclastic rudstone to floatstone with crinoids, bivalves and brachiopod occurred. These facies define the belt of higher-energy deposits close to the reef belt. This change in aspect and composition is ascribed to the increased energy of the environment (i.e. effect of storms, tidal channels) and to the bioclastic contribution of the peri-recifal zone. This high-energy deposits are characterised, close to the reef facies of the southern margin of the platform (Val Parina), by the presence of lenses of bioclastic limestones rich in open sea biota (ammonoids and pelagic bivalves) and different brachiopods, which allowed for a good dating of the succession (Jadoul et a., 1992; Fantini

Sestini, 1994; Torti & Angiolini, 1997). Biostratigraphic data indicate that the deposition of the Esino Limestone occurred between late Anisian and, at least, Late Ladinian above the inception area, whereas it is possible that the progradation of the Brembana platform lasted until early Carnian, as demonstrated by Balini et al (2000) for the Esino Limestone to the East (Lozio Basin).

The cyclic organization of the inner platform facies in the middle and upper lithozones is different. The inner platform facies are invariantly organized in shallowing upward cycles characterized by a subtidal lower part capped by stromatolitic bindstones with a fenestral fabric, but the average thickness of the cycles decreases from the lower part (aggrading stage, middle Lithozone) to the upper part (prograding stage, upper Lithozone), from about 1 m to about 30 cm. The reduction of the cycle thickness from the middle to the upper lithozone suggests a gradually decreasing accommodation from the beginning to the end of the deposition of the Esino Limestone.

b1) Massive reefal limestones

The inner platform facies are bordered by a reef belt consisting of massive light-gray limestones. The reef facies (lithozones 3 and 5 of Jadoul et al., 1992) are mainly characterized by massive limestones and patch reefs with metre-size coral framestone with calcisponges and intrabiolcastic packstone associated with *Tubiphytes* and plurimetric microbial mounds (Fig. 1.5). *Tubiphytes* and microbial mounds also colonize the upper part of the slope. The margin and perirecifal area are characterized by a pervasive network of cavities (decimetric to metric) partially or completely filled with isopacous grey to dark gray fibrous early-diagenetic cements (evinosponge; Jadoul & Frisia, 1988; Frisia-Bruni et al., 1989).

These facies are well-exposed on the southern margin of Brembana platform (Fig.1.6-1.7), whereas toward the north the outcrop conditions do not allow a detailed description of the reef associations (only coral and *Tubiphytes*-bearing limestone are observed; Fig.1.5). On the contrary, the transition from reef-upper slope to slope is preserved only in the northern margin.

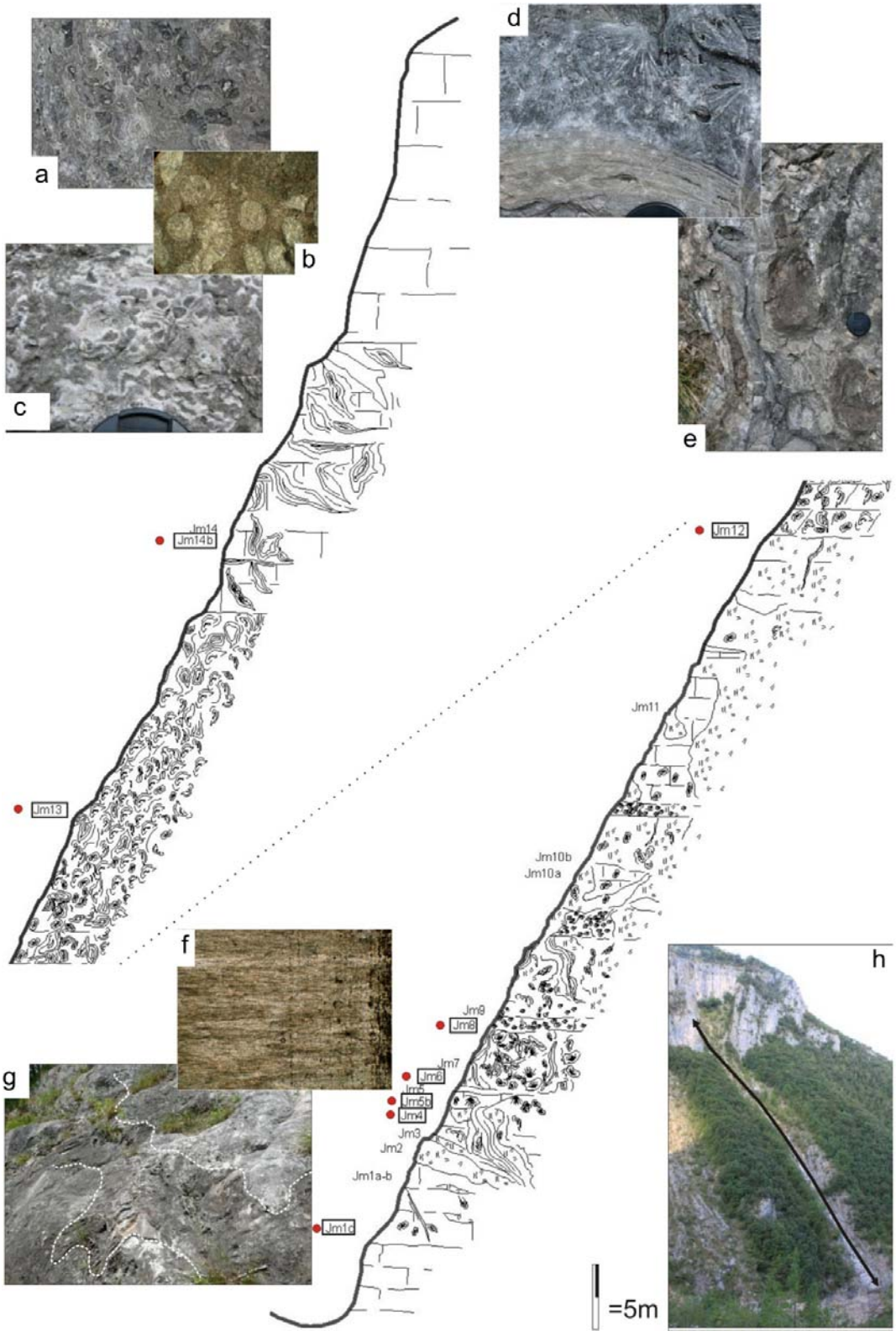

Fig1.6: *Val Secca section log.* ***a, c-*** *Biocostructions typical of the Upper slope of the Esino Limestone;* ***b-*** *photomicrograph of a framestone with recrystallized tubes of Problematica organisms;* ***d, e-*** *details of evinosponge-like structures, notice in d the sharp boundary between the laminated envelops of evinosponge and raggioni cements;* ***f-*** *photomicrograph of recrystallized crusts of an evinospongia;* ***g-*** *dolomitized fracture bordered by evinosponge-like crusts;* ***h-*** *trace of the section.*

From field evidence, the geometry and facies associations of the northern margin differ from those of the southern margin, probably for the different orientation with respect to the dominant wind/currents.

The southern margin (Fig.1.6), more aggradational, is characterized by a wide reef-upper slope area stabilized by microbial mounds (Fig 1.7 a), Problematica, calcisponge and *Tubiphytes* (Fig 1.7 b, d, f). Coral patch reefs are poorly represented. The transition between slope and basin is not preserved, but the transition to the slope is probably gradual, before a slope break located in the upper slope. The reef belt occupies a zone about 600 m wide and about 150-200 m thick. The size of the reef area on the southern margin probably reflects the aggratation and progradation of the reef belt.

The low-angle geometry of the upper slope to platform transition prevents the identification of a well defined reef, but a narrow belt with a high concentration of biocostructors can be recognized. The corals are poorly represented also in this area, and they represent a small part of the total reef volume.

Upper slope is characterized by plurimetric microbial mounds about 5 m high, which have flanks up to 20° steep. They are formed by elongated cavities with stromatactis fabric (Fig 1.7 c,e) occurring in patchy distribution or (often) as layers alternating with limestones, prevailing consisting of micrite (Fig 1.7 b, c). The stromatactis type cavities are filled by several generations of isopachous calcite cement, blocky calcite and late Fe-rich dolomite. Isopachous cement consist of cloudy or turbid fibrous (to bladed) crystals a few millimeter long. The borders of the cavities are characterized by dark, irregular micritic or biogenic (encrusting microbial organism) millimetric (up to 1-1.5 cm) crusts (Fig 1.7 b). The outer part of laminated biogenic encrustations are locally eroded and voids are filled by micrite. The limit with the host rock not well-defined. Between the mounds, Evinospongia-like (Jadoul & Frisia, 1988) cavities, up to 70 cm in size, can be observed. At the nucleous of these structures internal sediments with ostracods are locally preserved and testify the connection between reef cavities and the interface water/sediment.

The original depositional macro- and micro-facies and early diagenetical textures of upper slope rocks are often altered or destroyed by recrystallization acting during burial diagenesis

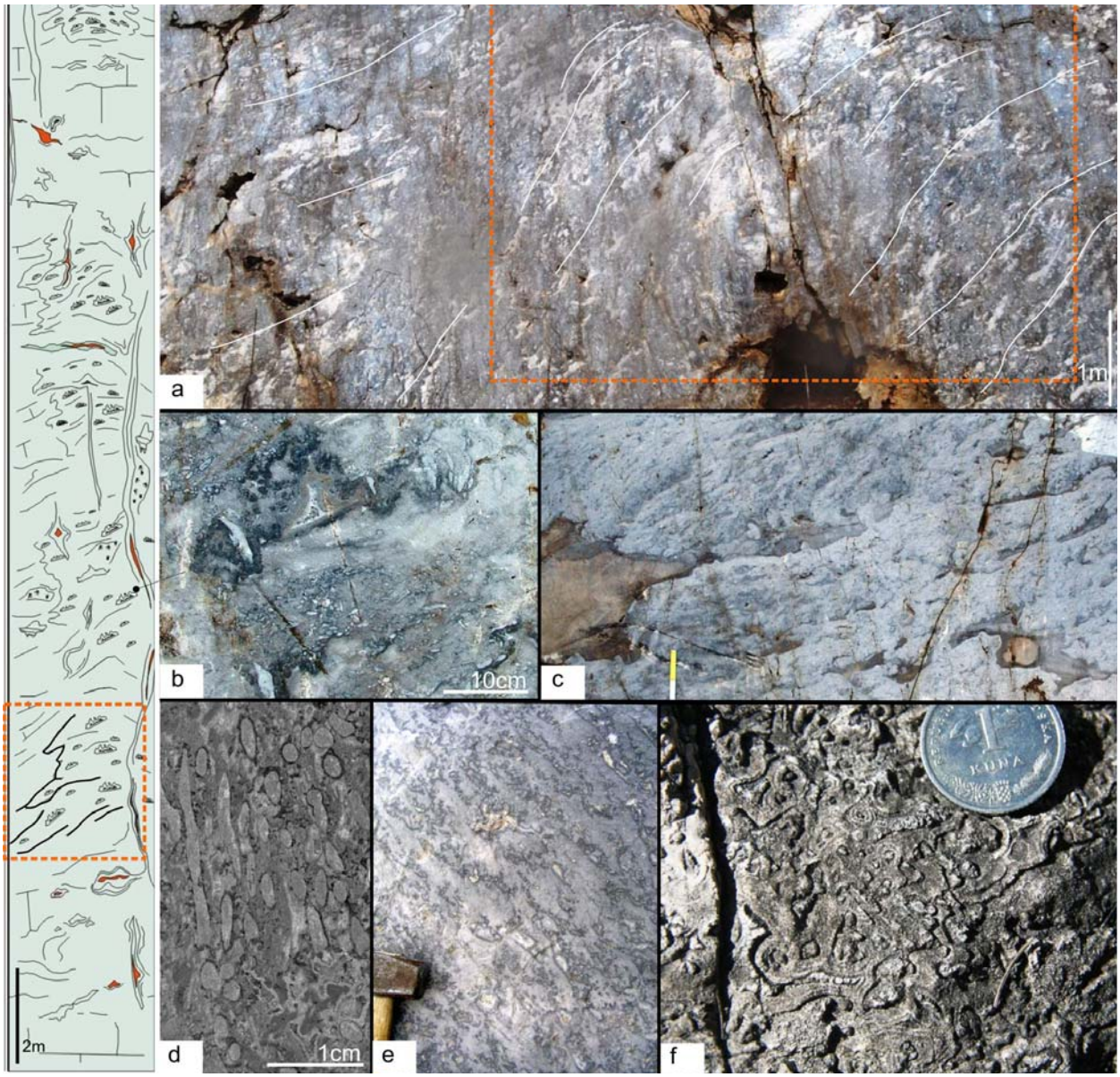

***Fig.1.7**: **a**- Overview of geometries microbial mounds characterizing the reef-upper slope domain of the southern margin; **b**- Small serpulids patch reef associated to stromatactis type cavity with biogenic envelops at the border and filled by fibrous calcite cement and late Fe dolomite; **c**- Microbial structure consists of Stromatactis type cavities aligned in layers wich alternate with limestones consisting prevailing by micrite. In the upper part prograding geometries of mound. Fig. a, b, c refers to Strada Gamba log (in the left of the figure). **d**-serpulids framestone; **e**- alignement of stromatactis type cavities stabilizing micritic sediment; f- reef facies made of microbial, Macrotubus, serpulids encrustations and early cements. Volume of micritic sediment is lower than volume of biogenic crusts and cements.*

Microbial contribute, rapid cementation (controlled by microbial activity) as well as assistance of encrusting organisms (Serpulids) are essential in the formation of these mounds: early lithification of framestones and microbialitic boundstones contributes greatly to stabilize a non-skeletal micritic sediment.

The original porosity of the reef facies was very high (up to 45%) as documented by the abundance of cements in the intergranular porosity. Cementation was an early-diagenetic event, as documented both by cathodoluminescence analyses and stable isotope geochemistry. The reef belt is generally a few metres wide and both the boundaries with the inner platform and slope facies are rapid.

The trajectory of the narrow reef belt is clearly highlighted by the rapid transition from the bedded inner platform facies to the massive, clinostratrified slope breccias, which build most of the prograding platform. The reef trajectory (Fig. 1.2) describes two different stages: a first stage where aggradation and progradation are roughly balanced (aggradation/progradation ratio ≈ 1) and a second stage where progradation prevails (aggradation/progradation ratio << 1). Due to this stratigraphic balance between accommodation space and carbonate production, the reef belt builds a narrow climbing belt during the deposition of the middle lithozone, whereas it develops as a time-transgressive, low-angle to sub-horizontal lithozone which marks the toplap surfaces of the slope clinoforms during the deposition of the upper lithozone.

b2) Massive bioclastic margin

During the late growth stage of the Esino Limestone, a rapid progradation toward the surrounding basins, with hight-angle clinostratified bodies of breccias, occurred. Similar progradation are registred also toward narrow and shallow intraplatform basins (Fig. 1.8 a, b) developed from the lower Ladinian.

In the Baita Muffi area (Middle Brembana Valley) a powerful basinal succession overlaying the Lumachella di Ghenia bioclastic deposits is preserved. This succession bears evidence of low bathymetry and high sedimentation rates. The evolution of the basin can be observed until the progradation of the Esino Limestone sutures it (Fig. 1.8 a).

***Fig.1.8**: **a**-Panoramic view of the intraplatform basin of Baita Muffi with highlined progradational clinoforms complex; and of **b**- relationship with inner platform domain (Mt. Menna); **c**-Upper part of the clinoforms with massive, high angle, reefall facies; **d**-tuffaceous layers intercalated to volcanic sands characterizing upper part of filling-basin succession.*

Mixed, well bedded, sedimentary succession (Fig. 1.8 d) filling intraplatform basin consists of intraclastic peloidal packstone, rarely bioclastic (mainly bivalves) intercalate with wackstone (often with black chert nodules) and laminated fine-grained packstone-mudstone (microsparite).

Rare lithoclasts in matrix-supported floatstone\rudstone (debris flows) can be observed. Alterated tufaceous silty shales (up to 1.5m thick) and volcanoclastic litharenites are also locally associated to carbonates.

***Fig1.9. a**- Bioclastic rudstone with packed, often articulated bivalvs (mainly) showing shelter porosity; **b**- Encrusting organisms and white envelops of fibrous radial calcite bound the bivalves*

The progradation above this succession is very rapid with sigmoidal clinostratified bodies, 30-40 m thick and about 30° steep up in the upper part (Fig 1.8 a, c).

The transition between inner platform facies and slope facies is sharp and takes place in a few tens of meters. Inside the transition between inner platform facies and slope facies, three sub-facies associations can be recognized, depending on the proximity to the platform.

- Sub-facies 1: Prevalence of detrital fragments of bivalves floating into fine grained carbonate. Pseudo-cyclic organization of the bioclastic layers can be locally observed. The bioclasts in these layers can be more or less densely packed. Moving toward the basin, the the bioclastic fraction decreases.

- Sub-facies 2: Narrow (few meters extension) deposit consisting of massive bioclastic (mainly bivalves) rudstone, in levels up to 70-110 cm thick. The valves are packed, often articulated and homogeneous in size (ranging between 0.8 and 5-6 cm) (Fig. 1.9). Encrusting organisms and envelops of fibrous radial calcite bound the bivalves. Orientation of the bioclasts generates shelter porosity.

- Sub-facies 3: Poorly bedded bioclastic deposits (40-60 cm thick) showing either clast or matrix support. Bioclasts consist of green dasycladacean algae, small gastropods and prevailing bivalves. The valves are often isooriented within a single layer.

c) Slope breccias

The narrow reef belt is bordered basinward by slope deposits, represented by a monotonous succession of massive to crudely bedded, clinostratified, clast-supported breccia deposits (Fig. 1.5). The maximum size of clasts often exceeds two metres and the average size is centimetric to decimetric. Cavities between the clasts are filled by fibrous cements, documenting the scarcity of fine-grained sediments. When the cavities are not completely filled by cements, laminated internal sediments are present. The presence of ostracods in these laminated internal sediments indicates the early (syndepositional) origin of the cement precipitation in marine waters and the connection of these cavities with the sea-floor. These data support the importance of the early marine carbonate cementation along the submerged slope, as observed in other platforms of the geological record (e.g. Van Der Kooij et al., 2010). Only in the deeper part of the slopes, where the size of the clasts decreases, fine-grained sediment locally fills the intergranular space.

Cavities partially or totally filled by isopacous and botryoidal cements (evinosponge: Jadoul & Frisia, 1988; Frisia-Bruni et al., 1989) are larger and more common in the upper slope. In the studied successions clasts are polygenic and they generally derive from reef-upper slope facies, as documented by the common occurrence of clasts with *Tubiphytes* bafflestones and coral framestones, together with coarse bioclastic packstones (often yielding gastropods and bivalves). Microbialites and clasts consisting of automicrite are also present, suggesting a contribution to the carbonate factory of the slope itself, as observed in other Ladinian platform of the Western Tethys (Keim & Schlager, 1999). Microbial layers probably testify episodes of reduced sedimentation between two events of breccia deposition. The grain size of the breccias decreases from the upper slope to the toe of the slope and locally it is possible to observe a crude fining upward trend within a single clinostratified depositional event. The source material was devoid of fine-grained sediments, as documented by the clast-supported fabric and by the rapid pinch out of the breccias bodies at the toe of the slope. These features, along with the heterogeneous composition of the clasts, their lithofacies and the high-angle of depositional surfaces (35–40°) fit a model for their origin of accumulation of coarse, non-cohesive and (almost) mud-free sediments (Kenter, 1990; Harris, 1994) produced by falls of unstable portions of the upper slope and reef belt. Between different episodes of breccia emplacement, cm to dm thick lenses of daonellids were deposited during the aggradational stage (Fig. 1.5). These bioclastic layers are interpreted as the evidence of periods of reduced sedimentation on the slope between two events of breccia deposition.

d) Basinal facies

The transition from the slope facies to the basinal succession is sharp, as the clinoforms pinches out interfingering with dark, bedded fine-grained calcarenites and mudstones that characterize the sedimentation in the open basin facing the carbonate factory. The lithological (and thus lithostratigraphical) features of the basinal facies change through time, so that the slope breccia deposits interfinger with and rest on different formations during the evolution of the carbonate system (Fig. 1.10). In the first stage the slope breccias cover the marly limestones of the Prezzo Limestone and interfinger with the cherty limestones (yielding ammonoids and rich in sponge spiculae and radiolarians) of the up to 20 m thick Buchenstein Fm. Later, the cherty basinal facies are substituted by dark, laminated, intraclastic packstone (Perledo-Varenna Fm.), which

are generally thin-bedded (average thickness around 10–20 cm, only rarely massive beds occur), and commonly show normal grading.

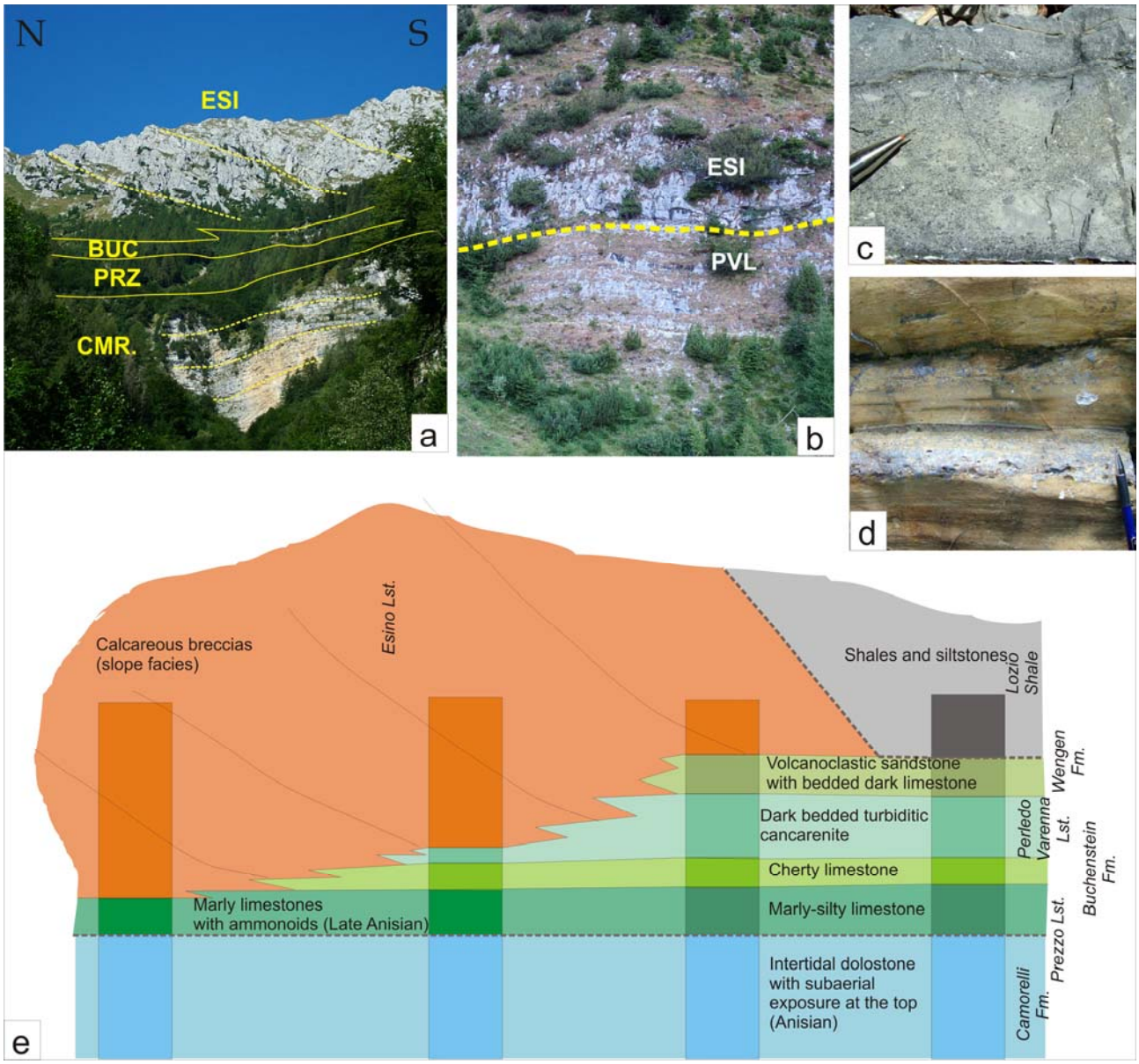

Fig. 1.10 *– Vertical and lateral distribution of the basinal facies during the different stages of the platform growth;* ***a-*** *Geometry of the transition between prograding slope breccias and basinal units, south of Monte Pegherolo;* ***b-*** *detail of the transition between the bedded basinal limestone of the Perledo-Varenna Limestone and the prograding slope breccias of the Esino Limestone, Valleve;* ***c-*** *aspect of the platform-derived resedimented limestone of the Perledo Varenna limestone;* ***d-*** *fine-grained marly siliciclastics of the Wengen Formation with lenses of calcareous rudstone.*

Composition and sedimentary structures indicate that the bedded calcareous deposits of this unit originate from resedimentation fed by the carbonate highs. Sponge spiculae and radiolarians are common in the laminated facies, which are interpreted as the evidence of intervals of reduced

sediment supply in the basin. The dark colour as well as the presence of well-preserved lamination and scarce burrowings indicates that the bottom were from anoxic to dysoxic. The carbonate deposits of the Perledo-Varenna Limestone are thicker close to the toe of the prograding slope facies, suggesting that they built a toe-of-the-slope fan which interfingered with the slope breccias. Locally, paraconglomerate beds up to a few decimetres thick are present, as well as cm-thick layers of clast supported slope breccias with centimetric clasts. Resedimented limestone beds reflects a rapid increase in carbonate delivery into the basin with respect to the underlying Buchenstein Fm., which is characterized by a reduced sedimentation rate. The increase in thickness and the facies changes in the basinal setting reflect the progradation of the carbonate platform basinward which is coupled with a higher exportation of carbonate sediments form the platform top to the basin. Locally the Perledo Varenna interfingers with or is substituted by the Wengen Formation (consisting of sandy to shaly volcanoclastic deposits alternating with thin-bedded resedimented limestones), which record the clastic input from the erosion of volcanic edifices at the border of the basin (Jadoul & Rossi, 1982).

Clastic input is clearly coeval with the progradation of the Esino Limestone, as the Wengen Formation interfingers with the slope breccias of the Esino Limestone, mainly north of the Brembana platform (Fig. 1.10).

Geometric relationships between platform and basin indicate that the evolution of the platform from a first stage of aggradation (with reduced progradation) followed by a major progradation pulse (which persisted until the demise of the Esino Limestone) is mirrored in the evolution of the basinal sedimentation. The change in depositional rates and facies assemblages of the basinal succession are interpreted as the basinal response to the changes in the lithofacies evolution on the inner platform: the stage of platform inception (lower lithofacies) and the prevailing aggradation stage (thick inner platform cycles and prevailing aggradation of the slope facies; middle lithozone of Jadoul et al., 1992) corresponds to the deposition of the low-sedimentation rates marly (Prezzo Lst.) and siliceous (Buchenstein Fm.) basinal deposits, whereas the progradation stage is recorded in the basin by prevailing resedimented limestones which reflect a higher sediment export from the platform to the basin (Fig. 1.10). The increased basinal delivery of limestone is ascribed to the decreased accommodation space for sediment storage on the platform top. The local and episodic volcanoclastic input (Wengen Fm.) probably reflects volcanic activity in the surrounding of the depositional basin.

PLATFORM DEMISE (EARLIEST CARNIAN?)

The progradational stage of the Esino Limestone came to a sudden end close to the Ladinian-Carnian boundary throughout the Lombardy Basin (Berra, 2007). The end of the Ladinian carbonate system (Esino Limestone) is recorded by different facies assemblages either on the platform top or on the slope.

a) Platform top

The platform demise is well-recorded at the top of the Esino Limestone on the south-eastern margin of the Brembana Platform.

The massive reef facies are abruptly capped by bedded peritidal-supratidal limestones along a slightly irregular surface (Fig. 1.8) with evidence of subaerial exposures and dissolution. From this erosional surface, sedimentary dykes filled with reddish and marly limestones are cut into the underlying reef facies up to 5-10 meters from this surface. Bedded peritidal-supratidal limestones above the surfaces are characterized by abundant cements and tepee structures which alternate with red marls. This dissolution surface marks the boundary between the Esino Limestone and the overlying "Calcare Rosso" deposits.

This unit reflects the changes in the carbonate production on the platform top triggered by a regressive trend at the top of the Esino Limestone (Assereto & Kendall, 1977; Assereto et al., 1977; Mutti, 1992; Berra, 2007). In the southern side of the Brembana platform (Cespedosio), facing a southern basin, the Calcare Rosso (KLR) reach maximum thickness of about 60 m. Moving to the nucleation zones of the Esino Limestone, corresponding to the inner platform domain (Fig.1.11), the 'Calcare Rosso' deposits decrease to a few meters (3-5 m). Above the bedded to massive inner platform facies (Fig.1.11 g,f,e,d) , they are characterized by both wide variety and rapid changes of facies and mainly consist of residual breccias (Fig.1.11 a) with tuffaceous levels intercalated. From the erosional surface that marks the demise of the Brembana Platform, collapsed karst structures (Fig.1.11c) are developed into the Esino Limestone up to 20 m.

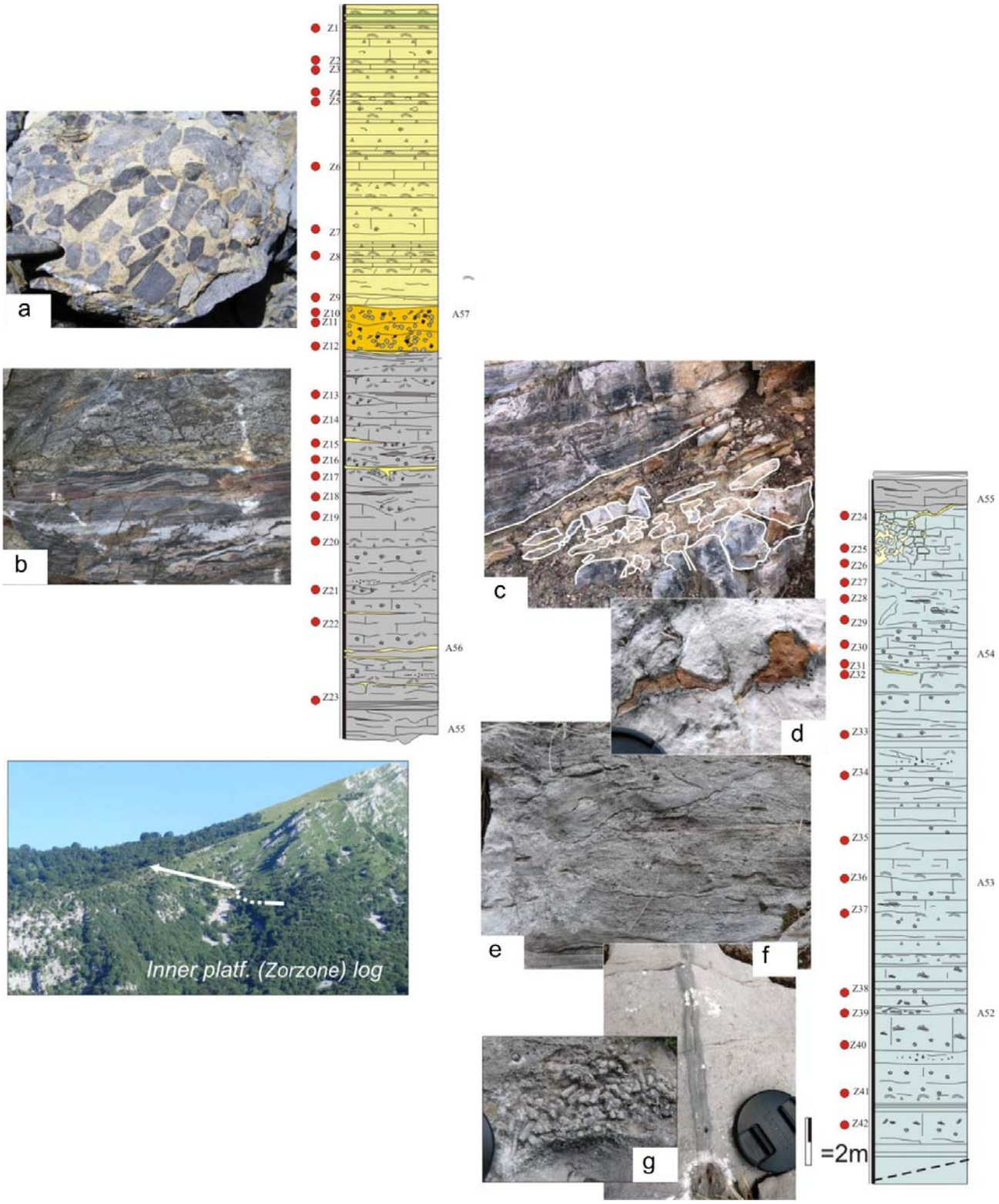

Fig. 1.11*: Platform demise and transition between inner platform facies of the Esino Limestone to Calcare Rosso (KLR) facies. In the upper part, Carnian deposits of the Breno Fm. is preserved (Zorzone log). Both photo a, b show the two mainly KLR facies in this area:* ***a****-residual breccias;* ***b****-peritidal tepee-deformed limestones, rich in cements and internal sediments (yellowish in the photo);* ***c****-collapsed-karst structures mark the subaerial exposure at the top of the Esino Limestone;* ***d****- solutional cavities (enlarging*

primary porosity) at the top of the Esino Limestone are filled by thin calcite cement rim and brown internal sediment; ***e****- sheet cracks (up to 10cm thick and 1.5 m long) filled by laminated crusts of fibrous radial calcite and internal sediment;* ***f****- fracture filled by crusts of 'coconut meat calcite';* ***g****- Green dasycladacean algae often articulated.*

Above the prograding part of the Esino Limestone (north of the Pegherolo Mt.) the boundary between the Esino Limestone and the "Calcare Rosso" is less pronounced, probably as the peritidal sediments which cover the prograding reef-slope facies are less affected by subaerial exposure.

Data from the platform top (where the toplap of the prograding slope breccias occurred) suggest that the demise of the Esino Limestone carbonate platform can be ascribed to a rapid sea-level fall, which changed the environmental conditions, thus reducing the efficiency of the carbonate factory, as observed in other coeval carbonate platforms in the Lombardy Basin (Berra, 2007).

b) **Slope and basin**

The change in sedimentation and environment on the platform top has a counterpart in the basin and along the slope. The open basinal setting is only partly preserved in the study area due to Alpine tectonics, nevertheless it is possible to follow the effect of the change along the slope (Fig. 1.10).

The slope facies, mainly represented a monotonous massive unit consisting of reef-derived, early- cemented breccias, continuously prograde for about 4 km to the north. These prograding facies interfinger with a younging basinal succession (Prezzo Limestone, Buchenstein Fm., Wengen Fm. and Perledo Varenna Limestone). The end of the progradation is marked by the onlap of shales with intercalation of siltstones (Lozio Shale), which unconformably rest on the last pulse of progradation of the Esino Limestone carbonate platform (Fig. 1.12). Between the Lozio Shale and the typical slope breccias of the Esino Limestone it is possible to observe the presence of a thin (up to 3 m thick) drape of dark, microbial limestone which are preserved from the middle slope toward the basin, whereas they are not present on the upper part of the slope. The deposition of this thin unit can be interpreted as the effect of the switch-off of the carbonate productivity on the subaerially-exposed platform top. The absence of this unit on the upper part of the slope probably reflects a bypass of the sediments on the upper (and steeper) part of the slope as well as the ceased production of slope breccias.

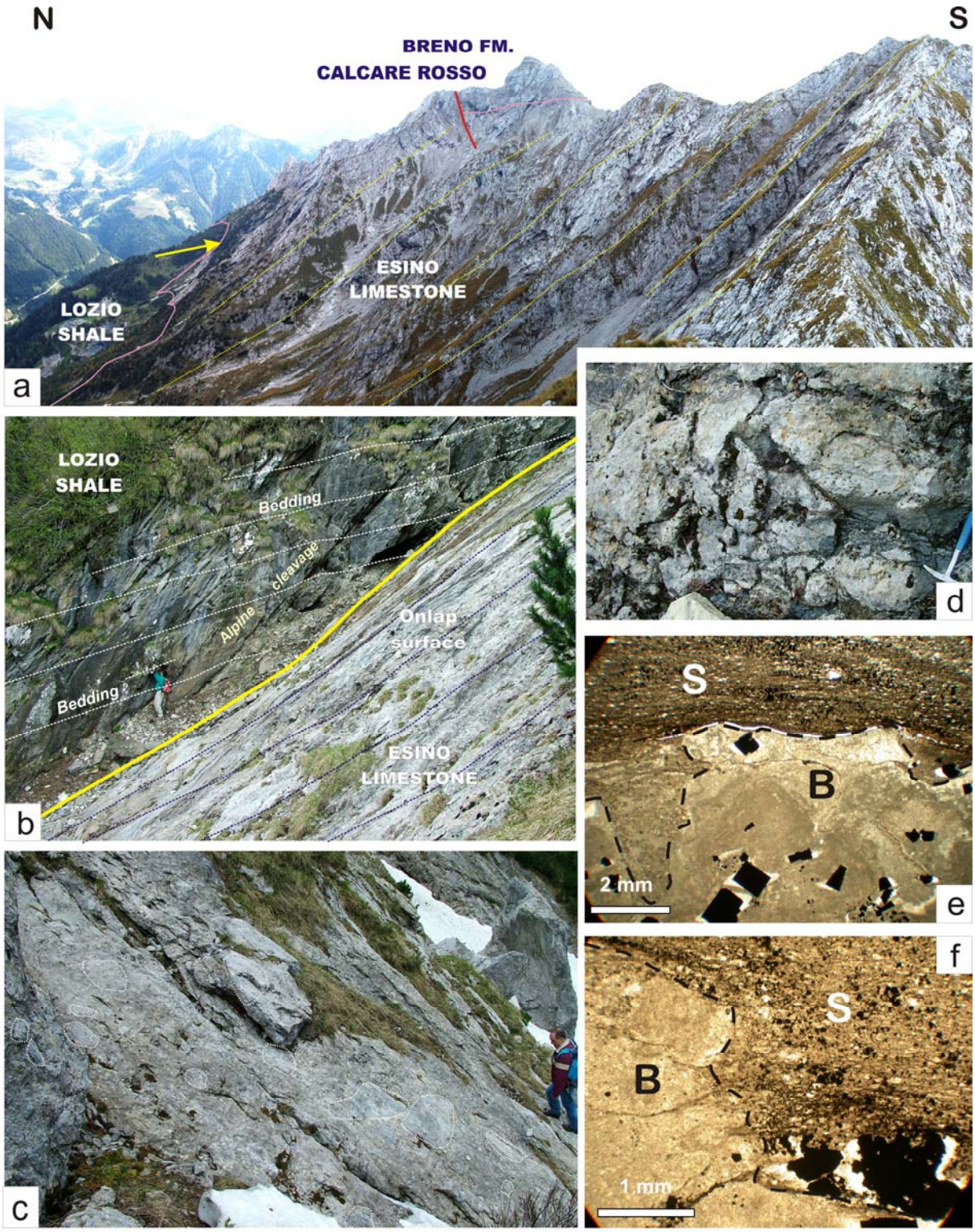

Fig. 1.12 *– Facies association reflecting the demise of the carbonate platform of the Esino Limestone along the slope.* ***a-*** *view of the northern slope of the Esino Limestone: note the clinostratified slope and the flat-lying younger units (Breno Formation, Early Carnian) on the former platform top of the Esino Limestone. The arrow points to the position of fib (b);* ***b-*** *detail of the onlap surface represented by the last clinostratified breccias of the slope of the Esino Limestone;* ***c-*** *distribution of breccia boulders on the onlap surface;* ***d-*** *detail of the onlap surface: note the shale that fills the intergranular voids between the*

unsorted breccia boulders at the top of the Esino Limestone; ***e, f****- microphotographs of the contact between the calcareous breccia boulders (B, Esino Limestone) and the shales (S, Lozio Shale). Note the abundant pyrite.*

The onlap surface is well exposed at different paleodepth, determined on account of the position of the toplap surface of the prograding wedge: about 350-400 m at the Valleve Quarry and 250-300 m at Mt. Cavallo. Geometric constraints allow the confident evaluation of the shelf to basin relief at the end of the progradation of the carbonate platform, which is about 450-550 meters. The final progradation of slope breccias is built by clast-supported breccias up to 1 m in size, which are directly onlapped by shales, which mantle the irregular top surface of the slope breccias. The present-day angle between the platform slope and the shales is about 25°: considering that the shale were deposited roughly horizontally and that, after deposition, the shales experienced a higher compaction with respect to slope breccias, it is possible to reconstruct an original angle around 30-35° between the originally horizontal shales and the carbonate slope (Fig. 1.12 b). This angle is compatible with the obtained dip of about 35° for the slope as deduced from geometric constraints. The contact between the breccia clasts and the shales (Fig. 1.12) is sharp and marked by pyrite, Fe-rich crust and hard-grounds, which supports the existence of a significant hiatus on the onlap surface.

The onlapping shales do not contains clasts of the slope facies of the Esino Limestone, suggesting that the process of breccia production ended (or at least decreased abruptly) before the onlap of the Lozio Shale). Burrowing in the Lozio Shale is generally reduced, pointing to dysoxic conditions. The rare occurrence of ripple marks in this unit a few hundreds of meters from the onlap surfaces supports the existence of bottom currents, as the reconstructed paleo-waterdepth for these structures is about 200-250 m, deeper than the expected storm-weather wave base. Carbonate sedimentation during the deposition of the Lozio Shale is extremely reduced and consists of dark mudstone lenses embedded in the Lozio Shale, thus recording the presence of a less-efficient and partly different carbonate factory, which exported a reduced amount of carbonates during the deposition of the Lozio Shale. Nevertheless, the composition and texture of these limestone highly support a change in the nature of the carbonate factory postdating the end/change of the processes which controlled the progradation of the Esino Limestone. The presence of quartz-rich siltstones suggests the erosion of a distal continental basement, supporting the possible origin from the European continent of the clastic material delivered in the northern part of the Lombardy Basin, as suggested by Berra & Jadoul (2002). Toward the south, the deposition of the Lozio Shale did not occur, as the carbonate highs

probably prevented the delivery of shales toward the south. Here, the clastic input during the Carnian is dominated by volcanoclastic deposits (Val Sabbia Sandstone) which were fed from south by the Southern Mobile Belt of Brusca et al. (1977).

RECOVERY OF THE VOLCANIC ACTIVITY

The Triassic volcanic activity in the Lombardy basin began in the Late Anisian-early Ladinian and continue until Lower Carnian (225Ma, Crisci et al. 1982; Jadoul & Rossi, 1982). It's characterized by several piroclastic horizons intercalated in the Buchestein Fm., Perledo Varenna Fm. (Grigne area, Pasquarè & Rossi, 1969), Esino Limestone and Breno Fm.

In the Brescian Prealps the Ladinian activity consists of the voluminous magmatism of Mt. Guglielmo, corresponding to the polyphase but substantially unitary explosive event with widely dominant pyroclastic deposits in association with abundant breccias and tuffs, without a regular horizontal distribution. Between Camonica and Trompia valley, several sub-vulcanic rock bodies so-called 'Montecampione group'(Corazzato et al. 2001) occurs. They consist both of sills (always apophyses of major bodies) and small laccoliths emplaced at different stratigraphic levels within lowermost part of Triassic sedimentary record. Mineralogical, petrographical and chemical data show variable changes and sometimes contrasting features that are difficult to interpret, from calc-alkaline to alkaline seriality and from acid to basic composition.

The radiometric dating (Rb-Sr, whole rock and biotite) of two sub-volcanic units (respectively M. Muffetto: 231±5 Ma and Dosso Sparviero: 226±4 Ma; Cassinis & Zezza, 1982), the detailed petrographical and geochemical analyses, as well as a tentative stratigraphical reconstruction allow to ascribe these igneous products to undefined Middle-Late Triassic times.

In the studied area, the second important Triassic volcanic event is registered close to the Ladinian-Carnian boundary (Jadoul & Rossi, 1982) and continue during the Carnian time.

Tuffaceous levels are interstratified at different stratigraphic position: in the Esino Limestone (Vachèe, 1966), Calcare Rosso, Calcare Metallifero (Assereto et al. 1977), and in the lower part of both Gorno Fm. and Arenaria di Val Sabbia. In addiction, in the Seriana Valley at the Mt. Alino, a mixed succession of volcanic to carbonate breccias, matrix to clasts-supported, with intercalated laminated grained silts, outcrops. This volcanoclastic unit was deposited above upper slope facies of the Esino Limestone and is capped by residual breccias of the Calcare Rosso. Therefore, the stratigraphic position confirms a Late Ladinian/Early Carnian age and the

facies analysis the proximity of the volcanic center to the southeastern areas of the Esino Limestone. Also the volcanic litharenites of the Arenaria di Val Sabbia are clearly connected with the erosion of the products of both a coeval (presumably early Carnian, Garzanti, 1985; Cassinis et al. 2008) igneous rocks and earlier volcanic edifices located southwards (probably along the so-called «Southern Mobile Belt» of Brusca et al., 1982), testified by the presence of Ladinian andesite clastics (Cassinis et al. 2008).

PLATFORM REBIRTH (EARLY CARNIAN)

The exposure of the platform top, marked by a reduction in the efficiency of the carbonate factory, is followed by a gradual reprise of the carbonate production. The physiographic setting of the basin has changed and the shalf to basin relief is reduced, due to the deposition of the Lozio Shale, which fills the intraplatform basins.

The filling of the basin is related to the increase of the sedimentation rate. The creation of accommodation space on the platform top and the reprise of carbonate production is recorded by the deposition of cyclic peritidal limestone (Breno Formation), whereas a gradual increase of carbonates in the Lozio Shale can be envisaged in the basin, mainly close to the former slopes of the Esino Limestone (Fig.1.13).

a) Platform top

After the subaerial exposure of the platform top and the deposition of the different facies of the Calcare Rosso, a reprise of the carbonate production is recorded by the deposition, on the flat top of the Esino Limestone, of up to 70 m of cyclic peritidal limestone (Breno Limestone). In the Brembana platform the thickness of the Breno Fm. is roughly constant, whereas on larger platforms the thickness generally increases (as it happens for the underlying Calcare Rosso) from the inner part of the platform toward the prograding facies of the Esino Limestone.

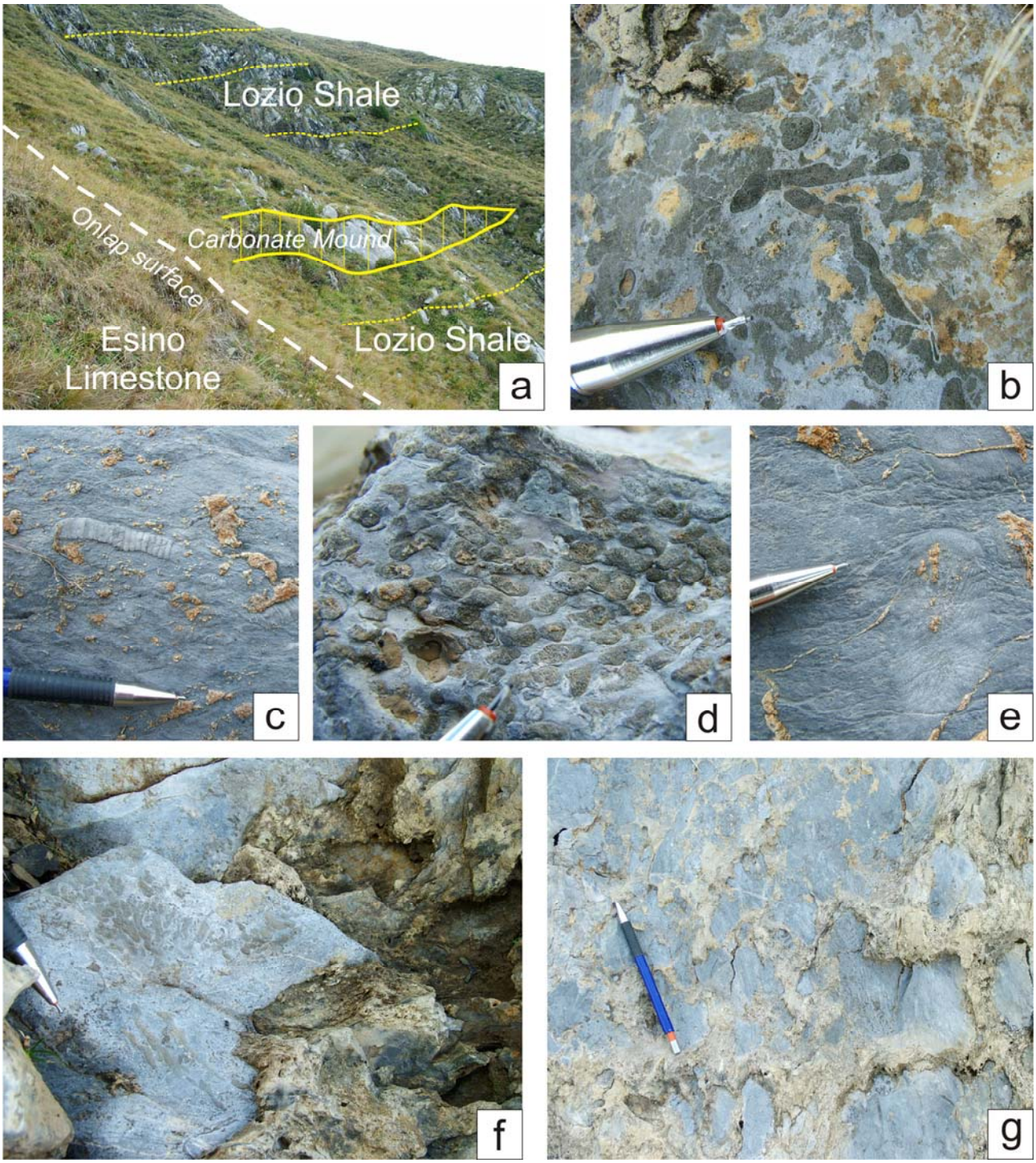

Fig. 1.13 *– Facies reflecting the "rebirth" of the carbonate factory close to Monte Cavallo:* ***a-*** *view of the onlap of the Lozio Shale on the slope of the Esino Limestone, with the intercalation of a meter-thick carbonate mound which pinches out in the shales;* ***b-*** *calcisponge in the carbonate mound; c- crinoids ossicles;* ***d-*** *coral colony;* ***e-*** *large solitary coral;* ***f, g-*** *muddy breccias with shaly matrix lateral to the carbonate mound. Note the different composition with respect to the slope breccias of the Esino Limestone and the presence of the muddy matrix.*

Peritidal cycles are characterized by a prevailing intertidal-supratidal part, which is much more developed in the Breno Limestone than in the Esino Limestone. This cyclicity suggests that sedimentation rates overpass the creation of accommodation space. A general drowning of the Breno Limestone is recorded by the transition to subtidal facies with marly intercalations of the overlying Calcare Metallifero Bergamasco which gradually evolves in the Gorno Formation (Assereto et al, 1977).

b) **Slope**

Carbonate sedimentation on the slope is recorded by the presence of the fine-grained muddy limestone beds which intercalate with dark shales on the lower slope (Fig. 1.13).

In the middle-upper slope the first evidence of in-situ carbonate production is recorded by meter-thick carbonate mounds alternating and interfingering with dark shales. These low-relief mounds reach a few tens of meters in width and 0.5 to 3 m in height. Lithologically, they consist of fine-grained limestones (mainly wackestone) containing calcisponges, gastropods, crinoids, corals (both isolated and colonial) and problematica. The mounds generally grow close to the slope of the Esino Limestone and pinches out in the shales that onlap the slope. Laterally to the mounds, intraformational breccias with mud clasts derived from the mounds and abundant muddy matrix are present. Transport and selection of the clasts is reduced and the low-relief mounds laterally pass to mound-derived breccias.

Chapter 2

DEPOSITS AND PROCESSES RELATED TO THE SUBAERIAL EXPOSURE OF THE ESINO LIMESTONE: CALCARE ROSSO (*KLR*) AND ASSOCIATED FACIES

A comprehensive description of regressive deposits related to subaerial exposure of the top of the Esino Limestone is complex as they are the final outcome of precarious balance (and complex interaction) of different depositional, erosional and diagenetical processes varying in time and space.

In this chapter an overview of a wide variety of both **a)** macro/microfacies of these deposits and **b)** effects on the underlying platform due to the subaerial exposure at the top of the Esino Limestone are provided.

a) Marine deposits are organized in 1) *peritidal cycles,* 2) *lagoonal/pond environments* and are capped or laterally replaced by paleosols or 3) *residual breccias*. The peritidal limestones show both thicker and more continuous sedimentary record characterized by marine deposition and superimposed subaerial exposure effects. Deformation degree and abundance of Terra Rossa material and, in addiction, internal sediments are the mainly features for distinguish Typical red peritidal facies (Tred) and Typical grey peritidal facies (Tgrey) of Calcare Rosso.

In literature Calcare Rosso (KLR) has been used as synonymous of Typical red peritidal facies (Tred). In this chapter Calcare Rosso is meant as group of the regressive facies at the top of the Esino Limestone.

b) The Calcare Rosso (KLR) succession records several discontinuity surfaces starting with the main one which separate the KLR from the underlying Esino Limestone. In correspondence with these surfaces, evidences of subaerial exposure and changes to depositional characteristics of the host rock can be recognized. Hiatus, early diagenetic modification and deformation are the most common occurrences. Both the deposits of the top of the Esino Limestone and of the KLR succession are affected by epi- and endo-karsic processes.

2.1

DEPOSITS AND PROCESSES ASSOCIATED WITH THE CALCARE ROSSO EVENT

Karst features on carbonate platforms

The subaerial exposure of flat-topped carbonate platform are likely to develop karst over a broad area and through a significant thickness (Mylroie 2005) depending on the entity of the sea level fall. Karst development is a very rapid geological process but paleokarst (Wright & Smart, 1994) is not common in the geological record due to its vulnerability to subsequent erosion and alteration.

Karst systems affecting carbonate rock present a pronounced lateral and vertical spatial complexity that results from a complex history of formation. Most of the known karst systems are epigenetic and they are the result of near-surface karst processes during periods of subaerial exposure and followed burial compaction and diagenesis (Pomar & Ardila, 2000).

Scale, morphology and spatial complexities of these karst systems on carbonate islands depend on many factors: carbonate rock solubility, preexistent morphology, hydrogeology (recharge), paleoclimatic conditions, lowering of base level (either by tectonic uplift or sea-level fall) and duration of subaerial exposure. Tectonic uplift, in addition, commonly induces fracturing and faulting that further control karst development.

On emergent carbonate platforms meteoric precipitation falls directly onto the carbonate land surface, and enters the subsurface vadose zone. Such input is known as **autogenic** recharge (Mylroie, 1984). The meteoric water, slightly acidic from incorporation of atmospheric CO_2, gains more dissolutional potential by addition of soil CO_2. Much of this dissolution potential is expended rapidly by interaction with the exposed carbonate rocks and, as a result, water enters the subsurface with significantly diminished dissolution capability. On the scale of hundreds of meters, water infiltration is relatively uniform over the exposed outcrop as diffuse input (Mylroie, 1984). Exceptions occur where carbonate platforms are on a continental margin, or on an island with significant outcrops of insoluble rocks: meteoric water collects in streams flowing onto the carbonates. In these cases the input is **allogenic**, because the water enters the limestone in appreciable volumes at point locations, and its dissolutional potential persists to significant depths in the limestone. Such allogenic inputs are restricted to the contact of the carbonates and

insoluble rocks; within the bulk of the carbonate outcrop, autogenic recharge, and the effects of that recharge, dominate.

Carbonate platforms that receive only autogenic recharge may appear to be a special case, but many areas in the world, both today and during the Pleistocene, fit this case. The Bahamas are the most notable example. With only regionally diffuse meteoric input, macroscopic karstic porosity and cave permeability occurs in three basic areas corresponding to major hydrological environments of the carbonate islands: the surface (epikarst), the vadose zone and the fresh-water lens in the phreatic zone. The boundary between the freshwater lens and the underlying saline groundwater may be a sharp halocline or a broad region of changing salinity called a mixing zone.

Shape and thickness of a fresh water lens are controlled primarily by recharge and annual water budget but also by lithology. In particular, low annual water budget (dry climate) as well as carbonate with high initial permeability (coarse) correspond to thick fresh water lens; conversely, high annual water budget (humid climate) as well as carbonate with low initial permeability (micritic) correspond to thick fresh water lens because lens will discharge slowly, thereby causing the water to "pile up".

Maximum dissolution occurs at the discharging margin of the freshwater lens (where vadose water mixes with the fresh to brackish groundwater lens, Fig. 2.1) due to the close juxta-position of the top of the groundwater lens, and at the base of the lens (where fresh to brackish groundwater mixes with underlying seawater) (Mylroie, 1984).

Recent study (Schwabe et al., 2008) propose an alternative model questioning the low dissolutional potential of the meteoric waters in the subsurface: the dissolutional capability is enhanced or maintained because the descending meteoric water accumulates microbially-generated CO_2 that is produced by heterotrophic bacteria residing in the pores of the host rock. In addition, bacteria in the fresh, mixed, and marine groundwater also contribute CO_2 and produce other organically generated acids that contribute to the dissolution of carbonate rocks (Schwabe et al., 2008). The end-product of carbon metabolism by these microbes produces PCO_2 levels of at least 3 to 4 times atmospheric concentration.

Therefore the resulting microbially-maintained acidic pH at these boundaries is responsible for the greater limestone dissolution that seems to have occurred at and around sea level (*sensu* Mylroie & Carew, 1988), rather than the actual physical mixing of different water masses.

The amount of emergence of carbonate terrains, and the rate at which this emergence occurs, interacts with climate and lithology to place karstic porosity and permeability, especially that developed within the fresh-water lens (Fig. 2.1), at a variety of locations within the carbonate section, but if subaerial erosion is significant it can remove all evidence of the caves, obscuring the important role of cave formation (Palmer, 1991; Mylroie & Carew, 1995). Because macroscopic dissolutional voids that are meters to tens of meters in size can form in as few as tens of thousands of years, even minor variations in the rate of sea level change can greatly affect the size and location of the caves (Mylroie, 2008).

If the emergence is slight, then the water table is just below the surface, and the epikarst communicates directly with the phreatic zone (Mylroie & Carew, 1995). The surface ecosystem has ample water supply and significant biological productivity, which results in high soil CO_2 that drives karst processes in the epikarst and vadose zone. Interior water bodies are likely to occur if topographic depressions intersect the top of the lens. If the climate is humid, these lakes will recharge the aquifer, and the water-filled depressions will enlarge by dissolution. If the climate is arid, the lakes will experience excessive evaporation and the underlying marine groundwater will be upconed, thereby partitioning the freshwater lens and this mixing of meteoric water with saline water in the epikarst results in an extremely jagged and fretted rock surface ("moonrock", Davis & Johnson, 1989).

If the platform is significantly emergent, then the epikarst is separated from the freshwater lens by a substantial vadose zone; the topographic depressions do not penetrate down to the top of the lens, and the epikarst is dominated by meteoric karst forms; and the surface ecology is diminished with consequent lower organic productivity and lesser amounts of karst (Mylroie & Carew, 1995).

Therefore, slight emergence will produce a better developed epikarst than significant emergence. Additionally, slight emergence will tend to superimpose the epikarst onto the dissolutional zone that occurs where vadose and phreatic waters mix at the top of the water table. In the rock record, the proximity of these dissolutional environments may lead to important permeability (J.E.Mylroie & J.R.Mylroie, 2003).When the platform is significantly emergent, two permeability zones develop with respect to the vadose zone: one at the surface epikarst and one at the top of the freshwater lens. Neither horizon is likely to be as permeable as the composite one developed when emergence is slight (Mylroie & Carew, 1995).

If a carbonate platform experiences slow, steady emergence through time, initially the freshwater lens will be a shallow lens (i.e. the epikarst will be in contact with the freshwater lens). If the emergence rate exceeds the denudation rate, then the epikarst will lose contact with the freshwater lens, and the vadose zone will enlarge with time. The mixing zone and its dissolutional effects will migrate downward through the carbonate platform (Mylroie & Carew, 1995).

If the rate of emergence is slow and does not exceed the karst denudation rate, the landscape will be lowered as well, and the platform will maintain a shallow lens configuration with the epikarst in contact with the freshwater lens (Mylroie & Carew, 1995). Because the denudation rate is controlled by climate, variations in climate could fortuitously combine with a variety of platform emergence rates to produce the same end result.

A steady, continual, and rapid emergence will result in a development of both phreatic and vadose dissolutional permeability through a large section the platform thickness, resulting in a relatively uniform but low level of porosity and permeability production (Mylroie & Carew, 1995). Slow, stillstand emergence will concentrate attendant effects of the mixing zone (physical mixing, organic carbon oxidation, and sulfur oxidation/reduction processes) on specific horizon approximating the elevation of the sea level stillstand. Not only is the rate of sea level change, but reversals in the direction of sea level change have a significant impact. The sea level fluctuations repeatedly subject the carbonate rocks of the platform to a variety of subaerial, vadose, freshwater phreatic, mixing zone, and marine phreatic conditions. The overprinting of the rock with multiple karst and diagenetic features from these fluctuations introduce a bewildering variety and complexity into the rock record. These complexities can be very difficult to resolve after millions of years (Mylroie, 2008).

Through time, emergent carbonate platforms may develop karst features faster than other diagenetic processes can alter the carbonate rock (Mylroie, 2008).The groundwater geochemistry that develops carbonate-platform karst features is affected by atmospheric and soil CO_2, subsurface oxidation of organic carbon to CO_2, inorganic mixing of fresh and saline waters, and oxidation/reduction reactions involving sulfur (Mylroie & Carew, 1995; Baceta et al. 2001). It's not well studied if these complex chemical reactions introduce unexpected variations in stable isotopes that may confuse results aimed at assessing the occurrence of exposure events.

Epikarst: follows surface topography and occurs only in the upper few meters of rock (Mylroie & Carew, 1995). Karst surface is a surficial, irregularly pitted and etched surface, with dissolution channels and networks of great complexity that extend through only the upper few meters of rock. The rock contains numerous tubes, holes, and enlarged joints in the size range of centimeters to tens of centimeters. The karst surface is all or partially covered by soil and weathered rock material which may subside into the underlying dissolutional network. This surficial karst and its soil mantle is referred to as epikarst or subcutaneous karst (Williams, 1983). The epikarst is intimately linked with soil development processes and biological activity. Despite the fact that the epikarst is very permeable, and that the carbonate rocks beneath the epikarst have large porosity, the epikarst is capable of significant water storage.

Paleosols: two more common deposits can be differentiated: calcarenite protosols from terra-rossa paleosols. Calcarenite protosols are fossiliferous, unstructured paleosols formed during brief emergence events or temporary pauses in carbonate deposition that occur within a single sea-level highstand. They represent a minimal exposure time for the carbonate platform. Terra-rossa paleosols are the result of the cumulative weathering effects of long-term exposure associated with sea level lowstands, and are underlain by a porous epikarst. Terra-rossa paleosols commonly separate carbonate deposits formed during different sea level highstands, and, therefore, represent a substantial exposure time for the carbonate platform.

The proper interpretation of paleosols and the past exposure surfaces in the rock record can be difficult in carbonate islands (Carew & Mylroie, 1991) because of:

-topography, whether depositional or erosional, can result in poorly-developed, thin paleosols on ridge crests, and well-developed, thick paleosols in topographic lows may lead an observer to incorrectly interpret multiple exposure events;

-apparent terra-rossa paleosol horizons can develop within existing carbonates as a result of shallow vadose flow and weathering and can be misinterpreted as exposure surfaces (Carew & Mylroie, 1991; Rossinsky, et al., 1992);

-paleosol material may be transported into vadose and phreatic caves at depth and because phreatic caves may form at common elevations, the collection of the soil infilling at specific horizons can be later misinterpreted as a surface paleosol formed at a true exposure surface (Carew & Mylroie, 1991).

Endokarst: Caves observed on carbonate platform can be related to three main categories: vadose, phreatic and fracture caves (Mylroie & Carew, 1995). The first consist of vadose shaft called pit caves: vertical and punctual dissolutional patways formed by water discending from surface toward the water table; the active lifetime (and the vertical development of individual pit cave) is brief and reflects the variability of the epikarst upstreams causing the formation of the pit complexes. Large phreatic caves ('banana holes' and 'flank margin caves') form along the margin of the discharging freshwater lens (Fig. 2.1) as a result of freshwater/saltwater mixing (Mylroie & Carew, 1990). These caves are not conduits but rather mixing chambers that receive water in the island interior as diffuse flow and discharge that water after mixing as diffuse flow to the sea. Because they are developed at the margin of the lens, where it thins near sea level, they are especially indicative of sea level position (Mylroie, 2008) but vurnerable to destruction by scarp and hillslope erosion during subsequent platform exposure. Fractures caves develop along the margin of carbonate platform as a result of mechanical failure of the platform margin.

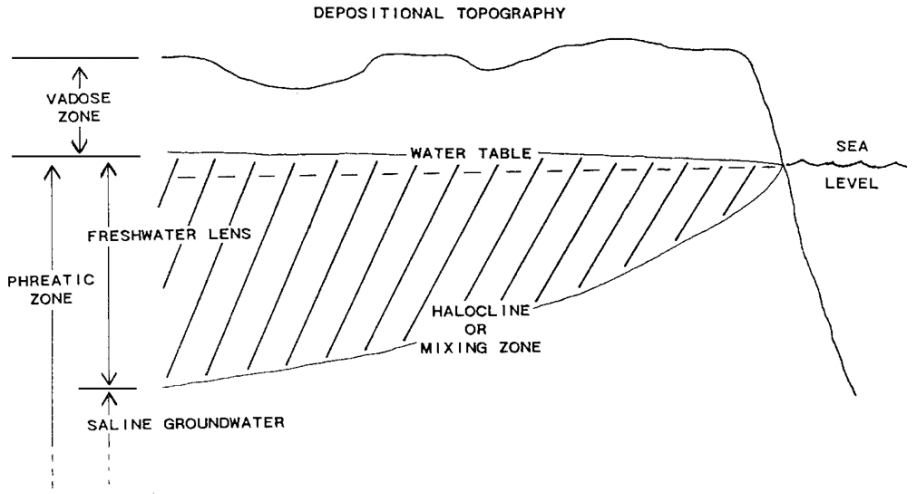

***Fig.2.1**: (da Mylroie & Carew, 1995) Diagrammatic representation of the main dissolutional features found on carbonate islands: epikarst (with paleosol), pit caves, banana holes and phreatic caves, and flank margin caves. Also shown are their positions relative to a freshwater lens and halocline. Changes in sea level move the position of the karst features. In the Quaternary, these sea level changes led to overprinting of dissolutional environments.*

Several composite unconformities in the stratigraphic record, carbonate sections display extensive karsting that leads to multiple development of cave systems (Esteban 2003; Sattler et al., 2005). These cave systems underwent extensive collapse and mechanical compaction with burial. Deformation of the overlying strata is associated with burial collapse of the cave system. Coalesced, collapsed-paleocave systems and associated suprastratal deformation appear to be prominent diagenetic/structural associated to composite unconformities and lead to correct

interpretation of original structures. Modern detailed (with submeter resolution) study of the three-dimensional architecture of the near-surface collapsed paleocave systems has been made with ground penetrating radar imaging (GPR) (McMechan et al. 1998; Loucks et al. 2004).

Successful identification of karst features in the rock record has important implications for sequence stratigraphy, paleo-environment and hydrocarbon reservoir because caves are regions of very high porosity and permeability but this identification is a 'daunting task'(Mylroie & Carew, 1995; Pomar & Ardila, 2000; Baceta et al. 2001;). The successful prediction of the occurrence of paleokarst caves in ancient carbonate platforms requires the use of additional information (Kerans, 1988) and evidence of exposure is a critical factor (Saller et al., 1994). Subaerial unconformities or evidence of mixing-zone diagenesis would be an important clue that pit caves and flank margin caves were possible. If subaerial unconformities in the carbonate section can be identified, the degree to which the epikarst has been developed can provide clues to the climate at the time of karstification, and the degree of separation of the surface from the water table (Webb, 1994).

The **methodology** used for the study on the Esino Limestone coincides with the unconformity-palaeokarst analysis proposed by Esteban (1991) following different steps: (a) unconformities mapping; (b) analysis of exposure profiles; (c) interpretation of exposure environments; and (d) analysis of underlying and overlying rocks to recognize immediately pre- and post-unconformity events

The **classifications** of cave products and cave facies is referred to Loucks (1999)* and Loucks & Mescher (2001)**.

Deposits:

Internal facies organization of the Calcare Rosso (KLR)

Facies			Characteristics	Thick -ness	Geometry of the beds
Typical peritidal deposits	***Red***	**Tred**	Peritidal lmst. rich in cements, TR and internal sediment, high deformed into tepees (mature)	<60m	m-scale, well bedded, often deformed in tepee, peritidal cycles
	Grey	**Tgrey**	Peritidal lmst rich in cements and internal sediments, deformed into tepees	30m	m-scale well bedded, often deformed in tepee, peritidal cycles
Lagoonal deposits	***dolomitized***	**Ld**	Dark dolomitized, laminated(stromatolitic?) lmst.	3m	cm- to dm-scale well bedded
	Fenestral	**Lf**	Dark lmst. rich in fenestral, bioturbation and (locally) with tepees	8-10m	dm-scale, well bedded
Residual breccias		**Rb**	Intraformational carbonate breccias	4m	Lens shaped

Fig. 2.2: *Summary table of distinctive features of three main facies characterizing the internal organization of 'Calcare Rosso' (KLR) deposits*

1. Typical peritidal deposits:

1a. Typical Red facies (*Tred*):

Field observations: Tred facies comprises peritidal cyclotemic limestones with abundant early carbonate cement precipitation, repeatedly capped by Terra Rossa paleosols (in particular at the base and in the upper part of the unit) and affected by complex deformations related to multiple events of subaerial exposures, such as highly evolved (mature) tepees (Assereto & Kendall, 1977; Mutti, 1992, 1994) (Fig.2.3 a, c) along with vadose pisolites. Locally, mainly in the upper part, decimetres-thick layers of red and green shales (tuffaceous?) intercalate. Internal sediment (Fig.2.3 b, c) with red and green clays, tuffaceous levels, dolomitizing and redox processes, and growth/precipitation of dark to grey to white cements provide a polychromatic aspect of the Tred deposits. Peritidal bedding of Tgrey succession is accentuated by intercalation of both Terra Rossa and millimeter to centimeter-scale shales (tuffaceous?) layers. Locally, supratidal and

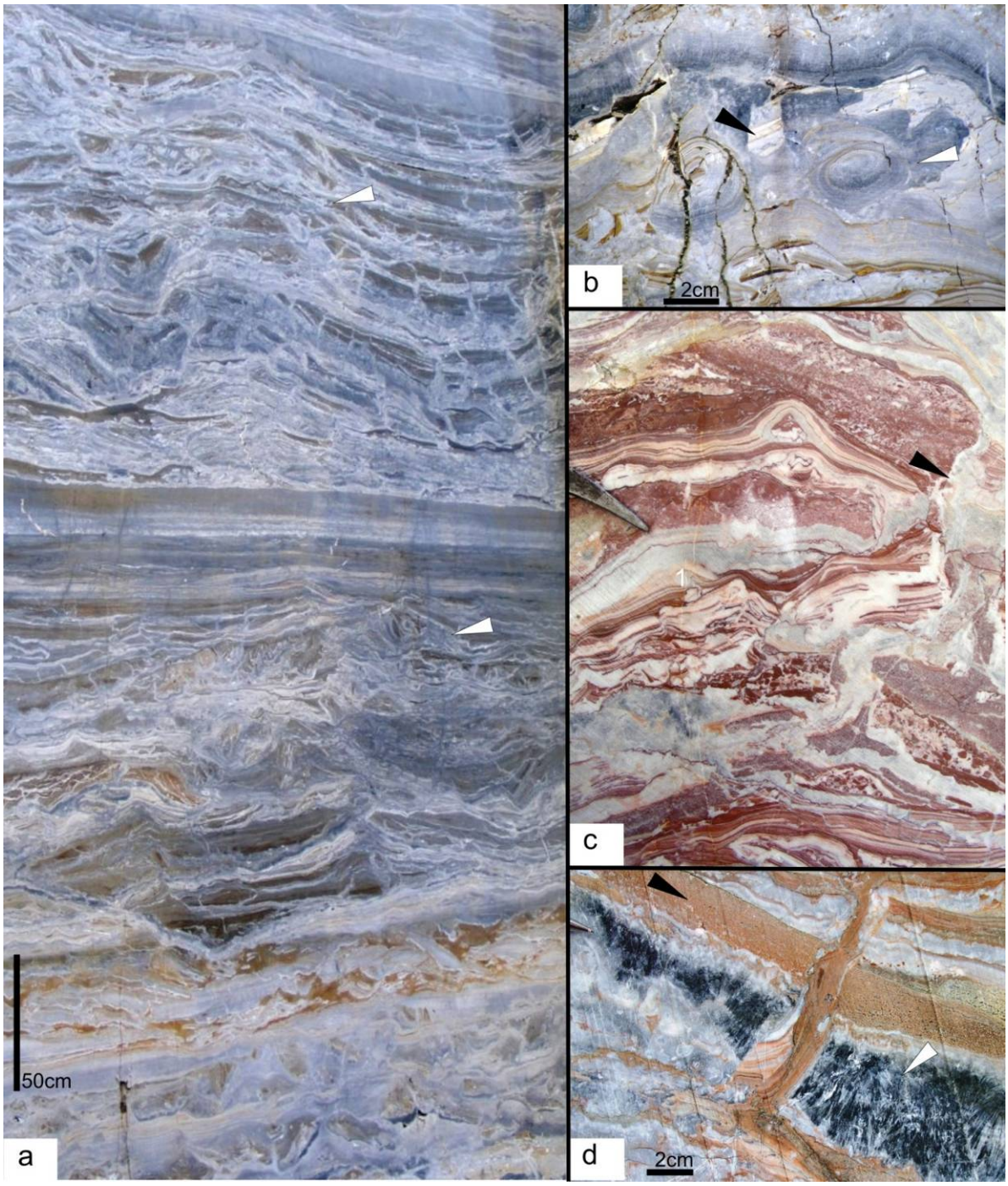

Fig. 2.3: *Tred macrofacies (Cava Gamba section).* ***a-*** *Vertical alternance of mature tepee-deformed (white arrow), undeformed layers and laminated internal sediments filling subhorizontal cavities;* ***b-*** *Pendant cements(white arrow) associated to several laminated polychromes internal sediments(dark arrow). Notice the typical blackening in the lower part of pendant strauctures;* ***c-****Internal laminated reddisj sediment at filling a mature tepee (Assereto & Kendall, 1977). A complex history of filling,deformation and fracturation can be observed;* ***d-*** *Dark 'raggioni'(Assereto & Folk,1980) crystals, growing from upper border of a subhorizontal cavity are cut by vein filled by reddish material and laminated internal sediments.*

diagenetic tepees (Assereto & Kendall, 1977) deformations ranging from simple antiformal structures (peritidal tepee, Assereto & Kendall, 1977) to composite breccias broke the regular stacking pattern (Fig.2.3 a).

The upper and lower surfaces of the beds show erosive and dissolutional features. Veins, sedimentary dykes and diagenetical deformations cut and modify these surfaces.

Meter-scale, shoaling upward, peritidal cycles consist of a vertical succession of grey to light grey, bioturbated, bioclastic subtidal facies; grey to rare dark-grey (in the lower part of the Tred succession) fenestral, stromatolitic intertidal facies with penecontemporary dolomitization; tepee deformations (Assereto & Kendall, 1977), pisolitic lens and Terra Rossa material (locally paleosols) with disperse dolomitized clasts (up to 10 cm in size) referred to sopratidal facies. The sopratidal deposits up to 50 cm thick are often eroded or deformed. Terra Rossa deposits (paleosols?) with lower erosive surface reach 30-40 cm in thickness; they are often flushed and preserved into paleokarst network (Fig 2.3 c) of veins and subhorizontal cavities (also 5-10 m long).

The thickness of intertidal deposits shows large variability ranging between 15 to 80 cm.

The subtidal deposits are 30-40 cm thick. Within subtidal deposits gastropods (*Trachynerites sp*.), green dasycladaceans algae (*Diplopora* sp. and *Clypeina besici - Pantic*, found by F. Jadoul in the Cadei Section, 10-15 m above the base of the unit), ostracods, (rare) ammonoids and foraminifera were found. Levels rich in oncoids (up to 2 cm in size) are common.

Primary depositional structures are modified by superimposed diagenetic and paleokarst processes (Fig.2.3a). Internal sediments and diagenetic cements filling large cavities, veins and sheet cracks, take up until 80% of the total rock volume in strata involved in senili tepees (Assereto & Kendall 1977; Mutti , 1992, 1994). The volume of cement and internal sediments dominate with respect to the host rock (Fig.2.3) and document an intense dissolution of the original sediments. Both isopachous and acicular cements ("raggioni" of Assereto & Folk, 1980) can be recognize (Fig.2.3 d). Isopachous cement crusts, up to 3 cm thick, covers generally the walls of cavities and veins. 'Raggioni' cements (Assereto & Folk, 1980) (Fig.2.3d) show different size (up to 15 cm) and fabric reflecting probably different origin or growth conditions. Assereto & Folk (1980) interpreted the raggioni as calcitic pseudomorphs on primary aragonitic

crystals growing in paleokarst cavities and tepees (Assereto & Kendall, 1977). Morphology of crystals changes depending on the polarity, with prevailing top-down growth (pendant raggioni, Assereto & Folk, 1980, Fig 2.3d). Nucleation starts from the borders of the cavities. Typical 'raggioni' cements (Assereto & Folk, 1980) consist of dark, calcitic, up to 5 cm in lenght rays organized in fan-like structure; growth of these crystals within internal sediments deforms or substitute the original lamination of the sediments.

Internal sediment (Fig 2.3 b,d) consisting of carbonatic and terrigenous material (clays and Terra Rossa material) flushed into vadose to phreatic conduits during several phases of cavities filling. These deposits are both thin and granular, laminated (with millimetre-scale lamination), polychromatic (green, red, grey) and contain ostracods.

In the depocentral areas of the southern margin (of the Esino Limestone), the lower 7-10 meters of the Tred succession (that pinch out rapidly northward) below the first paleosol show intermediate characteristics with the upper inner platform deposits of the Esino Limestone. Degree of deformation, abundance of early/shallow burial cements, richness of both internal sediments and tepees (juvenili and mature, Assereto & Kendall, 1977; Mutti, 1992, 1994) and stacking pattern are very similar to overlying deposits (of Tred), but is distinguishing the absence of intercalated TR material. This lower part of the Tred facies succession is named Tred *transitional facies.*

Paleosols: Several Terra Rossa (TR) levels have been recognized within the Tred facies succession, mainly in the lower and upper part of Tred facies. The highest abundance of TR layers does not correspond to the maximum thickness of the Tred facies; above the southern margin of the Esino Limestone, moving from the depocentral areas of the 'Calcare Rosso' (Cadei Quarry section) to the areas above the reef facies (Gamba Quarry, Remuzzi Quarry), the abundance of TR layers increases, while it decreases moving to backreef facies.

The Terra Rossa layers consist of subhorizontal deposits 3 to 50 cm thick redeposited into stratabound cavities (in vadose-phreatic conditions) or surface karst depressions. Few oldest pedogenic cycles are (partly) recorded by Tred succession and very little information are available for these. The best example of Terra Rossa paleosol within the Tred facies has been studied along Strada Gamba Section (Fig.2.4 a).

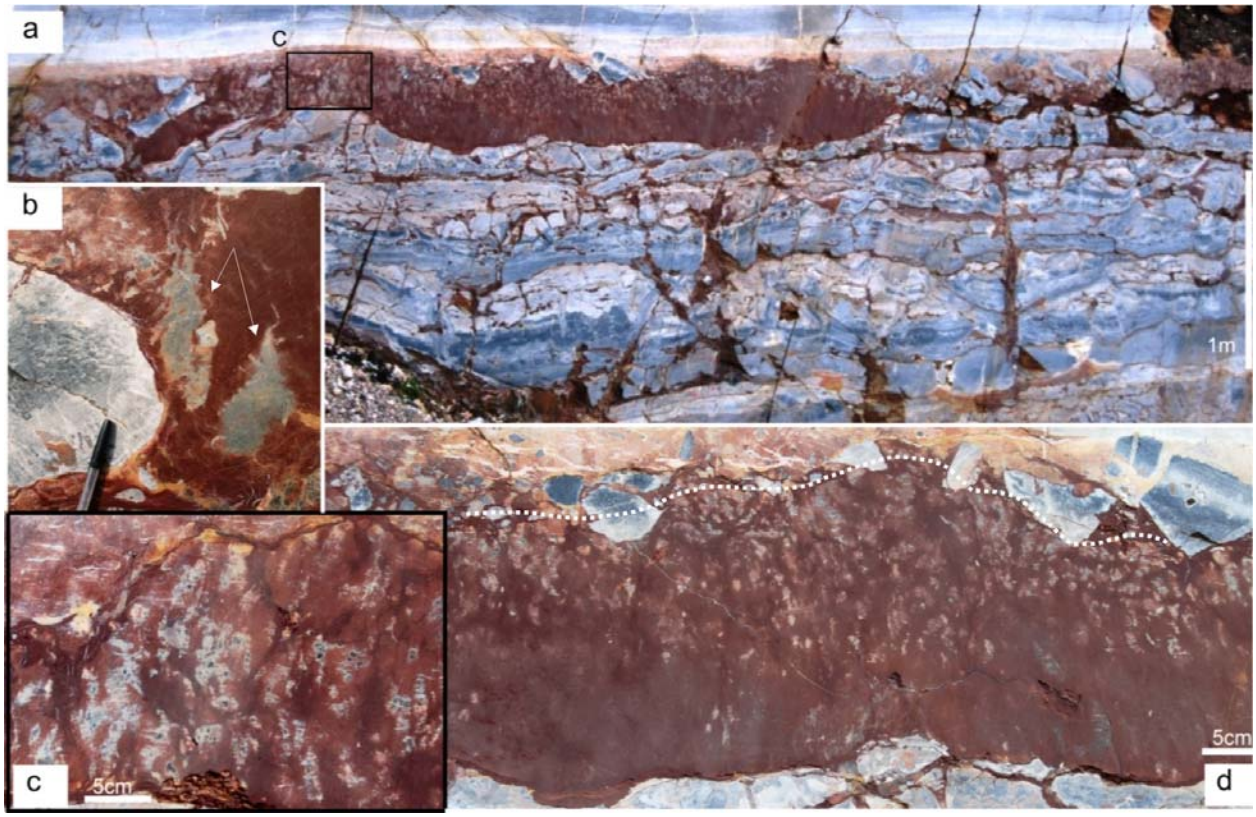

Fig.2.4: a- *General view of the truncated Terra Rossa-like paleosol preserved at the base of the Calcare Rosso succession (Strada Gamba section) and underlying paleokarst network of tubes and cavities;* ***b-*** *residual $CaCO_3$ concretions in the groundmass of the Terra Rossa horizon;* ***c-*** *a detail of decalcification features from the upper part of the paleosol (detail from the box in* a*);* ***d-*** *the decalcification features decrease along the paleosol, notice the upper boundary of the Terra Rossa horizon is truncated (dotted line)*

The buried paleosol marks the boundary between the Tred transitional facies and the Tred facies; it consists of a lenticular, 4 to 5 m large and 5 to 50 cm thick, truncated 'Terra Rossa horizon' that levels the irregular topography of the paleokarst surface.

The lower boundary (with well bedded, deformed peritidal deposits of the Tred Transitional facies) presents evidence for solutional processes. Paleokarst network of tubes, dissolution vughs and strata-bound cavities are characterized the Tred Transitional deposits up to 1.5 m. Cavities are filled by Terra Rossa material and locally by millimetric breccias, red clay; moreover, karst pores and fractures are lined by early calcitic cements. Few, more developed and up to 10 cm in diameter vertical tubes deepening up to 2.3 m from unconformity.

The upper boundary of the paleosol is a sharp and slightly irregular erosional surface, overlaid by several layers of matrix-supported carbonatic breccias, which groundmass shows analogies with the Terra Rossa horizon. The lateral continuity and correlability of the paleosol are highly

variable, ranging from tens to hundreds of metres. Carbonatic clasts from the breccias above the erosional surface are millimetric to centimetric (up to 12 cm), poorly rounded, recrystallized and often blackened. Rounding of clasts is partly due to intense dissolution of the margin.

The upper and lower boundaries of the paleosol are marked by green/red clay coatings (probably diagenetic), 0.5-1 cm thick; possibly they are affected by stylolitization. Millimetric layers of clay coat also the breccia clasts. The paleosol consists of well aggregated and cemented micritic Terra Rossa material (color: 10R3/6), without macrovoids; it presents residual $CaCO_3$ concretions, decalcification structures, and calcite veins. Carbonate pedofeatures are segregated into large (2-6 cm in diameter) subspherical features (glaebules) and into small (<= 1 cm diameter) filaments arranged into non– or weakly calcareous matrix. The carbonate pedofeatures decrease in number and complexity towards the bottom of the paleosol and in particular in the upper 20-30 cm.

Microfacies analysis: Only three samples from the paleosol and the paleokarst veins were analysed.

Paleosol: the porosity pattern is dominated by a network of channels, chambers, and planes, producing an open porphyric c/f related distribution; estimated total void space is 15%. The c/f (coarse/fine) ratio, with limit imposed to 10 μm, range from 10/90 to 20/80. The micromass consists of red to reddish yellow clay and fine silt (Fig.2.5 c). It is opaque with dotted luminescent areas and an undifferentiated b-fabric; locally a crystallitic b-fabric occurs.

The fine material is widely and intensely impregnated with reddish brown iron oxides and hydroxides. The coarse mineral grains are randomly orientated and consist of very well to well sorted, detrital and diagenetic quartz grains, autigen crystals of clay with low interference colours (developed mostly near the border of the pedofeatures), bioclasts, and fragments of microbial boundstone. Bioclasts consist of weakly rounded, recrystallized fragments of brachiopods (up to 1 cm) with evidence of dissolution and microboring. Fragments consist of poor rounded microbial boundstones and peloidal packestone (intra, bio-micrite) often laminated with oncoids, lumps, fragments of green dasycladaceans algae and small foraminifera.

Redoximorphic features point to strong hydromorphism. Orthic nodules of different types (typic, nucleic; Fig. 2.5 a, b) and size (10-20 μm to 200-300 μm in diameter) are moderately to partially impregnated, red brown to dark red, and generally with mamillate-serrate surfaces.

Irregular and poorly rounded nodules are impregnation of coarse fragments, bioclasts and grains.

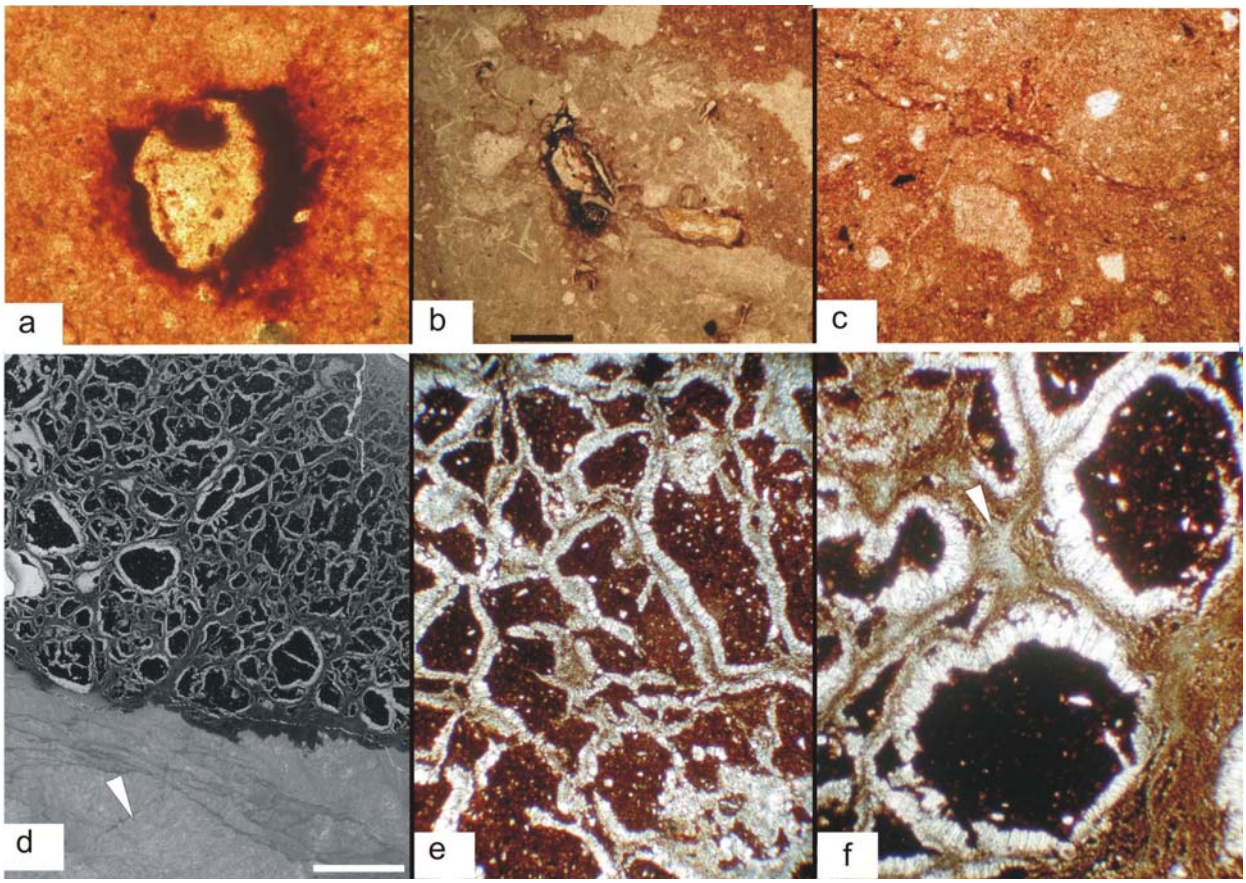

***Fig.2.5**: **a**- Possibly residual impregnative nodule of iron hydroxide; **b**- Impregnative nodule or hypo-coating of iron hydroxide; growth of autigen crystals in the groundmass; **c**- Intercalation of clay (linear clay concentration in the groundmass); **d**- scanned slide (grey scale) from the solutional boundary between the host rock and the infilling of a paleokarst tube; **e**- pedorelicts accumulated within a paleokarst tube, each pedorelict presents a rim of calcite; **f**- detail of* e, *notice the radial calcite crystals coating pedorelicts (cross polarized light).*

Occasional external hypocoatings of Fe and Mn oxides are also present, and generally related to the other features, as nodules, mineral grains or bioclasts.

Into the micromass, dispersed cavities (up to 200 μm in size) with irregular morphology are present. These cavities are filled by medium to coarsely crystalline quartz or recrystallized calcitic cements. Locally, two generation of calcite cement are preserved: isopachous crusts (20-30 μm thick) of fibrous radial calcite and sparry calcite at the nucleous.

Material infilled in cavities and veins: it shows an highly separated subangular blocky microstructure (Fig.2.5 d, e, f). The abundace of redoximorphic features point to strong hydromorphism: the micromass is widely and intensely iron–stained (reddish brown in colour).

Secondary carbonate pedofeatures are associated to a high porosity and made of fibrous radial calcite and microsparite. They occur in the form of typic coatings, hypocoatings and infillings, up to 150 µm thick. In the first case they form coats or bridge respectively around and between the peds.

The macro- and micro- morphological analyses reveal different and subsequent pedogenetic phases characterizing both the paleosol formation and the transport of unweathered material in cavities (Fig.2.5 d) of paleokarst network lied beneath: 1) strong weathering of the primary minerals and decalcification (leaching), 2) clay neoformation and illuviation; 3) strong rubefaction, 4) secondary calcite precipitation on carbonate-free parent material, and 5) erosion and soil truncation processes.

During the pedogenetic cycle responsible for the paleosol formation the climate was probably characterized by seasonal soil moisture availability (winter) and water deficit (summer), and quite high temperature during the long dry period (summer), which produced the rubification typical of the Fersiallitic soils (Dudal et al., 1966; Duchafour, 1977; Fedoroff, 1997; Yaalon, 1997). The high degree of pedogenic development suggests soil forming processes that acted for a long time.

Microfacies analysis: Tred microfacies are affected by diagenetic (vadose) processes that alter size, shape and arrangement of the crystals and obliterate the original depositional textures and constituents. Few examples of poor altered microfacies were observed.

Subtidal deposits are characterized by wackstone and subordinate packstone with peloids, large (up to 1 cm) aggregated grains (often microbial lumps) and bioclasts. In particular, faunas of restricted lagoon were observed: Gastropods, bivalves, ostracods, green Dasycladaceans algae (*Diplopora* sp.; *Teutoporella echinata*, Mutti, 1992; *Clypeina* sp.) and small foraminifera. Original fabric of shells and algal fragments are replaced by sparry calcite. Bioclasts are often rimmed by micritic envelops, biogenic encrustations (locally complex irregular meshwork structures, Stromatoporoids?) and isopachous cements. Isopachous crusts around the grains consist of radial fibrous calcite or needle-like (fibrous or acicular) crystals (Fig. 2.6 c) probably composed of Low-Mg calcite (typical mineralogical composition of fibrous calcite in ancient reef, Walls & Burrows, 1985) or with aragonitic precursor.

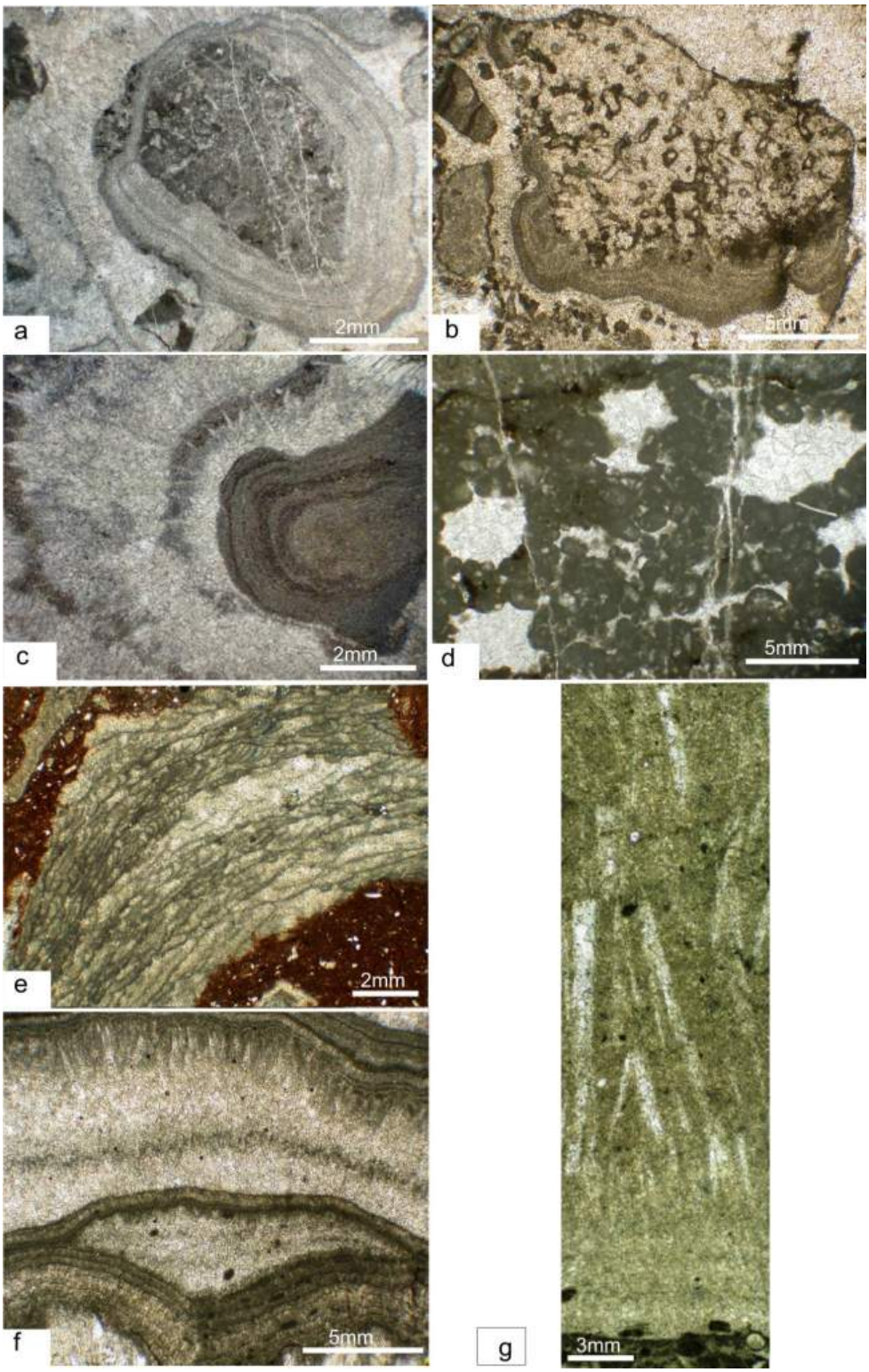

Fig.2.6: a- *Pisoid (Tred transitional; Strada Gamba section)**;** **b**-Coated grain with pendant structure (x18) (Cadei Section);* ***c*****-** *Detail of a pisoid with recrystallized autigenic "pseudoacicular" calcitc rays, growing into the outer layers;* ***d*****-***fenestrae fabric (Tred transitional; Strada Gamba section);* ***e*****-** *clasts of microbial boundstone floated into Terra rossa matrix;* ***f*****-***laminae of l internal sediments deformed by growth of raggioni (Assereto & Folk, 1980) cements;* ***g*****-** *Transition between peloidal sediments and recrystallized layer with remnants of peloids and mega ray of clear calcite (blocky).*

Bioclasts or fragments of bioclasts and intraclasts coated by concentric finely crystalline, biofilms and fibrous laminae form pisoids structures up to 3 cm in size (Fiog.2.6 a, b). Pisoid rudstone also contains broken and reworked pisoids.

Micritization is often limited to the borders of the grains but locally affects the whole grain.

Intertidal deposits, often dolomitized are characterized by fenestral peloidal packstone (Fig.2.6 d) and stromatolitic bindstone. Subordinate wackestone. Rare bioclasts (green dasycladaceans algae) were observed.

Above intertidal deposits, erosional surfaces often marked by Fe-ox accretion characterize the base of millimetre-scale rudstone with inter-, sub-tidal intraclasts and fragments of paleosols floated into micritic matrix. Supratidal clasts show early dolomitization.

Veins and fractures are filled by several generation of isopachous crusts of calcitic cements with intercalated biogenic films and internal sediments. Internal sediments consists of Terra Rossa material or peloidal sediments laminated with some dolomitized laminae. Laminations in peloidal sediments are often deformed and cut by growth of diagenetic cements (‘raggioni’, Assereto & Folk, 1980) (Fig.2.6 f, g). In particular, the growth of these acicular crystal seem to be influenced by gravity. The raggioni crystals (Assereto & Folk, 1980) are more developed downwards, whereas they form fans like structures at the base of cavities.

They are square-ended (probable evidence of a former aragonitic mineralogy of the cement, Assereto & Folk, 1976; Mazzullo & Cys, 1977, preserved after neomorphism to calcite) (Fig.2.6 g) or ‘plume’ habit. Dissolutional polyphasic processes involve both subtidal and intertidal deposits enlarging fenestrae and reopening depositional porosity.

Distribution: the Tred facies outcrops extensively above the upper slope/reefal facies of the southern margin of the Esino Limestone and rapidly pinches out laterally (wedge-shape). Furthermore, limited outcrops has been studied above the eastern margin of the Esino Limestone, in particular at the Mt. Vaccaro (2-3 m thick) and Ardesio-‘Ponte delle Seghe’ (15-20 m thick). Vachè (1966) describe Tred facies also in the Trevasco area and in the Valle dell’Orso. *Thickness:* above southern margin of the Esino Limestone maximum thickness is about 60 m.

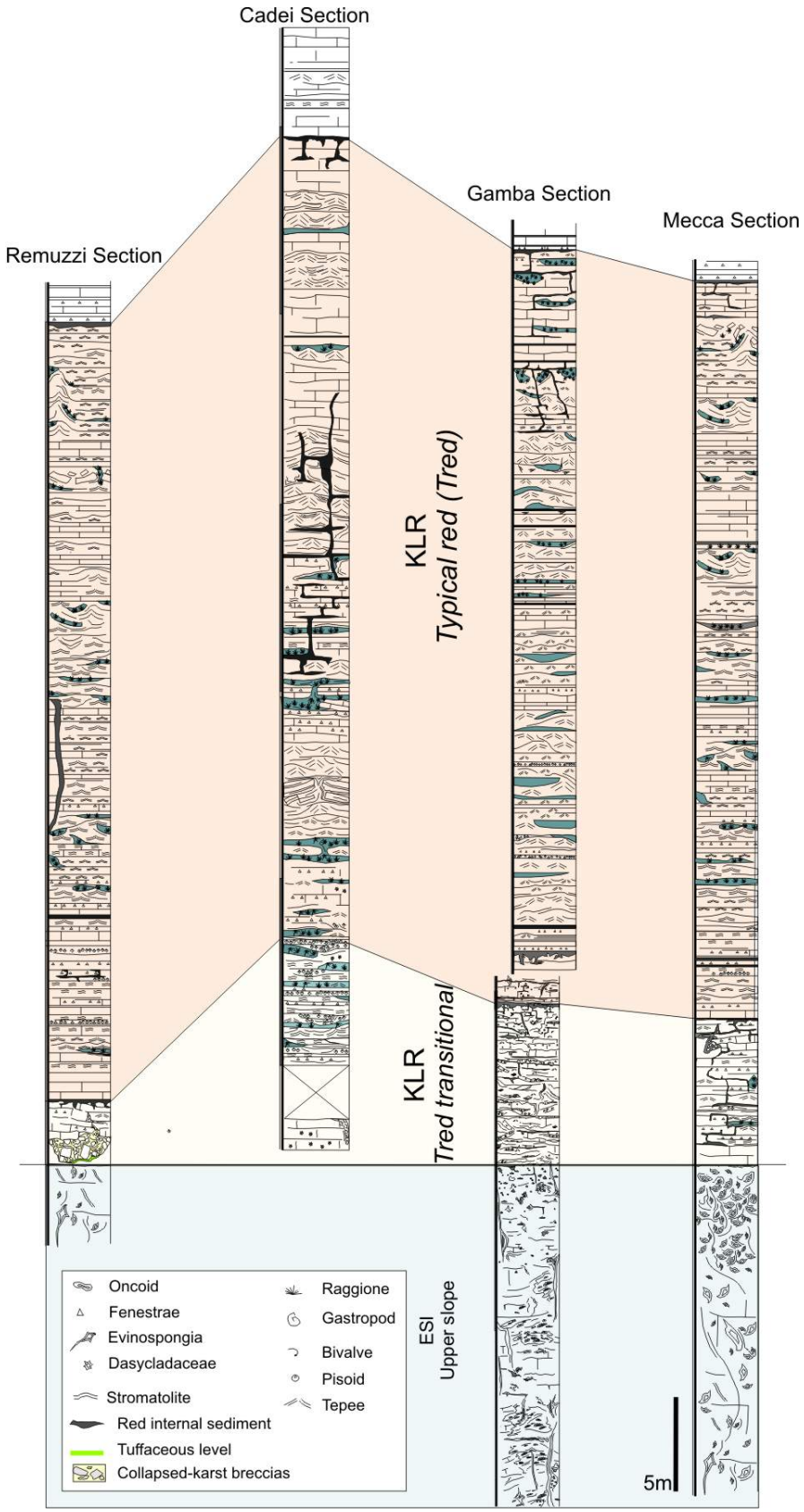

Fig.2.7: *Correlations table of the stratigraphic logs measured above the southern margin of the Esino Limestone in correspondence of the transition between Esino Limestone and Calcare Rosso deposits.*

2a. Typical Grey facies (*Tg*):

Field observations: the '*Typical Grey*' consists of well bedded grey limestone, organized in meter-scale peritidal cycles, with supratidal deformations (tepees; Assereto & Kendall, 1977) (Fig.2.10). Subtidal bioclastic deposits (green dasycladacee algae, gasteropods, bivalvs), with oncoidal lens and small coral patch reef, characterize the lower part of peritidal cycles.

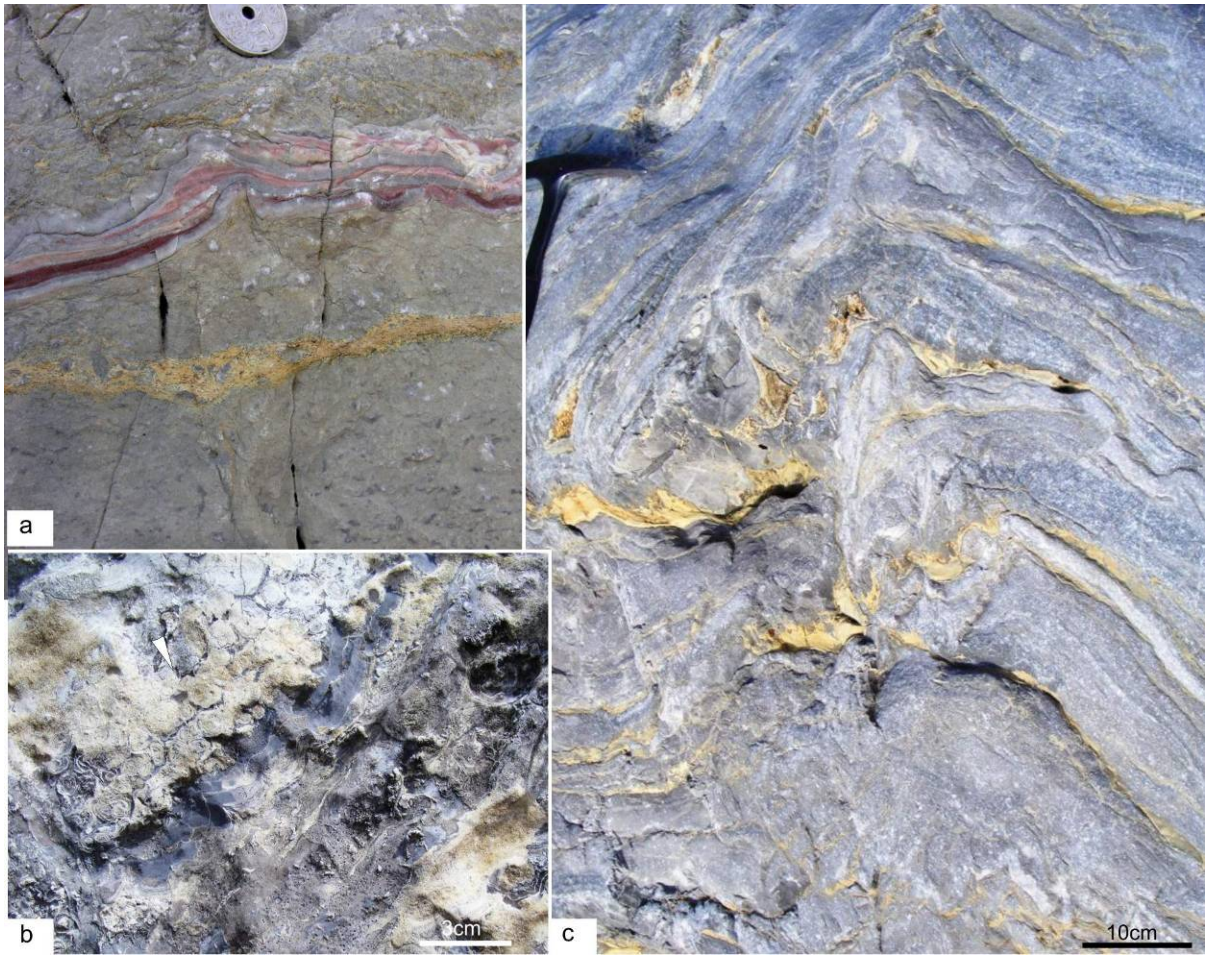

Fig. 2.8: a- *Sheet cracks developed into fenestral limestone filled by reddish laminated internal sediments and crusts of 'coconut meat calcite'. (Few centimetres below) Another subhorizontal cavities filled by carbonate breccias supported by yellow- greenish matrix;* ***b****-pisoidal crust with pendant cements;* ***c****- Meter-scale mature tepee (Assereto &Kendall,1977).*

Fenestral and stromatolitic limestones seldom capped by centimetre-scale intraformational breccias and permeated by dissolutional features filled by yellow matrix, often deformed in tepees (juvenili tepees, Assereto & Kendall, 1977; Mutti, 1992, 1994) (Fig.2.8 c) characterize the upper part of the cycles. Locally microbial mats or centimeter- to decimeter-scale microbial domical hemisferoids can be observed. Tepee deformations ranges from decimeter-scale (juvenili tepees, Assereto & Kendall, 1977; Mutti, 1992, 1994) to meter-scale (mature tepees,

Assereto & Kendall, 1977; Mutti, 1992, 1994) antiformal structures (Fig.2.8 c), to rare composite breccias floating in internal ocher sediments (senile tepees, Assereto & Kendall, 1977; Mutti, 1992, 1994). Associated to major supratidal /diagenetical deformation, dissolutional features, pisoids lens, sheet cracks with several generation of isopachous cements and internal sediments (Fig.2.8 a) and large amount of cements. In particular effects of intense vadose diagenesis are registred by growth of pendant cements (often dark and controlled by biogenic encrustations) (Fig.2.8 b) and 'raggioni' cements (single crystals fans, up to 5 cm in leght; coalescens 'raggioni': up to 2 cm; Assereto & Folk, 1980) (Fig. 2.10).

The thickness of the cycles range from 0.4 to 1.6 m. The thickness ratio between subtidal facies and inter-sopratidal facies range from 5:1 to 2:1.

The base of Tgrey facies is characterized by tuffaceous levels (5-10 cm thick, Mt. Trevasco) or intraformational carbonate breccias (20-40 cm thick, Mt. Pegherolo). In the lower part are often intercalated well bedded (25 to 40 cm thick) dark fenestral limestone rich in green dasycladaceans algae.

Bedding is marked by millimetric intercalations of dolomitized yellowish material (Fig.2.8 c).

Stacking pattern and depositional characteristics are very similar to the overlying peritidal deposits of the Breno Fm. but the peritidal cycles of the Tgrey facies are often thinner and the ratio between supra-tidal and to subtidal facies is higher.

Microfacies analysis: bioclastic and peloidal wackestone/packestone, lens of oncoidal rudstone, fenestral packestone and crusts of laminated (microbial) cements (Fig.2.9 d, e) characterize the typical peritidal cycle from base to the top. The subtidal fine grained limestone is characterized by lens of centimetre-scale oncoidal or (rare) pisoid rudstone and sheet cracks filled by several generations of isopachous crusts of fibrous radial calcite, carbonatic internal sediments laminated or ocher material dolomitized. Bioclastic wackstone with ceritid gastropods and green dasycladeceans algae (*Teutoporella echinata* Ott., *Diplopora* sp.) are common (Fig.2.9 c). Locally, recrystallized colonies of corals bafflestone (Fig.2.9 a, b). Penecontemporary dolomitization affects part of inter-, supra-tidal deposits. The fenestral peloidal layers, from 5 to 20 cm thick, consist of peloidal-intraclasts packestone/wackestone weakly bioturbated, not laminated and with spar-filled pores. Stromatolitic bindstone and laminated (microbial) cements

cap the cycle. Vadose dolomitized pisolitic crusts and pendant cements are often associated with the inter- supra-tidal deposits.

Into the more deformed strata, mature-senili tepees (Assereto & Kendall, 1977; Mutti, 1992, 1994) and sheet cracks filled by laminated internal sediment often recrystallized into mega-ray structures ('raggioni', Assereto & Folk, 1980) are common. Different degrees of development and size of 'raggioni' can be observed: coalescens fans-like crystals millimeter - to centimetre - scale and centimetre -scale dark isolated mega-rays. Cements and internal sediments form up to 60% of the total rock volume.

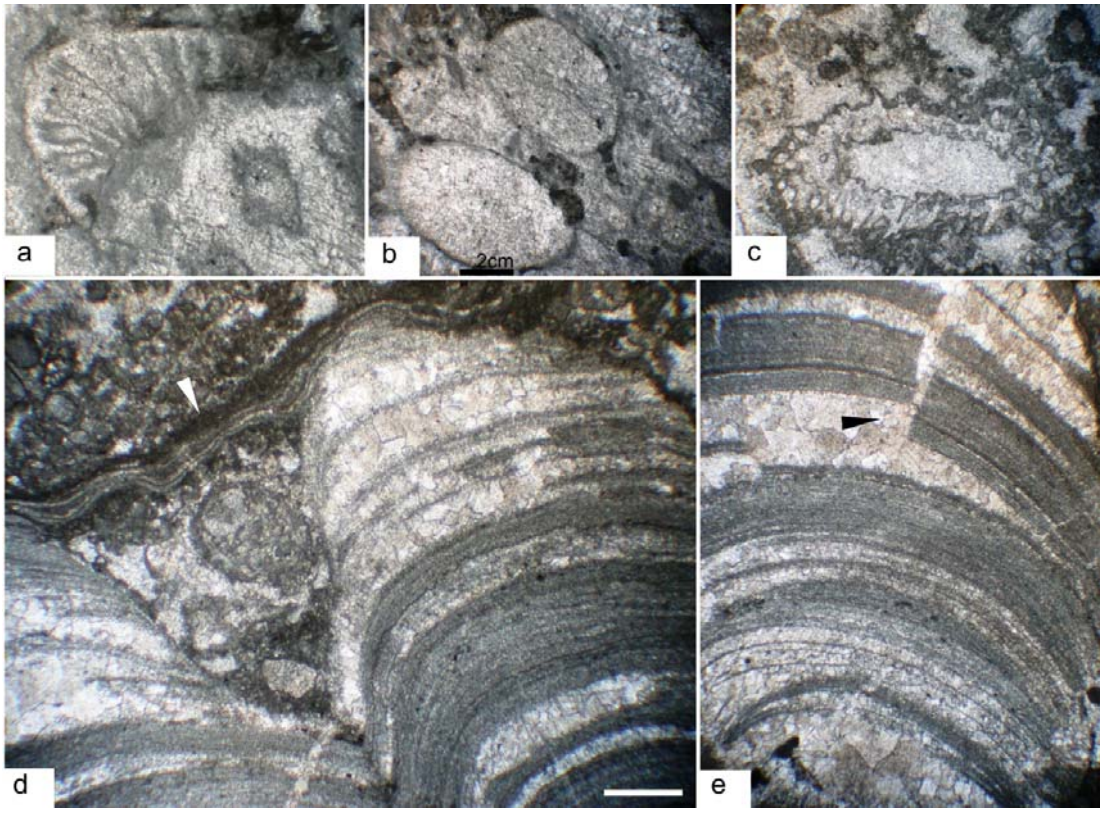

***Fig. 2.9: a, b**- Details of a recrystallized coral framestone with encrusting organisms (b); **c**- Thallus of a green dasycladaceans algae (Teutloporella echinata Ott.);**d**- Stromatolitic bindstone coated by laminated microbial envelop; **e**- (detail of d photomicrograph) stromatolite laminae crushed by aggrading recrystallization.*

Distribution: the *Tgrey* facies is typical on both the Northern margin and the Southeastern margin of Brembana platform, in particular it outcrops extensively both in the Brembana platform and in the Mt. Trevasco.

Thickness: maximum thickness is the 30-35 m in Brembana platform, it decreases northward from 35 m to 25 m; in the Trevasco area it's about 5-7 m.

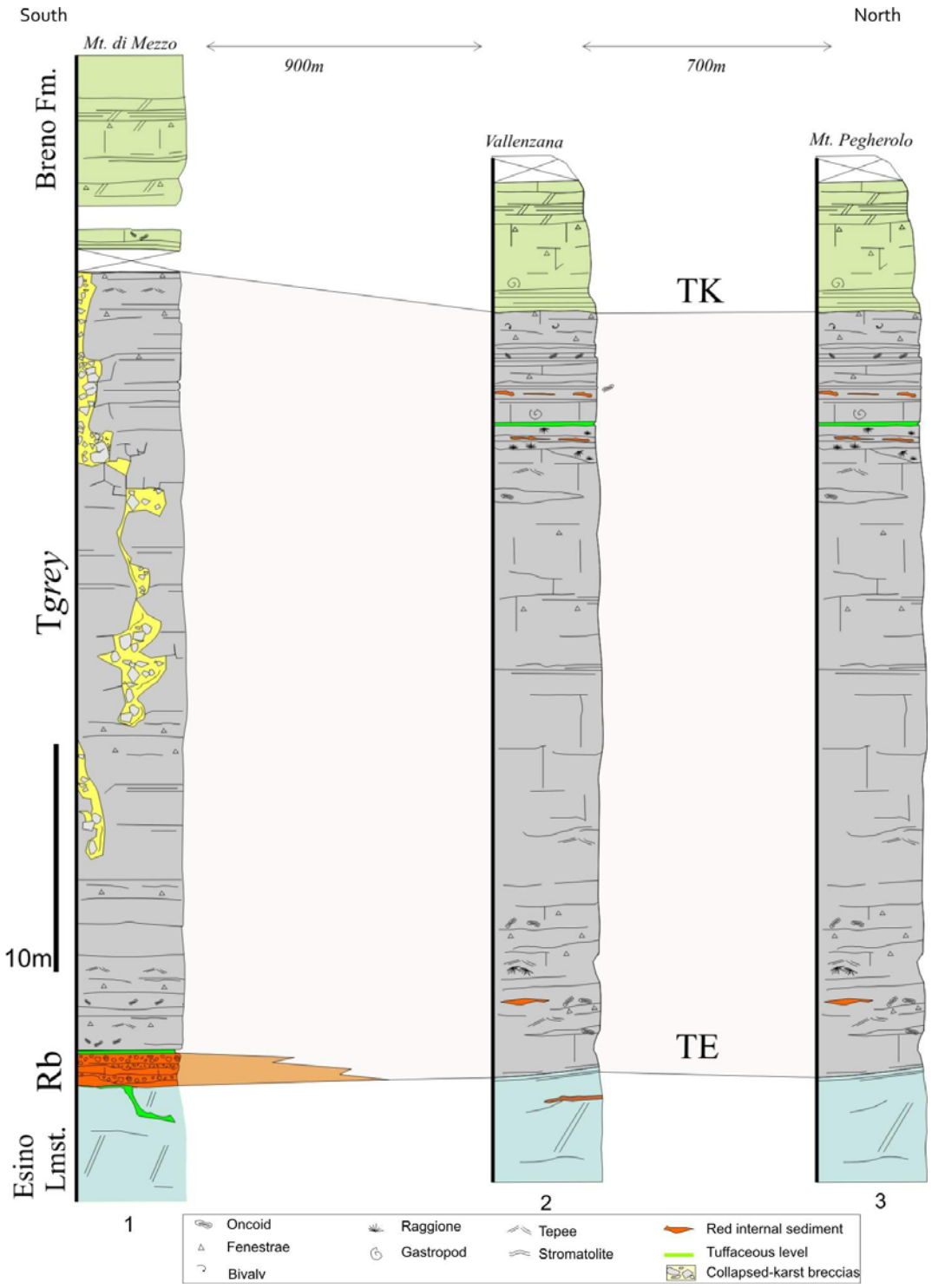

Fig.2.10: *Table of correlation of the measured stratigraphic sections in the regressive Tgrey facies above the thin dolomitized limestone of the Esino Limestone overlying the high relief clinostratified bodies of breccias of the progradational complex. In the section 1 (Mt. di Mezzo) vertical collapsed-karst structures are cut into Tgrey facies.*

2. Lagoonal deposits

2a. Dolomitized facies (*Ld*):

Fields observations: it consists of well bedded, 15-25 cm thick, dark grey dolomitized limestone. Centimetric green/yellowish tuffaceous/marly levels are often intercalated.

The facies are vertically arranged in shallowing-upward cycles (up to 1.6 m thick) with homogeneous subtidal limestone at the base, overlain by laminated carbonates without evidence of subaerial exposure. Boundaries of the cycles are marked by tuffaceous/marl intercalation. The subtidal/intertidal thickness ratio in the cycles is about 2:1 in the lower part of the succession and 1:1 or locally 1:2 in the upper part.

Microfacies analysis: the fine-grained subtidal deposits are characterized by unfossiliferous microsparite, with distinct mottling due to bioturbation.

The laminated peritidal carbonates exhibit (stromatolitic) bindstone consisting of wavy to crinkled fine laminae composed of couplets of grey micritic layers and layers with dark-grey peloids. Vertical burrows interrupt the continuity of the laminae.

Distribution: these deposits outcrop in the south-eastern part of the Esino Limestone, and they are preserved into depressions above residual breccias at the top of the volcanoclastic deposits Mt. Alino and often above paleokarst collapse deposits.

Thickness: ranges from 0.5 m in the paleokarst depressions to 3-4 m above the volcanoclastic deposits of Mt. Alino.

.

2b. Fenestral facies (*Lf*):

Fields observations: 'Lagoonal Fenestral' consists of well bedded, dark, dark-grey limestone, 15-30 cm thick often organized in shallowing upward cycles. Subtidal bioclastic fine grained limestone, rich in gastropods (Fig.2.11 d) and green dasycladaceans algae, are capped by fenestral and laminated limestone often deformed in tepees (Assereto & Kendall, 1977; Mutti, 1992,1994). Subtidal deposits show locally burrows (millimeter size) and vertical to sub-vertical oriented rhizoliths.

Microfacies analysis: the subtidal deposits are characterized by (rare) intraclastic rudstone and often bioturbated bioclastic/peloidal packestone/wackestone rich in gastropods and green dasycladaceans algae (Fig.2.12). Green dasycladacean algae are well sorted and rarely articulated.

The Gastropods fauna is oligotipic, including decimeter-size specimens of *Coelostylina* sp., *Pseudoscalite* sp., *Omphalopthyca* sp., *Natycopsis* sp., *Trachynerita* sp. and small *Neritaria sp*.(Fig.2.11 d). Locally (Mt. Valbona) small, spaced and recrystalized coral patch reefs are present.

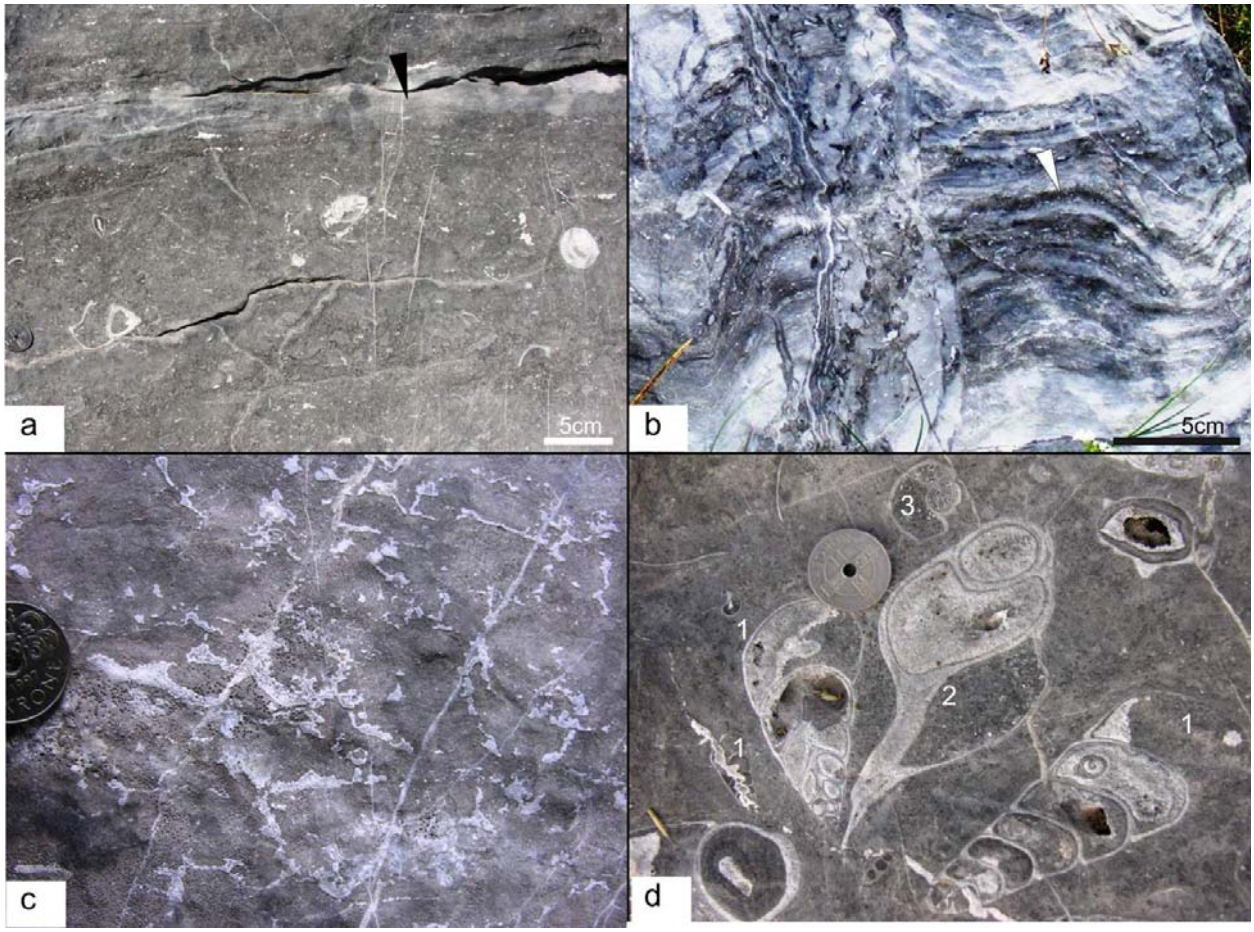

***Fig.2.11: a**- Dark, dark-gray bioclastic (bivalvs, green dasycladaceans algae and gastropods) and burrowed lagoonal deposits with sheet cracks filled by laminated and dolomitized grey internal sediments (dark arrow); **b**- Lateral linked stromatolitic emispheroids dolomitized and cut by several generation of fractures; **c**- subtidal deposits with voids filled by thin isopachous crusts and sparry calcite, interpreted as burrow; **d**- Gastropods faunas with 1) Coelostylina sp., 2) Omphaloptycha sp.,3)Trachynerita sp.*

The subtidal deposits are capped by dark fenestral packestone/wackestone and rare microbial binstone (Fig.2.11 b). Larger millimetre to centimetre open space structures irregularly

distributed or parallel to bedding planes form fenestral fabric or laminoid fenestral fabric. These voids are commonly filled by thin isopachous crusts and sparry calcite (Fig.2.11 c). Locally, the largest voids are filled by isopachous crusts and, at the nucleous, by sparry cement (only at the top) and fine-grained sediment (at the base) forming geopetal structure. Tubular cavities are interpreted as burrows or as the result of upward escape of gas bubbles biogenically produced within sediments (Flugel 2004).

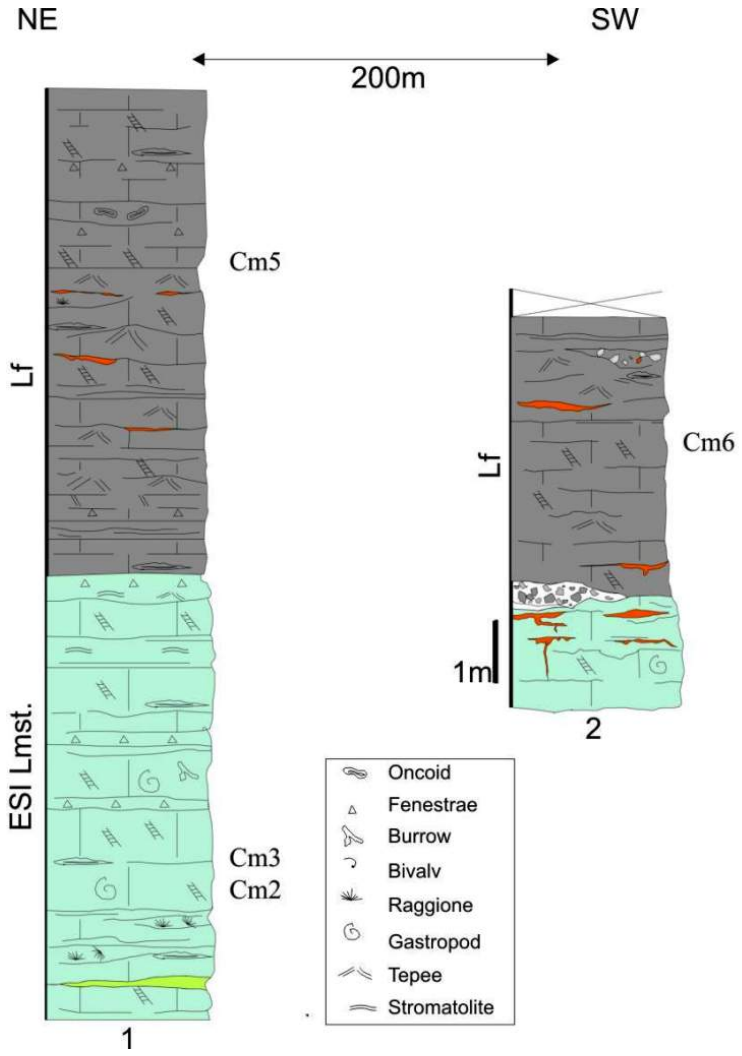

Fig. 2.12: *Stratigraphic logs of the lagoonal facies at the top of the inner platform succession of the Esino Limestone (Baitello di Menna; section 1is about 1km distant by Zorzone log)*

The subtidal/intertidal deposits ratio range between 10:1 to 5:1.

The top of several cycles is marked by decimeters-scale sopratidal deformations (juvenili tepees of Assereto & Kendall, 1977; Mutti, 1992,1994) and intense dissolutional processes which enlarge the fenestral vugs (Fig.2.12). Rare mature tepees (Assereto & Kendall, 1977; Mutti,

1992, 1994) reach 80 cm in height and involve the intertidal fenestral/laminated layers but often also the subtidal wackestone deposits.

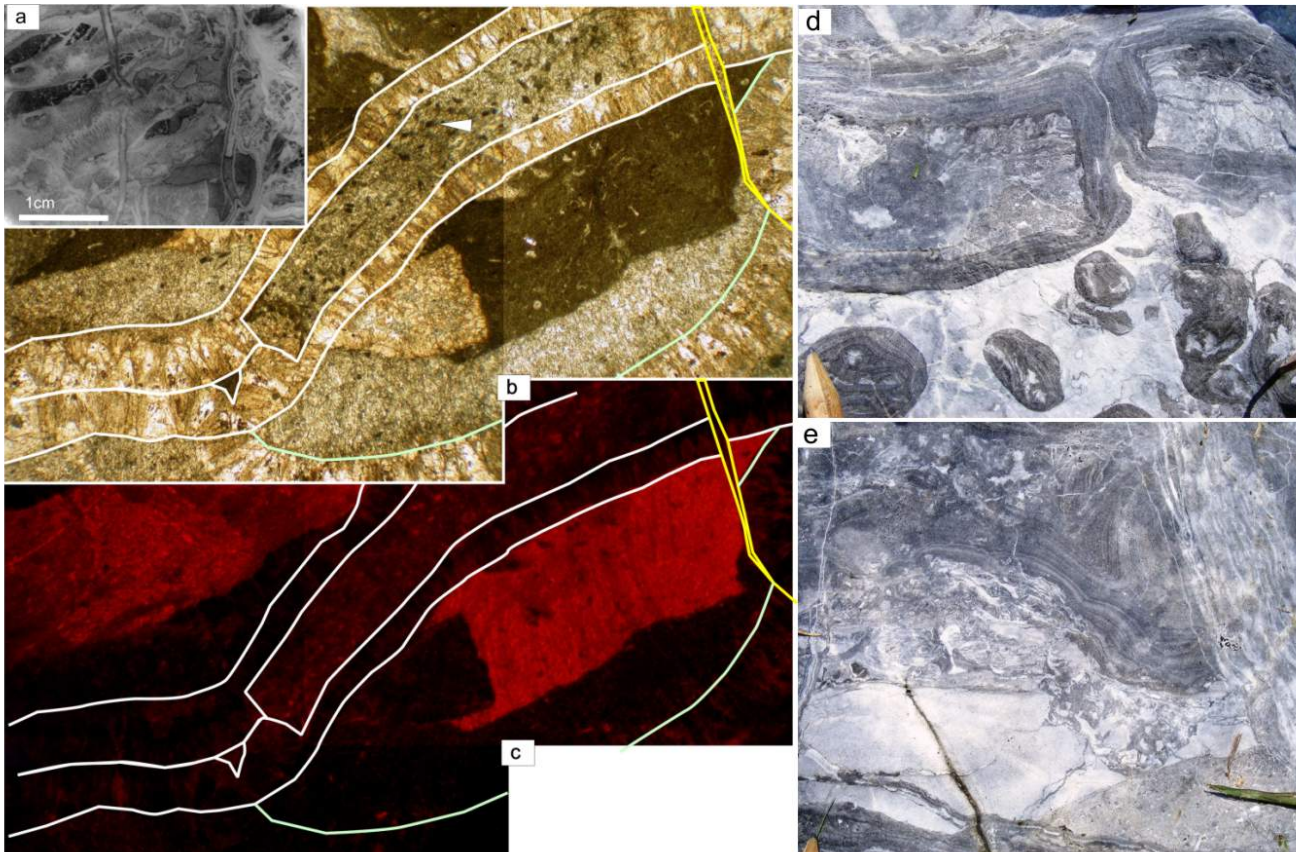

Fig.2.13 a- *Scanned thin section characterized by complex relations between fractures, sedimentary veins, host rock and acicular cements (raggioni);* ***b****- Transmitted light (composite) photomicrograph of several farctures filled by isopachous fibrous radial calcite, micritic and peloidal internal sediments;* ***c****- cathodoluminescence analysis (of same view). Crusts of fibrous radial calcite are non-luminescent (early cements). Fracturation, cementation and filling history;* ***d****- clasts breccias with dark laminated calcitic cement;* ***e****- Different fractures system are filled by different internal sediments.*

Associated to antiformal structures as well as to simple discontinuities, vertical dykes up to 8 cm in size and 40-50 cm deep and well developed sub-horizontal cavities (sheet cracks) (10 cm height and 1.5 m large) cuts into the subtidal deposits (Fig.2.12). Isopachous cements and internal marine laminated sediments (Fig.2.11 a) fill these cavities. Isopachous millimetre-scale crusts show emisferoidal structures (Fig.2.11 b) and arborescent growth typical of microbial control. Into the internal sediments also mega-rays (‘raggioni’, Assereto & Folk, 1980) can be observed. Locally, these vertical dykes and fractures has been observed associated to intraformational carbonate breccias characterized by angular to poor rounded clasts (up to 15 cm in size), often enveloped by millimeter to centimeter thick dark, laminated cement crusts, in

dolomitized thin grained matrix. The clasts of the breccias show early fracturation and the fractures not cut the dark cement envelops. Submarine formation of part of these vertical dykes and fractures is probably triggered by local synsedimentary tectonics (Fig.2.13).

Distribution: outcrops in most of the studied sections but well developed only in the areas characterized by intraplatform facies during the growth of the Esino Limestone.

Thickness: from 2-3 m (Mt. Ortighera) to 7-10 m ('Cascinetto di Menna'-Mt. Valbona)

3. Residual breccias

The term has been introduced by Norton (1917) in reference to breccias deposits developed on the karst topographies.

Fields observations: residual breccias consist of lens-shaped bodies of intraformational breccias with lateral extension up to tens of meters and variable thickness (0.3-4 m).

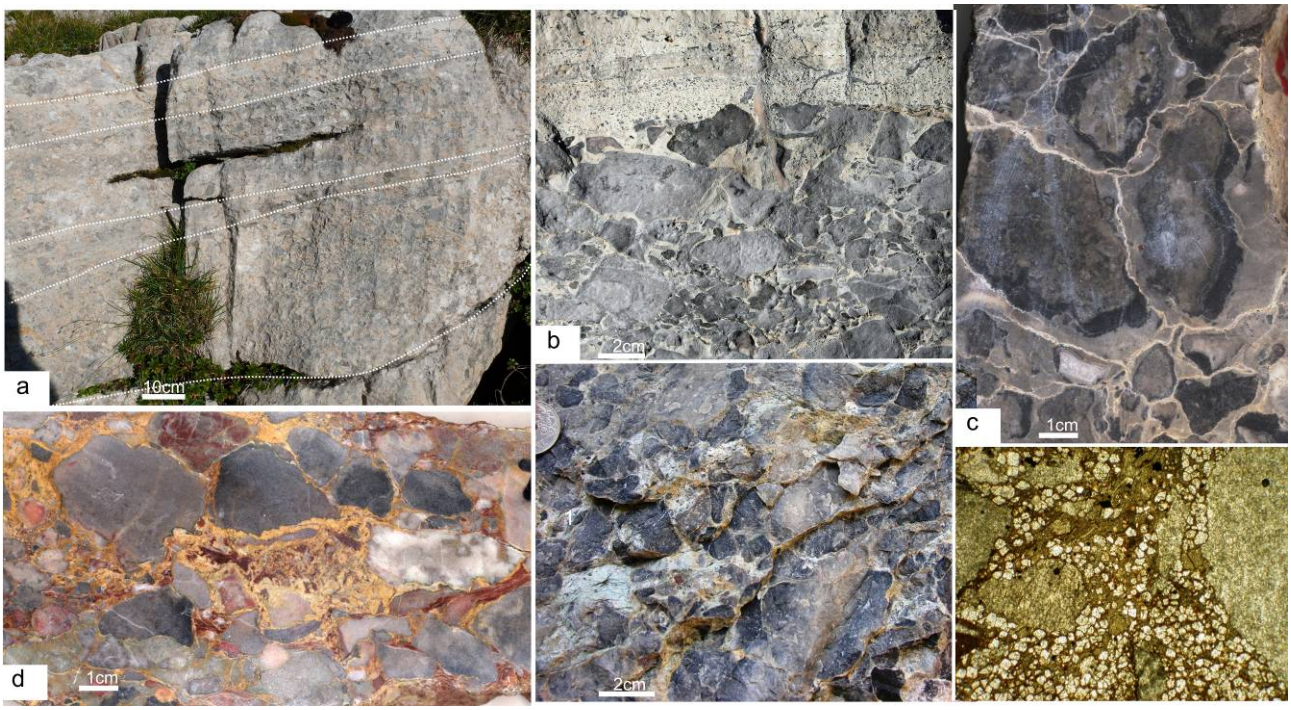

Fig.2.14: ***a****- Lenticular, poorly bedded bodies of breccias with erosive base (Mt. Arera);* ***b****- Sharp boundary between centimetre-scale, clasts-supported breccias and millimetre-scale matrix-supported breccias grading to calcarenites (Mt. Arera);* ***c****- Clasts of carbonate breccias with blackened rims and pendant cements (Mt. Pegherolo);* ***d****- Intraformational breccias with not-sorted, angular to poor rounded carbonate clasts and slabs of Terra Rossa paleosols (Val Mora);* ***e****- Blackening of the clasts is more common feature in the residual breccias and develops from the border of the clasts. Small clasts is often completely blackened. In this sample matrix consists of green, alterated shales (Mining tunnel Trevasco);*

***f**- Photomicrograph of residual breccias samples. The border of carbonate (recrystallized) clasts show dissolutional features and the matrix is dolomitized.*

These lenticular bodies are massive, often amalgamated or poorly bedded (only the thicker deposits) and show erosive or channelized conctacts (at the base) with underlying deposits and sharp and flat top boundary (Fig.2.14 a). The inverse or normal grading can be observed and breccias deposits are often capped by poor laminated calcarenites or millimetre-scale breccias (Fig.2.14 b). Locally yellow-greenish tuffaceous levels (<10 cm thick) and grey-dark grey (wackestone-packstone) carbonatic strata (10-15 cm thick) are intercalated.

Characteristics of the residual breccias deposits change in the different areas of the Esino Limestone. Three mainly types of residual breccias can be recognized on the basis of composition both of clasts and matrix, roundness of the clasts, fabric and packing.

1) *Residual breccias above* i*nner platform facies* (Zorzone section, Mt. Pedrozio, Mt. Arera, Mt. Vetro, Val Mora section): lithological composition ranges from monomict to (rare) polymict. Grey/dark carbonatic clasts and slabs of red paleosols (Fig.2.14 c)are associated to volcanoclastic to mixed varicolor matrix (Fig.2.14 d). Fabric is often clasts support. Angular to poor rounded (rare to rounded) millimeter to centimeter-size clasts show moderate sorting and the packing is close to open and the fitting is not primary;

2) *Residual breccias on the northern margin* (Mt. Pegherolo) (Fig.2.10): composition of both angular centimeter-size clasts and matrix is carbonatic. Fabric is clasts supported and packing is close. Dark, pendant cement crusts are common;

3) Residual breccias on the southern margin (Ardesio section, mining tunnel 'Ribasso Trevasco' section): poor rounded clasts are carbonatic, with moderate sorting and often blackened. Size range from millimeter to centimeter. Fabric range from clast to matrix support. Matrix consists of green shales probably alterated tuffaceous material.

All types of residual breccias show sharp clast/matrix boundary, solution voids at the border and developement of blackening processes from the borders.

The ratio between clasts and matrix is variable (from 9:1 to 1:2).

Both differences in microfacies, fitting, size and rounding of the clasts and change in matrix types reflect the erosion of different parts of a carbonate platform (Fig.2.14 c).

Microfacies analysis: the microfacies analysis of the clasts highligts the occurrence of two main group of lithologies: 1) grey fenestral peloidal wackstone/packstone; boundstone; algal, oncoidal packstone/grainstone or rare (Tubiphytes) bafflestone often recrystallised; 2) dark-dark grey laminated limestone (with reddish levels), rich in cements, recrystallized. The first group of microfacies can be referred to typical facies of the underlying platform (Esino Limestone); the second to 'Calcare Rosso' facies. In addition, greenish shale fragments and well rounded clasts, exhibiting both reddish microspar and laminar/nodular paleocaliche often dolomitized, characterize the residual breccias. The clasts float within a reddish, fine graded, non-cohesive, dolomitized matrix (Fig.2.14 f). The recristallization processes prevent a detailed microfacies characterization. Matrix of the residual breccias overlying the Mt. Alino volcanoclastic deposits and in general of the neighbouring areas (Middle Seriana Valley) consists of reddish dolomitized microspar and green shale material. On the northern side of the Esino Limestone, the matrix consists of recrystallized fine-grained calcite.

The carbonatic clasts are well cemented, seldom fracurated and early diagenized. Different phases of cementation and fracturation (restricted to the clasts) can be recognized with the catodoluminescence analysis of the clasts. Therefore the source rocks experienced early fracturation and different conditions of cementation.

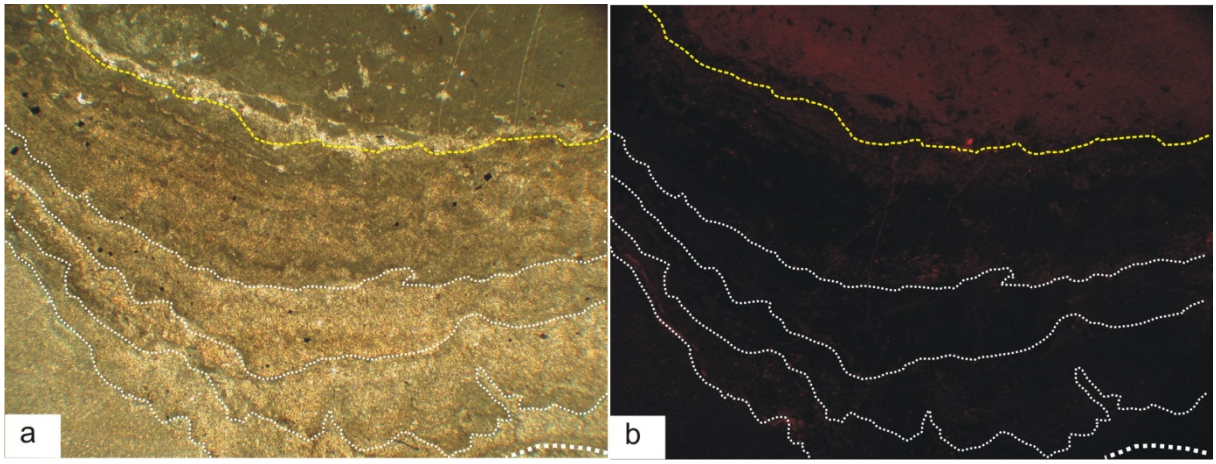

***Fig.2.15: a**- Photomicrograph (transmitted light) of clast of residual breccias with dark-grey pendant crusts made of recrystallized microbialitic envelops/cements; **b**- cathodoluminescent analyses an the same sample of a. The microbial rims are NL.*

Inception of gradual blackening as dark rims or thin lineation developed from edge to center characterize the finer-grained, often recrystallized, carbonate clasts.

Into the carbonate residual breccias (Mt. Pegherolo), millimetre-size dark-grey pendant crusts of microbialitic envelops/cements has been observed (Fig.2.10; 2.14 c; 2.15).

Distribution: the lens-shaped bodies of the residual breccias are widespread and overlain the inner platform facies of the Esino Limestone. Residual breccias has been observed also: on the northern margin (Mt. Pegherolo, Fig.2.10) of the Esino Limestone above reef-backreef facies at the base of the Tgrey facies; on the eastward margin of the Esino Limestone above the Mt. Alino volcanoclastic deposits; (locally) at the top of the Tred succession both on the southern and on the eastward margin of the Esino Limestone. The rapid thickness changes reflect the paleotopography conditions at the top of the underlying platform and the erosional nature of these deposits.

Volcanoclastic-carbonate breccias (Alino unit):

It consists of a mixed succession of volcanic to carbonate breccias, matrix to clasts (up to 35-40 cm in size) supported, with intercalated fine grained layers locally well laminated. The amount of the carbonatic clasts decrease from the base and slightly increase in the upper part.

Thickness: The maximum thickness (measured) of unit is about 40 m (Trevasco mining tunnel).

Outcrop area: The unit outcrops in the Seriana Valley, only in the Mt. Alino area. More complete section have been measured in the lower part of the Nossana Valley (2 km south-eastward from Mt. Alino) in the Trevasco mining tunnel but the lowermost part is not preserved.

Stratigraphic relationships: The unit lies with a tectonic contact on upper slope facies of the Esino Limestone and is overlain by residual breccias of the KLR. The upper boundary with the overlying deposits of the KLR (Residual facies) is marked by erosive surface.

Facies association:

In the Trevasco mining tunnel serie 5 facies associations (from the base to the top) are recognized (Fig.2.16):

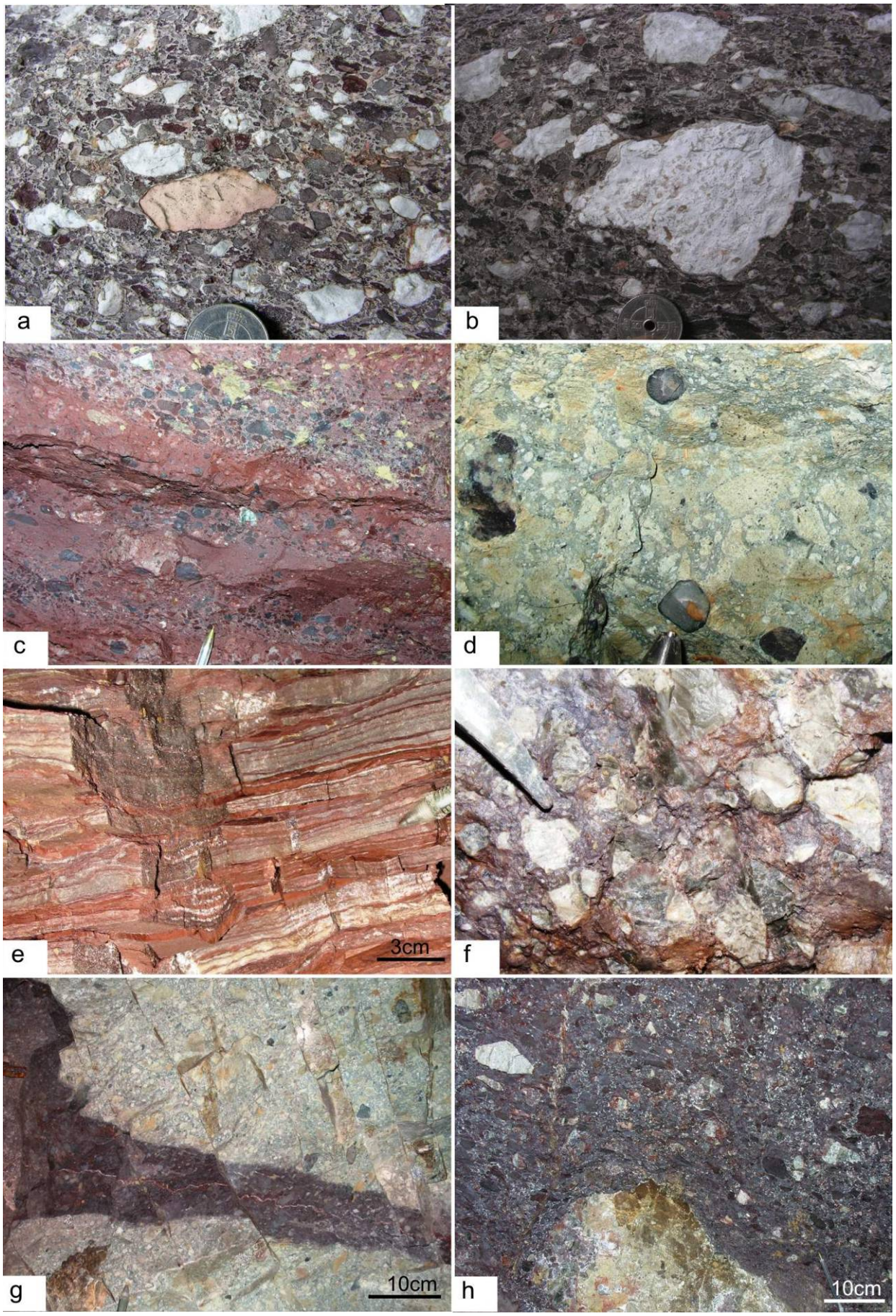
a
b
c
d
e
3cm
f
g
10cm
h
10cm

Fig.2.16: ***a****- volcanic clast with trachytic fabric due to the alignement of prismatic phenocrystals;* ***b****- quartz grain;* ***c****- lamination (Facies C) marjed by changes granulometrie, degree of recrystallization and layers rich in oxides;* ***d****- volcanic clast with vescicles and prismatic phenocrystals (undeterminables) in ashy altered matrix* ***e****- vescicles in a volcanic clast;* ***f****- carbonatic clasts made of pel-sparite in volcanic matrix. Altered clays coating cover evidence of dissolution at the border of the clast;* ***g****- Volcanics clats showing trachitic structure and dissolution features at the borders, surrounded by diagenetic sparry calcite;* ***h****- scanned thin section of lower part of Facies B. Clasts are surrounded by diagentic rims of isopachous fibrous radial calcite and porosity is filled by sparry calcite Carbonatic clasts (10-15%) are recrystallized and volcanic clasts (pumices) are very altered.*

Facies A – Breccia deposit made of centimetric volcanic and carbonate clasts, angular to rounded, matrix supported. Volcanic clasts are very altered, usually subrounded, light yellow in colour and constituted probably of both pumices and minor lavas. In the upper part carbonatic clasts increase in size and abundance (until 35 cm and 80%), whereas the volcanic clasts are smaller (centimetric in size). In the carbonate clasts are recognized: a) cements and microbial crusts (typical of the underlying upper slope facies); b) fenestral, laminated (stromatolitic?), oncoidal, peloidal fine grained limestone associated with crusts of 'coconut meat calcite' (of the inner/open platform domain); c)dark-grey recrystallized limestone, rich in cements and with reddish laminae (KLR deposits?). The clasts are often recrystallized in microsparite and show Liesegang ring formation. Thickness: 5.1 m

Facies B – Breccias deposit at the base shows normal gradation and a progressive decreasing both of carbonatic clasts and the matrix, in the middle a succession of decimetric layers alternated rich in volcanic and carbonatic clasts, in the upper part a composition made of volcic clasts with few carbonates (less than 30%) (Fig.2.16 b, h) The deposit is matrix supported except at the top of the lower part, clasts are rounded and centimetric in size. Volcanic clasts are very altered, light gray in colour and constituted probably mainly of pumices. The deposit presents isorientation of the clasts when matrix supported.

Thickness: 12.5 m

Facies C – Succession made of volcanic breccia alternated to fine laminated grained silts (Fig.2.16 e). Moving to the top the fine laminated grained silt gradually increases and the volcanic breccia disappears. The base of the breccia layers is erosive, whereas the top is usually transitional (few are sharp) and the breccias show a normal gradation with maximum size of 2 cm. Thickness of the breccia layer ranges from 25-30 cm to 2-3 cm to the top. The fine laminated silts present a well organised fabric to the top with an alternation of red and grey

colour millimetric laminations, whereas at the base the lamination is undulated, not well defined, red in colour. In the thin section, silts appear to be very recrystallized and the alternation of couplets of grey/red laminae correspond to alternation of prevaling carbonate/volcanic material. Depositional alternation is highligned by pressure solution resulting (locally) in stylolaminated fabric with non-sutured wispy parallel sets of dissolution seams. The breccias are made of rounded or subrounded clasts, mainly red lavas and scoria, whereas small yellow pumices are present at the top in thin (1 cm) layer.

Thickness: 6.2 m

Facies D – Fine-grained silts with lenses of volcanic breccias showing normal or reverse to normal gradation. Lenses are 20-25 cm thick and metric long and decrease in size to the top. The base is erosive, whereas the top boundary is gradual. The breccias are made of mainly rounded or subrounded pumices.

Thickness: 4.3 m

Facies E – Homogeneous fine grained silt with some lenses of volcanic to carbonate breccias, up to 10 cm thick, intercalated in the lower part (2-3 m from the base) of the layer. Sedimentary structures are not observed (Fig.2.16 c).

Thickness: 7 m (distributed into two layers: 3.2 m thick (lower); 3.8-4 m thick (upper))

Facies F - Breccia made of mainly carbonate clasts and rare volcanics. Clasts are angular, 4-10 cm in size, with scarce matrix (Fig.2.16 f). This facies can be related to phreatomagmatic activity or to avalanche. Thickness: 1.4 to1.8 m

Underlying Esino Limestone deposits

The Esino Limestone deposits observed both below Mt. Alino and Trevasco mining tunnel section consists of bioconstrued/microbial stabilized limestone and they are rich in centimeter- to decimeter-scale 'Evinospongie'(Jadoul et al., 1989) structures (Fig.1.6; 1.7) typical of the upper slope domain. The nucleous of some 'Evinospongia' cavities is infilled by shales probably due to Quaternary paleokarst. The rock is dolomitized, fracturated and recrystallized.

Microfacies analysis:

In thin sections, volcanic clasts, generally subrounded (rare subangular), are in a carbonatic matrix formed for late recrystallization of an original ashy matrix, testified by few remnants. Volcanic clasts are characterised by almost complete transformation of glass and phenocrystals. Lava porphyritic index varies from 20 to 30%. Phenocrystals are usually transformed in calcite except for a few quartz grains in Facies B, are characterised by a prismatic shape and by isorientation, sometimes showing a trachytic structure. We can observe the late growth of calcite inside the vescicles (maximum 20% - usually elongated). Glass is often very altered, showing a late growth of oxides and few microsparites.

In thin sections (Fig.2.17), *carbonate clasts* are angular to subrounded and 500 μm in size. Often recrystallized, and surrounded by isopachous calcitic rims (150 μm in size), they are characterized by:

a) isopachous calcite crusts, Problematica framestone, microbial boundstone;
b) fenestral packestone-wackestone, laminated (stromatolitic?) bounstone, pel-, intra-micrite, unsorted biosparite (gastropods fragments, foraminifera);
c) microsparite sligthly laminated.

Diagenetical features: growth of white isopachous rims (Fig.2.17h) of fibrous calcite 0.2-1 mm in size, orange in Cathodoluminescence analysis, surround the volcanic/carbonate clasts in the A (rare B) Facies.

The unit has been observed only in two points of the Mt. Alino (Seriana Valley) area, above upper slope facies of the Esino Limestone, aligned to south-eastern margin platform trajectory reconstructed. Despite its narrow outcrops areas, thickness and stratigraphic position (between Esino Limestone top and Residual breccias of the KLR) make them attractive.

The Mt. Alino deposits are the first evidence of a recovery of a volcanic activity in the central part of the Lombardy basin after the recess of the Upper Ladinian.

The carbonate clasts of the breccias show a different source: a) and b) are typical of the underlying Esino Limestone. In particular: a) bioconstrued upper slope facies; b) peritidal inner/open platform facies. c) can be referred to deformed, rich in cements, reddish facies of the KLR (Tred or Tgrey) deposits.

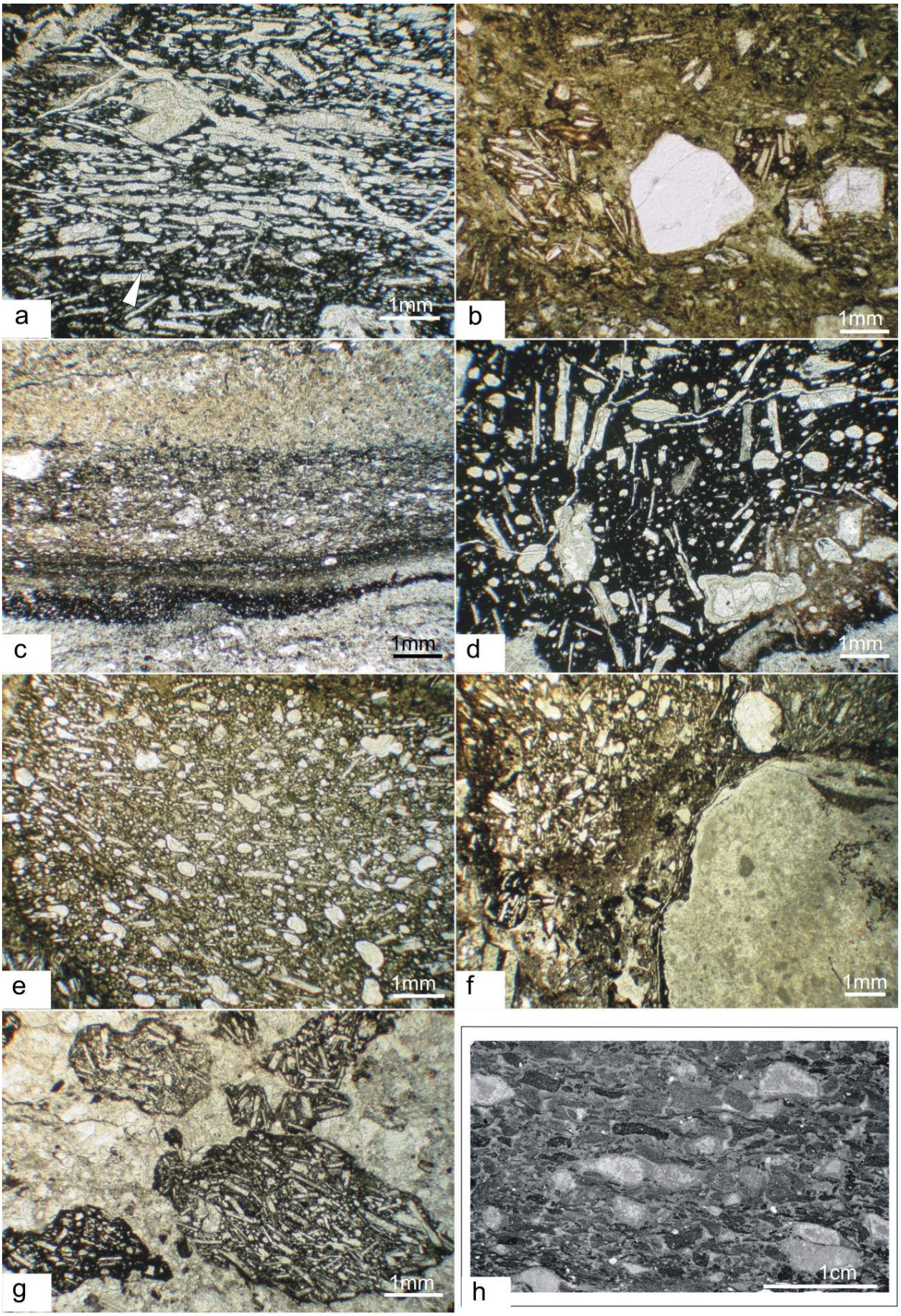
a
1mm
b
1mm
c
1mm
d
1mm
e
1mm
f
1mm
g
1mm
h
1cm

***Fig.2.17**: **a**- Breccias with very altered volcanic clasts constituted probably of both pumices and minor lavas and larger carbonate clasts (Upper part of Facies A); **b**- Particular of fenestral carbonatic clasts (Upper part of Facies A); **c**- Fine-grained silts with lenses of volcanic breccias (Facies D); **d**- Breccia with pumices and rare micritic carbonate clasts blackened at the border (Facies B); **e**- Laminated silt (Facies C); **f**- Breccia with angular, mostly carbonate clasts. This facies seem related to phreatomagmatic activity or to avalanche (Facies F); **g**- diagenetics structures due to redox reactions (Facies B); **h**- Volcanic breccias with decimetre-scale carbonate clasts often recrystallized (Facies A).*

The Esino Limestone deposits observed both below Mt. Alino and mining tunnel of 'Ribasso Trevasco' section consist of bioconstrued/microbial stabilized limestones and they are rich in centimeter- to decimeter-scale 'Evinospongie'(F. Jadoul, 1989) structures typical of the upper slope domain. Open/Inner platform facies outcrops 1-1.5 km northward and Tred facies has been described in the mining tunnel of Trevasco (Vachèe, 1966).

Karst on Esino Limestone Platform

The emergent Esino Limestone platform is a spectacular case study for an ancient polyphase karst related to subaerial exposure of the carbonate platform. The development of karst in correspondence to subaerial exposure of the top of the Esino Limestone has been described by Assereto, et al. (1977). The paleokarst effects on the overlying deposits of the Calcare Rosso (KLR) has been studied by Mutti (1992, 1994) that 1) explains the lens-shaped depression filled by these deposits as a tectonic-controlled feature or as a karst-processes related to incised-valley associated to a major eustatic cycle; and 2) focuses on the close relationship between senili tepees (Assereto & Kendall, 1977) and karsting at the top of the peritidal cyclic facies of the Calcare Rosso supposing a coeval development.

Vertical development, spatial distribution, and diagenetic evolution of the karst structures can be characterized (Fig.2.16). The Esino Limestone and the overlying deposits of the Calcare Rosso offer the possibility to observe the karst evolution on a well exposed transect from the margin to the inner platform in response to a sea level fall. The stratigraphic record at the top and above of the Esino Limestone show the overprinting of the multiple karst and diagenetic features associated to several unconformities.

Most of these discontinuity surfaces characterize the peritidal deposits of Calcare Rosso (Tred, Tgrey) and they are marked by both Terra Rossa layers and epikarst features.

Endokarst structures into the Calcare Rosso deposit are more rare. Instead, they are well developed into the massive (upper slope/reef facies) or bedded (inner platform facies) deposits of submergent top of the Esino Limestone.

It’s often trick to make a distinction between endo- and epi-karst in these paleokarst examples. Depth measured from paleosurface can be partly alterated by erosive processes (during exposure time or subsequent marine transgression); or similar deposits and depositional processes can be related to different burial conditions.

For example, collapse breccias at the top of the Esino Limestone has been interpreted as both endokarst and epikarst deposits. In the first case (endokarst), the breccias has been interpreted as due to collapsed caves because overlain by deformed beds and separated by subaerial exposure surface. In the second case (epikarst), the breccias deposits, preserved into surface depressions,

are due to collapse ceiling cavities or passages because bounded by sub-planar unconformity and overlaid by not deformed beds.

	Structures	***Size***	***Deposits***	***Process***
EPIKARST	Pitted and etched surface		Red/yellow dolomitic limestone, locally laminated (tuffaceus?)	Chemical/biological dissolution enlarging the sindepositional porosity
	'Swiss cheese'	cm-scale		
	Vertical veins and dyke	m-scale	Marine calcarenites	
	Network of fractures and cavities	m-scale	Flushed paleosols	
	Lens of collapsed material	m/Dm scale	Chaotic to matrix-rich mosaic breccias	? dissolution and superficial collapse
	Paleosols	m-scale	TR material	Pedogenetic processes
ENDOKARST	Composite deformed areas: Lower part: chaotic Upper part: sag struct. fractured and faulted	Dm-scale	Chaotic breccias Cave sedimentary filling Tilted strata	Coalescent collapse and suprastratal deformation
	Vertical shaft	m/Dm-scale	Crackle to matrix rich mosaic breccias	

Fig.2.16*: Resumptive table of characteristics of karst structures recognized at the top of the Esino Limestone and within 'Calcare Rosso' deposits.*

Epikarst (Fig.2.16)**:** The unconformity at the top of the Esino Limestone is characterized by dissolutional process related to subaerial exposure. Irregularly pitted and etched karst surfaces and several structures involving the upper few meters the Esino Limestone, can be observed both in the inner platform domain and in the upper slope-reef areas. Enlarged syndepositional voids and reactivated network of fractures are the major features.

In particular, in the southern margin, below the sharp (etched) boundary between the Esino Limestone and the overlying Calcare Rosso, the upper 4-5 m of the rocks show a ***'Swiss cheese'***

features (Fig.2.17 a) (Baceta et al, 2000). It's characterized by centimeter-scale (3-7 cm) dissolutional cavities (5-15 cm evenly spaced between them) filled by fine reddish limestone (Fig.2.17 b). Their distribution is favoured by hight porosity characterizing the upper slope facies of the Esino Limestone (Fig.2.17 c). When it's possible to recognize the original cavities, the dissolutional enlargement seem to be more pronounced toward the lower part of the cavities. The upper part of the re-opened voids is partially filled by reddish shales (probably related to upper unconformities) or by ankeritic dolomite. Often these cavities show geopetal structure. Lamination or gradation are not observed. Blackening processes interest the walls of the dissolution vugs for 2-3 cm in thickness (into the host rock) and seem to be gravity controlled.

Fig. 2.17: ***a-*** *distribution of dissolutional cavities ('Swiss cheese feature')at the top of the Esino Limestone (Strada Gamba section);they are partly filled by isopachous cements crusts, fine reddish limestone and late dolomite cements.* ***b-*** *dissolutional cavities showing geopetal structure, filled by fine reddish limestone and late Fe-dolomite (Strada Gamba section);* ***c-*** *distribution of the cavities is favoured by hight porosity characterizing the upper slope facies of the Esino Limestone (Strada Gamba section)*

Above the karsified top of the Esino Limestone, well developed epikarst structures can be observed associated to discontinuity surfaces characterizing the lower part of the Tred succession (Fig.2.18 a). In particular the transition between Tred transitional facies and Tred facies (above the southern margin of the Esino Limestone) is marked by a partially preserved paleosol. The lateral continuity of paleosol deposits is limited, whereas the dissolutional network of cavities, vertical and subhorizontal fractures developed below this discontinuity surface, characterizes the Tred transitional facies for several kilometers.

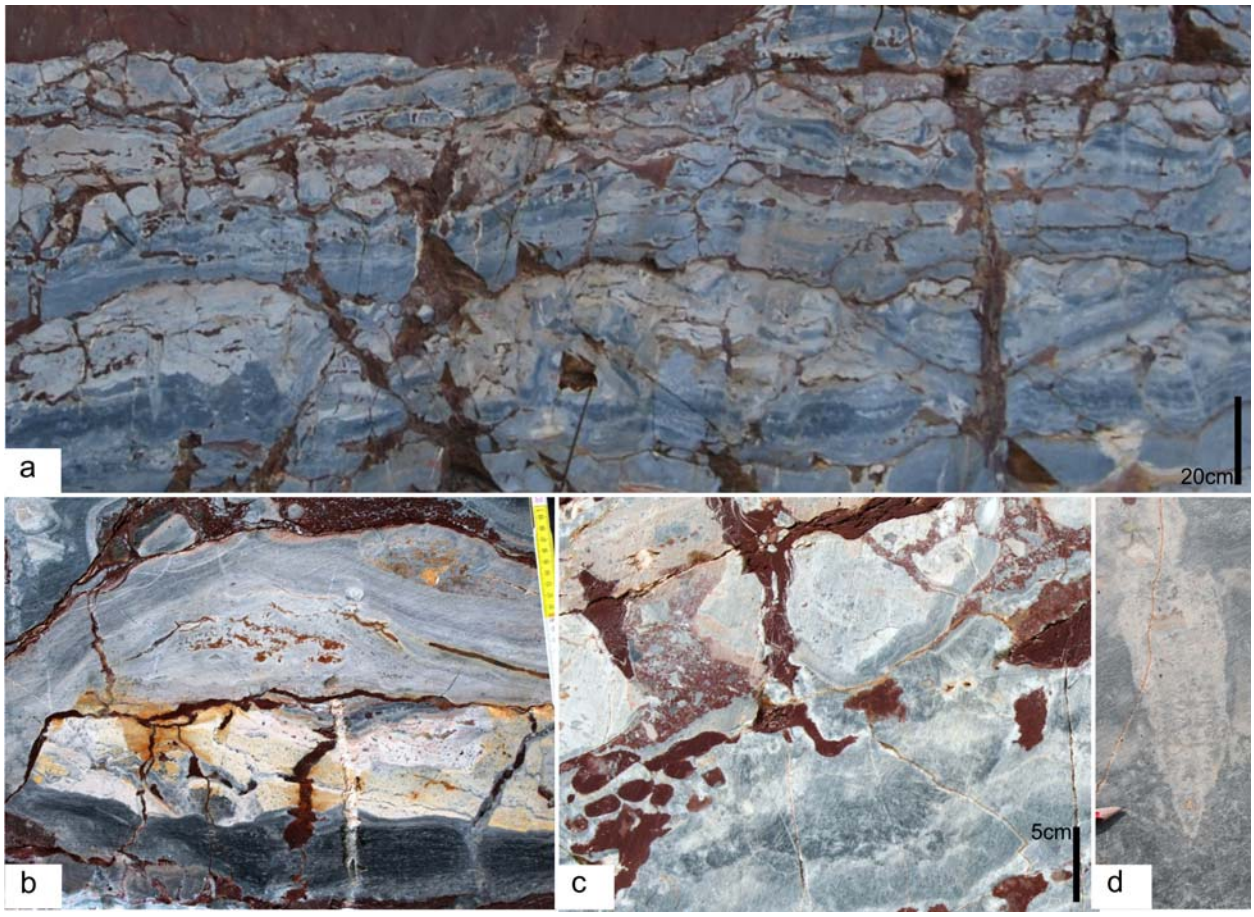

Fig.2.18*: *a- *paleokarst network of veins and cavities filled by Terra rossa and breccias deepening about 2 m below the Terra rossa paleosol;* ***b-*** *Terra rossa filling highlight the effects of the dissolution on peritidal, deformed in tepee (Assereto & Kendall, 1977) host rock (clast and internal sediment associated to senile tepee of Tred transitional facies, Assereto & Kendall, 1977 s);* ***c-*** *dissolution structures are filled by Terra rossa and/or rudstone with Terra rossa matrix. Veins and fractures are cut into early cemented clasts and internal sediments (with' raggioni' cements, Assereto & Folk, 1980) of a brecciated mature tepee layers;* ***d-*** *vein filled by cements and interal carbonate sediments cut peritidal deposits of Tred transitional facies and internal sediments (recrystallized in 'raggioni' Assereto & Folk, 1980).*

It forms a continuous meter-scale layer with high secondary porosity (Fig.2.18a). Dissolutional network characterize the upper two meters of Tred Transitional facies and consists of enlarged fenestrae and shelter porosity, small (up to 10 cm in size) pits, veins and fractures (Fig.2.18 b, c, d) and subhorizontal cavities (up to 8-10 cm high and 3-4 m wide).

This dissolutional network is filled by carbonate breccias in TR material (Fig.2.18 c), isopachous cements, clays and TR weathered material (often laminated) that replace almost the 40% of the host rock.

Above the disconformity at the base of the Calcare Rosso, the Tred deposits show large spectrum of paleokarst features often associated with sindepositional or diagenetical deformations. More

common epikarstic features are meter-scale sheet cracks with associated vertical veins and sedimentary dykes often 30-60 cm deep. Both polychromatic internal sediments with laminated limestone and shales and cements fill these structures.

In the **open/inner platform domain** the broad erosional processes prevent the preservation of paleosols but TR material deriving from paleosols are preserved into paleokarst structures.

The peritidal subaerial exposed rock contains numerous holes, tubes and enlarged joints ranging in size from centimeters to tens of centimeters. These features and fenestral to mouldic re-opened porosity and bedding parallel sheet-craks are filled by tuffaceous material and reddish limestone probably due to flushed soil or from exposure surface.

In the Mt. Trevasco the discontinuity surface at the top of the Esino Limestone is marked by ***lenses of carbonate breccias*** (Fig.2.19**)** up to 6 m thick, about 8 m large and 10-20 m spaced. The breccias are preserved into close-contour depressions and capped (locally) by dark-grey, bioclastic fine grained limestone (Lagoonal facies of Calcare Rosso) 0.3-1 m thick or by Tgrey facies. Beds both of the Lagoonal and of the Tgrey facies of KLR are not deformed.

Laterally and beneath to the lens of carbonate breccias, centimeter-scale matrix supported breccias are fluted in strata-concordant or vertical veins (up to 1 m in size) (Fig.2.19 c) deepening up to 3-4 m from the discontinuity surface at the top of the Esino Limestone.

The lens of carbonate breccia are (generally) clasts supported with deep-red (volcanoclastic?) matrix and the clasts consist of subangular to poorly rounded limestone of the Esino Limestone facies ranging from 2 to 50 cm in size. Layers of centimeter-scale matrix (rich or matrix) support breccias (Residual breccias of KLR, Fig.2.19) with poor rounded to rounded, blackened carbonate clasts and rare slab of paleosol are intercalated to close-packed breccias. Blackening processes involve carbonate micritic clasts from the border.

Centimeter-scale cavities (into the clasts) filled by reddish material and etched/pitted edges of the clasts testify an intense dissolutional processes (Fig.2.19 b).

The wide variety of the facies observed in the carbonate breccias lenses can be explained as result of two processes: a) mass flow transported material (residual breccias) from the surface to sub-surface passages and b) meters-scale ceiling collapse of open cavities and/or near surface passages. The lenses of carbonate breccias resulted from the polyphasic filling of epikarstic,

close contour depressions developed on the exposed and previous karsified top of the Esino Limestone.

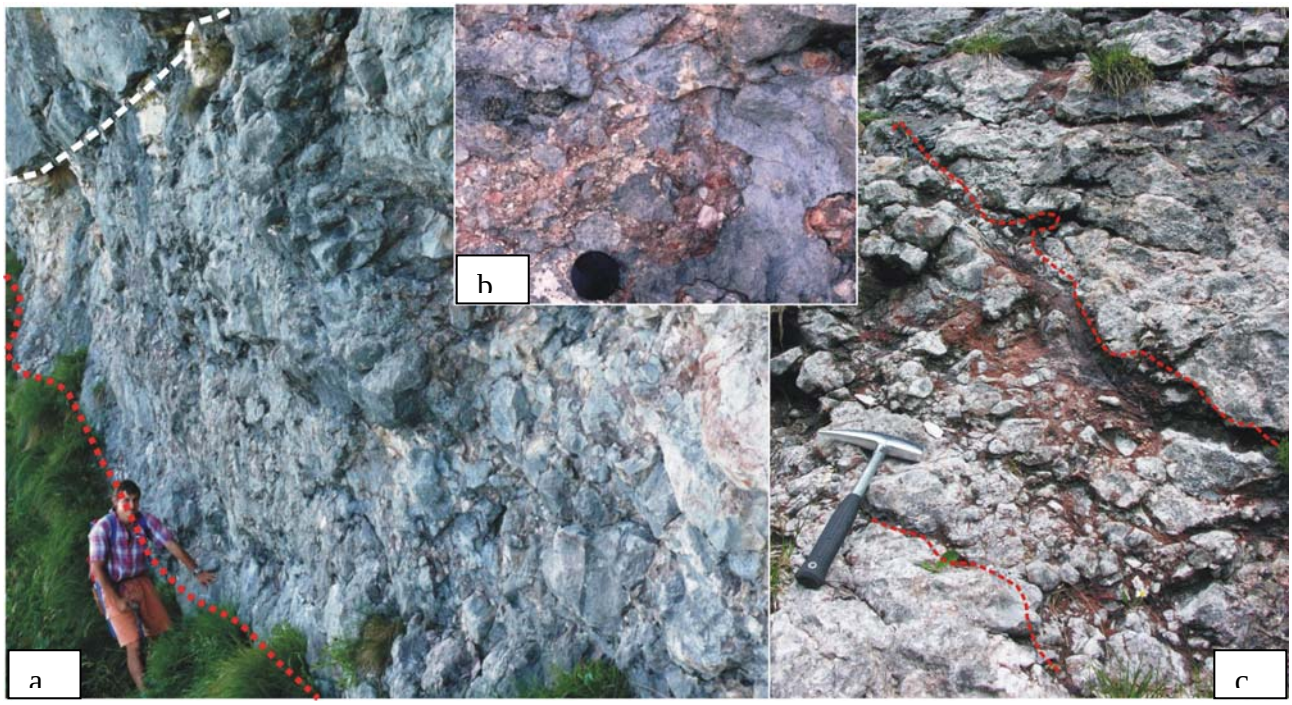

Fig.2.19: ***a-*** *Lens of carbonate breccias preserved into close-contour depressions and overlain by peritidal tepee-deformed Tgrey facies. Breccias are clasts supported with deep-red (volcanoclastic?) matrix and the clasts consist of subangular to poorly rounded limestone of the Esino Limestone facies;* ***b-*** *dissolutional features at the borders of angular to poor-rounded breccias clasts;* ***c-*** *matrix supported breccias are fluted in vertical (or strata-concordant) veins deepening up to 3-4 m from the discontinuity surface at the top of the Esino Limestone.*

Endokarst (Fig.2.16): three main cathegories of endokarst deposits and structures have been recognized at the top of the Esino Limestone and into the overlying deposits of the Calcare rosso: Veins, sedimentary dykes, fractures; cavities; coalescent collapse breccias.

1) Veins, sedimentary dykes, fractures: these features are widespread on the massive upper slope deposits at the top of the Esino Limestone but were observed also into the overlying peritidal deposits of the Calcare Rosso (Tred).

From the unconformity at the top of the Esino Limestone, veins and sedimentary dykes cut into a underlying upper-slope deposits (of the Esino Limestone) reaching 7-8 m in depth (Fig.2.17 a,2.20 a). Preliminary field measurements highline their preferential parallel orientation to the hypothesized direction of the southern platform margin.

Veins and sedimentary dykes present a complicated polyphasic filling history due to subsequent karstic reactivation. Centimetric crusts of isopachous (marine) cements cover the walls; grey marine grainstone with rare bioclasts and fine reddish limestone (partially) fill the secondary porosity; further stages consist of shales seeped trought fractures from overlying unconformity In fact, part of the major structures were reopened by dissolution processes during subsequent subaerial exposure events and filled by flushed materials headed by syndepositional fractures. These structures, probably cut into underlying deposits from the top of Tred succession, are 10-15 cm in size and filled by millimeter- to centimeter- breccias with reddish matrix support and recrystallized carbonate clasts (often blackened). The boundaries between different filling materials are marked by dissolutional features.

2) Cavities (Fig.5): a peculiar zone from 10 to 20 m below the top of the reef-upper slope facies of the Esino Limestone are characterized by large cavities up to 1.7 m in size, partly filled by marine mammellonary structures 'Evinosponge' -like (Frisia et al., 1989). The bioconstrued reef-upper slope facies of the Esino Limestone are a very porous system but porosity decreased rapidly for abundance of early cementation. These large scale reef cavities are part of a complex network of veins, cavities and subhorizontal pipes connected to subaerial exposure surfaces. Cavities, stabilized by recrystallized laminated microbial envelops are partly filled by alternations of microbial films (Russo, 2006) and isopachous cements (10 to 35 cm thick). Millimetric to centimetric crusts of cave calcite is the more internal concentric filling layer; reddish limestones and unconsolidated Terra Rossa deposits partly fill the cavities.

Part of these cavities show uncomplete filling. The conctact with host rock is irregular and blurred, locally sharp. The 'host rock' is characterized by intense recrystallization in dark-grey microraggioni, irregular thin microbialitic envelops and sparry white dolomite. Intensive recrystallization and superimposition of polyphasic diagenetic conditions complicate the interpretation of these cavities: nature and timing of alteration and the effects on the microbial (?) envelops have not yet been understood.

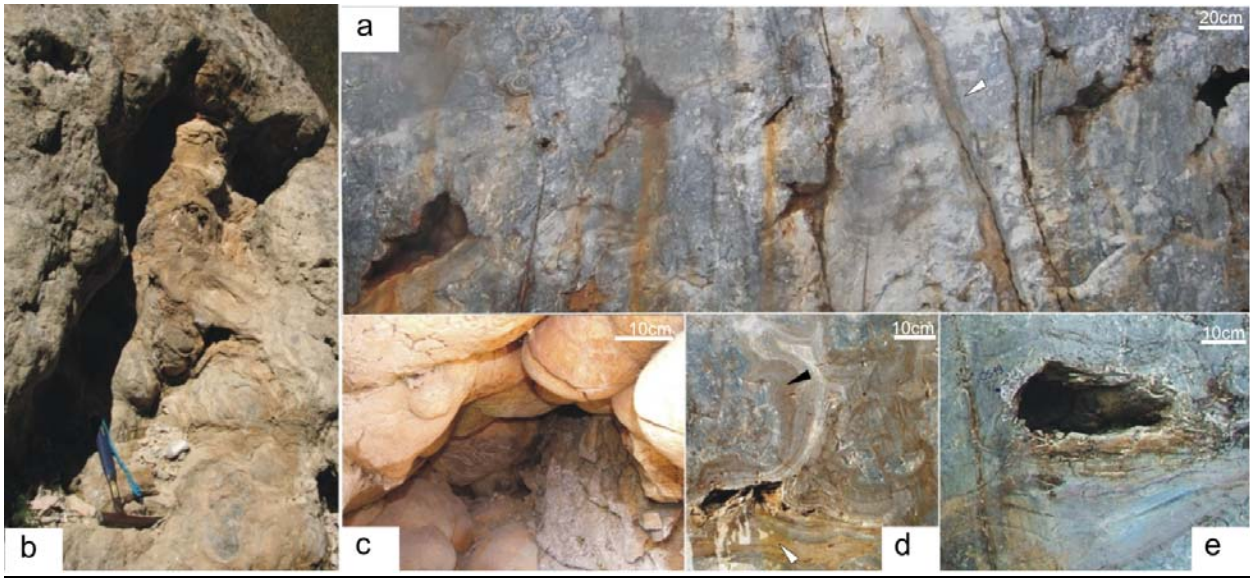

***Fig.2.20**: **a-** Porous network of sedimentary dykes(white arrow) and large cavities characterize the upper 10-20 m of bioconstrued reef-upper slope facies of the Esino Limestone (Strada Gamba section); **b-** Large cavity evinospongia-like with mammellonary crusts; **c-** Cavity with mammellonary crust of isopachous cements on the walls; **d-** Cavity are partly filled by recrystallized, laminated microbialitic envelops (dark arrow), reddish limestone (white arrow) and unconsolidateTerra Rossa materal at the nucleous; **e-** Wheatered microbial envelops in the lower part of the cavity.*

3) Coalesced, collapsed-karst*:* it consist of meter- to decameter-scale karst structures involving both the upper meters of the Esino Limestone (Mt. Arera; Mt. Vaccareggio; Parina valley) and the Calcare Rosso deposits (Mt. Trevasco, Pegherolo massif). These collapse karsts can be locally stacked up or coalescent. From the reef to the open platform domain frequency and size of these structures increase, decreasing to the inner platform domain. In the Calcare Rosso deposits, different facies correspond to different morphology of the karst structures .

***Coalesced collapsed-paleocave system with associated suprastratal deformations:** Mt.Arera – Mt. Vaccareggio*

Coalesced, collapsed-paleocave system has been recognized in Mt. Arera and Mt. Vaccareggio, in the inner/open platform domain of the Esino Limestone. In Mt. Vaccareggio the upper part of the collapsed structure is not preserved and the only well-preserved example of coalesced collapsed-paleocave system with associated suprastratal deformations outcrops in Mt. Arera, 25-30 m thick and up to 10 m wide. This collapsed structure involve Tred facies of the Calcare Rosso deposits and well bedded facies of the top of the Esino Limestone.

The architecture of the Mt. Arera paleokarst system can be divided into two zones (Fig.2.21 a,b): lower collapsed and upper deformed zones.

Lower collapsed zone (Fig. 2.21 *b)*: it consists of massive chaotic breccias. The definition of the lateral boundaries (walls of the paleocave) of this structures is complicated because the transition between host rock and collapse breccias is not sharp: a gradual increase of fracturing and deformation can be observed.

Moving from the breccias deposits to the host rock in the collapsed zone all the basic cave-collapsed facies can be recognized (Loucks & Mescher, 2001) (Fig. 2.21 b):

-coarse clasts chaotic breccias: they are characterized by a mass of a very poorly sorted granule- to boulder-sized chaotic- breccias with clasts approximately 0.2-1.5 m long. Two main lithologies of the clasts were observed: grey to light brown peritidal, bioclastic limestone of the upper Esino Limestone and dark grey, cement-rich limestone of the overliyng Tgrey facies more common upward. Breccias are commoly clasts supported.

These breccias are interpreted as collapse-breccia cavern fill produced by ceiling and wall collapse.

- centimeter to decimeter-grained chaotic breccia: mass of clasts-support moderately sorted granule- to cobble-size clasts with vary amount of matrix. Deposits can be graded.

- carbonate cave sediment with chips, slabs and blocks often deposited in lenticular strata: collapsed and tilted m-scale strata surrounded by chaotic breccias and overprinted by crackle breccias; in the upper part of Mt. Arera section the tilted strata form an antiformal structure.

-disturbed host rock: the bedding continuity of the host rock can be recognized but it is disturbed by folds and offset by small fractures and faults.

-undisturbed host rock

The lower zone could correspond to single large paleocave but the complexity of the structure and the lack of a ordered distribution of the facies could be interpreted as outcome of polyphasic collapse of multiple staked paleocaves/passages.

The boundary between lower collapsed zone to the upper deformed zone of the karst structure is not sharp but is a transitional area corresponding to the boundary between Esino Limestone and Tgrey deposits marked by a discontinuous and folded layer (20-50 cm thick) of Terra Rossa reworked deposits.

Upper deformed zone (Fig. 2.21 *b)*: it consists of a large sag structures containing faults and fractures.

The strata (Calcare Rosso deposits) are less chaotic that lower zone and the bedding continuity is partly preserved. The strata are characterized by crackle to mosaic to matrix-rich breccias (preserved into veins and stratabound layers). The degree of deformation increase toward the

middle part of the sag, where the disturbed host rock are offset by faults and partly collapsed and decrease upward.

Upper deformed zone is overlain by undeformed well bedded deposits of the Breno Fm.
Also the lower collapsed zone is delimited at the base by undeformed bedded deposits of the Esino Limestone. The whole coalescens collapsed structure, delimited by undeformed deposits measure 25 m in height and several meters in size. Near this major coalescens collapsed structure, collapsed-structures up to 10 m deep outcrops .
The outcrop conditions don't permit observation of their pattern in map view: commonly this structures displaying a rectilinear pattern (Loucks 2007).
In the Mt. Vaccareggio another collapsed-paleocave system area can be observed but only part of the lower zone of the collapsed structure is preserved. The deposits are characterized by coarse chaotic carbonate breccias, clast or matrix supported, and disturbed host rock in the upper part, with vertical and subhorizontal fissures filled by fine grained breccias and shales. Rare strips of internal sediments consisting in dark laminated marls (Jadoul personal comunication) are preserved.

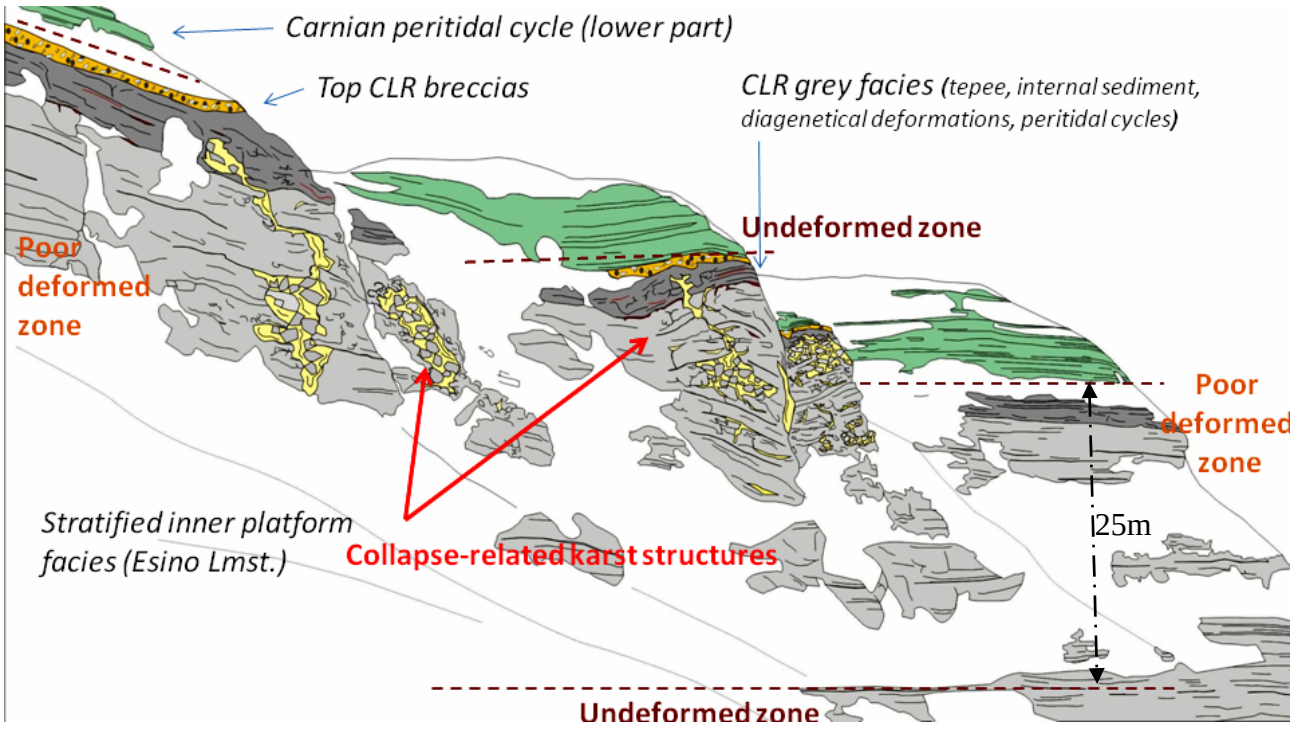

***Fig. 2.21a*:** Schematic general view of the collapsed- karst system characterizing the top of the Esino platform and the lower poart of the Calcare Rosso (KLR)

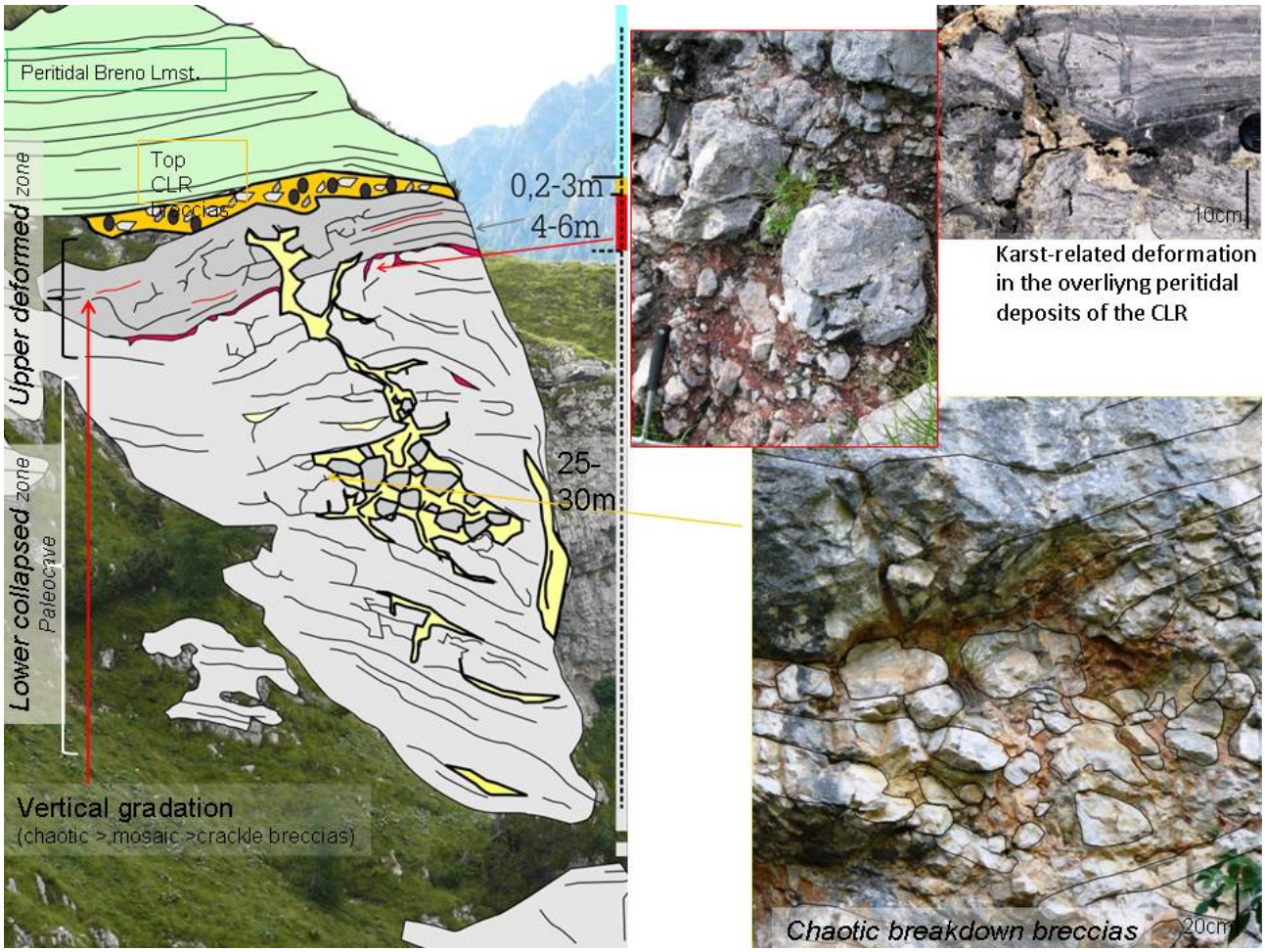

Fig. 2.21b: *Most developed collapsed structure outcrop in the Mt. Arera. Detail of the breccias filling the cavities between the rotate clasts.*

Vertical collapse shaft: *Trevasco, Pegherolo – Remuzzi quarry*

Vertical collapse shafts has been recognized in the Tgrey facies of KLR both in Trevasco Mt. and Brembana platform and into the transitional deposits at the base of Tred facies that outcrop in Remuzzi quarry (Parina valley).

In the Brembana platform (Fig.22), these karst structures sink into the Tgrey well bedded facies for 15-20 m with size ranging from about 0.5 to 2.5 meters. The same vertical shaft (Fig22c) is often characterized by several thicker compartements connected by thin pipes or fractures. In the Trevasco Mt. they reach 5-6 m of vertical development into the Tred transitional facies at the base of a Remuzzi quarry.

Crackle breccias and mosaic or (rare) matrix-rich mosaic breccias with yellow dolomitized fine matrix (Fig.22 a,b) are the predominant facies and the conctact with the host rock is often difficult to define. The clasts, 5 cm to 60 cm in size, consist of peritidal, oncoidal rich, fenestral

or stromatolitic limestone, early dolomitized (Fig.22 b). These features and the lack of granular and fossiliferous marine material suggest a vadose genetic conditions.

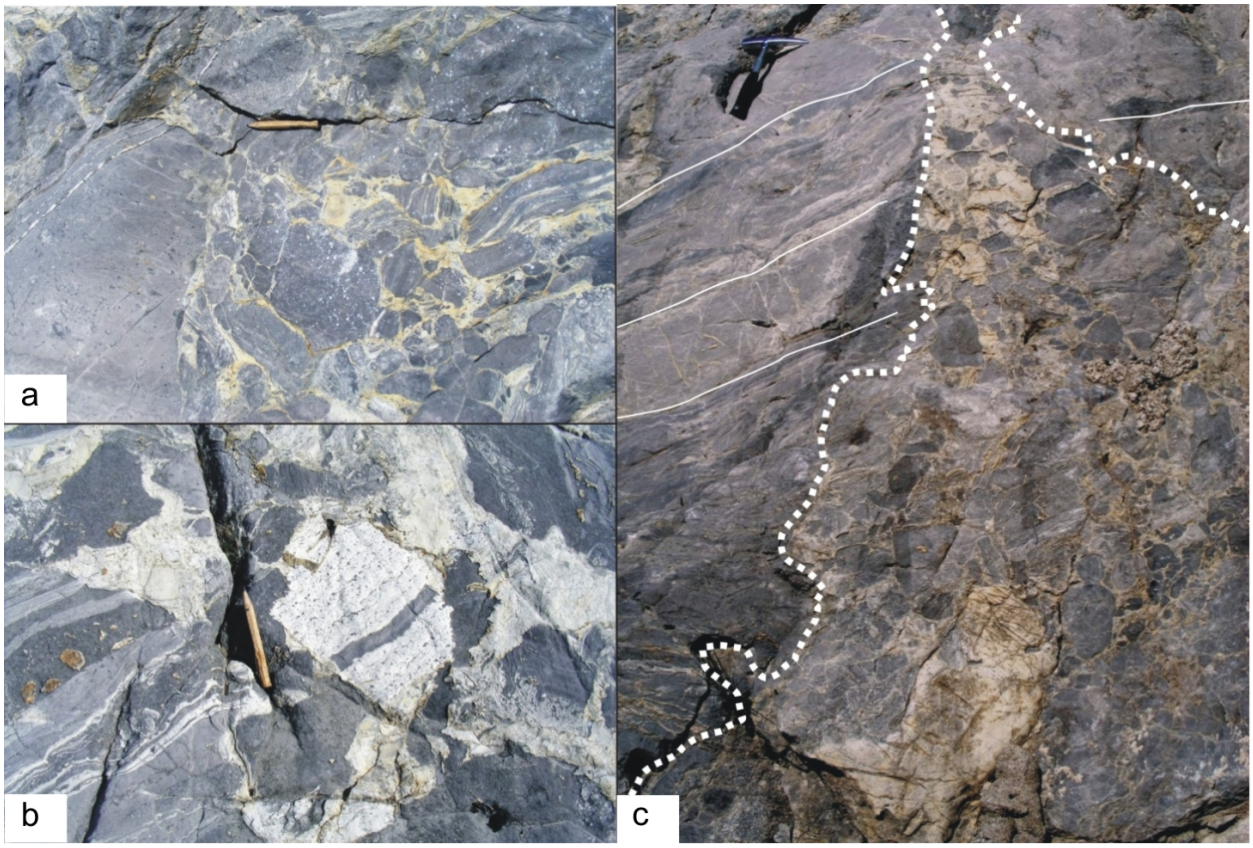

Fig. 2.22: a- *matrix-rich crackle breccias filling V-shape fracture;* ***b-*** *Breccias clasts are characterized by intertidal facies with penecontemporary dolomitization;* ***c-*** *vertical shaft filled by poor rounded carbonate clasts. Micritic clasts are often blackened.*

	Tred	Tgr	L	R	Thick. (m)	Varia b.	ESI	KLR		Depht (m)
INNER PL.	x		x	X	0,5<<12	hight	K, (V),D	D		Up to 5-8m
OPEN PL.	X	X	x		6<<20		K, D	K, (V,D)		Up to 25m
REEF/UPPER SLOPE	X			X	1,5-60	low	V,D	Trz.	Tred	Up to 10-15m
								K, D	D,V, K	

Fig. 2.23: *Resumptive table both of karst structures and Calcare Rosso facies distribution above Esino Limestone.*

2.2

DISCONTINUITIES ASSOCIATED WITH THE CALCARE ROSSO EVENT

Discontinuity surfaces in the sedimentary record

Discontinuity surfaces are features in the sedimentary record related to breaks in sedimentation (*hiati*) and reflect reactions of sedimentary system to rapid and drastic environmental changes (Heim, 1924; Brombley, 1975). Their identification and interpretation are of significance for palaeoenvironmental and palaeogeographic reconstructions, diagenetical interpretations, sequence stratigraphy, and petroleum reservoir assessments (Budd et al., 1995; Clari et al., 1995; Sattler et al., 2005; Chow & Wedte, 2010).

Discontinuity surfaces have been studied by numerous authors (e.g. Heim, 1924; Shinn, 1969; Bromley, 1975; Marshall & Ashton, 1980; Riding & Wright, 1981; Allan & Matthews, 1982; Wright, 1994; Clari et al., 1995; Fouke et al., 1995; Hillgartner, 1998; Immenhauser et al., 2000; Wilson & Taylor, 2001; Immenhauser & Scott, 2002), but little research has been done yet to demonstrate how characteristic features such as surface morphology, petrography and facies change across a discontinuity and how geochemistry changes spatially along the surface (lateral variability) (Sattler et al., 2005; Chow & Wedte, 2010). Ignoring the lateral variability of a discontinuity surface can result in poor correlations of spatially separated sections and misinterpretations in sequence stratigraphy (Kauffman et al., 1991). The impact of a given discontinuity surface on reservoir compartmentalization strongly depends on its lateral extent and lateral variability, and on the associated diagenesis of underlying rocks.

Criteria for the recognition of discontinuity surfaces include geometrical relationships, facies contrasts, depositional and diagenetic features, and biostratigraphic data (Clari et al., 1995; Hillgartner, 1998).

Subaerial discontinuity surfaces differ from other discontinuity surfaces for a variety of palaeokarst and palaeosol features characterizing the underlying profile (Esteban & Klappa, 1983; James & Choquette, 1984; Goldstein et al., 1991; Wright, 1994), and they testify intervals characterized by markedly different digenetic histories.

The **methodology** used for the study on the Esino Limestone coincides with the unconformity-palaeokarst analysis proposed by Esteban (1983) following different steps: (a) unconformities mapping; (b) analysis of exposure profiles; (c) interpretation of exposure environments; and (d) analysis of underlying and overlying rocks to recognize immediately pre- and post-unconformity events.

Discontinuity surfaces related to the Calcare Rosso event

The Ladinian-early Carnian succession of the Lombardy basin records various discontinuities. This chapter focuses on the lateral extent and morphology of these surfaces formed as a consequence of a regional sea level fall at the top of the Esino Limestone and during several exposure events characterizing the deposition of the overlying Calcare Rosso (sl.) succession (in particular in the lower and upper part). Petrographic facies and geochemical changes across these discontinuities have been analyzed. The spatial and temporal distributions of surfaces are compared in several physiographic domains (inner platform, open platform, margin-upper slope). Field observations, combined with petrographic data, suggests that a few surfaces are laterally extensive. In contrast, a large number of laterally limited surfaces (< 0.5 km) are related to locally active processes. Moving to the open and inner platform domain the number of the discontinuity surfaces decrease rapidly and several surfaces merge into one.

The Middle Brembana valley, the Arera, Trevasco and Pegherolo areas provide optimal outcrop conditions for the identification of the more important unconformities from the top of the Esino Limestone to the top of the Calcare Rosso. Lack of major tectonic structures and several quarries lead to detailed characterization of these surface, of their lateral extent as well as the sedimentological analysis of the associated deposits.

The studied areas belong to different paleogeographic domains of the Esino Limestone: southern, eastern and northern margin platform; open platform and inner platform.

Surface		Position	Nature	Facies change
UPPER SLOPE - REEF domain				
TK		*Between* KLR (Tred)/BRE Fm.	Erosional-(*tuffaceous material)*	*peritidal deformed (tepee) lmst. to peritidal lmst.*
Internal (major)	**K2**	*Within* KLR *(Lower part)*	Erosional -*TR deposit*	*Not significative changes*
	K1	*Within* KLR *(Between Tred/Tred transitional)*	Erosional-*Paleosols*	*Increase in Vol% of TR material*
TE		*Between* ESI margin/KLR (Tred)	Angular, Erosional-(*mm-scale breccias)*	*Massive lmst. to peritidal deformed lmst.*
OPEN PLATFORM domain				
TK		*Between* KLR (*Tgrey-Residual breccias)/* BRE Fm.	Simple	*intraformational breccias (or peritidal deformed lmst.) to peritidal lmst.*
Internal K		*Within* KLR *(within Tred or between Residual breccias/Tgrey)*	Erosional *(locally with TR material)*	*Not significative changes or peritidal deformed (tepee) lmst. to intraformational al breccias*
TE		*Between* ESI open platf./KLR (*Tgrey-Residual breccias*)	Erosional	*bioclastic lmst.to peritidal deformed (tepee) lmst (to intraformational breccias)*
INNER PLATFORM domain				
TK		*Between* KLR (Residual breccias - Tgrey)/BRE Fm	Simple (*–tuffaceous material)*	*intraformational breccias (or peritidal deformed lmst.) to peritidal lmst.*
Internal K (rare)		*Within KLR (Between Residual breccias/Tgrey)*	Erosional	*peritidal deformed (tepee) lmst. to intraformational al breccias*
TE		*Between* ESI margin/KLR (Residual breccias)	Erosional	*bioclastic lmst.with sheet cracks and tepee to intraformational breccias or to peritidal deformed (tepee) lmst.*

Fi.g2.24.: *Summarizing table of the characteristics of the major Discontinuity surfaces at the top of the Esino Limestone and within Calcare Rosso deposits, above different paleogeographic domains.*

Discontinuity surfaces above the platform margin area (Middle Brembana valley):

In the Middle Brembana Valley the transition between Esino Limestone and Tred Calcare Rosso (KLR) deposits is marked by a major unconformities (**TE**) and another important surface (**K1**) into the KLR (Tred) deposits eight meters above. Furthermore several discontinuity surfaces characterize the KLR (Tred) succession. In particular, has been take account of both **K2** in the lower part of KLR, used as marker for the quarry activity and discontinuity surface at the top of the KLR (Tred) succession (**TK).** The physical correlations of the major erosional surfaces and the presence of tuffaceous/terra rossa layers represent the only tools for correlations across different environment of the Esino Limestone (Assereto et al., 1977).

These discontinuity surfaces are traceable for a few km then they merge into two surfaces: at the base (TE, K1, K2) and at the top (TK) of the KLR deposits (fig.2.24).

In this area, moving from the southern depocentral zone of the Tred (KLR) deposits northward or eastward, from upper slope to open platform facies of the underlying Esino Limestone (Fig.2.24), the thickness Tred decrease from 60 m (Cadei Quarry Section) to 1.5 m (Paglio Pignolino Section) in 1.4 km. This thinning trends, well exposed in this zone, is typical of the all margins of the Esino Limestone except for the northern margin.

Both thickness decrease and facies transition of KLR deposits, lead to a reduction of the number and a change in the characteristics of discontinuity surfaces.

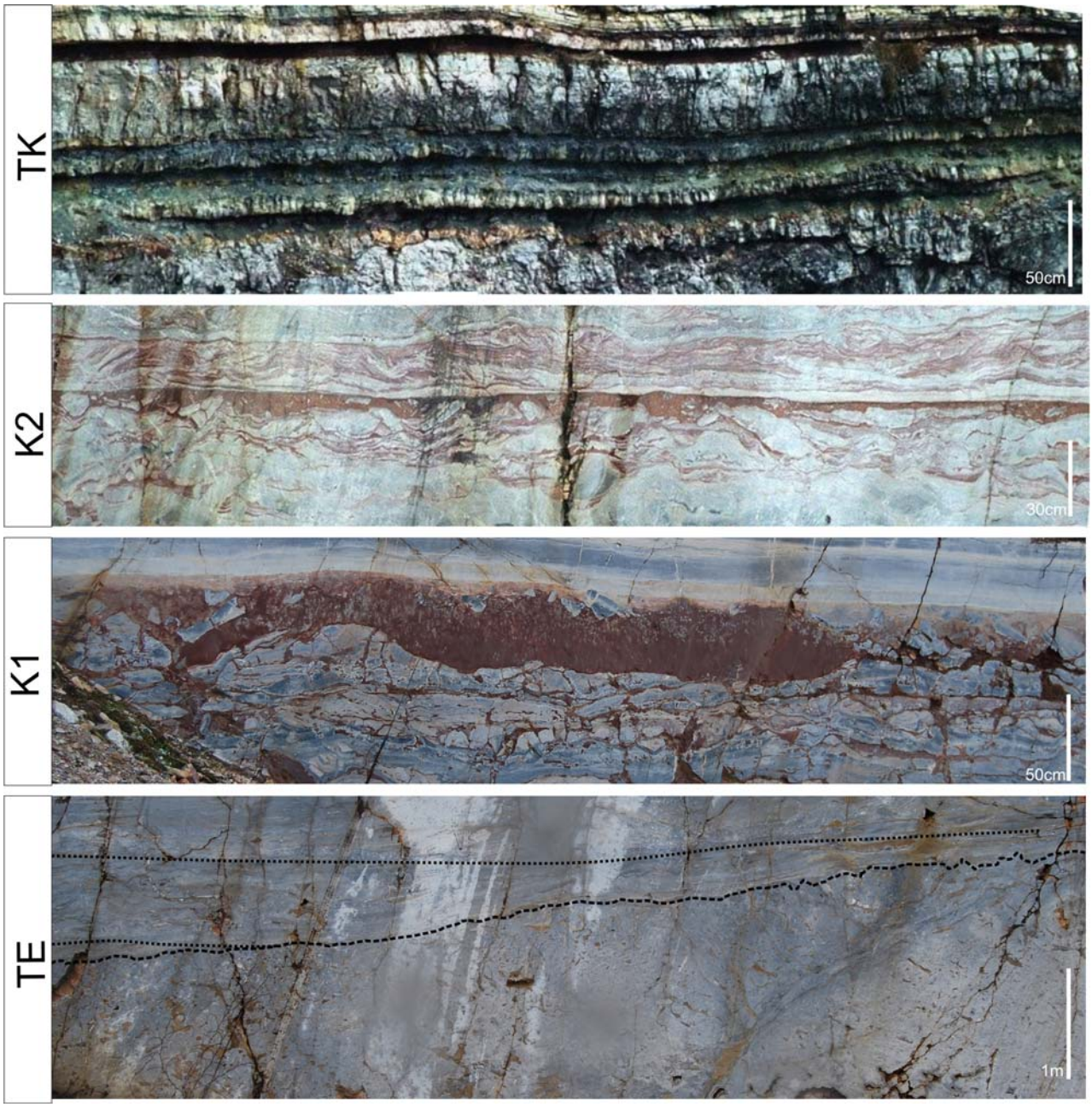

Fig.2.25: *For major discontinuity surfaces (D.S.) characterizing the regressive facies of Calcare Rosso (Tred) above the platform margin area (Esino Limestone).* ***TE****: disconformity between massive upper slope facies of the Esino Limestone and peritidal, deformed in tepee Tred (transitional) facies of the KLR;* ***K1*** *and* ***K2****: unconformity within Tred succession, characterized by (respectively) by TR truncated paleosol and underlying paleokarst network (K1) and TR material with dispersed dolomitized intertidal angular clasts;* ***TK:*** *subaerial exposure sub-planar surface characterized by hardened crust at the top of loferitic breccias with dolomitized clasts and tuffaceous level.*

UPPER SLOPE-REEF DOMAIN:

Discontinuity surfaces at the top of the Esino Limestone

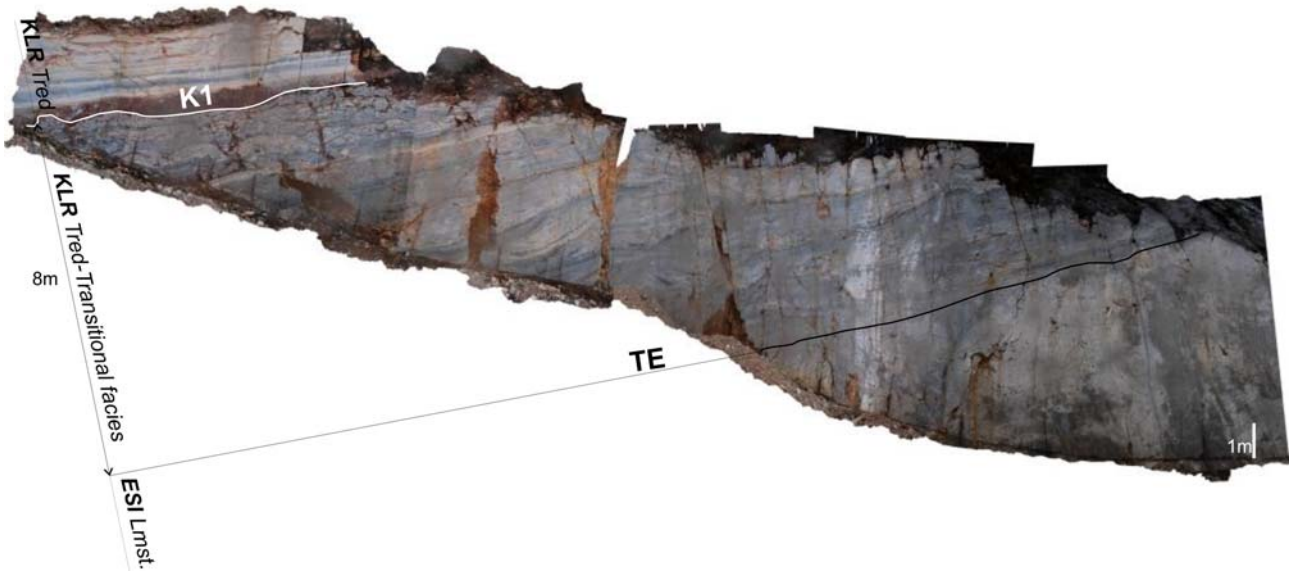

Fig. 2.26.*: panoramic view of the discontinuity surfaces (*TE *and* K1*) characterizing the transition between massive upper slope-reef facies of the Esino Limestone and well bedded peritidal deposits deformed in tepees of 'Calcare Rosso' (KLR, Tred-Tred transitional). Tred transitional facies differ by Tred facies for lower abundance of TR material.*
TE *disconformity marks the top of Esino Limestone deposits.* K1 *consists of paleosol deposit and marks the transition between Tred transitional and Tred facies.*

TE disconformity *(Fig2.25; 2.26)**:*** The TE disconfomity is a slightly irregular, sub-planar surface due to subaerial exposure and subsequent trasgressive flooding. This surface caps massive microbial boundstone of the Upper slope of the Esino Limestone and it's overlain by onlapping ciclotemic bedded and deformed fenestral packstone.
Intraclastic rudstone grades up into reddish limestone often with disperse carbonatic clasts and millimeter-scale vugs filled by sparry calcite, bound the subaerial exposure surface. These discontinuous deposits are preserved as millimeter- to centimeter-scale crusts or into small depressions leveling the top of underlying rocks, and they are erosion truncated by subsequent marine transgression.
A variety of sedimentary structures and fabrics interpreted to have formed during subaerial exposure occurs down to a depth of about 4-5 m below the unconformity.

From this surfaces, sedimentary dykes, filled with polyphasic reddish and marly limestone and marine grainstone- rudstone more or less laminated, cut into the underlying facies. These sediments fill the pervasive sindepositional network of evinosponge and cavities characterizing the microbial mounds and the cemented veins and fractures parallel to the margin, reopened by dissolutional processes. The centimeter-size solution vugs, filled (or partially filled) by reddish sediments and evenly spaced into the upper 3-4 m of rocks underlying the disconformity, form a 'Swiss cheese' (Baceta et al., 2001) feature. Just below (0.5-1 m) this surface, these cavities show a geopetal fill with reddish or granular sediments in the bottom and isopachous cements at the top. The remaining voids are filled by spatic calcite or more common late dolomitic cements. Blackening processes interest the walls of the dissolution vugs for 2-3 cm in thickness (into the host rock) and seem to be gravity controlled. The TE surface correspond also at the upper limit reached by dolomitizing fluids.

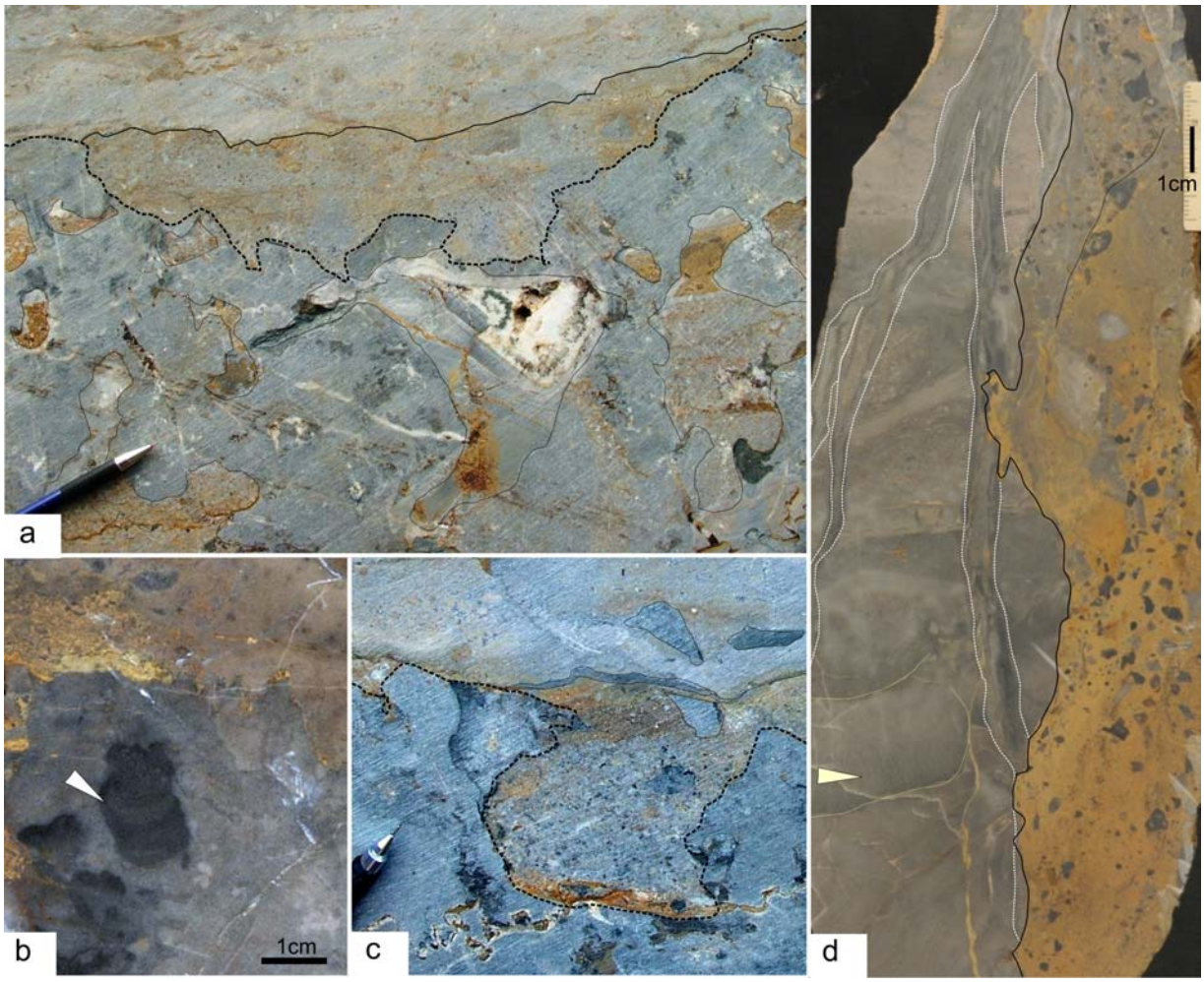

Fig. 2.27: ***a-*** *centimetre-scale solution vugs that form a typical Swiss-cheese structure (Baceta et al., 2001) of the upper 3-4 meters of the massive facies of the Esino Limestone; cavities show*

polyphasic filling: reddish limestone, carbonate micro-breccias, spatic calcite or more common late dolomitic cements. Lower part of the cavities show blackening processes; small depression on the TE surface are filled by intraclastic rudstone; ***b****- the sample shows dark-grey pendant cements filling cm-scale cavity just below TE surface;* ***c****- Intraclastic rudstone grades up into reddish limestone often with disperse carbonatic clasts and millimeter-scale vugs filled by sparry calcite, bound the subaerial exposure surface and they are preserved in depression. Thin clay coating marks the upper boundary of these deposits;* ***d****- two generations of fractures (outlined with white ink) are cut into Tred transitional deposits and deep below TE surface. An older system of fractures, filled by early microbial controlled cements (marine?) is cut by younger fractures filled by matrix support carbonate breccias. Breccias consists of millimeter-size, rounded to poorly rounded and often blackened clasts in reddish carbonate matrix. Arrow point to pendant cements (recrstallized in' raggioni', Assereto&Folk, 1977) in of host rock.*

Discontinuity surfaces within 'Calcare Rosso' (Tred)

K1 unconformity *(Fig.1;2)****:*** less of 10 meters above the first (TE) disconformity, the sedimentary record is characterized by the K1 sharp, sub-planar, subaerial exposure unconformity.

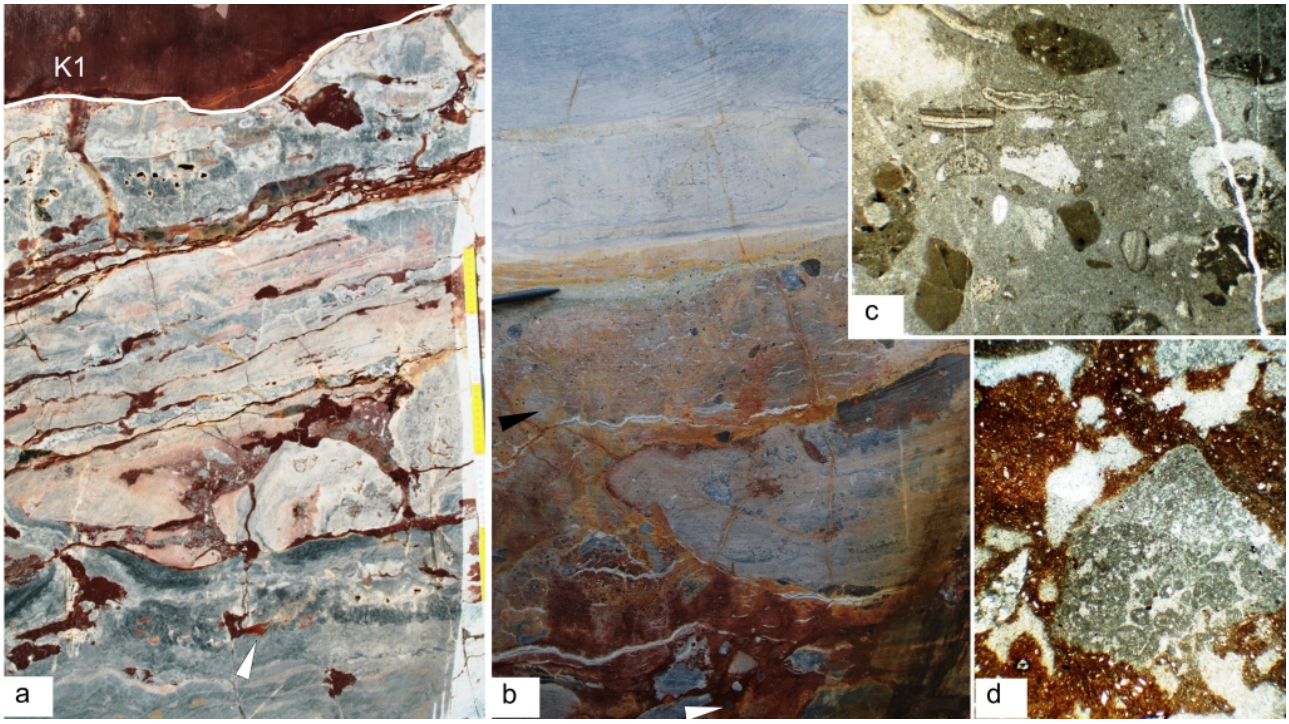

Fig.2.28: ***a****- Erosional surface corresponding to K1 unconformity overlain by Terra rossa paleosol. Below K1 surface paleokarst network with veins, subhorizontal cavities and small solution vugs filled by Terra rossa material and intraclastic breccias;* ***b****- Two layers of carbonate breccias corresponding to erosive truncation of the paleosol (above K1*

*unconformity);**c-** phoromicrograph of upper breccias layer; d-poor rounded clast with dissolution features at the border and vugs filled by sparry calcite at the top of the paleosol.*

This erosional surface marks the transition from onlapping peritidal deformed in tepee (Assereto & Kendall,1977) limestone of the Tred Transitional facies to overlying Tred facies. The Tred facies differs from Transitional facies for degree of diagenetical deformation and, in particular, for abundance of infilled green-red shales and (primary or flued) Terra rossa layers. Veins and sedimentary dykes cut the Tred transitional facies and the TE surface, deeping for some meters (less of ten) into the massive limestone of the Esino Limestone reef-upper slope facies. Outcrop conditions prevent observation of upper surface of development of these vertical structures: probably it coincides with K1 or surfaces slightly above or below. These veins and fractures, 10-15 cm in size, are filled by matrix-supported carbonate breccias. Breccias consist of millimeter-size, rounded to poorly rounded and often blackened clasts in reddish carbonate matrix. Clasts are recrystallized, weathered and show dissolutional features at the border. The filling history of these fractures is complex. Several phases of infilling TR breccias were observed. In addiction, discontinuous, centimeter-thick crusts of cements, coating the walls of the fractures, testify reopening of the older fractures system (3-7 cm in size). This older fractures system are filled by early (marine?) cements, probably microbially- controlled, and seem to be parallel to the orientation of the Esino Limestone reef belt.

The best outcrop of surface K1 occurs at the top of Upper slope-reef complex in the Section of the road to the Gamba quarry (Fig.2.25), with a erosional truncated TR paleosol up to 70 cm high.

Peritidal limestone under this unconformity are affected by a paleokarst network of fractures and centimeter-scale solution vugs and solution enlarged cracks. Solution vugs and enlarged cracks are filled with red shale and paleosol material (with subangular blocky structure, rims of calcitic cements and evidence of poligenyc and policyclic genesis).

***K2 unconformity** (Fig.2):* Rapresents a marker level for the quarry activity in the MAO quarry of the Middle Brembana Valley. It's a scalloped sub-planar surface traceable for several kilometer in the lower part of the KLR (Tred) and corresponds to decimeter-scale TR material with dispersed dolomitized intertidal angular clasts. The upper boundary of this layer is marked by green tuffaceous intercalations.

Discontinuity surfaces at the top of 'Calcare Rosso' (Tred)

TK unconformity *(Fig.2.25)**:*** The uppermost deposits of the Tred of the Calcare Rosso (KLR) consist of deformed peritidal strata into juvenili to mature tepees with flushed layers of Terra Rossa deposits.

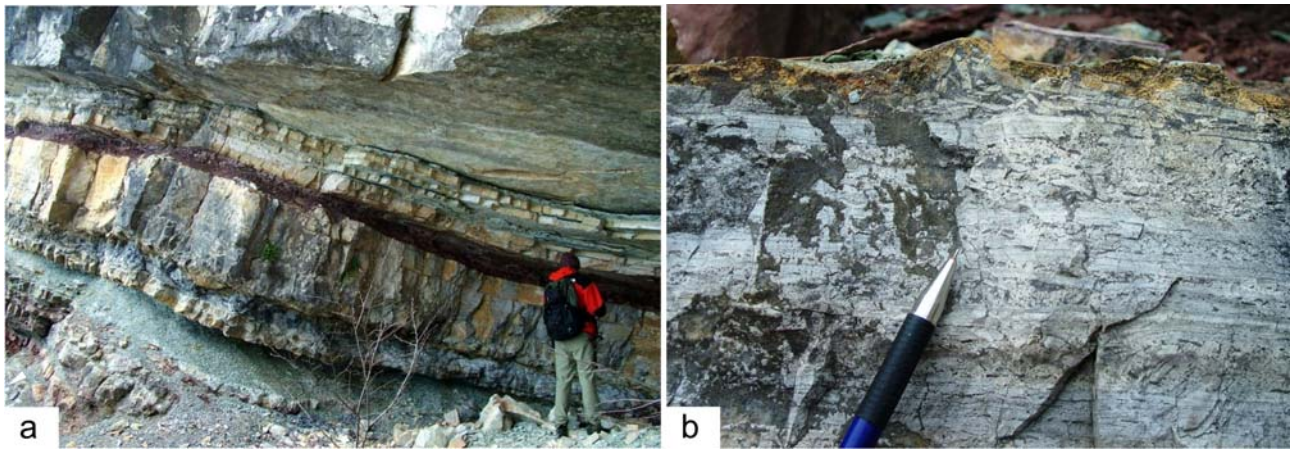

Fig.2.29:*a-* *Several green/red decimeter-scale tuffaceous layers alternated to laminated-fenestral and thin grained limestone mark the transition between Tred facies of Calcare Rosso (KLR) and peritidal deposits of Breno Fm.;* ***b-*** *TK erosional surface characterized by hardened crust caps dolomitized inter-supratidal deposits of Tred facies of KLR. Dissolutional features (centimeter-scale veins, enlarged fenestrae) characterize underlying deposits.*

The transition to the Breno Fm. is marked by close alternation of decimeter-scale laminated-fenestral and thin grained dark grey limestone with reddish internal sediments, often dolomitized and green-red decimeter-scale shales (-tuffaceous) layers (Fig.2.27). The TK is a subaerial exposure sub-planar surface characterized by hardened crust at the top of loferitic breccias with dolomitized clasts. Centimeter-scale veins filled by cements cut into underlying deposits. Dissolutional processes enlarge millimeter-scale fenestral layers alternated to stromatolitic layers, equally thick more developed (meter-scale) palokarstic features including meter-scale network of veins and subhorizontal fractures characterize that top surface of KLR in the Gamba and Mecca Quarry sections.

OPEN PLATFORM DOMAIN:

Lateral evolution of the Discontinuity surfaces: up to open platform domain

Moving to (backreef) open platform domains the discontinuity surfaces characterizing the boundary between the Esino Limestone and the Calcare Rosso (KLR) deposits show a important changes. In particular the discontinuity surfaces at the top both of the Esino Limestone (TE) and of the Tred facies of KLR (TK) can be described in detail.

From reef (Gamba Quarry section, Remuzzi Quarry section) to backreef facies (Costa Pagliari section, Sonzogni tunnel), both the thickness of the Tred transitional facies and the gap between TE and K1 decrease. At the same time, an increasing in percent of replaced host rocks and a major sinking in the underlying deposits are observed. A dissolutional network of cavities (cm- to decimeter- size), irregularly spaced sub-horizontal sheet cracks (with smooth and rounded margins) and veins filled by TR material outcrops extensively below the K1 surface for at least 0.4 km (observed) but probably up to 1 km. Locally (Remuzzi Quarry), paleokarst-dissolutional processes allow to collapse of this pervasive network of solution cavities and consequent formation of sag of breccias. These structures 5-7 m deep and 3-4 m in width involve the peritidal limestone of the Transitional facies of the KLR as showed by lithologic analysis of the clasts of the breccias. The dolomitized bioconstrued rocks of the underlying Esino Limestone are not involved.

No paleosols corresponding to K1 surface are observed but Terra Rossa material or Terra Rossa thin breccias probably correspond to K1.

1 km northward of Sonzogni Quarry, above the open platform facies (Antenna Section) TE surface merge into K1 surface; subsequently (1.5 km northward respect to Antenna Section; Corna Grossa) also K2 surface merge into the one-surface at the base of the KLR deposits: thickness decreases and facies change of the KLR deposits allow to decrease of the number of the discontinuity surfaces within KLR deposits.

Unlike discontinuity surfaces characterizing the lower part of KLR deposits, the discontinuity surface (TK) at the top of these deposits, along the transition from the upper slope to the open platform domain, remain a planar surface with tuffaceous layers with poor developed paleokarst structures.

When Tred facies grade to residual breccias and all the discontinuity surfaces merge into two: generic TE and TK surface.

In the Middle Brembana Valley, the lateral evolution of discontinuity surfaces and their associated deposits/paleokarst structures moving to upper slope to backreef domain is very similar both on the S-N (Cadei-Sonzogni) and W-E (Cadei-Remuzzi transect). Instead the transition to open platform domain is different northward (described) and eastward.

Fig.2.30*: Moving from the margin to the open platform domain KLR facies pinch out rapidly. Thickness decrease from 40 m to 3 m in less than 1 km. Facies change from peritidal, tepee-deformed (Assereto & Kendall, 1977) Tred to few peritidal strata with residual breccias and tuffaceous levels intercalated.*

Eastward to the depocentral area, along the Parina Valley the KLR deposits decrease in thickness more rapidly than along other transect studied: from 35-40 m (Remuzzi Quarry) to 0.5 m (Paglio Pignolino Section) in less than 0.7 km. In the Paglio Pignolino Section the KLR consists of thin strata of both fenestral and breccias with tuffaceous levels intercalated. The lower boundary is characterized by well developed sedimentary veins (partially) filled by shales cut into the underlying massive facies of the Esino Limestone for about 10 m depth.

Also in this section and along the whole transition from the upper slope to the open platform domain, the discontinuity surface at the top of these deposits is a planar surface with tuffaceous layers overlying poor developed paleokarst structures.

INNER PLATFORM DOMAIN:

Decrease in thickness and facies change of the KLR deposits above the inner platform domain (of the Esino Limestone) coincides with the reduction of the registered discontinuity surfaces: only TE and TK are often observed.

These surfaces bound discontinuous lens of mass flow breccias intercalated to centimetric tuffaceous intervals and (in the upper part) decimetric laminated limestone (bindstone). The thickness of the deposits between the two unconformities is about 1-3 m.

The ***TE*** is a composite surface with subaerial exposure and erosional features. This surface caps peritidal deposits rich in algal fragments (Dasycladacee) and stromatolitic bindstone organized in meter-scale cycles. Locally the upper strata (1-2 m thick) of the Esino Limestone beneath this surface record the effects of a subaerial exposure: sindepositional deformations, dolomitic crusts, selective dolomitization and seldom, silicification and breccia-like texture (patchy recrystallization?).

The ***TK*** is a planar discontinuity surface marked by a green tuffaceous level and is overlain by thin stratified dolomitic stromatolitic deposits of the Breno Fm.

However KLR deposits on the inner platform domain of the Esino Limestone are characterized by rapid local changes in thickness and facies. These rapid changes are due to reduced accommodation space and wide range of morphologies of inherited topography. Therefore, in certain areas of the inner platform domain also the characteristics of discontinuity surfaces are very different.

Three areas are a perfect examples of these locals changes: Zorzone, Mt.Trevasco and Mt.Arera (Fig.).

Zorzone section: upper part (ten of meters) of the inner platform facies of Esino Limestone is characterized by decrease in thickness of the peritidal cycles (from 1 m of the Middle Esino Limestone to 30 cm), often capped by juvenili tepees (Assereto & Kendall, 1977) and cut by sheet cracks. Isopachous crusts of ‘coconut meat calcite and laminated/graded internal sediments fill the dissolution cavities. The boundary between the Esino Limestone and ‘Calcare Rosso’ Tgrey deposits correspond to subaerial exposure surface (TE) marked by green tuffaceous level (10-15 cm thick). Beneath this surface, paleokarst network of dissolutional cavities filled by tuffaceous material is developed for 2-4 m at the top of the Esino Limestone. Sag of mosaic (to matrix-rich mosaic) breccias with clasts from 5 to 15 cm in size are due to collapse of this

network. Size of these collapsed bodies has not been observed. Across the TE surface, facies and geometry not significantly change.

The top of the KLR Tgrey deposits are characterized by an erosional discontinuity surface (not observed) at the base of residual breccias

Subplanar surface (TK) marks the transition between Residual breccias facies and well bedded, bioclastic (bivalvs) peritidal deposits of the Breno Fm. Cycles thickness of the Breno Fm. range from 80 to 150 cm, with prevailing subtidal facies.

Trevasco area: the effects of a major subaerial exposure corresponding to ***TE*** discontinuity surface are documented by paleokarst features with different degrees of development. In particular, decimeter-scale veins and dissolutional vugs (up to 1 cm in size) filled by TR material characterize the upper 1-3 m of the well bedded, bioclastic (green dasycladaceans algae) limestone of the Esino Limestone beneath the TE surface. Locally, TE surface is marked by lens of carbonate breccias filling depressions 3-6 m high, 5-8 m large and 10-20 m spaced. Below these collapsed deposits, centimeter-scale breccias are fluted in strato-concordant or vertical cavities, deepening up to 4-5 m from TE.

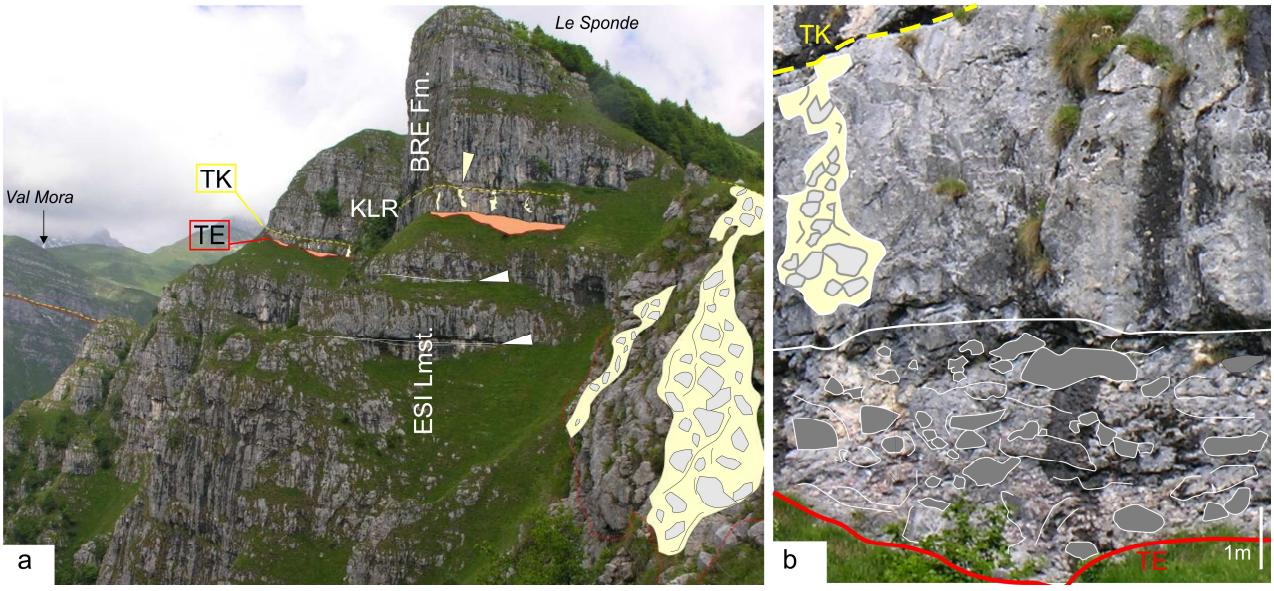

Fig.2.31 : *a-* *Panoramic view of the tracks of the major and more continuous unconformities TE and TK (red line: Top Esino Limestone and yellow line: Top 'Calcare Rosso') above inner platform facies of the Esino Limestone. Ki (within KLR deposits) surface separate the lens of collapsed paleokarst deposits (reddish area) and Tgrey facies with vertical collapsed structures. Arrows indicate two major exposure surfaces in the upper part of Esino Limestone deposits with tepees and pisolitic lens;* ***b-*** *two not-coalescens paleokarst collapsed breccias characterize the*

KLR succession in this area. Above TE surface, lens of carbonate breccias with volcanoclastic matrix fill depressions at the top of subaerial exposed platform. Below TK surface vertical shafts filled by matrix rich mosaic to mosaic to crackle breccias are cut into the Tgrey deposits for 3-4 m. Surface between the top of lower breccias deposits and the Tgrey facies are marked by tuffaceous level.

15-20 meters below this unconformity a less important exposure surface has been recorded by peritidal deposits with pisolitic cements, small tepees (Assereto & Kendall,1977) and tuffaceous lens.

The TE surface, marked by tuffaceous level, is overlain by Tgrey facies of the KLR, 4-6 m thick.

TK is a planar surface between poorly-deformed peritidal deposits of Tgrey facies and peritidal deposits of Breno Fm. From this unconformity vertical shafts filled by matrix rich mosaic to mosaic to crackle breccias are cut into the Tgrey deposits (for 3-4 m). These structures, less to 1.5 m in size occurs 4 to 10 m spaced and their lateral boundaries are difficult to define for the scarcity of matrix and the weak dislocation of the clasts.

In this area favourable outcrop conditions allow the characterization of the lateral evolution of both TE and TK discontinuity surfaces from inner to open platform domain, for at least 5.7 km.

Moving from the inner (Val Mora Section, Fig.2.32) to open platform (Mt. Vaccaro section, Fig.2.32) domain thickness and facies of the KLR deposits between these major surfaces (TE, TK) show important changes. In the Val Mora section, the KLR deposits are 3 m thick and consist of residual breccias with intercalated tuffaceous levels. In the ‘Sponde’ section, the KLR deposits are up to 12 m thick and they are characterized by lens of collapsed breccias overlain by Tred facies. In the Vaccaro section thickness decrease and Lagoon and Tgrey facies are replaced by Tred facies.

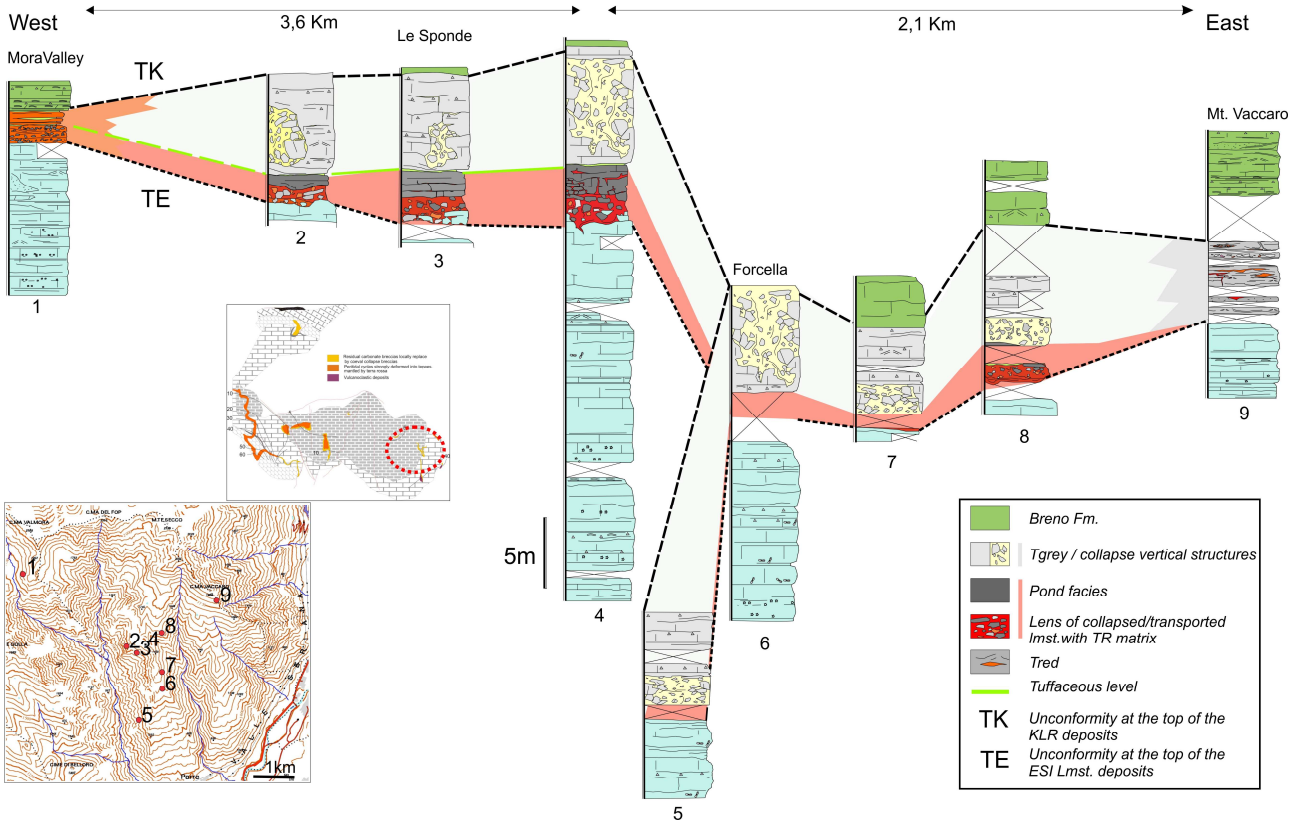

Fig.2.32: *Correlations of the measured sections at the top of the Esino Limestone above inner platform facies (Val Seriana)*

Arera area: in this area the KLR deposits are characterized by two facies: 4-6 m of Tgrey facies overlaid by 0.2-3 m of residual breccias. Therefore three main discontinuity surfaces can be recognized: a sharp erosional surface (Ki) that marks the transition between the two facies, TE and TK surfaces.

TE is a irregular subaerial exposure surface between the peritidal deposits green rich in dasycladaceans algae of the Esino Limestone and the deformed (tepees; Assereto & Kendall, 1977), rich in cements peritidal deposits of the KLR Tgrey facies. This surface is cut by large scale paleokarst collapsed structures, 3-8 m large and 25 m high, deepening from the ***Ki*** surface. Overlying Tgrey deposits are fracturated, tilted and partly deformed.

TK is a planar discontinuity surface that mark the transition between Tgrey facies and overlying thin stratified, dolomitized, stromatolitic deposits of the Breno Fm..

Chapter 3

DIAGENETIC CHARACTERIZATION AND EVOLUTION OF THE UPPER ESINO LIMESTONE-CALCARE ROSSO SUCCESSION

A multidisciplinary approach was followed to characterize the diagenetic events that are recorded in the upper Esino Limestone (late Ladinian-early Carnian?) and during the deposition of the Calcare Rosso. Detailed light-transmitted and CL microfacies observations, VDX and fluid inclusions data have been integrated with geochemical analyses (162 analyses for $\delta^{18}O$ and $\delta^{13}C$ on calcite and a few analyses for the Sr^{87}/Sr^{86} ratio). Porosity changes related to the diagenetic processes (dissolution, fracturing, internal sediment and cementation) were investigated with a procedure that integrates (from outcrop to thin-section scale) field observations and image analyses. Porosity in the different lithofacies of the Esino Limestone was evaluated at different diagenetic stages.

MACRO, MICROFACIES CHARACTERIZATION

A classification and definition of the macro and microfacies observed during the field work is proposed in Fig.3.1 with a legend of symbols and codes. This classification relies both upon field observations and on the study of more than 70 thin sections, mainly from the upper Esino Limestone and the lower part of the Calcare Rosso (Tred facies). Residual facies has been also considered.

Here, the main features of the different facies are summarized.

HOST ROCK: facies association observed during sampling for diagenesis were synthesized in 5 categories: ***f***, ***g***, ***b***: texitural and syndepositional; ***r***, ***d***: diagenetically modified.

The distribution of the host-rock types in the different facies of the **Esino Limestone** is as follows:

Inner platform: fine-grained packstone (rich in intraclasts and peloids), coarse bioclastic grainstone\fine rudstone with dasycladaceans (*Diplopora* cf., *Teutloporella* sp.), gasteropods, bivalvs and intercalated oncoidal rudstone. Inter-sopratidal facies, locally dolomitized, are represented by stromatolitic fenestral bindstone and lithoclastic rudstone. Prism cracks and large sheet cracks (up to several decimetre long) are developed mainly in shallow subtidal carbonates.

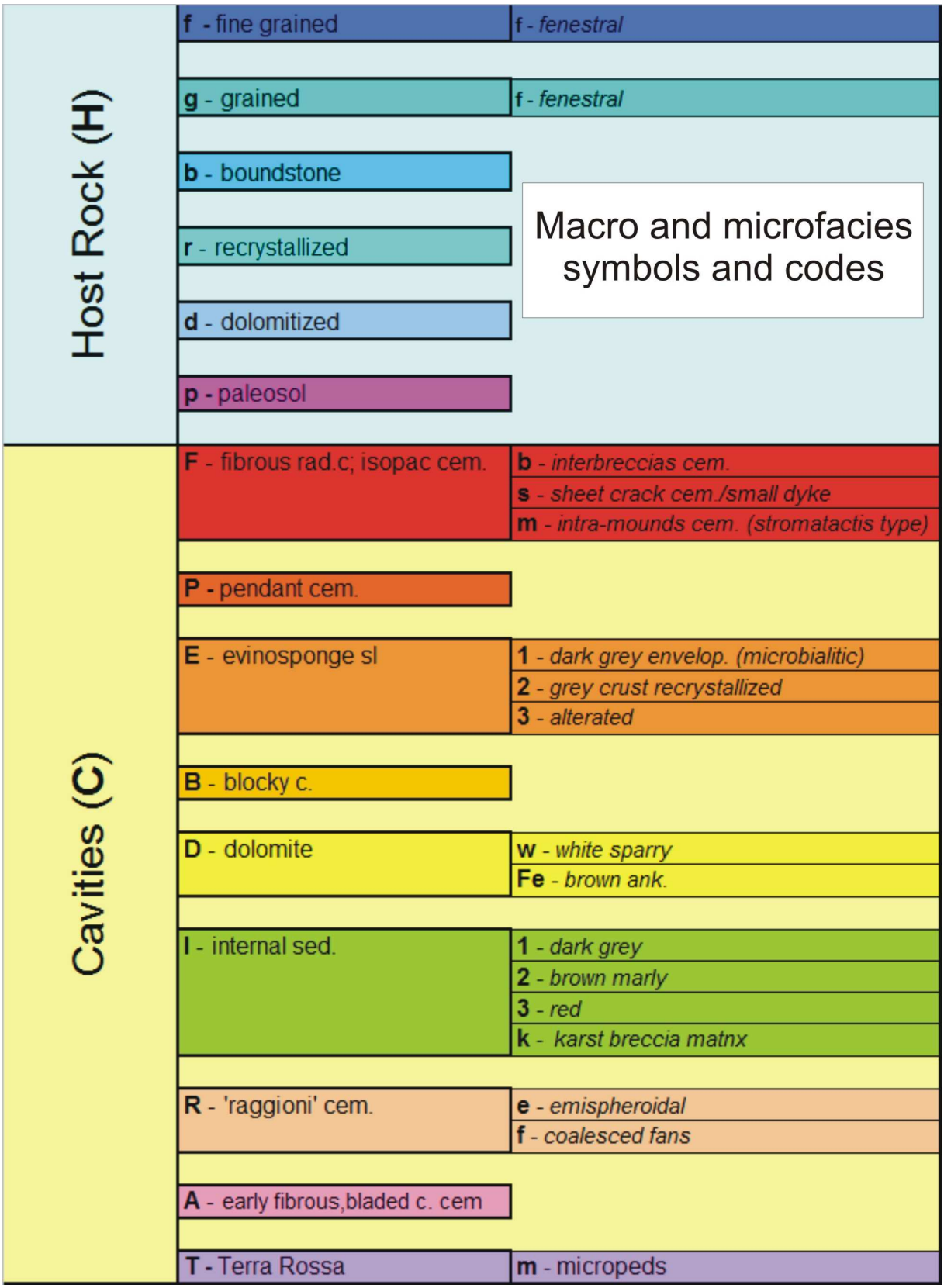

Fig 3.1: *Key to the symbols for macro and microfacies used in the ph.D. thesis.*

Open platform (f,g): coarse bioclastic-peloidal and intraclastic oncoidal packstone with bioclastic rudstone (gasteropods, brachiopods often associated with open marine biota: crinoids, brachiopods, ammonoids and pelagic bivalves) in the back reef area (wash-over storm and flood delta deposits).

Reef (b,g): massive coral framestone and microbial, algal stabilized bafflestone (*Tubiphytes* sp., *Macrotubus* sp., Problematica).

Upper slope (b,g): bafflestone\bindstone mounds with *Tubyphites*, problematica, serpulids and microbial crusts (in stromatactis-type cavities). Litho-bioclastic rudstone stabilized by encrusting organism, sinsedimentary dykes and veins, filled by carbonatic/silty internal sediments and/or isopachous (microbialitic?) cements (evinospongia type). Typical early lithification. The subvertical dykes of the upper slope, mainly developed parallel to the platform margin, are up to a few decimetre wide with a lateral decametric vertical continuity.

Lower slope (f,g): lithoclastic rudstone with clasts mainly deriving from the upper slope/reef associated with bioclastic rudstone. In the distal slope transition to intraclastic grainstone-packstone.

Intraplatform basin (f,g): intraclastic peloidal packstone, rarely bioclastic (mainly bivalves). Packstone facies intercalate with wackstone and laminated fine-grained packstone-mudstone (microsparite). Rare lithoclasts in matrix-supported floatstone\rudstone (debris flows). Wackstone with black chert nodules, alterated tufaceous silty shales, volcanoclastic litharenites are also locally associated to carbonates.

Dolomitized facies (d): well developed in the upper slope/reef facies of the southern margin. Selective strata-bound dolomitization (thickenss up to 10 m) is observed in the Val Parina back-reef succession.

The distribution of the host-rock types in the different facies of the **Calcare Rosso** is as follows:

Tred- *Typical peritidal red* (r,f,b):. Intraclastic, peloidal fine grained packstone, bioclastic wackestone, coarse bioclastic grainstone (dasycladaceans, gasteropods, bivalves) and intercalated oncoidal/pisoidal rudstone. Intertidal facies are represented by lithoclastic rustone and stromatolitic fenestral binstone often deformed in tepees and capped by Terra Rossa paleosols. Polychromatic laminated sediments and cements fill veins, cavities and sheet cracks. Tred facies is affected by diagenetic (vadose) processes that obliterate the original depositional textures and constituents. Into more deformed layers (mature and senile tepees) volume of internal sediments and cements is up to 80% of total rock volume.

Tgrey- *Typical peritidal grey* (r,f,b): similar to Tred facies but depositional characteristics are less modified by supratidal, diagenetical deformations (tepees). The volume both of the internal sediments and the cements is lower. Terra Rossa paleosols were not preserved/developed.
Ld- *Lagoonal dolomitized:* dark subtidal unfossiliferous and often bioturbated microsparite capped by laminated (stromatolitic?) bindstones.

Lf- *Fenestral dolomitized* (d,f,b,r): dark, dark-gray subtidal intraclastic rudstones and fossil-rich (Dasycladaceans, Gasteropods) peloidal wackestone-packestone are capped by intertidal dark fenestral packestone/wackestone and rare microbial binstones. Supratidal deformations in tepees and sheet cracks with laminated,carbonatic internal sediments are common.

Rb- *Residual breccias:* intraformational breccias with angular to rounded carbonatic clasts and paleosol slabs floated within a reddish, fine graded, non-cohesive, dolomitized matrix. Carbonate clasts show lithologic composition similar to inner platform facies of Esino Limestone; dissolutional and blackening processes at the border are common.
Paleosol: Terra rossa paleosol strongly weathered.

CAVITIES: this is the most important category for the diagenetic analyses (Fig.3.1) Cavities are filled by cements and internal sediments (E, I, R, P) or exclusively by cements (F, B, D, A).
The different types of cavities have been grouped in classes as follow:
F: fibrous radial calcite isopachous cements. Isopachous calcitic crusts, coconut meat calcite like (Fig.3.1), maximum thickness on average 3-4 cm, grey to dark grey. They are typical of inner platform and marginal-slope facies of the Esino Limestone, as well as of inter-supratidal facies of the Calcare Rosso. Three sub categories were distinguished: cements occluding intergranular porosity on the slope breccias (b), dissolution and shrinkage fractures in the peritidal carbonates (s), intramound cements in the stromatactis-type cavities on the upper slope (m).

V: Pendant cements (Dripstones). dark-gray, grey cement crusts with distinct thickening beneath roofs of solution vugs and grains (breccia clasts). Thickness ranges from 2 mm to 5-7 cm. Two subunits were distinguished: grey, dark-gray, cm-scale, pendant cements developed beneath roof of cavities (p); dark-gray, laminated, mm-scale pendant cements beneath grains (breccias clasts) with beard-like pattern; lamination is due to alternated biogenic films and cement layers (d).

E: evinsponges: concentric mammellonary envelops\crusts of grey to dark grey calcite locally fibrous radial. These facies fill cavities (up to more than 1 meter size) characterizing the Ladinian platform margin and slopes of the Tethyan domain (Frisia et al, 1988; Russo et al, 2006) (Fig.3.2).

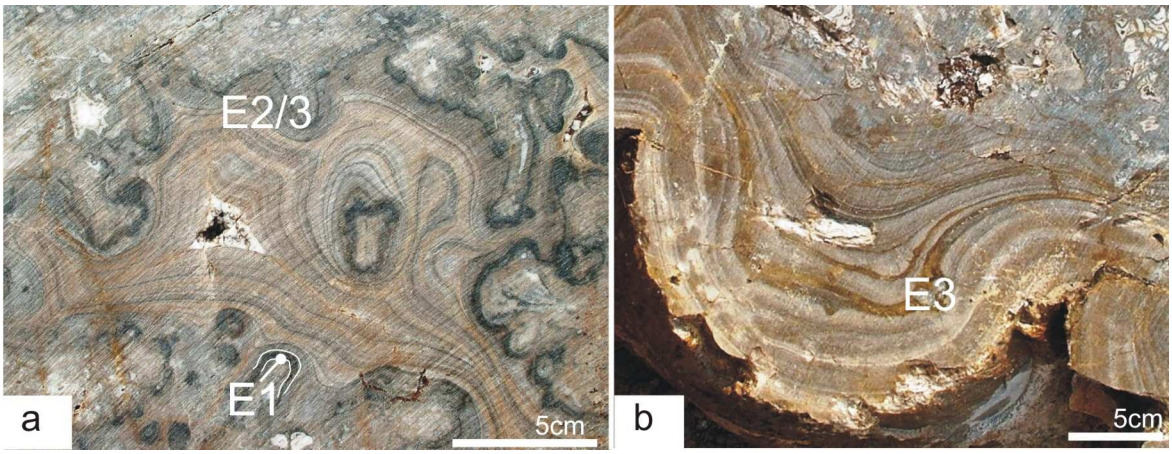

Fig.3.2: *Examples of concentric mammellonary envelops\crusts of calcite (Evinosponge) with indicated different subunits:* ***a****- black (microbial controlled) crusts stabilizing walls of the cavities and showing dissolutional boundary with host rock (E1); concentric (not isopachous) recrystallized (and altereted) calcitic layers showing thin layering of fibrous radial calcite and millimetre microsparitic intercalation (E2/3);* ***b****- altereted brownish layers of calcite and microcrystalline calcitic dolomite (E3) due to diagenetic (dolomitization processes) transformation of E2 or recent alteration/weathering (Pleistocene karst?).*

Three sub-units were recognized on the base of diagenetic modifications:

E1, fine (max centimetric) black crusts (Fig.3.2 a). It represents the first phase of stabilization of the walls of the cavities. Dissolution surfaces mark the contact between horst rock and this crust. Probably the dissolution is due to the acidification role played by microbial colonies.

E2, grey recrystallized crusts (Fig.3.2 a). They consist of concentric calcitic layers, not perfectly isopachous, characterized by calcite with diagenetic fibrous radial aspect owing to recrystallisation and crystals growth along c-axis. Macro observations show alternation of concentric, millimetre to centimentre thicks, ligh grey to dark grey layers. Microfacies show a finer layering (about 1-2 mm), marked by microsparitic intercalations (100-150 micron) characteristic of primary crusts and by preserved peloids in the fibrous radial calcite. Small crystal of idiomorphic quartz and autigenic megaquartz were found.

E3: evinsponges with altereted brownish layers of calcite and microcrystalline calcitic dolomite (Fig.3.2 a,b). E3 is a diagenetic transformation of E2, controlled by dolomitization processes

occurring on the southern margin of the Esino Limestone, possibly due to recent alteration/weathering (Pleistocene karst?)

B: blocky calcite. White spatic calcite filling intergranular porosity, syndepositional fractures of inner platform and the nucleous of stromatactis-type cavities.

D: dolomite. w=White sparry dolomite filling nucleus of small geodic cavities, fractures, small evinsponges. Fe= brown ankeritic/Fe dolomia, which characterize the last millimetric boundaries of Dw crystals.

I: Internal sediments. 1= calcitic, fine granular, ligh-grey, fine-laminated, graded sediments; locally with erosional surface at the base. In the Esino Limestone they were observed within syndepositional fractures and occluding intergranular voids in the slope breccias. In the Calcare Rosso they are associated to raggioni and F type cement, filling concordant and discordant fractures.

2.3 = varicolor (ochre-brown to green-grey), calcareous marly, silty and clayey internal sediments. They fill discordant fractures and small paleokarstic cavities at the top of the Esino Limestone and into Calcare Rosso deposits.

k= polichrome matrix consisting of silty calcareous, marly, clayey and locally volcanic (altereted and reworked tufite and vulcanite) material. They are common in the collapse breccias and residual pedogenic breccias.

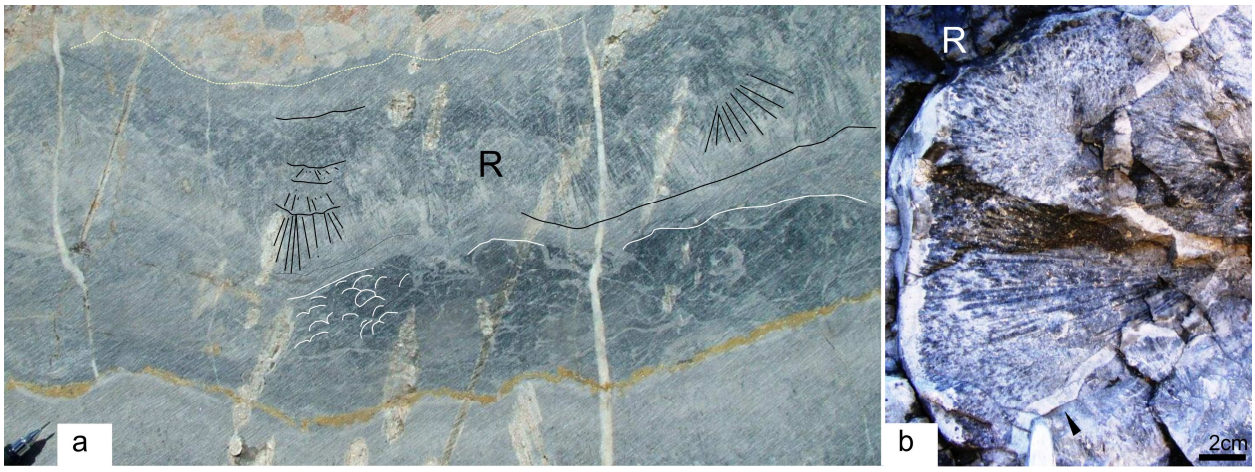

Fig.3.3: ***a****-'Raggioni' (Assereto&Folk, 1980) crystals in subhorizontal cavities with prevailing top-down growth (pendant raggioni). Nucleation starts from the borders of the cavities;* ***b****-fans shape dark raggioni with accretionary (dolomitized) micritic crusts.*

R: raggioni. Typical structures consisting of giant rays of dark gray calcite organized in large crystals with plume-acicular geometry and competitive growing in fan-like structure (Fig.3.3).

Coalescent fans of crystals reach a centimetric to decimetric size. If recrystallized, the colour changes from dark grey to grey or whitish. Square ended and feathery crystal terminations. Assereto & Folk (1980) interpreted the raggioni as calcitic pseudomorphs on primary aragonitic crystals growing in paleokarst cavities and tepees. Morphology of crystals changes depending on the polarity (Fig.3.3 a), with prevailing top-down growth (pendant raggioni). Nucleation starts from the borders of the cavities.

Rf= coalescent fans - An additional class of raggioni ("diagenetic raggioni", not considered in this work) is characterized by growth in sediments within preexisting fractures and cavities. These "diagenetic raggioni" show scalenoedric crystal termination that locally deform or substitute the laminations in the sediments. In thin sections, raggioni consit of a mosaic of small blocky calcite with irregular boundaries and wavy extinction under polarized light. Macro fibrous radial geometry is still visible.

Early fibrous, bladed calcite cement (A): typical syndepositional cements, which also precipitate during early diagenetic stages. They fill the primary porosity during the major cementation stage of the inner platform facies of the Esino Limestone and Calcare Rosso.

Terra Rossa (T): Mostly reddish clays ("Terra Rossa") filling veins, fractures, sheet cracks and paleokarst network associated to major subaerial exposure surfaces.

CATHODOLOMINESCENCE (CL)

About 50 thin sections were studied with CL8200 Mk 5-1 Optical Cathodoluminescence System operating at 10-12 KV and 50-70 current mA. Observations allow the definition of primary and late diagenetic features in cements form different types of cavities.

A synthesis of the CL characterization on different types of cements and studied diagenetic structures follows.

F - Fibrous radial calcite and other syndepositional isopachous cements: all Fb, Fs, Fm cements are not luminescent. In Fm we distinguish two stages of cementation: Fm1 is the first, dominant cementation episode and is characterized by luminescent microfractures; Fm2 shows dogtooth crystal terminations and is mainly not luminescent because microfactures are rare and more spaced. A few samples from the Calcare Rosso show thin luminescent zonations in F cements.

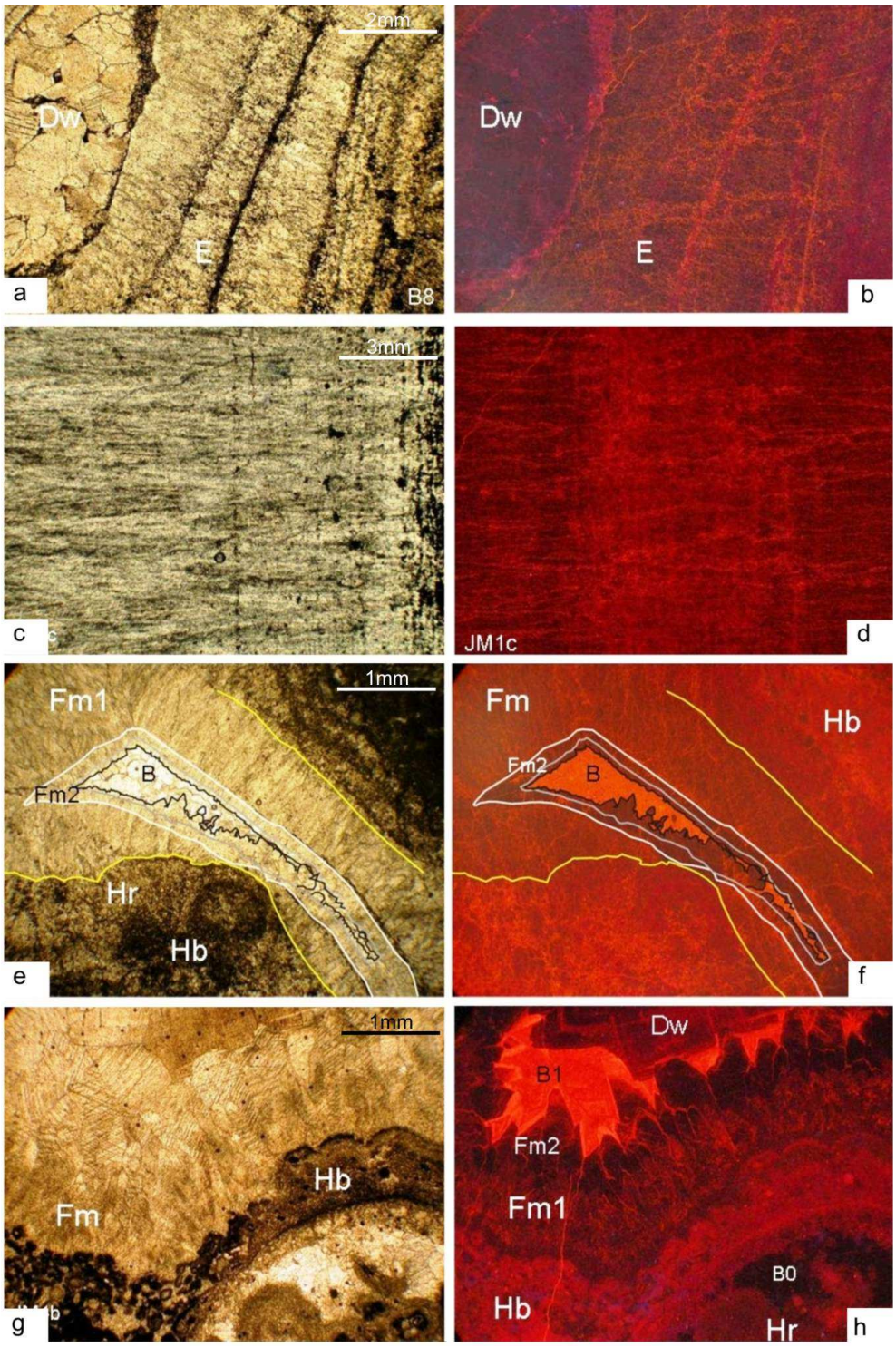

Fig 3.4- a,b*- Cathodoluminescence observations of fibrous calcite (E) of a recrystallized evinospongia with sparry dolomite at the nucleus (Dw);* ***c,d****: Cathodoluminescence observation of recrystallized evinospongia with raggioni-like crystals growth;* ***e,f****: Cathodoluminescence analysis of the upper Esino Limestone, calcite cements. Hb= microbialic host rock with dissolution at the boundary with the first fibrous radial non-luminescent calcite (Fm), as the precipitation phase shows scalenoedric terminations (Fm2) B: blocky calcite (B1) is bright orange luminescent and poorly zoned;* ***g,h****- cathodoluminescence analysis of the lower Calcare Rosso; paragenesis is similar to e,f sample but the nucleous of the cavity is filled by Dw.*

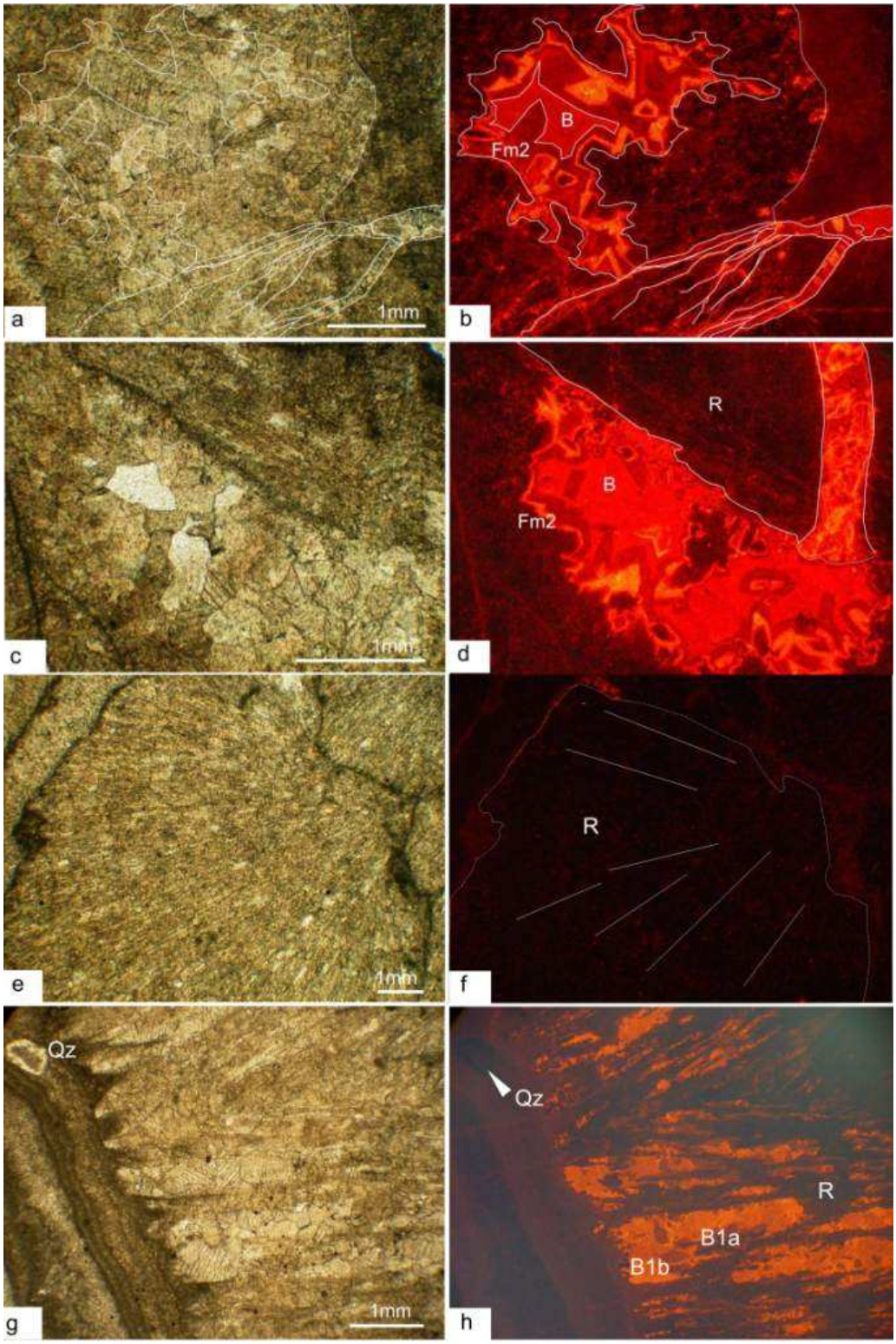

***Fig.3.5**: **a, b**-Zoned and L cementation phases in CL (Fm2, B) highline the burial fracturing reopening the porosity; **c,d**- NL in CL raggioni fan is cut by burial fractures with L cements (B); **e**-Fan of 'raggioni'crystals, NL in CL (**f**); **g**- Blocky calcite pseudomorps over raggioni "mega rays" with dog tooth termination and growing into a cavity filled by dark grey laminated internal sediment Q: autigenic quarz; **h**- detail in CL analysis of fig g) with two types of calcite: NL (early cements) and orange luminescent (late diagenetic; B1a, B1b related to dissolution followed by precipitation).*

E- evinospongia: layers of primary evinsponges E2 are non-luminescent, a weak diffuse luminescence is frequently caused by orange luminescent microfractures (Fig 3.4 b, d.). Orange luminescence of thin micritic-peloidal intercalation and microbialitic laminae of E1 (but also the host rock Hb) is possibly related to concentration of organic matter.

R- raggioni : The primary structure of calcitic raggioni is not luminescent (Fig 3.5 d, f, h). Bright blocky calcite (Fig3.5 f, h: B1a, B1b) showing two cementation stages (B1a dull poorly zoned, B1b light orange luminescent) replaces dissolved raggioni crystals.

D- dolomite: two different types of dolomite (Dw and DFe) have been identified. Dw is not luminescent to poorly zoned (sub-phase Dw1) to red luminescent (phase Dw2). DFe is similar to Dw1 but more zoned.

VDX ANALYSES

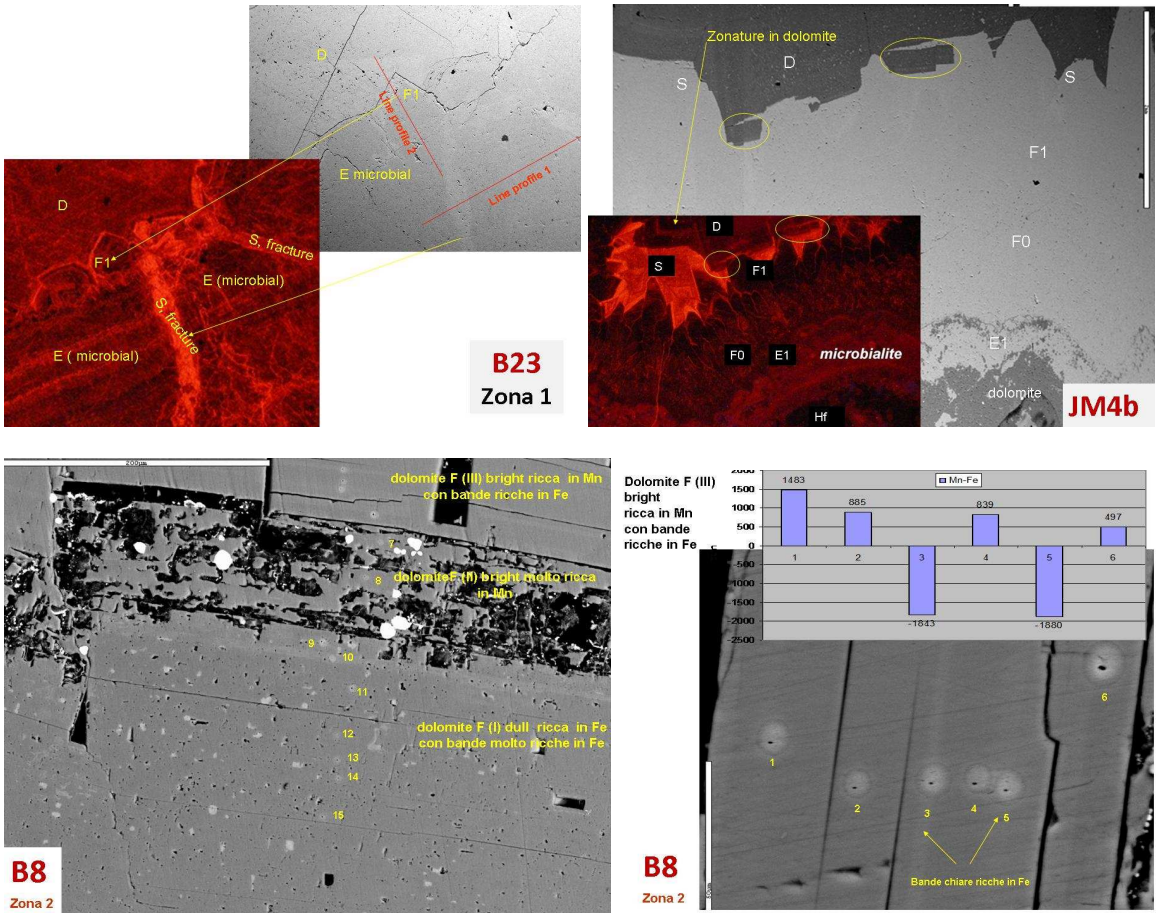

***Fig3.6**: Examples of WDX investigation on carbonate cements of upper Esino Limestone and lower Calcare di Esino (E. Previde , ENI laboratory).*

Five samples have been investigated with WDX technologies at ENI laboratories in Bolgiano (dott. E. Previde): 1 samples from upper slope of the Esino Limestone, 2 from the transitional facies Esino Limestone-Calcare Rosso and 2 from the lower Calcare Rosso.

The VDX analyses focussed on early to late diagenetic cementation phases, previously recognized by CL. For each stage, ppm concentration of Mn, Mg, Fe, Sr were returned.

The Wdx analyses confirm and support the CL data:

-luminescents zones show hight ratio Mg/Fe;

-blocky calcite (b) shows an average values of Mn-Fe of 172 ppm (early cementation phases),

- non-luminescent (E, F, R) cements show lower values of Mn-Fe.

esino	Not lumine Cements	F1	D	S	dolomite	dolomite incl
Mg	1629	1907	1956	1605	116957	116132
Mn	97	173	150	1060	471	414
Fe	122	282	484	888	764	1242
Sr	85	144	74	30	116	24
Mn-Fe	-25	-109	-334	172	-293	-827

Calcare rosso	Not lumine Cements	F1	D	S	dolomite	dolomite incl
Mg	3634	1435	2891	2285	106884	103130
Mn	75	72	351	442	1268	43
Fe	182	139	223	144	6054	910
Sr	131	25	112	40	45	0
Mn-Fe	-108	-67	127	298	-4785	-867

Fig3.7*: Table with the average of WDX analyses of the different phases of cementation (E. Previde. ENI laboratory)*

Stable isotope ($\delta^{18}O$, $\delta^{13}C$)

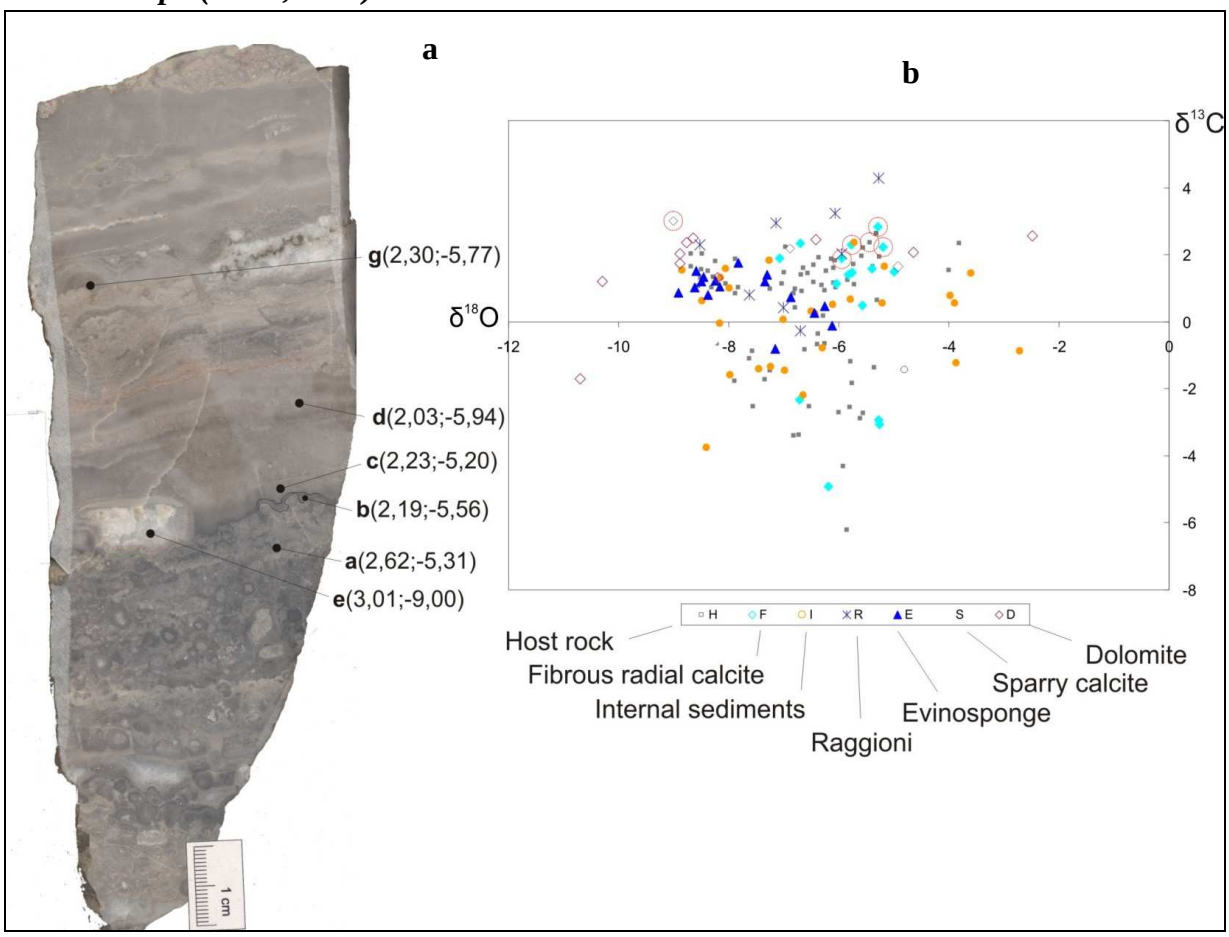

Fig3.8*- Polished sample of Calcare Rosso with position of microdrilling sampling and results of the analyses; b- Table with all the stable isotopic data (162 samples).*

The stratigraphic and sedimentological study was integrated by geochemical characterisation of different macro and microfacies of the upper Ladinian platform and of the overlying regressive lower Carnian peritidal carbonates.

At the ENI laboratories at Bolgiano 162 geochemical analyses has been performed on samples from 11 stratigraphic logs (two logs, Gamba quarry and Zorzone, were sampled in higher detail) (Fig 3.9). 91 microdrilling samples come from the upper Esino Limestone: 50 from the upper slope of the southern margin of Camerata Cornello; 40 from the inner platform, 1 from the northern slope of Pegherolo. 68 samples came from the lower Calcare Rosso: 44 from the typical facies of the Camerata Cornello quarries, 23 samples from the grey\residual facies of Zorzone (Seriana Valley) 1 from the vulcanoclastic succession of Monte Alino. 4 samples came from the Carnian peritidal limestone of the Breno Fm.

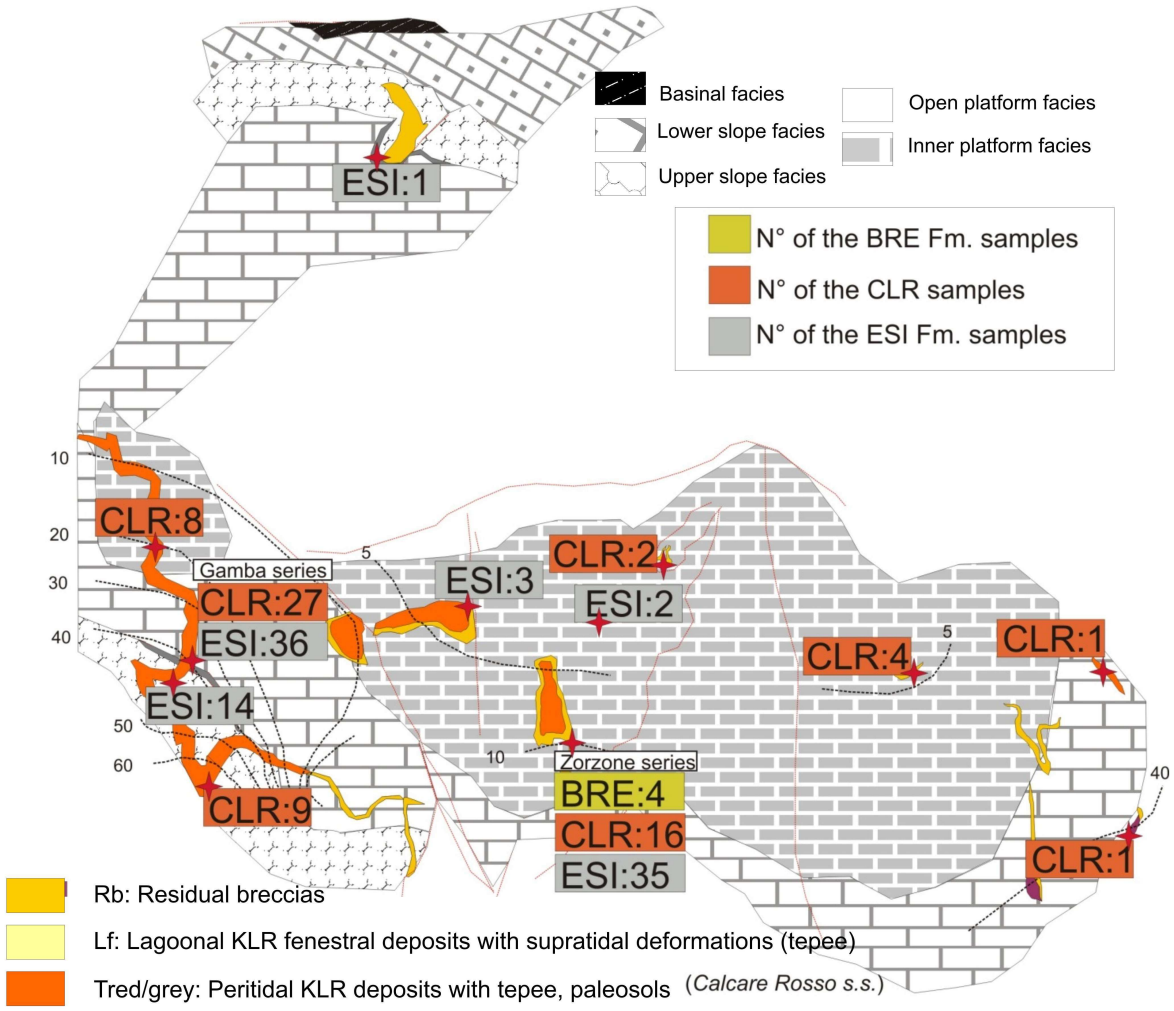

Fig.3.9 *- Paleogeographic distribution of the 162 samples (11 stratigraphic logs in the upper Esino Limestone, Calcare Rosso and Breno Formation).*

Fig.3.10: *Plot of the isotopic signature of the Esino Limestone grouped according to geographic position of stratigraphic sections and lithostratigraphiy*

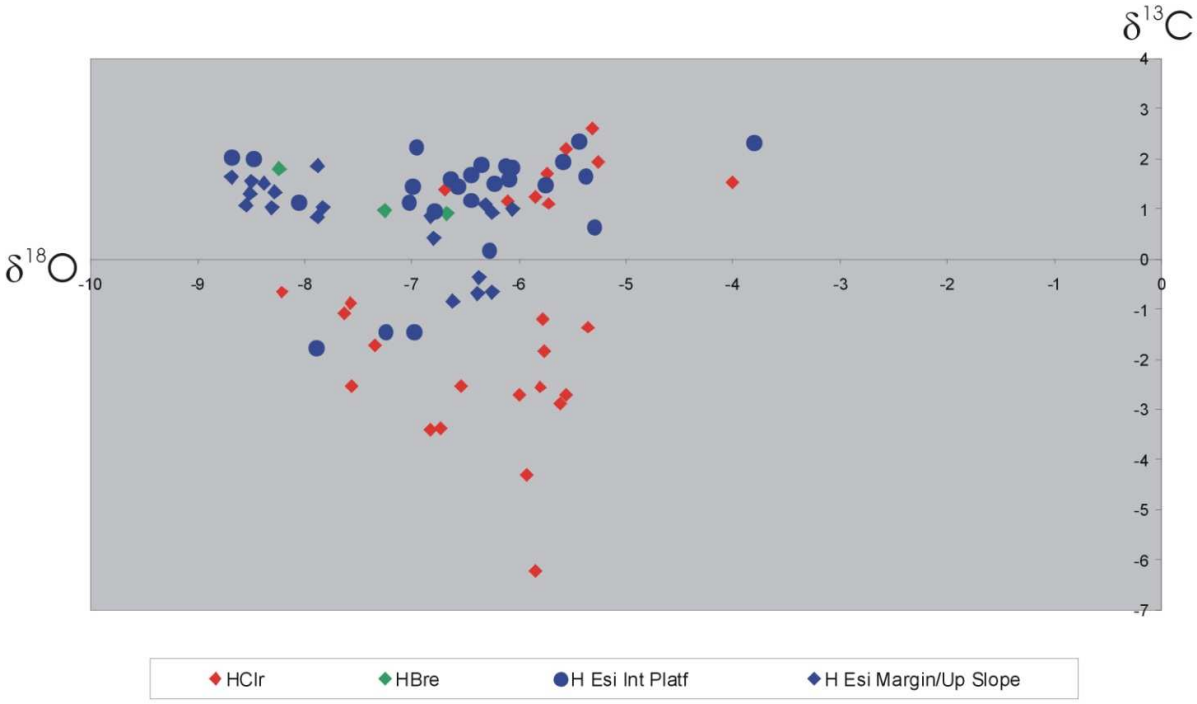

Fig.3.11: *Plot of the isotope signature of the Esino Limestone/Calcare Rosso samples grouped according to lithostratigraphy and facies.*

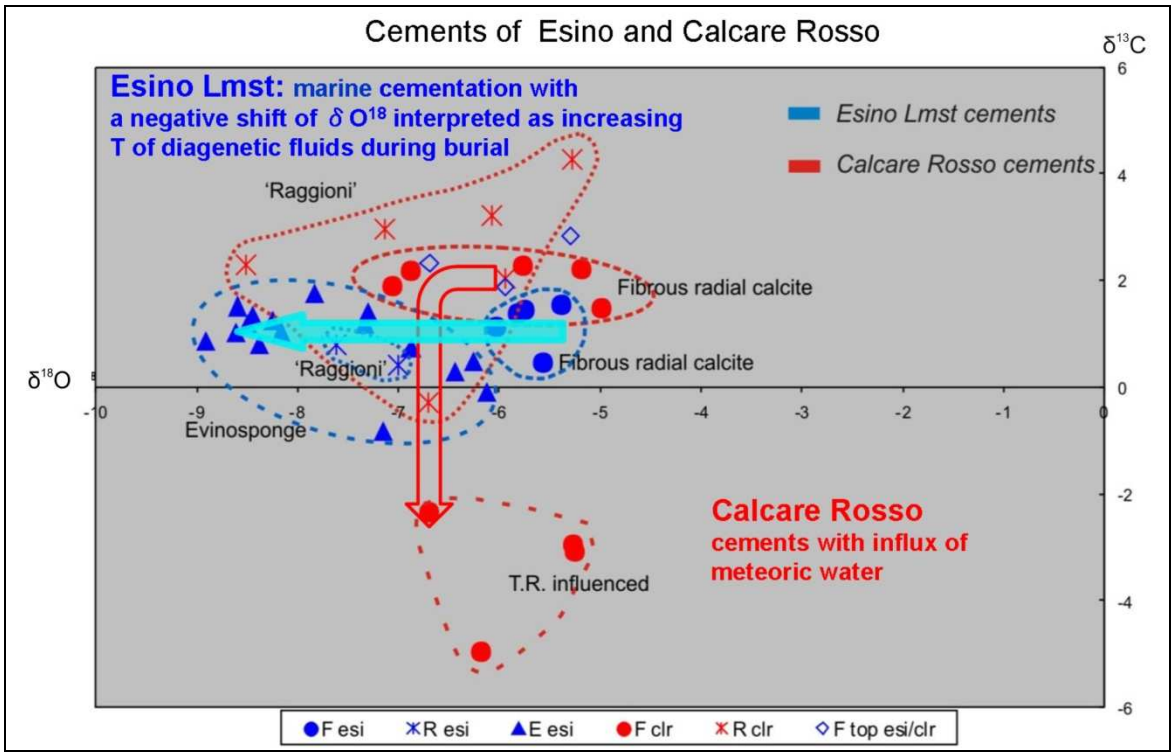

***Fig.3.12**: Interpretative plot of the stable isotope data of Esino Limestone\Calcare Rosso cements.*

SAMPLING METHOD

Samples have been drilled with an electric drill (diameter 4 mm) each 1-1.5 meters along the sections. Samples came from single cements or undifferentiated host rock.

Carbon and oxygen analyses of calcite and dolomite were measured in ENI laboratory of Bolgiano, the $Sr^{87/86}$ was measured at CNR laboratory of Pisa.

Data are reported as PDB in the standard per mil notation.

The same classification of Fig. 3.1 was used, leading to the clustering of the analyses in 7 groups: H (Host rock), F (Fibrous radial calcite), I (Internal sediment), R ('Raggioni' cement), E ('Evinspongiae'), S (Sparry calcite) and D (Dolomite).

CHEMOSTRATIGRAPHIC ANALYSES

The isotopic data have been discussed according to the geographic distribution of the sampled sections, the depositional setting and the stratigraphic evolution. The distribution of the isotopic values across the different domains of the platform evidenced that a major shift in isotopic values is observed comparing the Esino Limestone and the Calcare Rosso. In order to verify this

observation, two detailed stratigraphic sections have been measured across the boundary between Esino Limestone and Calcare Rosso both on reef-upper slope settings (Cava Gamba) and in inner platform settings (Zorzone).

The chemostratigraphic analyses were performed to:

- evaluate the effect of a subaerial exposure of the top of the Esino Limestone in inner platform settings (Zorzone log) and marginal platform successions(Cava Gamba log) on the isotopic composition of calcite;
- identify the existence of geochemical events (negative, positive shifts and trends in the isotopic stratigraphy) that could highlight a correlation between the two stratigraphic sections;
- characterize a possible chemostratigraphic curve for the Ladinian-Carnian boundary.

Data were collected along the road to Gamba quarry (950 m above s.l.) and along the private road from Zorzone to Cascinetto di Menna (1380 m above s.l.). The obtained isotopic curves permitted to characterize the isotopic signature of the facies associations and the cavities fillings close to the boundary between Esino Limestone and Calcare Rosso.

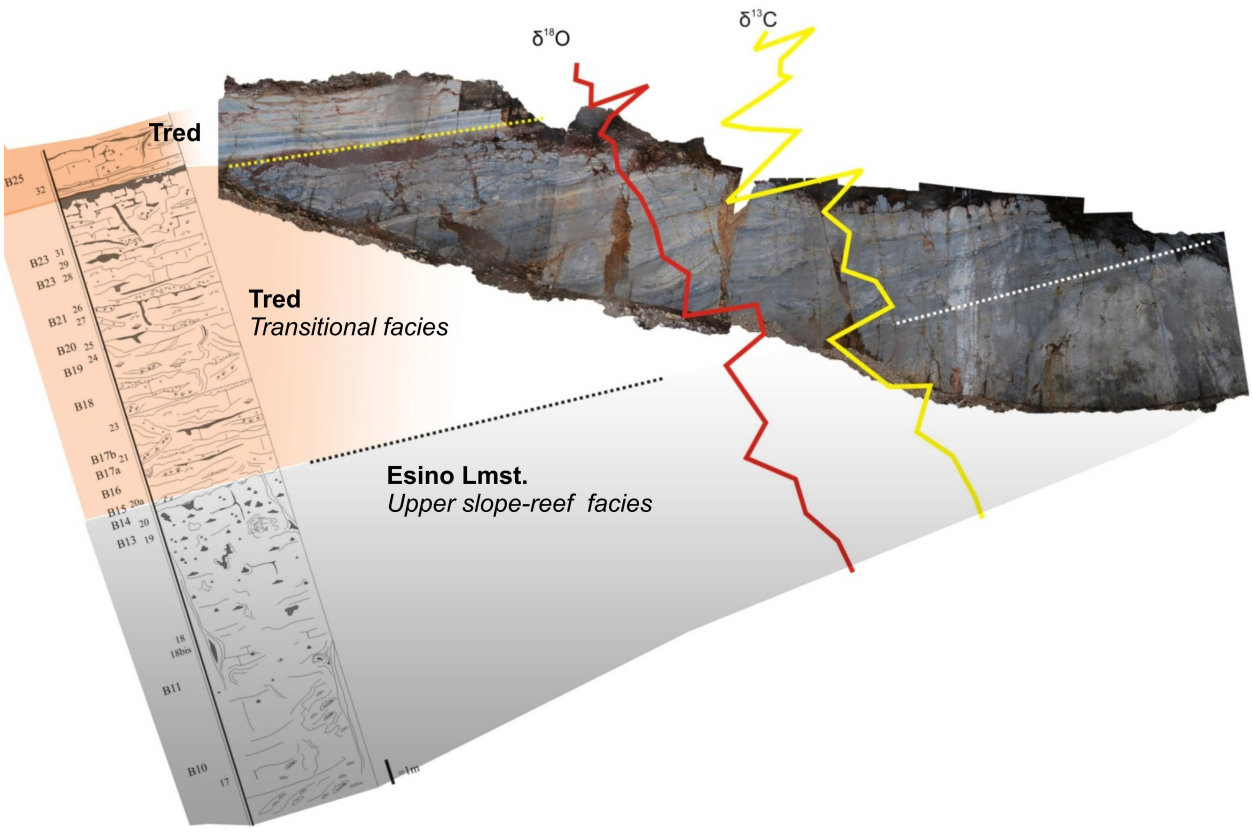

Fig. 3.13 *- Stratigraphic log of the upper Esino\Calcare Rosso transition along the road to Gamba quarry and isotopic curves characterizing the first disconformity in the southern margin.*

CHEMOSTRATIGRAPHIC RESULTS

The chemostratigraphic curves show a comparable trend in the two sections (Fig.3.14).

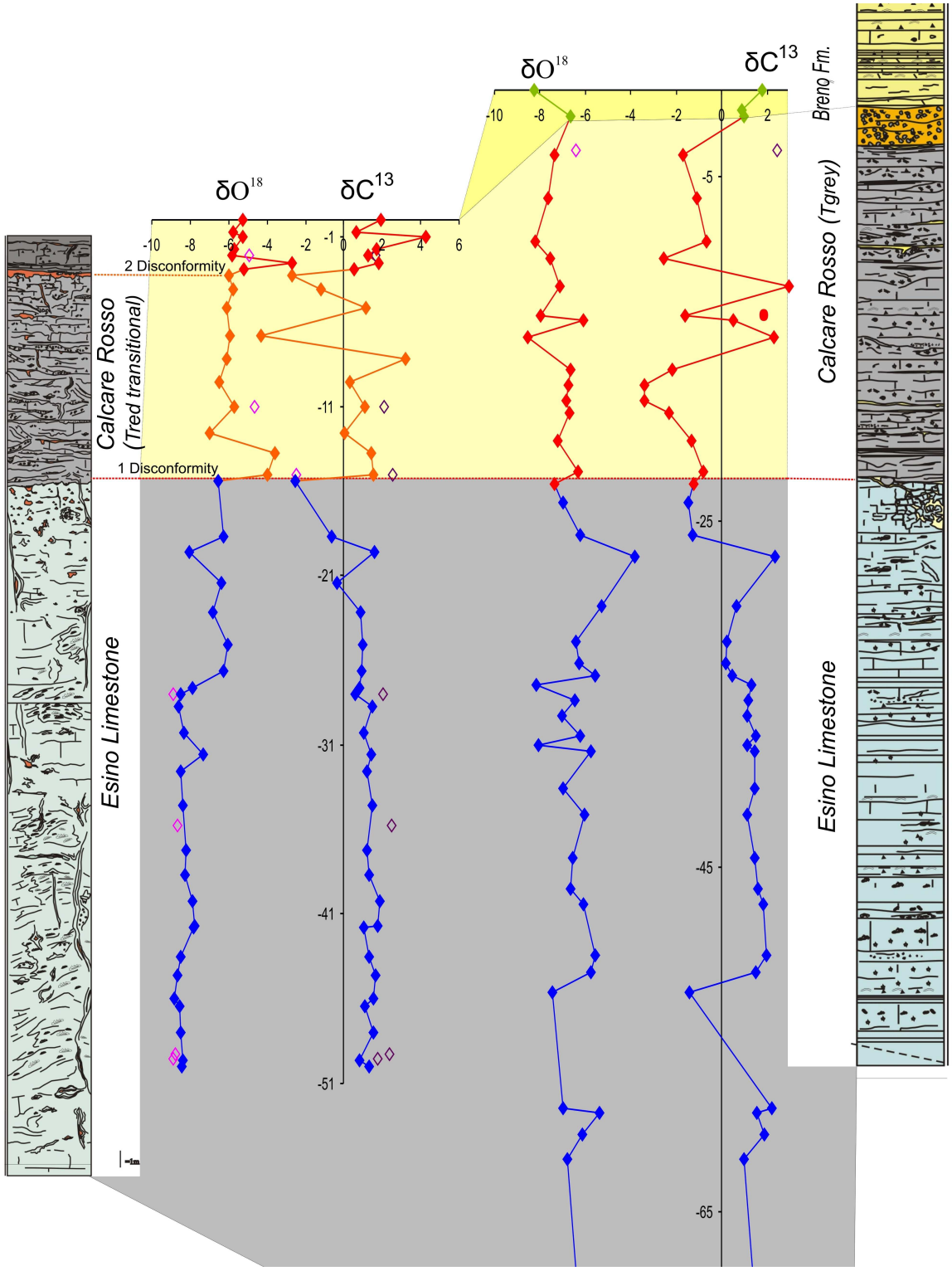

Fig.3.14 - *Stable isotope trends in two stratigraphic logs around the Esino/Calcare Rosso boundary in the inner platform and upper slope southern margin successions (left: Gamba Quarry, right: Zorzone).*

- *Upper Esino*: $\delta^{18}O$ values show an essentially homogeneous trend with a slightly positive shift in the marginal platform facies. The average values are between -5 and -8. Also the $\delta^{13}C$ values are comparable, homogeneous and positive (between +1 and +2) until 3-4m below the first disconformity in both logs (Fig.3.13).

- *Esino Limestone -Calcare Rosso boundary*: a negative shift of the $\delta^{13}C$ curve (about 4‰, +2 to -2) marks the most important chemostratigraphy event at the Esino Limestone-Calcare Rosso boundary. In the two logs (inner platform and margin) this geochemical event is highlighted by three samples and starts 4-5 m below the first disconformity. In the 'Gamba quarry log' the $\delta^{13}C$ values are positive in the lower part of the transitional carbonate facies of the Calcare Rosso.

In the Zorzone log, a negative shift (up to $\delta^{13}C$ =-3.5‰) is present in the supratidal carbonates of the lower Calcare Rosso, 8-9 m above the basal disconformity (9 samples).

3 samples from the residual breccias outcropping at the top of the Menna inner platform succession and equivalent to the Calcare Rosso (Valmora and Vindiolo logs) were studied. The data obtained by matrix sampling are very variable ($\delta^{13}C$ =-3.75 to $\delta^{13}C$ =0.54).

Calcare Rosso: data on the entire Calcare Rosso succession have been collected only along the Zorzone log, where the unit is only a few meters thick. The values of $\delta^{13}C$ are generally negative: 12 out of 15 are between $\delta^{13}C$ =-3.40 and $\delta^{13}C$ =0.66. Positive values have been observed only in internal sediments and 'raggioni'.

Along the Gamba quarry log, only the lower Calcare Rosso and the transitional facies of the Esino Limestone were sampled. The trend is generally positive, with minimum values between -$\delta^{13}C$ =4.32 and $\delta^{13}C$ =-1.19. Analyses on the samples collected for diagenetic investigations show negative values of -6.22.

Geochemical data from the 'Antenna log' (Cespedosio, Val Brembana) and Cadei Quarry complete the chemostratigraphic curve of the Gamba quarry log. Data from the Cadei Quarry (lower part of the Calcare Rosso) are positive (1.65 to 3.01). Data from the 'Antenna log' are both positive and negative.

The $\delta^{18}O$ data from the Gamba quarry log show a sligtlhy positive trend (Fig. 39, 40): average values between $\delta^{18}O$ =8.89 (at the base) and $\delta^{18}O$ =6.06 (at the top). At the Esino Limestone/Calcare Rosso boundary the trend of the $\delta^{18}O$ is similar to that of $\delta^{13}C$

The $\delta^{18}O$ trend of the Zorzone log data is comparable but with frequent and remarkable negative shift of 2.5‰. Negative values range between $\delta^{18}O$ =-5.3 and $\delta^{18}O$ =-8.68‰.

The Calcare Rosso $\delta^{18}O$ values from the Zorzone log ($\delta^{18}O$ =-5.90 to -7.8) are quite similar to those of the Esino Limestone. Those of the 'Strada Gamba log' are 2‰ more positive (-4 to-6).

DIAGENETIC CHARACTERIZATION OF DIFFERENT CEMENTS

Multiple analyses were performed on different structures\cements from single rock samples (Fig.34) in order to compare (at the micro scale) the isotopic signature of the host rock with the isotopic signature of different cavity infillings and cements.

76 analyses were performed on samples from the Esino Limestone from the road to Gamba quarry (7), Val Secca (14), Valbona (3), Menna (2) and from the lower Calcare Rosso, from the road to Gamba quarry (9), Cadei Quarry (9), 'Cespedosio Antenna' (8), Vindiolo pass (2), Val Mora (4), Mt.Vaccaro (2), Alino (2).

Results:

$\delta^{13}C$ values:

The cements and sediments that fill the cavities at the top of the Esino limestone show a homogeneous and mainly positive (-0.8 to +1.8) values.

The values of the typical cements of the Calcare Rosso shift from -5 to +4. The negative values can be referred to facies affected by contact with paleosols and/or meteoric fluids.

$\delta^{18}O$ values

The values of the cements and internal sediments in cavities at the top of the Esino Limestone show a high variability, from -5.5 to -9. The less negative and more homogeneous values are registered in the marine fibrous radial cement. Evinsponge show a large range (from -6 to -9), with average values similar to those of the raggioni growing associated with them (upper slope, Val Secca log).

Fillings of the Calcare Rosso cavities ranges from -5 to -8.4, showing values similar to those of the cements of the Esino Limestone but more positive with respect to values from evinsponge. Negative values from -5 to -7 are typical of early marine cements (fibrous radial); the most negative are from the diagenetic (modified) raggioni.

Dolomitisation of the southern margin

Only a few samples have been analyzed. The $\delta^{13}C$ values are positive (+2) and the $\delta^{18}O$ values range from -5 to -7. The spatic white dolomite (Dw) shows similar $\delta^{13}C$ values, whereas $\delta^{18}O$ values are more negative, ranging from -8.5 to -9.

FLUID INCLUSIONS

Fluid inclusions analyses were performed on 5 samples by the FIT Fluid Inclusions Tecnologies Inc Laboratory of Brocken Arrow (OK, USA). The following analyses were performed:

a) 3 analyses on the lithofacies of the Upper Esino: 1) sample B8 Strada Gamba section) is a calcitic cement of a stromatactis-type cavity (facies F and B); 2) sample JM1c is a recrystallized (with diagenetic raggioni) evinospongia grown in a the sedimentary vein in the upper slope (Val Secca: facies E,R); 3) sample A45bis is a fibrous radial isopachous cement from the breccias at top of the inner platform facies of the Esino Limestone (Mt. Valbona, facies F,B).

b) 2 analyses are from on the Calcare Rosso: 1) sample M12 is a raggioni calcite (facies R); 2) sample JM4 is a fibrous radial, blocky calcite and dolomite filling small cavities (facies F, B, Dw).

The results can be summarized as follow:

Esino Limestone: fluid inclusions show high T° (about 100-115°) and salinity, typical of fluids with hydrothermal or evapotic origin (salinity higher than 10-15%). The inclusions in the early cements can be interpreted as secondary inclusions. Fluid inclusions in the late spatic white dolomite indicate temperatures of 160-165° and high salinity (15-19%). Oil inclusions are absent.

Calcare Rosso: the values of inclusions in early cements are similar to those of the Esino Limestone: the range of variability is wide and temperature is high (95-130°). Salinity ranges from typical values of hydrothermal/evaporitic fluids (11-22%) to normal marine salinity to brackish (0.0-3.7%) (raggioni). Sample JM4 contains oil inclusions, possibly biodegraded and not quantifiable.

$^{87}Sr/^{86}Sr$ RATIO

$^{87}Sr/^{86}Sr$ ratios were measured at the CNR Laboratory, Pisa: 23 analyses on the 9 samples from the Calcare Rosso (including Volcanoclastic Alino deposits) and Esino Limestone (inner platform and margin). Measurements were made using a Finnigan MAT 262 multi-collector thermal ionization mass-spectrometer. Measured $^{87}Sr/^{86}Sr$ ratios have been normalized to $^{87}Sr/^{86}Sr = 0.1194$.

The quoted error on single measure is the standard deviation of the mean (2□m). Replicate analyses of international reference standard NIST 987 (SrCO3) gave an average value of 87Sr/86Sr = 0.710261±0.000013 (2□D). 3-10 mg of samples were dissolved into Savillex screw-

top beakers using a HCl 6.2N. Sr were separated using Sr.SpecElChroM resin. Two total blank were measured at the beginning and at the end of the sample analyses.

The obtained results show congruent values within the range of standard values for Ladinian-Carnian time. A single sample of blocky calcite from the Cadei Quarry show a higher ratio, reflecting the diagenetic origin of the cement.

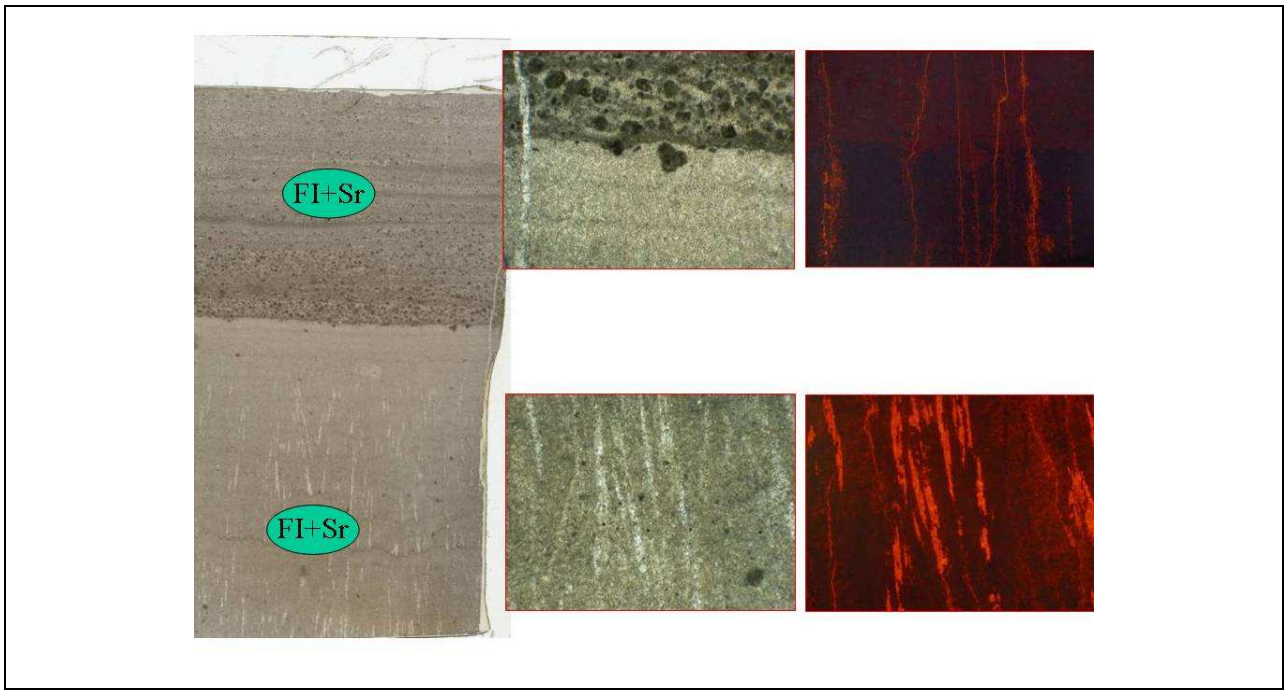

Fig.3.15 *- Example of a sample (Jm1c) studied for fluid inclusion and Sr isotopic composition (upper Esino Limestone).*

POROSITY EVOLUTION AND QUANTIFICATION

The facies of the Esino Limestone are characterized by a wide range of textures which control their physical properties. In detail, the porosity of the recognized facies is dependent upon the nature of the depositional processes and upon the diagenetic history.

In order to quantify the porosity changes from deposition to the present, a procedure has been developed. Porosity has been evaluated identifying the abundance of the different components of the rock (e.g. cements, internal sediments, different types of host rock, fractures) and the different episodes of porosity destruction and creation, determined with the diagenetic study. In detail, we focused on the quantification of the original porosity of the sediments a) before the cementation (both early and late, i.e. depositional porosity), b) during the early diagenetic stage

(after early cementation) and c) after burial (present-day porosity). Due to the different size of the elements which built the rocks (from breccia boulders to fine mud) the porosity evaluation has been performed at different scales (from outcrop to thin section), producing a work flow which can be applied to the different facies. The obtained porosity is mainly based on the presence of voids from outcrop to thin section scale, thus underestimating the porosity related to very fine-grained sediments (mud). Therefore, the inner platform sediments are likely characterized by a higher porosity than the one obtained from our work flow, due to the abundance of mudstone. This porosity was reduced heavily by compaction of the sediments during deposition. The obtained values of porosity for the different facies of the carbonate platform can be considered a proxy of the permeability of the facies at the different stages of evolution (due to the size of the considered pores) whereas the porosity not related to permeability (pores not connected in mudstone) is not considered.

METHOD

The different characteristics of the facies identified in the Esino Limestone and the wide range of grain size, required a procedure that takes into account porosity at different scales. It is possible to identify a macro-porosity (outcrop scale) and micro-porosity (thin section scale) which have been evaluated with different approaches on digital images.

Nature of porosity is different (in terms of distribution and size of the voids) in the different facies. The inner platform facies are characterized by frequent small cavities (mm/cm) filled by fibrous (early) and blocky (late) calcite cements and/or internal sediments. A network of sheet cracks (with internal sediments) is locally observed. Blocky calcite also fills dissolution vugs. In the reef-margin area the distribution, size and shape of the cavities is controlled by the existence of bioconstructions. Cavities are larger than 1 m, often associated with early fractures with fibrous cements (evinsponges) or internal sediments. In the slope the porosity is mainly related to the interparticellar cavities in the clast-supported breccias. Cements are fibrous and locally internal sediments fill the cavities.

The use of image analyses software packages on outcrops was not satisfactory as too many variables (light conditions, shadows, humidity, lower contrast between different facies and so on) affected the process. On the contrary, the image analyses approach was efficient on thin section images. Therefore, a two-levels approach was followed: at outcrop scale a manual definition of

different areas was performed, whereas a computer-aided definition of homogeneous components was used on thin sections. In order to return confident average values of the porosity, the work flow has been applied to different settings. In detail, outcrop-scale elaboration were performed on more than 30 images, whereas 8 thin sections (6 from inner platform and 3 from the upper slope) have been processed.

WORKFLOW

The first step considers the manual definition of areas corresponding to sub-facies with homogeneous porosity, large voids and cements on the outcrop and on its images. At the end of this stage, we have the subdivision of the facies in homogeneous areas. The existing voids and cement-filled cavities reflect the large-scale porosity, whereas the microscale porosity is evaluated for each subfacies with studies on thin sections (image analyses; second step). Once porosity has been calculated at different scales, it is possible to estimate the porosity that existed ad different stages of evolution of the unit. At this step, it is important to know the different diagenetic episodes which in turn created or destroyed the porosity, allowing a confident evaluation of the existing porosity at different diagenetic stages. The followed workflow allowed the measurement of the porosity at the time of deposition (before early cementation), during the early diagenesis (after precipitation of the fibrous early cements) and after burial (late diagenesis) when porosity is represented by present-day voids and open fractures.

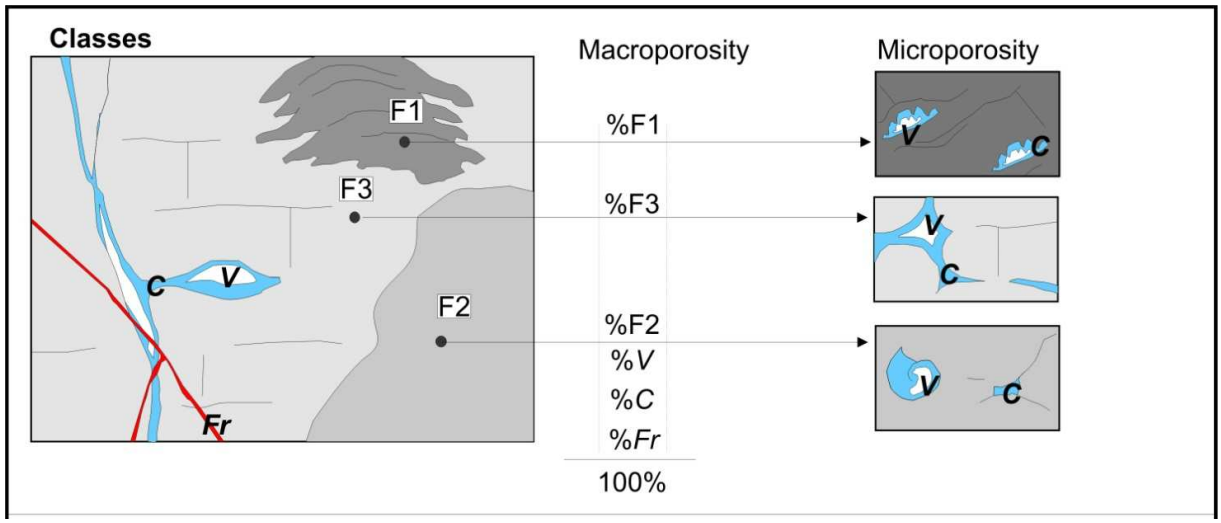

***Fig3.16**. – Procedure for the evaluation of the porosity at different diagenetic stages on the studied successions.*

In detail different types of classes of facies/events have been identified: 1) Early cements: Evinospongia, microbial coating, isopachous cements; Early fractures cements; 2) Terra rossa cavities and fracture filling; 3) Burial cements (calcite and dolomite); 4)Residual porosity (remaining voids after cementation); 5) Recent fractures; 6) Host rock.

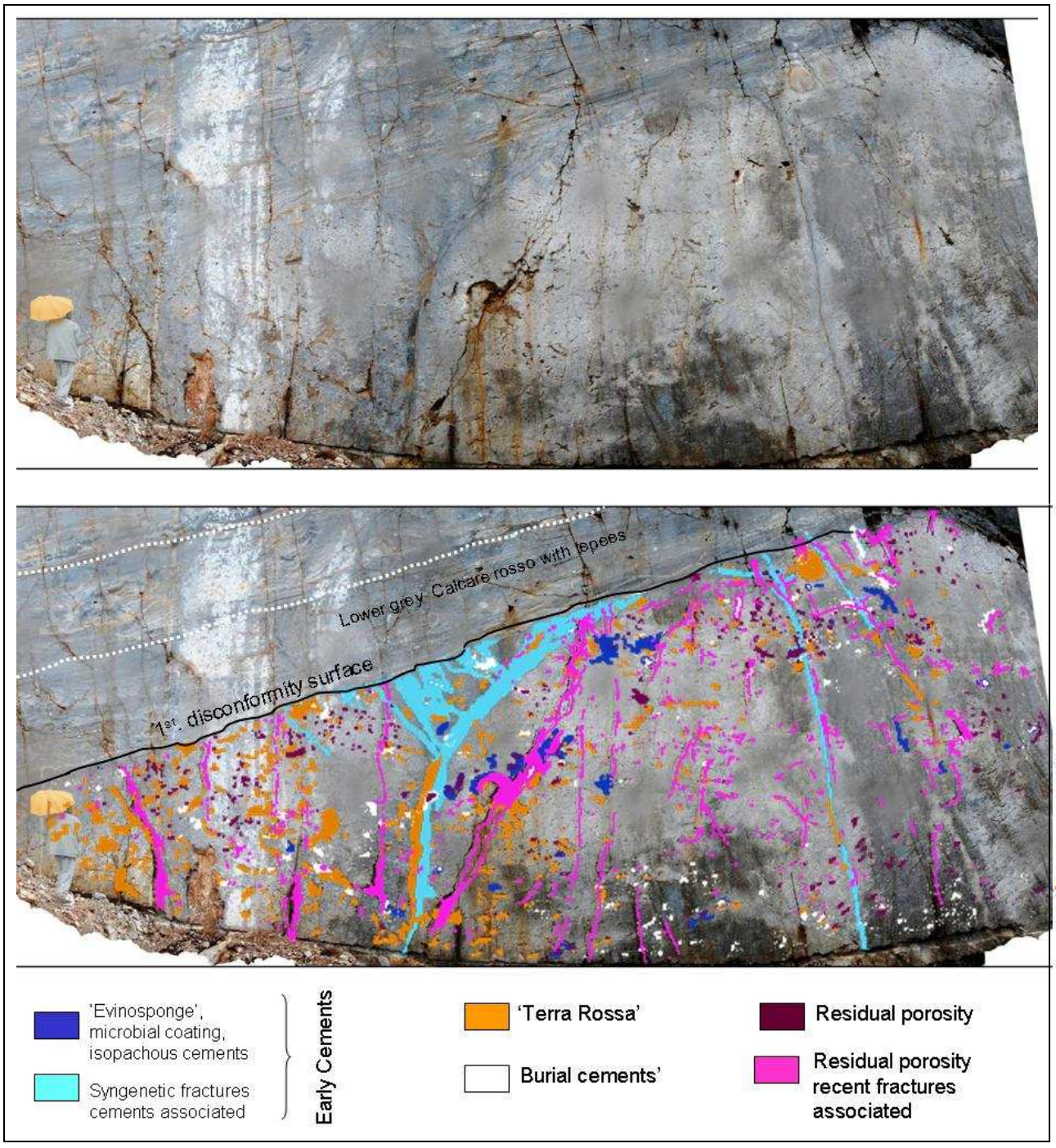

Fig.3.17 *- Top of the Esino Limestone (marginal facies) unconformably covered by the Calcare Rosso along a subaerial exposure surface. Coloured areas show distribution, size, shape and nature of cavities filled by cements, internal sediments and residual voids. Effects of exposure are marked by infilling 'Terra rossa' deposits in fractures and voids. Major cavities are partly to totally filled by isopachous*

cements (i.e. evinsponges). The host rock has been divided in different sub-facies, which have been defined on the outcrop surface and then reported on the picture (inage analyses software were not able to confidently identify these different sub-facies).For each sub-facies, a larger-scale porosity has been calculated.

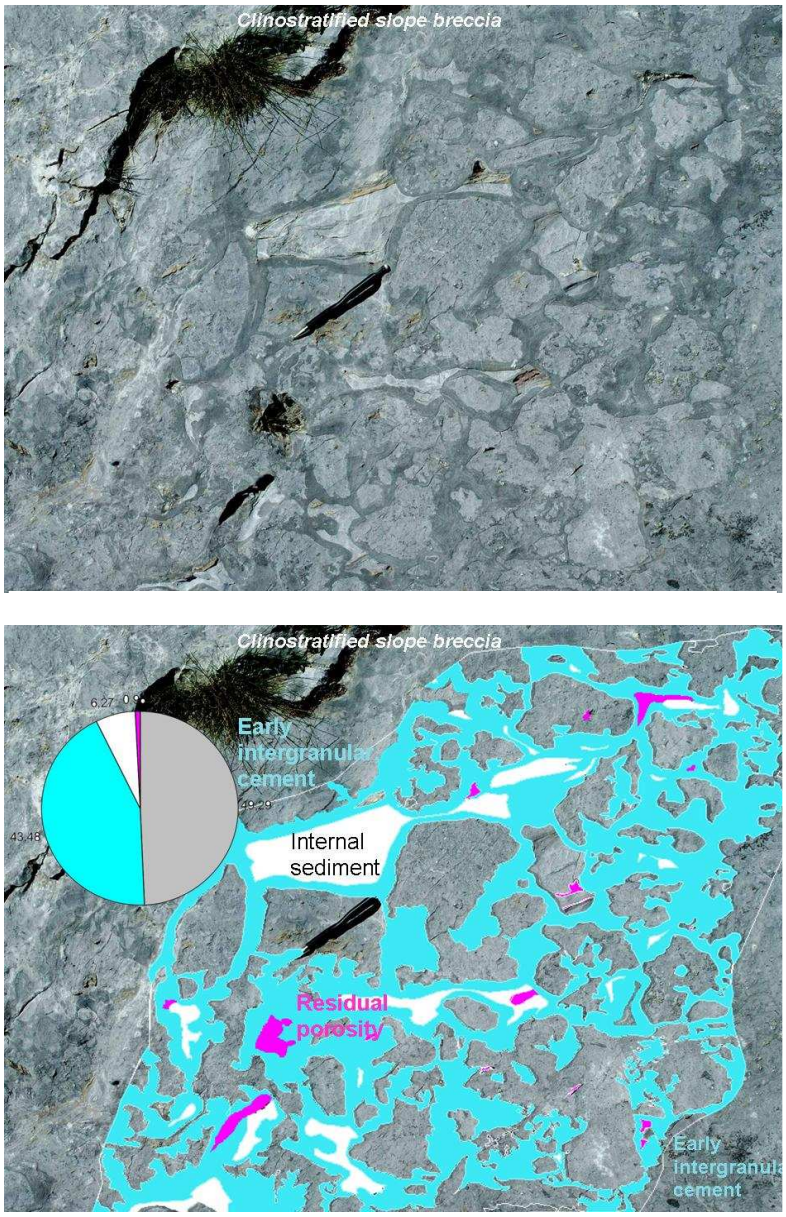

Fig.3.18 *- Porosity evaluation of slope breccias. In this case, the original porosity is represented by intergranular voids, filled during early diagenetic stages by isopachous fibrous cements (blue, belos) and internal sediments (white). Note the existence of a residual porosity (purple) in some of the original voids.*

This approach resulted extremely powerful when working on cut quarry walls (Fig. 3.17) or clean outcrop surfaces (Fig.3.18), where direct observations are possible with continuity on the outcropping surface, so that the distribution of the different facies can be precisely transferred on digital images.

The determination of the porosity of the different sub-facies was obtained by the evaluation of the different porosity on hand-specimens and on thin sections.

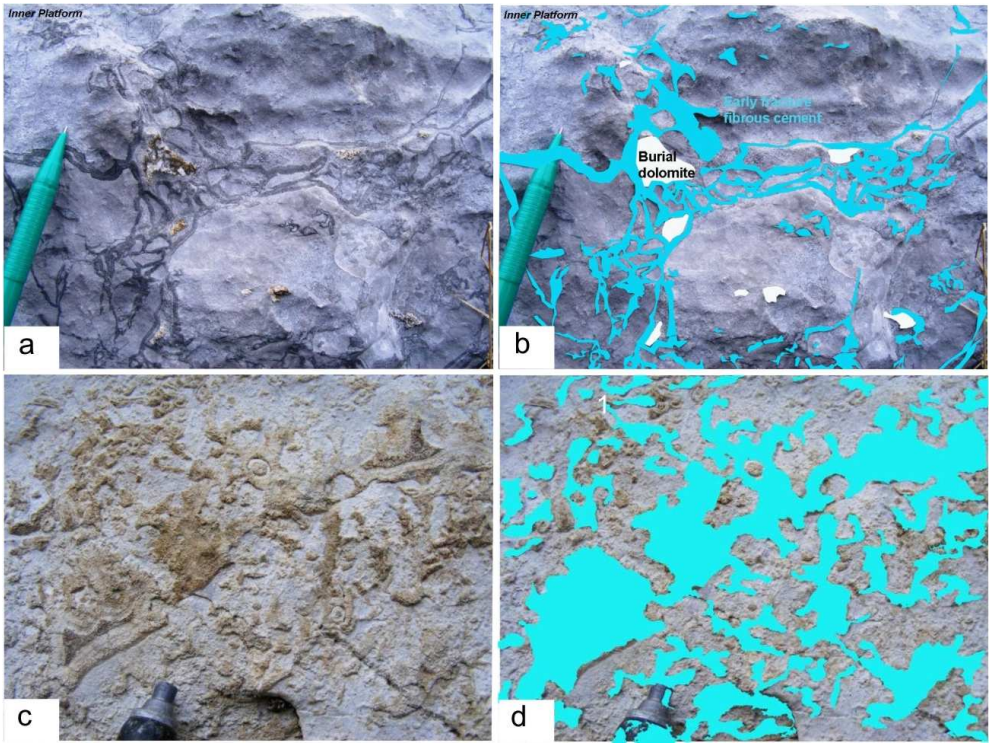

Fig3.19*- Examples of images used for the evaluation of the porosity in the inner platform facies. Top: Network of early diagenetic fractures with dark cements (blue) and burial dolomite (white); Bottom: intergranual porosity with different generation of early cements (blue). All the definition of the sub-areas are hand-made.*

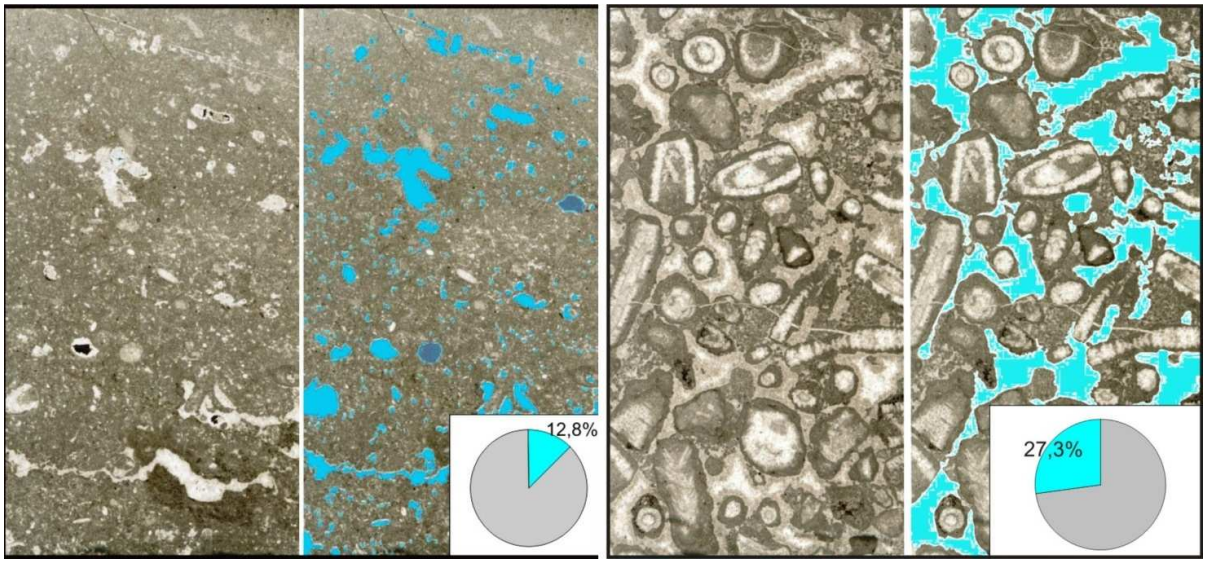

Fig3.20 *- Images in thin section from inner platform facies. On the left fine-grained packstone with fenetral fabric, on the right bioclastic packstone/grainstone with dasycaldaceans. The percentage of*

cement-filled voids (blue on the thin section) ranges from 12.8% to 27.3% of the section. Definition of the sub-areas from image analyses.

At the end of the work flow, it was possible to quantify the existing porosity after deposition, during early diagenesis (early cementation stage) and after burial (present-day porosity).

The evaluation of the porosity at different stages allowed the definition of a porosity that existed at each diagenetic stage and an ideal maximum porosity which results form the sum of the porosity at each stage. This latter porosity is higher than the maximum porosity at each stage, but it is considered to be an indicator of the efficiency of the processes did destroyed the porosity along the history of the rocks, from deposition to late diagenesis. This parameter has been called "max diagenetic porosity". The max diagenetic porosity thus represents the result of the depositional porosity plus the porosity produced at different events after the sediment deposition.

Considering the diagenetic history of the Esino Limestone, the max diagenetic porosity is mainly controlled by the primary porosity related to sedimentation.

In order to compare the effect of the subaerial exposure of the top of the Esino Limestone before the deposition of the Calcare Rosso, the max diagenetic porosity has been calculated ad different depth from the subaerial exposure surface (Fig. 3.17). In this case, the late diagenetic porosity (i.e. fractures) has not been considered in the maximum diagenetic porosity. The effect of the subaerial exposure on the porosity is responsible for a slight increase of porosity (about 5% on an average original porosity of about 45%; Fig. 3.17). The effect of the subaerial exposure is therefore not able to significantly change the porosity of the sediments, thus suggesting that, in the case of the Esino Limestone, dissolution and erosion processes did not affect in a detectable way the original porosity of the sediment. This reduced effect of the subaerial exposure on the generation of porosity can be ascribed to the reduced entity of the sea-level in a greenhouse period (such as the Triassic), whereas different effects could be possible in case of higher sea-level excursions in icehouse intervals. It is interesting to highlight that in the deepest part of the succession the depositional porosity is mainly destroyed by early cementation, whereas close to the exposure surface (up to 5-6 from the surface) most of the cavities are filled by terra-rossa deposits. The evaluation of the max diagenetic porosity in the different parts of the platform (inner platform, margin-reef, slope) returned similar values (Fig.3.20; about 40-45%) which were everywhere highly reduced during early diagenetic precipitation of calcite cements.

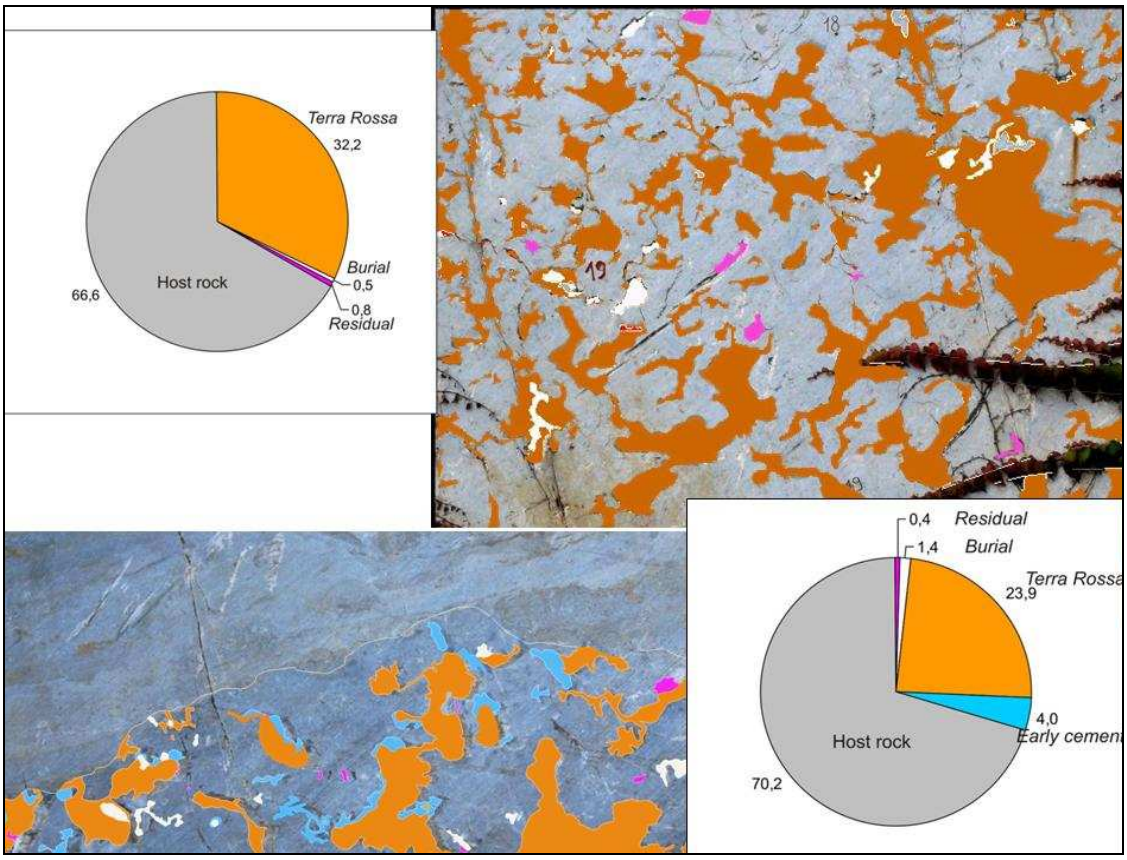

Fig. 3.21 *- Effects of the platform top exposure on the margin/upper slope facies with microbial stabilizated rocks. Primary voids and dissolution cavities were filled by 'Terra rossa' deposits. b. Detail of disconformity surface. Colors highlight 'diagenetic porosity'represented by the sum of early and burial cements, 'Terra rossa' deposits and residual porosity.*

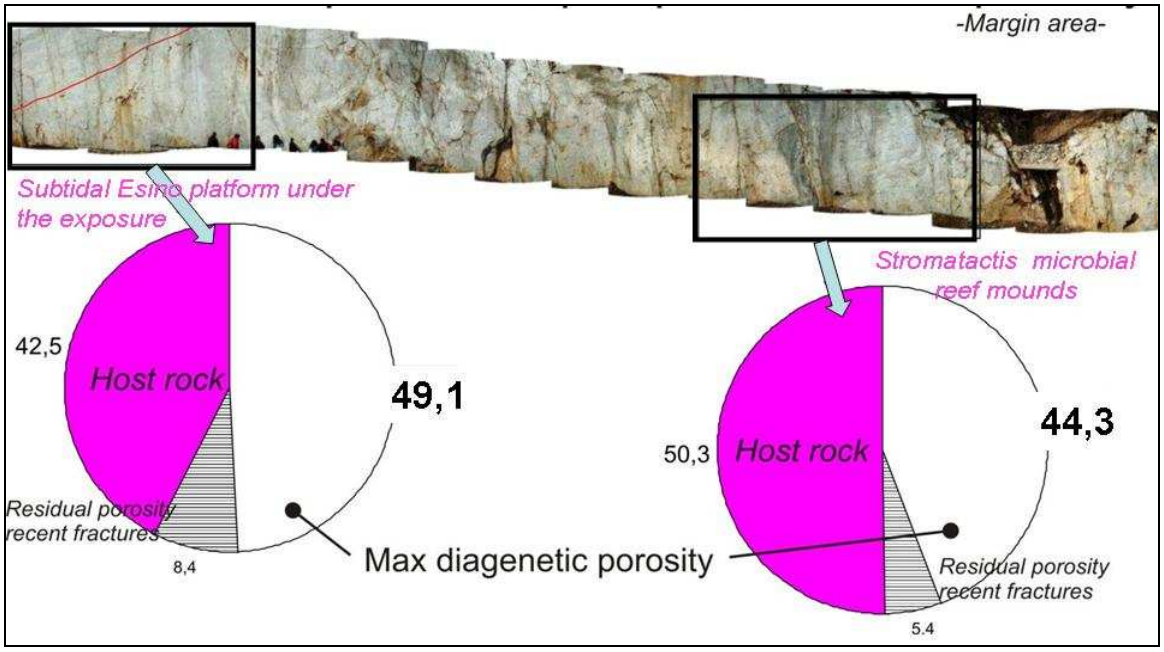

Fig3.22*. - Comparison between porosity in the margin-reef area close to the subaerial exposure surface (left) and at higher depth (right).*

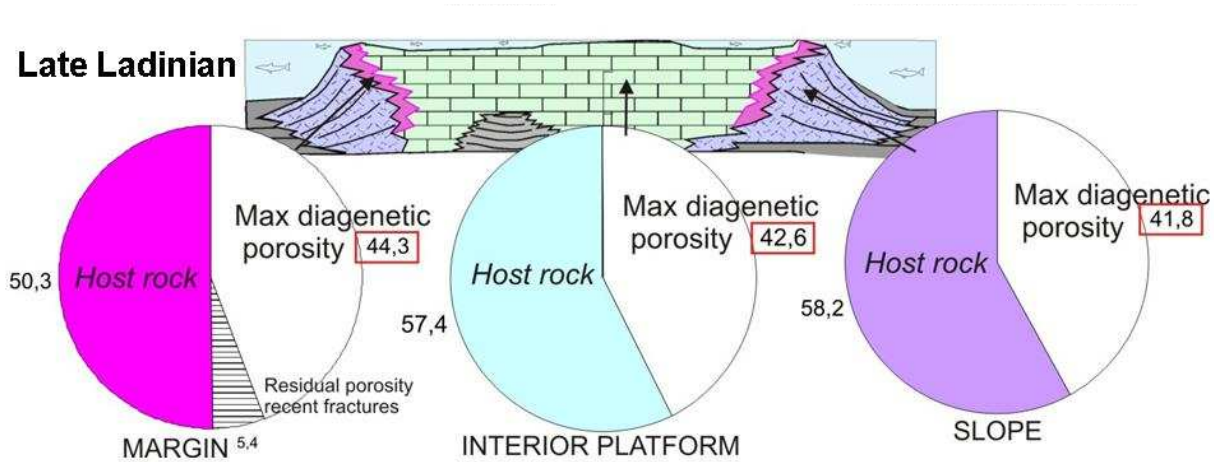

Fig. 3.23 *- Comparison among porosity values in different settings of Esino Limestone.*

Chapter 4

RESULTS

STRATIGRAPHY

Close to the Ladinian-Carnian boundary, a major sea level fall leads to exposure of the flat-topped, prograding Esino Limestone carbonate platform in the Central Southern Alps (Assereto et al., 1977; Jadoul & Rossi, 1982; Gaetani et al., 1998).
The subaerial exposure reduced the size and efficienty of the carbonate factory, as observed in other coeval carbonate platforms in the Lombardy Basin (Berra, 2007).

The reduced accommodation at the top of progradational platform led to the deposition of the thin (from a few to a 60 m) regressive unit of the Calcare Rosso (KLR). This unit groups the all deposits of the Brembana platform associated with the regressive stage: Typical (Tred, Tgrey) peritidal, tepee-deformed limestones capped by paleosols, Lagoonal restricted facies (Lf: fenestral, Ld: dolomitized) and Residual breccias.

The analyses of the facies distribution in the Calcare Rosso and Esino Limestone indicate that:
a) the ***distribution of the Calcare Rosso facies is strictly related to the distribution of the underlying facies of the Esino Limestone*** (Fig.4.1).
b) ***facies changes in the Calcare Rosso deposits are associated to changes in thickness.***

In particular, Typical (red, grey) facies (Tred, Tgrey) were deposited generally above the reef-upper slope domain; Lagoonal (Lf, fenestral; Ld, dolomitized) facies, as well as Residual breccias, were deposited above the inner platform domain. The Residual breccias are widespread above the inner platform facies but outcrop also in the reefal areas associated (above or below) to the Typical facies.
Moving from the upper slope to the inner domain, the thickness of the Calcare Rosso deposits decrease from the 60 m of the Tred facies to the 0,3 m of the Residual breccias in less than 2 km.

In the inner platform domain, the Calcare Rosso deposits range from 10 m to 0.3 m, and from Typical grey and/or Lagoonal facies to Residual breccias in less than 1 km.

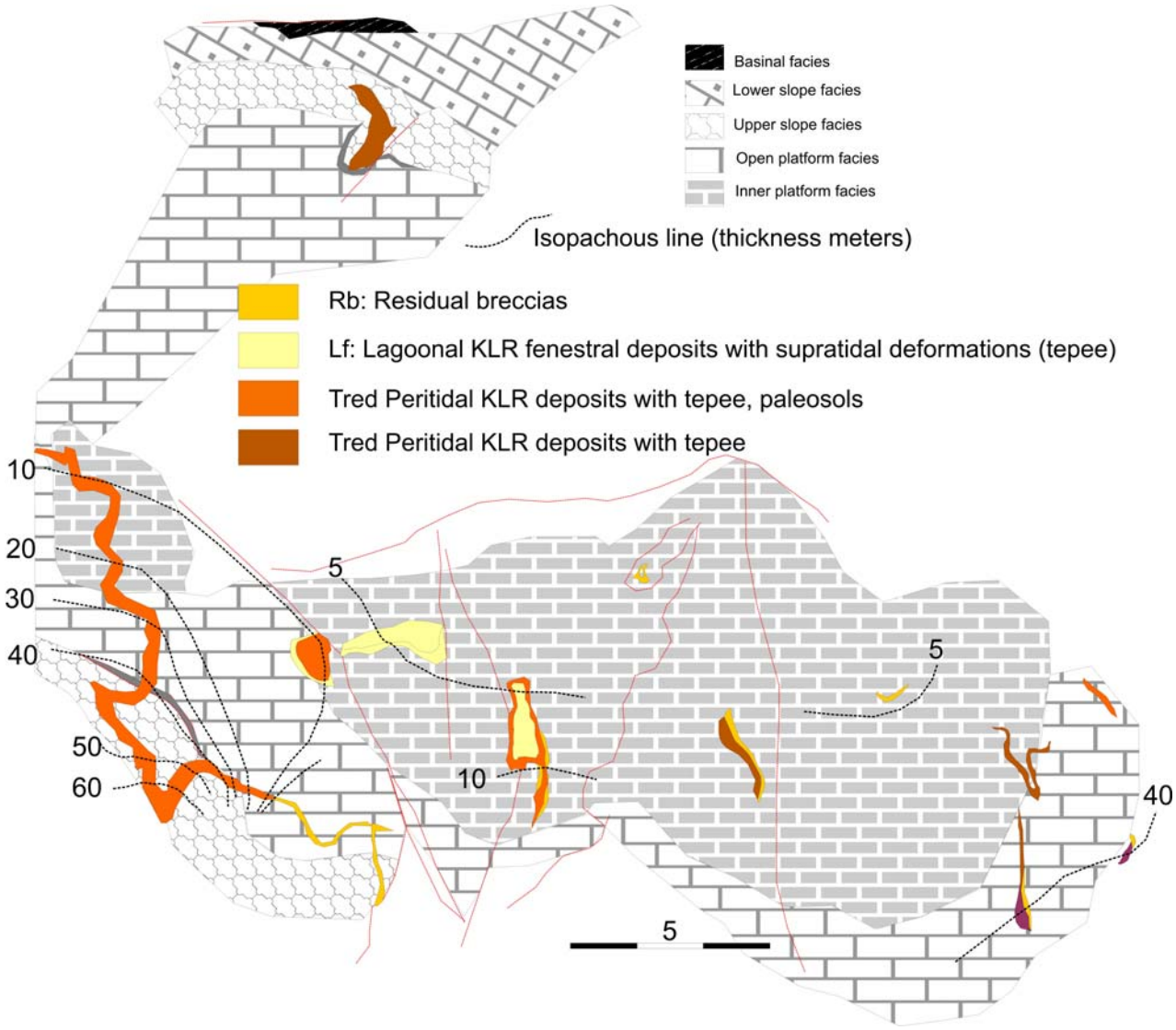

***Fig.4.1**: Paleogeogrophic map showing the relationships between Esino Limestone facies and both isopachous and distribution of the facies of the overlying Calcare Rosso.*

An ***high variability*** of ***facies in the inner platform*** reflects differentiated environments at the top of the Esino Limestone; moreover, the high variability is a significant effect of the reduced accommodation space.

In the inner platform the original topography of the Esino Limestone may have suffered karst processes, which resulted in the deepening of former shallow depressions. The evolution of surface karst features led to the deposition of erosional sediments (residual breccias) within depressions, followed by the onset of pond depositional environment. Karst depressions were filled by sediments and the surface flattened before the deposition of the subsequent Tgrey formation.

Narrow lagoons and ponds, where dark-gray bioclastic limestones were deposited, border exposed areas, in which paleosols and karst features developed. Therefore, at the same time, in the inner platform domain contrasting erosional and depositional processes took place. The evolution of different sub-environments (lagoon, pond, ...) in the inner platform was controlled by local factors. Sedimentation and erosion rates could be extremely variable. Above the intraplatform basins which were not sutured by the platform progradation (Mt. Valbona) or marked by high subsidence for compaction of thick basinal succession, the sedimentation of several restricted-lagoon cycles capped by tepee (Assereto & Kendall, 1977) occurred (Fig.2.11). These deposits (0,3 m) rapidly pinch out towards subaerially-exposed areas (Mt. Menna). During the regressive phase, the interplay between erosion and deposition in the inner platform areas produced a progressive levelling of the topographic surface.

In the ***upper slope***, the more continuous sedimentary record was characterized by cyclic alternation of marine deposition and subaerial erosion and by repeated superimposition of different diagenetic modifications, due to greater accommodation space. Peritidal cycles are capped by paleosols and repeatly affected by karst processes (Fig.2.3). In the southern margin of the Brembana platform the balance between sedimentation, subsidence and sea level oscillations preserves the most complete sedimentary record (the Tred facies of the Calcare Rosso, Fig.2.7) of the regressive phase. The subtidal/ peritidal ratio into the cycles of the Tred shows a prevalence of the peritidal deposits with respect to the Tgrey facies (Fig.2.8). Tgrey facies are often underlain by karst-breccias deposits (Fig.2.31-2.32) or residual breccias (Fig.2.10) and could register only the upper part of the regressive phase.

In the reef-upper slope area of the southern margin four major ***discontinuity surfaces*** has been characterized in terms of geometry, lateral extent, surface morphology, facies contrast and associated deposits/structures: the disconformity at the boundary between Esino Limestone/Calcare Rosso (TE); the unconformity internal at the Calcare Rosso (K1, K2); and the unconformity at the top of the Calcare Rosso deposits (TK) (Fig.2.25).

These surfaces can be traced from upper slope to the open platform facies for several kilometres (up to 5 km) and they represent an important tool for the correlations. In addition, the study of the karst structures associated to the discontinuity surfaces, provides data on the sea level changes and it's essential for understanding porosity changes related to unconformities on carbonate platforms, the reservoir degradation below subaerial exposure surfaces and the development of permeability patterns (Saller et al. 1995, Budd at al. 1995; Wagner et al. 1995).

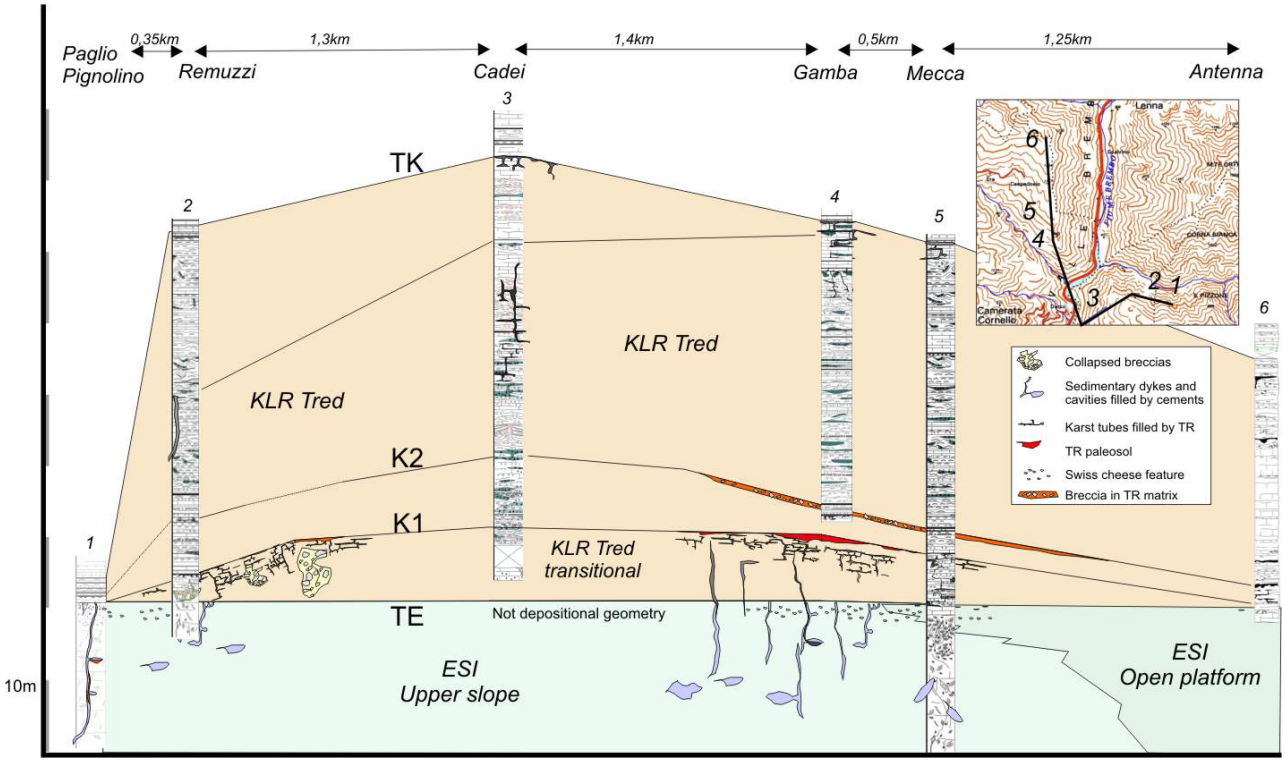

Fig.4.2: *Correlation table of the major discontinuity surface at the transition between Esino Lmst. and Calcare Rosso deposits and within Calcare Rosso deposits.*

Moreover the study of the paleosols associated to discontinuity surfaces provides constrains on the reconstruction of the climatic conditions (Fig. 4.2).

Karst structures are developed below the major discontinuity surfaces both in the Esino Limestone and Calcare Rosso deposits, and range from centimetre scale dissolution cavities to coalescent collapsed-karst systems up to 20 m deep.

Karst structures show wide range a) of distribution in the sedimentary record (Esino Limestone and KLR) and above various domains of the Esino platform; b) of sizes; c) of morphology.

Several local factors control the development of the karst structures and explain these large ranges of characteristics, but at least on the southern margin, moving from the reef-upper slope areas to the open platform of the Brembana platform, it's possible to recognized an 'homogeneous trends' in the lateral evolution of these structures (associated to the discontinuity surfaces at the transition between Esino Limestoine and Tred, as well as in the lower part of the Tred). 1) development of network of tubes and cavities up to 2 m below the K1 surfaces within Tred transitional facies; 2) increase in size and depth (up to 4-5 m from K1) of these structures, locally collapsed; at the same time, development of the network of veins and cavities

(Evinospongia-like) up to 7-8 m below TE surface; 3) paleosols preserved in correspondence to K1; development of a network of centimetre scale cavities (Swiss-cheese structures) up to 4-5 m from TE surface; development of the fractures from K1 (or from discontinuity surfaces slightly beneath) that cut TE surface and deep into Esino Limestone reopening network of cavities and veins; 4) decrease in size and frequency of the karst structures.

The recognized trend of karst development suggests the sea level change and the porosity of the host rock as major factors of control on the karst development. Therefore the vertical development of the karst structures helps in constraining the entity of the sea level changes in the exposed carbonate platform.

Above the southern margin, the fractures cut into Tred transitional and Esino Limestone deposits from the K1 surface measure 15-18 m.

In the inner platform, the distribution of the karst structures is not regular and also morphology and size varies greatly. Only the association of the vertical pit caves (filled by collapsed breccias) and Tgrey facies is common. In the Tgrey facies, these structures deepen up to 6-7 m from TK in the Trevasco area; above the northern margin of the Brembana platform the pit cave developed in the Tgrey facies up to 20 m in depth from TK surface (Fig.2.21).

Similar values of the sea level fall may be inferred from vertical development of the coalescent collapsed karst system observed in the Mt. Arera. Karst structures are cut into the deposits at the top of the Esino platform for about 20 m and the overlying 3-4 m of the Calcare Rosso deposits are deformed.

In conclusion, in the inner platform and in the reef-upper slope areas the recorded maximum amplitude sea level fall is likely about of 20-25 m. This value is obtained by the analyses of the distribution in depth of the collapse breccias above the inner platform facies of the Esino Limestone. Another important sea level fall is recorded in correspondence of the TK surface but its amplitude is not easy to be determined.

Several Terra Rossa layers characterize the Tred succession but the best preserved **paleosol** (Fig.2.4) correspond to the K1 unconformity, that marks the transition between the transitional facies and the typical facies of the Calcare Rosso. The macro- and micro- morphological analyses reveal different and subsequent pedogenetic phases characterizing both the paleosol formation and the transport of unweathered material in cavities of paleokarst network lied beneath. In particular the strong weathering of the primary minerals and the decalcification (leaching), the clay neoformation and the illuviation and the strong rubefaction suggest that during the pedogenetic cycle responsible for the paleosol formation the climate was probably

characterized by seasonal soil moisture availability (winter) and water deficit (summer), and quite high temperature during the long dry period (summer), which produced the rubification typical of the Fersiallitic soils (Dudal et al., 1966; Duchafour, 1977; Yaalon, 1997).

The creation of accommodation space on the top of the Esino Limestone can be ascribed to three more prominent controlling factors: 1) syndepositional tectonics; 2) differential subsidence; 3) regional tilting.

1) Sharp changes in thickness and facies of the KLR deposits referred to syndepositional tectonic activity has not been observed.

2) Instead, in the upper slope facies of the Esino Limestone and within the overlying Calcare Rosso Tred deposits, fractures filled by isopachous crusts of marine cements, aligned with the margin platform, has been found. These extensional fractures can be ascribed to stresses triggered by the compaction of the basinal facies overlain by rapid progradation of the Esino platform during the last evolutionary stages. The major thickness of the regressive facies on the marginal areas reflects differential subsidence of these areas with respect to the inner platform areas. As the margin of the prograding Esino Limestone rests on thick (about 150-200 m) of loose, fine grained basinal sediments it is possible that the compaction of the thicker basinal succession favoured a compaction-induced subsidence (Fig. 4.3). Therefore the gradual increase of the subsidence of the prograding complex can explain the wedge-shaped deposits of the Calcare Rosso above the reef-upper slope facies. Nevertheless, to verify this hypothesis, detailed numerical elaborations are needed.

The scarcity of biostratigraphic data in the upper part of the Esino Limestone and in the Calcare Rosso succession prevent a confident dating of the age of the observed stratigraphic events. The only tools for correlations of the regressive facies across different environments of the Esino Limestone consist of physical correlations of the major depositional/erosional surfaces and the presence of tuffaceous/Terra Rossa layers (Assereto et al., 1977). The Calcare Rosso event is likely coeval across the Central Southern Alps according to the continuity of the unit and the well-defined stratigraphic position and the correlation to the sea-level changes across the whole Southern Alps (Gaetani et al., 1998). It is therefore possible to suggest an Early Carnian age for the regressive event, as constrained by conodont and ammonoid data from the basinal facies interfingering with the Esino Limestone in the Concarena massif (Balini et al., 2000). In

particular, the conodont marker species *Paragondonella polygnatiformis* (Burdurov & Stefanov) occurs in this interval. The fossil marker *Clypeina besici* (Pantic) was found 10 m above the base of the Calcare Rosso (Tred) (Jadoul, Cadei Quarry). This fossil was considered Carnian in the past, but a recent revistion of its stratigraphic distribution (FAD in Late Ladinian) is not in contrast with the proposed Early Carnian age.

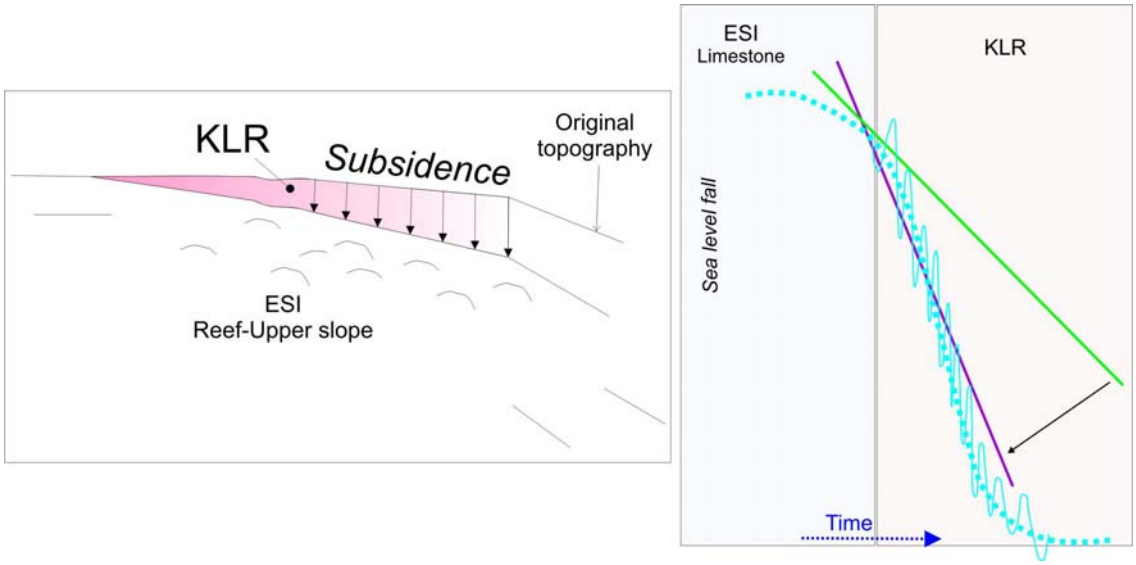

***Fig. 4.3**: Semplified scheme of the differential subsidence in from the inner platform to the upper slope domains in the Esino platform (left). The differential subsidence during the deposition of the wedge-shaped Calcare Rosso is responsible (right) for the different recording of the high-frequency sea-level falls in the inner platform (less subsiding, green line) with respect to the marginal area (purple line), where several cycles are recognized due to the interplay between sea-level fall and subsidence.*

The presence of the Ammonoid (Jadoul et al. 1992) in the upper part of the open platform facies of the Esino Limestone in (Parina Valley) indicates an Upper Ladinian age. This apparently different timing of the 'Calcare Rosso event' might be explained by a reduced accommodation at the top of the Esino Limestone during the last evolutionary stages.

The recovery of the volcanic activity close to the eastern areas of the Esino plarfom is recorded by proximal volcanoclastic deposits of Mt. Alino (Fig.2.16). The origin of part of the Terra Rossa material may be volcanic. The common presence of terra rossa deposits on the southern margin and in the eastern part of the Esino platform confirms this hypothesis.

DIAGENETIC CONSIDERATIONS

Macro/microfacies characterisation

Macro and microfacies characterisation has been performed on the different sub-environments of the carbonate system. The analyses has been locally hampered by regional recrystallisation and by intense dolomitization. Regional deep burial diagenetic processes are partly related to the burial of the succession (from 2.5-3 km), mineralization processes and alpine tectonics.

Evinsponges represent the most problematic and interesting structure on the upper part of the slope and margin. These structures are characteristic of the Ladinian platform of the southern Tethys margin and have been interpreted as a) cements that fill the major cavities/fractures probably related to subaerial exposure (Jadoul & Frisia, 1988), b) reef cements stabilizing margin platform (Frisia et al, 1989), c) reef cavities stabilized and filled by microbial carbonate crusts (Russo et al. 2006).

Macro and micro-analyses allow a partial genetic review: we suggest to restrict the term 'evinospongia' to large, concordant or discordant mammellonary structures in the margin facies of the Esino Limestone, whereas isopachous, centimetre size crust of cement of fibrous radial calcite occurring in the slope breccias are not considered evinsponge. The term evinospongia is thus referred to globular, metric structures or to discordant sedimentary veins filled by early cements. Concretionary crusts are formed by layers on non-isopachous cements and by dark-grey coatings at the contact with the host rock. The latter can be interpreted as early cements that stabilize the upper slope facies, controlled by (endo) microbial activity. Observations suggest a relationship between pH conditions in cavities (i.e. early diagenetic environment with low pH) and microbial activity, responsible of partial dissolution at the sediment-water interface. Micritic-peloidal intercalations alternating with calcitic crusts support the hypothesis of the origin of these cements form chemical precipitation. Some of the fibrous radial crusts have probably a secondary origin and result from recrystallization (mega rays mm/cm; raggioni like) of early layered cements. The presence of ostracods in internal sediments which were deposited after the precipitation of early cements confirms a syndepositional origin of these cements and the fact that precipitation occurred close to the depositional surface, allowing the connection between partly closed cavities and the sea-bottom. The globular evinsponge are interpreted as reef cavities, which were formed in the reef and upper slope facies. Instead, the interpretation of

the larger evinsponge-like structure (metre-scale) is unresolved. They can be interpreted as reef cavities due to early diagenetic dissolution of not preserved reefal organisms, early diagenetic removal/dissolution of metastable carbonates accumulated on the upper slope or (more probable) large voids between bioconstructions, partially enlarged by aggressive waters during the subaerial exposure if the top of the Esino platform (Fig.2.20).

The evinsponges cements in sedimentary dykes (Val Secca log, Fig.1.6) may be related to the opening and filling of syndepositional fractures on the upper slope, parallel to the margin (Canning Basin model; Frost & Kerans, 2009).

Raggioni (Assereto & Kendall, 1971, Assereto & Folk 1980) are interpreted as pseudomorphs of calcite on 'aragonitic hemispheroids', typical of caves or reef cavities. Two types of raggioni, probably reflecting different origins, have been recognized: a) dark raggioni, consisting of hemispheroids and coalesced fans filling sedimentary veins and strato-concordant cavities (top of the Esino Limestone and Calcare Rosso), interpreted as typical speleothems (Assereto & Folk 1980, Assereto & Kendall, 1971, 1979); b) morphologically similar structures but characterized by recrystallization, of cements in internal cavities, sedimentary veins and evinsponges. Their diagenetic origin is supported by the relationships between mega-rays and internal sediments in which they grow. Diagenetic recrystallization of raggioni is locally documented by gradual changes in colour from dark grey (original early raggioni cement) to grey-whitish.

PETROGRAPHIC AND GEOCHEMICAL DATA: CONCLUDING REMARKS

The ***CL observations*** indicate an early diagenetic origin of the marine, not luminescent calcitic cements (Fig. 4.4; fig. 4.5). Early cementation is responsible for the lithification and stabilization of the sediment, occluding most of the primary porosity immediately after deposition. Evinsponges, raggioni, crusts of fibrous radial calcite and part of the blocky calcite can be all classified as early cements. CL observations on the crusts of the fibrous radial calcite allow the identification of a dog tooth calcite (Fm2) growing on older generations of fibrous radial calcite (Fm1). This calcite was generally considered to reflect the effects of meteoric influxes (Flugel & Koch, 1995) but it is considered by other authors a typical marine or shallow burial cementation (Melim et al. 1995). Our observations confirm this latter interpretation.

Luminescent, poorly-zooned blocky calcite documents precipiration during burial. This late cements are volumetrically less important that the early cements.

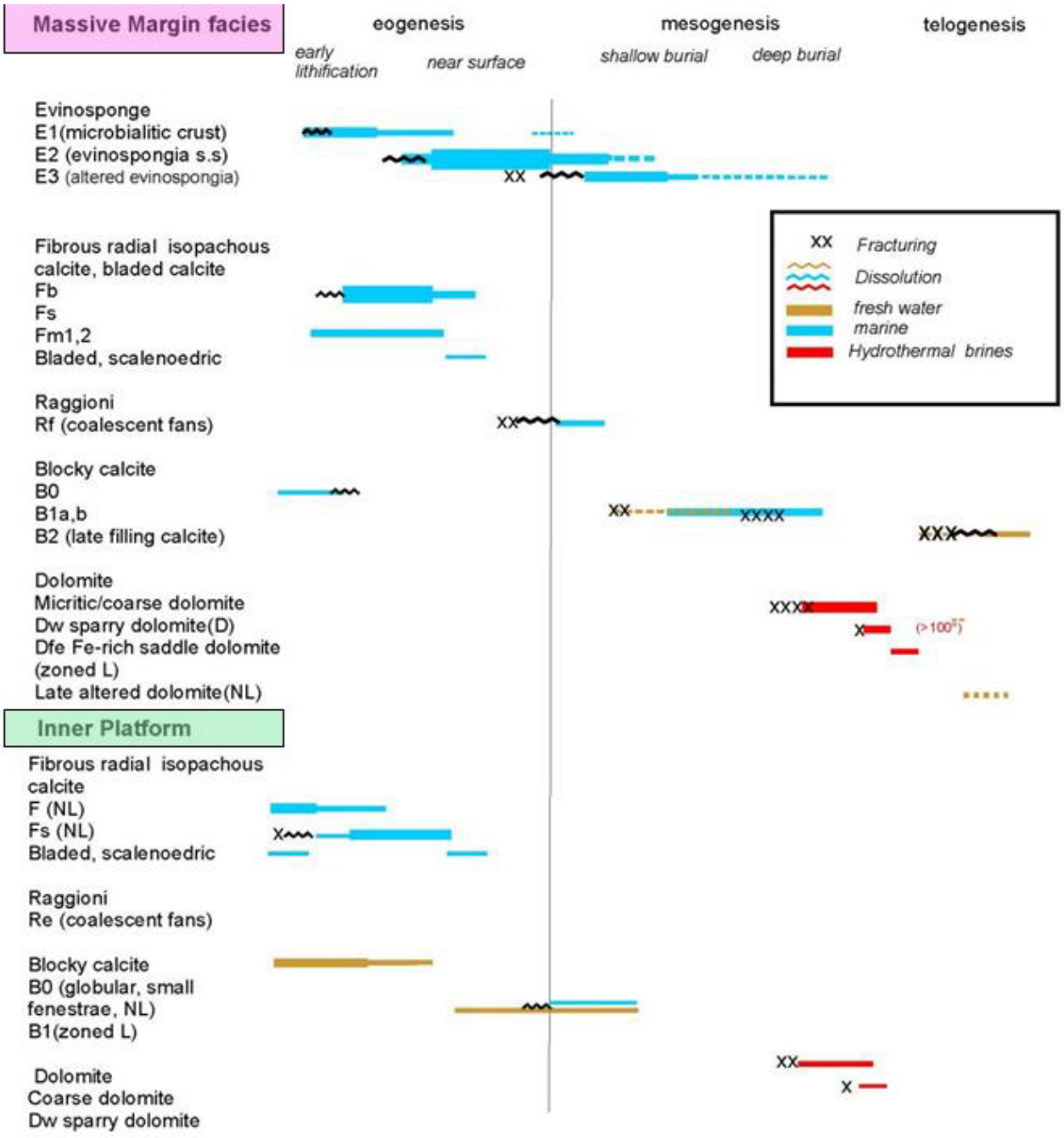

Fig.4.4*- Paragenetic synthesis of cementation and dissolution phases in the upper Esino Limestone.*

The transition between early, not luminescent cements and burial luminescent cements is marked by a network of microfractures which affects both the host rock and the early cements. Burial cementation is not affected by microfractures, as it seems related to a new opening of the diagenetic system (Frisia et al., 1988). This fracturing increases the micropermeability of the rock, favouring the circulation of late diagenetic fluids, which were able to destroy, with the precipitation of cements, the residual or secondary porosity. Microfratures are well-preserved in

the evinsponges (Fig 3.4), where they often develop along the direction of crystal growth (in fibrous radial calcite, Fm1) whereas fractures are more spaced in the dog tooth calcite (Fm2) (Fig.3.4).

In the raggioni partial and preferential dissolution in the mega ray is observed along with burial cementation with luminescent calcite (Fig. 3.5). The CL observations highlight two types of white spatic dolomite (Dw): the first is non-luminescent or dull; the second is zoned. Between the two dolomitic cements, a narrow boundary of not luminescent Fe-dolomite is present. CL studies, geometric relationships between cement and host rock, isotopic and fluid inclusions data confirm their late diagenetic origin. The origin of this dolomite is probably related to hydrothermal fluids, likely related to the development of strata-bound mineralizations (Mississippi Valley type ore deposits of the Gorno-Dossena District, Assereto et al., 1977) which characterize the Carnian succession of the study area.

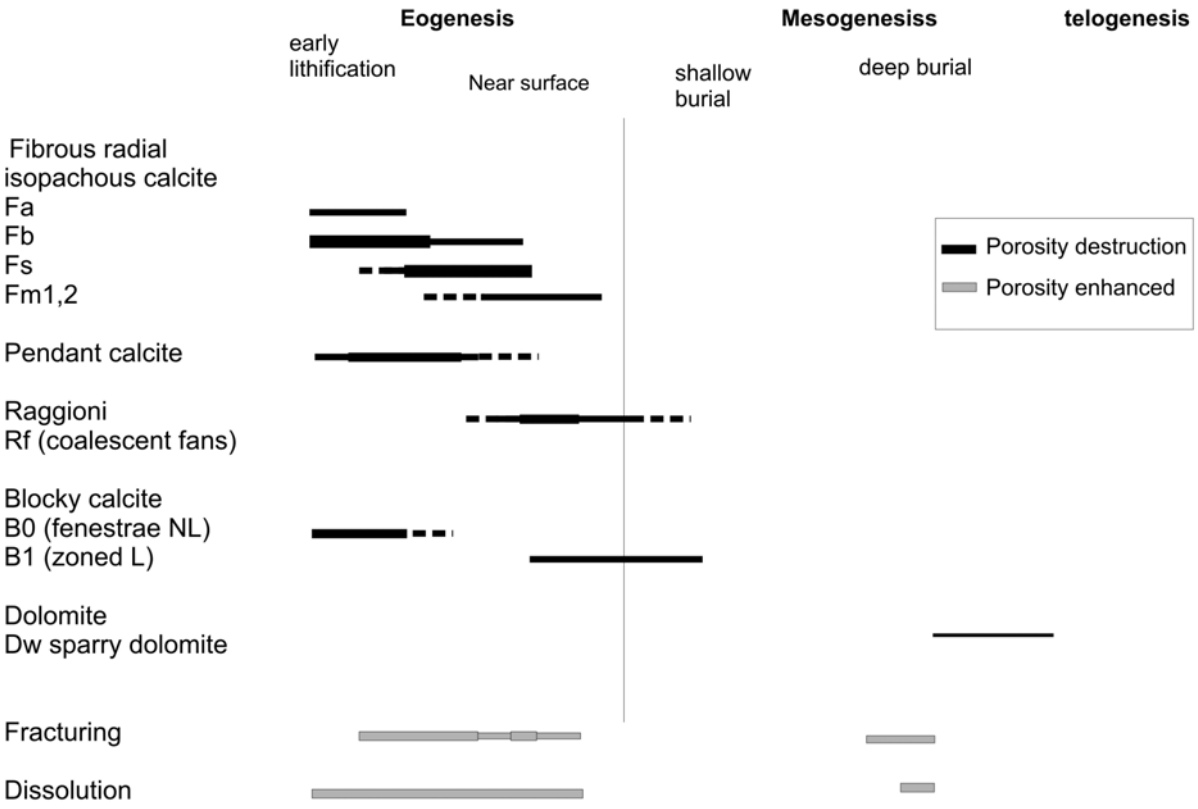

***Fig. 4.5**- Paragenetic synthesis of cementation and dissolution phases in the Calcare Rosso.*

Petrographic-cathodoluminenscence analyses were integrated with ***isotopic characterization*** of the host rocks and the different generations of cements (Fig.3.9). The negative values of $\delta^{18}O$ (on average lower than -5‰) likely reflect a regional negative shift which can be ascribed to homogenization during late diagenesis due to a) hydrothermal fluid circulations during mineralization processes and/or b) burial (5 km about) and heating of the middle Triassic succession of the Bergamasc Prealps (Berra & Carminati, 2010).

$\delta^{13}C$ data at the top of the Esino Limestone show a first negative shift (2‰) which corresponds to the first exposure surface on the top of the Esino Limestone (unconformity surface with the Calcare Rosso) (Fig.3.13). This event is traceable from the inner platform to the platform margin (Fig.3.14). The homogeneous and positive isotopic values of the upper Esino Limestone are interpreted as the result of marine diagenesis. Influx of meteoric waters at the top of the Esino Limestone (corresponding to the negative shift) are restricted to the uppermost 4-5 m of the unit, immediately underlying the disconformity and correspond to the distribution of the paleokarst network of cavities observed in two logs. A second major shift in isotopic values matches the second disconformity marked by Terra rossa paleosols in the Gamba log, within the lower part of the Calcare Rosso. Chemostratigraphic correlations between the Calcare Rosso sections are not possible due to the difference in thickness and facies (and likely in the difference in sedimentation rates and dissolution) in the Gamba log and Zorzone log, where the Calcare Rosso is extremely reduced and mainly represented by breccias. Above the second unconformity, $\delta^{18}O$ and $\delta^{13}C$ values of the Calcare Rosso are more negative than the values from the lower part of Calcare Rosso, suggesting a major role played by meteoric diagenesis.

The isotopic data collected in the cavity fillings at the top of the Esino Limestone are typical of marine conditions. The most negative $\delta^{18}O$ values in the evinsponges and raggioni are interpreted as the effect of homogenization between early isotopic signature (-5,-6‰) and late-diagenetic cements in the microfractures (-8,-9‰).

The general trend and wide range of the $\delta^{13}C$ values from the Calcare Rosso deposits (particularly in the fibrous radial calcite associated to the Terra Rossa deposits) resemble the trend of marine carbonates influenced by meteoric diagenesis (James & Coquette, 1988).

This isotopic trend, suggesting a major role played by meteoric diagenesis and the preliminary results of the paleosols characterization suggest a climatic shift to more humid conditions.

Fluid inclusion investigations highlight the presence of burial fluids with high T° and salinity also within early cements (evinsponges, raggioni) (Fig.3.15). We interpret these data (apparently contrasting with microfacies and cathodoluminescence analyses) as related to fluids migration driven by the microfracture network. Therefore, we suggest that fluid inclusions are not primary (i.e. trapped during the crystal growth) but they were formed during burial when the microfracture network developed and late, burial luminescent cements precipitated. The high salinity of the fluids could be likely related to evaporitic brines or to hydrothermal fluids. Fluid inclusions from spatic dolomite support an origin related to circulation of hot hydrothermal fluids during cement precipitation.

POROSITY

The study of the porosity has been effectuated in the Esino Limestone, focusing on the effects of the subaerial exposure in the different domain of the platform. The quantification of the syndepositional porosity in inner platform, reef-upper slope, slope domain exhibits similar values, about 45-50%.(Figs.3.18; 3.19; 3.20). The subaerial exposure is responsible for a slight increase of porosity (about 5%) in the upper ten meters of the Esino Limestone (Figs.3.21; 3.22). Only in the upper 2-3 m at the top of the platform the porosity increase up to 15%. The effect of the subaerial exposure is therefore not able to significantly change the porosity of the sediments, thus suggesting that, in the case of the Esino Limestone, dissolution and erosion processes did not affect in a detectable way the original porosity of the sediment (Fig.3.17). Furthermore, karsic cavities and tubes are filled by reddish sediments during the subsequent marine trangression. This reduced effect of the subaerial exposure on the generation of porosity can be ascribed to the reduced entity of the sea-level excursions in a greenhouse period (such as the Triassic), whereas different effects could be possible in case of higher sea-level excursions in icehouse intervals. Slight emergence will produce a better developed epikarst than significative emersione but will tend to superimpose the epikarst onto the dissolutional zone that occurs where vadose and phreatic waters mix at the top of the water table. In the rock record, the proximity of these dissolutional environments may lead to important permeability (J.E.Mylroie & J.R.Mylroie, 2003). It is interesting to highlight that in the deepest part of the succession the depositional porosity is mainly destroyed by early cementation, whereas close to the exposure surface (up to 5-6 from the surface) most of the cavities are filled by Terra Rossa deposits. The evaluation of the max diagenetic porosity in the different parts of the platform (inner platform,

margin-reef, slope) returned similar values (about 40-45%) which were everywhere highly reduced during early diagenetic precipitation of calcite cements (Fig.3.23).

Chapter 5

CONCLUSIONS:

The stratigraphic and sedimentological study of Esino platform and the overlying regressive lower Carnian peritidal carbonates (Calcare Rosso) were integrated by microfacies analyses (transmitted light and cathodoluminescence), image analysis and geochemical analyses (O, C and Sr) for the evaluation of porosity. This study allows for the following conclusive remarks.

1. STRATIGRAPHY AND FACIES ANALYSIS OF THE REGRESSIVE DEPOSITS

- Close to the Ladinian/Carnian boundary a major sea level fall, traceable in the whole Sudalpine, led to exposure of the flat top, early cemented carbonate platform of the Esino Limestone;
- vertical development of the karst structures within the Esino Limestone indicates a maximum sea level fall of nearly 25 m, which is in agreement with the sea level excursion expected during a greenhouse period such as the Triassic;
- the Calcare Rosso, which caps the Esino platform, comprises several different types of facies that were deposited during the regressive event and may be considered as lithostratigraphic unit;
- distribution and thickness of the Calcare Rosso facies are strictly related to the distribution of the underlying facies of the Esino Limestone. Typical facies (Tred) of the Calcare Rosso rests above the reef-upper slope facies of the Esino Limestone. Moving toward the inner platform, the Calcare Rosso thickness decrease from 60 m to 0,3 m and the Typical facies are replaced by Residual breccias.
- facies distribution and thickness of the Calcare Rosso is mainly controlled by differential subsidence within the Esino platform. The reef-upper slope was generally characterized by an higher subsidence than the inner platform. This depends upon compaction of the basinal sediments beneath prograding clinoforms of the Esino Limestone. Furthermore the heterogeneity of Calcare Rosso mirrors the distribution of platform facies of Esino Limestone;
- the Calcare Rosso deposits are the final product of the precarious balance and complex interactions among different depositional, erosional and diagenetical processes that have varied in time and space;
- the facies organization indicates multiple events of subaerial exposures and superimposed diagenetic transformations;

2. DIAGENESIS AND POROSITY

- The isotopic analyses pointed out the influx of meteoric fluids during diagenesis in the Calcare Rosso;
- preliminary results of the paleosols characterization support a climatic shift toward more humid climatic conditions that occurred in the Early Carnian;
- absence of vadose cements and high dissolution rates recorded in the Esino Limestone may be explained considering a phreatic lens that occurred close platform top;
- primary porosity of the Esino Limestone is very high, in particular in the upper slope domain, but it was filled early by marine cements;
- secondary karst porosity is generally low. During exposure, karst processes were mainly restricted to few meters below the platform top where cavities and tubes were formed and were rapidly filled by Terra Rossa or marine sediment during transgression events. The rare occurrence of large-scale karst features such as decameter-scale caves is related to major sea level falls and are followed by cave collapse processes.
- a late stage of porosity formation occurred during the burial history and is related to the formation of fractures and the migration of Mg-rich fluids.

REFERENCES:

ALLAN J.R. & MATTHEWS R.K. (1982) - Isotope signatures associated with early meteoric diagenesis. *Sedimentology*,29, 797–818.

ARDILA P.A.R., DURAN J.J. & POMAR L. (2004) – Paleocollapse structures as geological record for reconstruction of past karst processes during the upper miocene of mallorca island. *International Journal of Speleology*. 33(1/4): 81-95.

ASSERETO R. & CASATI P. (1965) – Revisione della stratigrafia permo-triassica della Valle Camonica meridionale (Lombardia). *Rivista italiana di Paleontologia e Stretigrafia*. 71: 999-1097.

ASSERETO R. & KENDALL C.G.ST.C. (1977) - Nature, origin and classification of peritidal tepee structures amd relative breccias. *Sedimentology*, 24: 153-210., Oxford.

ASSERETO R. & FOLK R.L. (1977) - Brike-like texture and radial rays in Triassic pisolites of Lombardy, Italy: a clue to distinguish ancient aragonitic pisolites. *Sedim. Petr*. 16: 205-222, Tulsa.

ASSERETO R. & FOLK R.L. (1980) - Diagenetic fabric of aragonite, calcite and dolomite in an ancient peritidal-spelean environment: Triassic Calcare Rosso, Lombardia, Italy. *Journ. Sedim . Petrol*. 50: 371-394, Tulsa.

ASSERETO R., JADOUL F. & OMENETTO P. (1977) - Stratigrafia e metallogenesi del settore occidentale del distretto a Pb, Zn, fluorite e barite di Gorno (Alpi Bergamasche). *Riv. It. Paleont. Strat.* 83: 395-532, Milano.

BACETA J.I., WRIGHT V.P., PUJALTE V. (2001) – Paleo-mixing zone karst features from Palaeocene carbonate of north Spain: criteria for recognizing a potentially widespread but rarely documented diagenetic system. *Sedimentary Geology 139*. pp. 205-216.

BALINI M. (1992) - Ammoniti e biostratigrafia del Calcare di Prezzo (Anisico Superiore, Alpi Meridionali). *Tesi di Dottorato*: pp. 191, Univ. Milano, Milano.

BALINI M., GERMANI D., NICORA A. & RIZZI E. (2000) Ladinian/Carnian ammonoids and conodonts from the classic Schilpario-Pizzo Camino area (Lombardy): revaluation of the biostratigraphic support to chronostratigraphy and paleogeography. *Riv. Ital. Paleontol. Stratigr.*, 106(1), 19-58.

BERRA F. (2007) - Sedimentation in shallow to deep water carbonate environments across a sequence boundary: effects of a fall in sea level on the evolution of a carbonate system (Ladinian-Carnian, eastern Lombardy, Italy). *Sedimentology*, 54, 721-735.

BERRA F & JADOUL F. (2002) - Sedimentological and paleontological evidences of a "Mid Carnian" transgression in the Western Southern Alps (S. Giovanni Bianco Fm., Lombardy, Italy): stratigraphic and paleogeographic implications. *Riv. It. Paleont. Strat*., 108, 119-131.

BERRA F., JADOUL F. & ANELLI A.(2009) - Environmental control on the end of the Dolomia Principale/Hauptdolomit depositional system in the central Alps:Coupling sea-level and climate changes. *Palaeogeography,Palaeoclimatology,Palaeoecology*. 290,138-150.

BERRA F, RETTORI R. & BASSI D. (2005) - Recovery of carbonate platform production in the Lombardy Basin during the Anisian: paleoecological significance and constrain on paleogeographic evolution. *Facies*, 50; 615-27.

BLENDINGER, W. (2001) Triassic carbonate buildup flanks in the Dolomites, Northern Italy: breccias, boulder fabric and the importance of early diagenesis. *Sedimentology*, 48, 919-933.

BOSAK P. (2003) – Karst processes from the beginning to the end: How can they be dated? *Speleogenesis and Evolution of Karts Aquifers.* 1(3): 2-24.

BOSELLINI A. (1989) – Dynamics of Tethyan carbonate platforms. In: P.D. Crevello et al. (Editors), Controls on Carbonate Platform and Basin Development. *Soc. Econ. Paleontol. Mineral. Spec. Publ.* 44: 3-13.

BROMLEY (1975) – Sediment structures produced by a spatangoid echinoid: a problem of preservation. *Bulletin of the Geological Society of Denmark.* 24: 261-281.

BRUSCA C., GAETANI M., JADOUL F. & VIEL G. (1981) - Paleogeografia e metallogenesi del Sudalpino. *Mem. Soc. Geol. It.*, 22, 65-82.

BUDD D.A., SALLER A.H. & HARRIS P.M. (1995) - Unconformities and porosity in carbonate strata. *AAPG Mem.*, 63, 313.

CASSINIS G. CORTESOGNO L., GAGGERO L., PEROTTI C.R., & BUZZI L. (2008) – Permian to Triassic geodynamic and magmatic evolution of the Brescian Prealps (eastern Lombardy, Italy). *Boll. Soc. Geol. It. (Ital. J. Geosci).* 127(3): 501-518.

CAREW J.L. & MYLROIE J.E. (1991) - Some pitfalls in paleosol interpretation in carbonate sequences. *Carbonates and Evaporites*. 6: 69-74.

CHOW N. & WENDTE J. (2010) – Palaeosols and palaeokarst beneath subaerial unconformities in an Upper Devonian isolated reef complex (Judy creek), swan hills formation, west-central Alberta, Canada. *Sedimentology*. pp. 1365-3091

CLARI P.A., DELA PIERRE F. & MARTIRE P.L. (1995) – Discontinuities in carbonate successions:identification, interpretation and classification of some Italian example. *Sed.*

Geol. 100: 97-121.

CRISCI C.M., FERRARA G., MAZZUOLI R. & ROSSI P.M. (1984) – Geochemical and geochronological data on Triassic volcanism of the Southern Alps of Lombardy (Italy): genetic implications. *Geol. Rdsch.* 73: 279-292.

DAVIS R.L. & JOHNSON C.R. (1989) – Karst hydrology of San Salvador. *In: Mylroie J.E., ed., Proceedings of the Fourth Symposium on the Geology of the Bahamas. Port Charlotte, Florida: Bahamian Field Station.* pp. 118-135.

DOGLIONI C. & GOLDHAMMER R.K. (1988): Compaction-induced Subsidence in a margin of a carbonate platform. *Basin Research*, 1/4, 237-246.

DUCHAFOUR PH. (1977) – Pédologie. Vol.1- Pédogenèse et classification 477p., Masson Edit. Paris

DUDAL R., TAVERNIER R. AND OSMOND D. (1966) - Soil Map of Europe, UN Food and

Agricultural Organization, Rome

ESTEBAN M. & KLAPPA C.F. (1983) – Subaerial exposure environment. Carbonate Depositional Environments. *AAPG Memoir*. 33: 1-54.

ESTEBAN & TABERNER C. (2003) - Secondary porosity development during late burial in carbonate reservoirs as a result of mixing and/or cooling of brines. *Journal of Geochemical Exploration.*

FANTINI SESTINI N. (1994) - The Ladinian ammonoids from the Calcare di Esino of Val Parina (Bergamasc Alps, Italy). Part.1. *Riv. It. Paleont. Strat*., 100: 227-284, Milano.

FEDOROFF N. (1997) - Clay alluviation in Red Mediterranean soils. *Catena Elsevier*. 28: 171-189.

FLUGEL E. (2004) – Microfacies of carbonate rocks. *Springer*

FORCELLA F. & JADOUL F. (a cura di) (2000) – Carta geologica della Provincia di Bergamo alla scala 1:50.000 con relativa nota illustrativa. 3 fogli geologici e vol. di 300 pp. Assessorato all'Ambiente della Provincia di Bergamo. Monti ed., Bergamo.

FOUKE B.W., ZWART E. W., EVERTS A.J.W. & SCHLAGER W. (1995) – Subaerial exposure unconformities on the Vercors carbonate platform (SE France) and their sequence stratigraphic significante. *Geol. Soc. Spec. Publ.* 104: 295-320.

FROST & KERANS (2009)

GAETANI, M., GNACCOLINI, M., JADOUL, F. AND GARZANTI, E. (1998) - Multiorder sequence stratigraphy in the Triassic system of the Western Southern Alps. In: Mesozoic and Cenozoic Sequence Stratigraphy of European Basins (Eds P.C. de Graciansky, J. Hardenbol,

T. Jacquin and P.R. Vail), *SEPM Spec. Publ*., 60, 701–717.

GOLDESTEIN R.H., ANDERSON J.E. & BOWMAN M.W. (1991) – Diagenetic responses to sea-level change: integration of field, stable isotope, paleosol, paleokarst, fluid inclusion, and cement stratigraphy research to determine history and magnitude of sea-level fluctuation. Sedimentary modelling: computer simulations and Methods for improved parameter definition. *Kansas Geol. Surrv. Bull.* 233:139- 162.

HANDFORD, R., AND LOUCKS, R. G. (1993) - Carbonate depositional sequences and systems tracts responses of carbonate platforms to relative sea-level change, in Loucks, R, G. and Sarg, Rick, eds., Carbonate sequence stratigraphy: recent advances and applications: *American Association of Petroleum Geologists Memoir* 57, p. 3-41.

HARRIS, M.T. (1994) - The foreslope and toe-of-slope facies of the middle Triassic Latemar buildup (Dolomites, Northern Italy). *J. Sed. Res*., B64, 132-145.

HEIM A. (1924) – Uber submarine denudation und chemische sedimente. *Geologische Rundschau.* 15: 1-47.

HILLGARTNER F. (1998) – Discontinuity surfaces on a shallow-marine carbonate platform. *Journal of Sedimentary research.* 68: 1093-1108.

IMMENHAUSER A. & SCOOT R.W. (2002) – An estimate of Albian sea-level amplitudes and its implication for the duration of stratigraphic hiatuses. *Sed. Geol*. 152: 19-28.

JADOUL F. & ROSSI P.M. (1982) - Evoluzione paleogeografico- strutturale e vulcanismo triassico nella Lombardia centro-occidentale.In: A. Castellarin (Ed.): "Guida alla geologia del Sudalpino centro-occidentale. *Guide Geol. Reg. S.G.I".:* 143-155, Bologna.

JADOUL F. & FRISIA S. (1988) - Le evinosponge: ipotesi genetiche di cementi calcitici di cavità nella piattaforma ladinica delle Prealpi Lombarde (Alpi Meridionali). Riv. It. *Paleont. Strat*., 94: 81-104, Milano.

JADOUL F., FRISIA S. & WEISSERT H. (1989) - Evinosponges in the Triassic Esino Limestone (Southern Alps): documentation of early lithification and late diagenetic overprint. *Sedimentology.* 36: 685-699, Oxford.

JADOUL F., GERVASUTTI M. & FANTINI SESTINI N. (1992) - The Middle Triassic of the Brembana Valley: preliminary study of the Esino Platform evolution (Bergamasc Alps). *Riv. It. Paleont. Strat*., 98: 299-324, Milano.

JADOUL, F., NICORA, A., ORTENZI, A. & POHAR, C. (2002) - Ladinian stratigraphy and paleogeography of the Southern Val Canale (Pontebbano-Tarvisiano, Julian Alps, Italy). *Soc. Geol. Ital. Mem*, 57, 29-43.

JAMES N.P. & CHOQUETTE P.W. (1984) - Diagenesis 9. Limestones – The meteoric diagenetic environment. *Geosci. Can*., 11, 161–194.

KAUFFMAN J., MYERS W. J. AND HANSON G.N. (1990) - Burial cementation in the Swan Hills Formation (Devonian), Rosevear Field, Alberta, Canada. *J. Sed. Petrol*., 60, 918–939.

KEIM L. & SCHLAGER W. (1999) - Automicrite facies on steep slopes (Triassic Dolomites, Italy). *Facies*; 41, 15– 26.

KENDALL C.G.ST.C., AND W. SCHLAGER (1981) - Carbonates and relative changes in sea level: *Marine Geology* v. 44, p. l8l-2l2. l980

KERANS C. (1988) – Karst-controlled reservoir heterogeneity in Ellenburger Group carbonates of west Texas. *AAPG Bulletin.* 72: 1160- 1183.

KENTER J.A.M. (1990) - Carbonate platform flanks: slope angle and sediment fabric. *Sedimentology*, 37, 777-794.

LOUCKS R.G. (1999) – Paleocave carbonate reservoirs: origins, Burial-Depth modifications, spatial complexity, and reservoir implications. *AAPG Bulletin.* 83(11): 1795-1834.

LOUCKS R.G. & MESCHER P. (2001) – Paleocave facies classification and associated pore types. *American Association of Petroleum Geologists, Southwest Section, Annual Meeting, Dallas, Texas, March 11-13, CD-ROM, p. 18.*

LOUCKS R.G. (2007) – A review of coalesced, collapsed- paleocave systems and associated suprastratal deformation. *Time in karst.* pp. 121-132

MAURER, F. (2000) - Growth mode of Middle Triassic carbonate platforms in the Western Dolomites (Southern Alps, Italy). *Sed. Geol*. 134: 275-286.

MELIM L.A., SWART P. K. & MALIVA R.G. (1995) Meteoric-like fabrics forming in marine waters: Implications for the use of petrography to identify diagenetic environments. *Geology*, 23, 755-758

MCMECHAN G.A. (1998) - Ground penetrating radar imaging of a collapsed paleocave system in the Ellenburger dolomite, central Texas. *Journal of Applied.*

MYLROIE J.E. (1984) – Hydrologic classification of caves and karst. In R.G. LaFleur, ed., Groundwater as a geomorphic agent: Boston, Allen and Unwin. pp. 157-172.

MYLROIE J.E. & CAREW J.L. (1988) – Solution conduits as indicators of Late Quaternary sea level position. *Quaternary Science Reviews.* 7: 55- 64.

MYLROIE J.E. & CAREW J.L. (1990) – The flank margin model for dissolution cave

development in carbonate platforms. *Earth Surface processes and Landforms.* 15:413-424.

MYLROIE J.E. & CAREW J.L. (1995) – Karst development on carbonate islands. *Unconformities in Carbonate Strata. AAPG Memoir.* 63: 55-76.

MYLROIE J.E. & MYLROIE J.L. (1995) – Quaternary tectonic stability of the Bahamian archipelago: Evidence from fossil coral reefs and flank margin caves. *Quaternary Science Reviews.* 14:145-153.

MYLROIE J.E., JENSON J.W., TABOROSI D., JOCSON J.M.U., VANN D.T. AND CURT WEXEL (2001) – Karst features of Guam in terms of a general model of carbonate island karts. *Journal of Cave and Karst Studies*. 63(1): 9-22.

MYLROIE J.E. &. MYLROIE J.L (2003) – Karst development on carbonate island. *Speleogenesis and Evolution of Karst Aquifers*. 1(2): 2-20.

MYLROE J., STAFFORD K., TABOROSI D., JENSON J., MYLROIE J.R. (2005) – Karts development on Tinian, Commonwealth of the Northern Mariana Islands: Control on dissolution in relation to the carbonate island karst model. *Journal of Cave and Karst Studies*. 67(1): 14-27.

MYLROIE J.R. & MYLROIE J.E. (2007) – Development of the carbonate island karst model. *Journal of Cave and Karst Studies*. 69(1): 59-75.

MYLROIE J.E. (2008) – Late Quaternary sea-level position: Evidence from Bahamian carbonate deposition and dissolution cycles. *Quaternary international 183*. pp. 61-75.

MUTTI M. (1992) - Facies a tepee del Calcare Rosso (Ladinico superiore, Alpi Lombarde): meccanismi di formazione ed implicazioni per la stratigrafia del Ladinico-Carnico lombardo. *Giorn. Geol*., 54 (1): 147-162, Bologna.

MUTTI M. (1994) - Association of tepees and paleokarsts in the Ladinian Calcare Rosso (Southern Alps, Italy). *Sedimentology*. 41: 621-641, Oxford.

MUTTI. M., AND HALLOCK, P. (2003) - Carbonate systems along nutrient and temperature gradients: a review of sedimentological and geochemical constraints. *International Journal of Earth Sciences*. 92: 465-475.

PALMER A.N. (1991) – Origin and morphology of limestone caves. *Geological Society of America Bulletin.* 103:1-21.

POMAR L. & ARDILA P.R. (2000) – Upper Miocene karst collapse structures of the east coast. Mallorca, Spain. *Acta Carsologica.* 29/2(12): 177-184.

PATRINI P. (1927) - I fossili della scogliera dolomitica di Costa Pagliari presso Lenna (Valle Brembana). *Riv. It. Paleont. Strat*. 33: 47-70, Milano.

PERLMUTTER M.A., MATTHEWS M.D. (1989) - Global cyclostratigraphy—a model. In: Cross, T.A. (Ed.), Quantitative Dynamic Stratigraphy. Prentice Hall, pp. 233–260.

POMAR L. (2001) - Types of carbonate platforms: a genetic approach. *Basin Research*, 13, 313-334.

RIDING R. & WRIGHT V.P. (1981) – Paleosols and tidal-flat/lagoon sequences on Carboniferous carbonate shelf: sedimentary associations of triple disconformities. *J. sed. Petrol.* 51: 1323-1339.

ROSSETTI R. (1967) - Considerazioni sui rapporti tra le diverse facies ladiniche nella zona del Pizzo Camino e della Concarena (Bresciano nord-occidentale). *Atti Ist. Geol. Univ. Pavia,* 17, 124–142.

ROSSINSKY V. Jr., WANLESS H.R. & SWART P.K. (1992) - Penetrative calcretes and their stratigraphic implications. *Geology.* 20: 331-334.

RUSSO F., GAUTRET P., MASTANDREA A. & PERRI E. (2006) - Syndepositional cements associated with nannofossils in the Marmolada Massif: Evidences of microbially mediated primary marine cements? (Middle Triassic, Dolomites, Italy). *Sedimentary Geology*, 185, 267–275

SALLER A.H., BUDD D.A. & HARRIS P.M. (1994) – Unconformities and porosity development in carbonate strata. Ideas from a Hedberg Conference. *AAPG Bulletin.* 78: 857-871.

SATTLER U., IMMENHAUSER A., HILLGARTNER H., ESTEBAN M. (2005) – Characterization, lateral variability and lateral extent of discontinuity surfaces on a Carbonate Platform (Barremian to lower Aptian, Oman). *Sedimentology*. 52: 339-361.

SCHWABE S.J., HERBERT R.A., CAREW J.L. (2008) – A hypothesis for biogenic cave formation: a study conducted in the Bahamas. *Special publication of 13th Symposium on the Geology of the Bahamas and other Carbonate Regions.* pp. 141-152.

SATTLER U., IMMENHAUSER A., HILLGARTNER H., ESTEBAN M. (2005) – Characterization, lateral variability and lateral extent of discontinuity surfaces on a Carbonate Platform (Barremian to lower Aptian, Oman).*Sedimentology*. 52: 339-361.

SCHLAGER W. (2003) – Accomodation and supply – a dual control on stratigraphic sequences. *Sed. Geol.* 86: 111- 136.

SHINN E.A. (1969) – Submarine lithification of Holocene carbonate sediments in the Persian Gulf. *Sedimentology.* 12: 109-144.

TOMMASI A. (1911) - I fossili della lumachella di Ghegna in Valsecca presso Roncobello.

Parte I: Alghe, Anthozoa, Brachiopoda, Lamellibranchiata. *Paleont. Italica*, 17: 1-36, Milano.

TOMMASI A. (1913) - I fossili della lumachella di Ghegna in Valsecca presso Roncobello. Parte II: Scaphopoda, Gastropoda, Cephalopoda. Appendice, Conclusione. *Paleont. Italica*, 19: 31-101, Milano.

TORTI V. & ANGIOLINI L. (1997) - Middle Triassic brachiopods from Val Parina, Bergamasc Alps, Italy. *Riv. It. Paleont. Strat.*, 103, 149-172.

VACHE' R. (1966) - Ricerche microstratigrafiche sul "Metallifero" di Gorno (Prealpi Bergamasche). *Riv. It. Paleont. Strat*., 72: 53-144, Milano.

VAN DER KOOIJ B., IMMENHAUSER A., STEUBER T., BAHAMONDE J.R. AND MERINO TOMEO (2010) - Controlling factors of volumetrically important marine carbonate cementation in deep slope settings. *Sedimentology*. 57(6): 1491-1525.

WALLS R.A. & BURROWS O.G. (1985) - The role of cementation in the diagenetic history of Devonian reefs, western Canada. *Carbonate Cements, SEPM Spec. Publ.*. 36: 185-220.

WEBB G.E. (1994) – Paleokarst, paleosol and rocky-shore deposits at the Mississippian Pennsylvanian unconformity, northwestern Arkansas. *Geological Society of America Bulletin.* 106: 634-648.

WEBER L.J., FRANCIS B. P., HARRIS P.M. AND CLARK M. (2003) - Stratigraphy, facies, and reservoir distribution, Tengiz Field, Kazakhstan. *AAPG Mem*., 83, 351-394.

WILLIAMS P.W. (1983) - The role of the subcutaneous zone in karst hydrology. *Journal of Hydrology.* 61: 45-67.

WILSON M. & TAYLOR P.D. (2001) – Palaeoecology of hard substrate faunas from the Cretaceous Qahlah formation of the Oman Mountains. *Paleontology*. 44: 21-41.

WRIGHT V.P. & SMART P.L. (1994) – Paleokarst (dissolution diagenesis): its occurrence and hydrocarbon exploration significance. *Sedimentology 51*. pp. 489-502.

WRIGHT V.P. (1994) – Paleosols in shallow marine carbonate sequences. *Earth-Science Reviews.* 35:367-395.

YAALON D.H. (1997) – Soils in the Mediterranean region: what makes them different? *Catena Elsevier*. 28: 157-169.

... a Flavio e Fabrizio

...a Paola

... a tutto il gruppo di lavoro, tra cui Gianluca, Irene, il Mussu, Andrea, Enrico e Dario, i miei due omonimi, la zia di Sara e Sara

... a nonno Antonio e nonna Gidia,

... a Marcellino e Lella, Tina, Teo e Tommy, Igino e Enrico